iJERGS International Journal of Engineering Research And General Science

Journal which deals with research, Innovation and Originality

International Journal Of Engineering Research and General Science

ISSN 2091 - 2730

Table of Content

CHIEF EDITOR BOARD

Message from Associate Editor In Chief

Let me first of all take this opportunity to wish all our readers a very happy, peaceful and prosperous year ahead.

This is the Forth Issue of the Fifth Volume of International Journal of Engineering Research and General Science. A total of 16 research articles are published and I sincerely hope that each one of these provides some significant stimulation to a reasonable segment of our community of readers.

In this issue, we have focused mainly on theGlobal challenges and its innovative solutions. We also welcome more research oriented ideas in our upcoming Issues.

Author's response for this issue was really inspiring for us. We received many papers from many countries in this issue but our technical team and editor members accepted very less number of research papers for the publication. We have provided editors feedback for every rejected as well as accepted paper so that authors can work out in the weakness more and we shall accept the paper in near future. We apologize for the inconvenient caused for rejected Authors but I hope our editor's feedback helps you discover more horizons for your research work.

I would like to take this opportunity to thank each and every writer for their contribution and would like to thank entire International Journal of Engineering Research and General Science (IJERGS) technical team and editor member for their hard work for the development of research in the world through IJERGS.

Last, but not the least my special thanks and gratitude needs to go to all our fellow friends and supporters. Your help is greatly appreciated. I hope our reader will find our papers educational and entertaining as well. Our team have done good job however, this issue may possibly have some drawbacks, and therefore, constructive suggestions for further improvement shall be warmly welcomed.

Er. Pragyan Bhattarai,

AssociateEditor-in-Chief, P&REC,

International Journal of Engineering Research and General Science

E-mail -Pragyan@ijergs.org

Situational Factors influences on Impulse Buying Behaviour of Working Women in Informal Sector

F.B.Kennedy, DEPARTMENT OF BUSINESS ADMINSTRATION,
PhD Research Scholar, Annamalai University, Tamil Nadu, India - 608002
And
Dr.B.Vimala, DEPARTMENT OF BUSINESS ADMINSTRATION
Assistant Professor, Annamalai University, Tamil Nadu, India - 608002

ABSTARCT - Impulse buying is one of the most fragmented concepts in consumer behaviour. There are difficult factors researched in relation to study the impulse buying behaviour. This research investigate the relationship between situational factors: money availability, time availability and family influence on Impulse buying behaviour through urge to buy on impulse. Urge to buy on impulse plays a mediator role in impulse buying behaviour.

Respondents for this study are 230 working women in informal sector of employment. They were administrated with structured questionnaire. The findings state that money availability, family influence are positively influencing impulse buying behaviour of women in informal sector whereas time availability is not supporting the hypothesis.

Keywords: Impulse buying behaviour, Situational Factor, Working women and urge to buy on impulse

INTRODUCTION

Impulse buying is a mystery in Marketing. It is a spontaneous purchase. Consumers decides to purchase the object on the spur of the movement not in response to a previously recognized problem. Impulse buying is investigated about more than seven decades in the research paradigm. Research state that situational factors (Rook and Fisher, 1995; Ito and Nakamura, 1998), along with intrinsic factor of consumers' (Kacen and Lee, 2002), extrinsic stimuli as visual merchandizing (Vinamra et al., 2012; Buttle, 1988; Frings, 1999) and shopping environment (Morrison, 2002; A. Ali.ASF Hansu, 2013) and consumers' cultural factors (Muruganandham and Bhakat; 2013) influence the impulse buying behaviour. Moreover, the demographic factors as age, gender, educational qualification, income level and occupation also affect impulse buying.

Women Sri Lanka are very traditional but now there seems to be very different in their buying behaviour especially in dressing including purchasing of apparels. Research found women tend to buy symbolic and self-expressive goods which are associated with their appearances and emotional aspects. Working women in informal sector are not exceptions in expressing their purchasing behaviour in this line. Therefore, apparels are taken as investigating object in finding the relationship between situational factors and impulse buying behaviour of working women in Batticaloa District.

Review of Literature and Hypothesis Development

Impulse Buying Behaviour

The four types impulse purchasing pure, reminder, suggestion or fashion oriented and planned impulse buying are recognized by Stern (1962). Pure impulse buying is when the buyer breaks the usual shopping trend and purchase the products. Reminder impulse is when a consumer reminded about the purchase when she/he sees the products in the store. The other concept of suggestion or fashion-oriented impulse buying is also introduced by Stern (1962) *ie* without any prior experience the buyer suggesting a new product for themselves. Han et al. (1991) described fashion-oriented impulse as a type of suggestion impulse where the purchase is motivated by self-suggestions to buy the new fashion products. Dittmar et al. (1995) found that products bought on impulse can reflect gender identity.

Situational Factors and Urge to buy on Impulse

Situational factors are attributed to person's situation, related to availability of money (Pattipeilohy and Rofiaty, 2013; Beatty and Ferrell, 1998), time (Pattipeilohy and Rofiaty, 2013; Beatty and Ferrell,1998) and family influences (Lin and Chen, 2012; . Anić and Radas, 2006). The theory of Reasoned Action emphasized human social behaviour follows reasonably and often spontaneously from the information or beliefs people possess about the behaviour under consideration (Fishbein and Ajzen 1995).

Urge to buy on impulse is different from impulse buying behaviour. Beatty and Ferrell, (1998) suggested that as consumers feel stronger urges, their likelihood of buying impulsively goes up. The immediate urge to buy is a state of desire reached through an encounter with a product (Beatty & Ferrell, 1998). Hirschman (1985), forwarded that consumer's own train of thoughts was considered to trigger the desire to make an unanticipated purchase, and once triggered, the urge supposedly becomes so powerful and persistent that it demands immediate action. This finding explains that urge to buy impulsively is the stage prior to and leading towards the actual stage of impulse buying.

Therefore, these literature led to develop the following hypothesis for this study.

H1a: There is a positive relationship between Money availability and Impulse buying behaviour

H1b: There is a positive relationship between Money availability and urge to buy on impulse

H2a: There is a positive relationship between Family Influence and Impulse buying behaviour

H2b: There is a positive relationship between Family Influence and urge to buy on impulse

H3a: There is a positive relationship between Time availability and Impulse buying behaviour

H3b: There is a positive relationship between Time availability and Urge to buy on impulse

H4: There is a positive relationship between Urge to buy on impulse and Impulse buying behaviour

Methodology

Sample and Area

This study concentrates with situational factors through urge influences on impulse buying behaviour of working women in informal sector. This study was carried out with 230 working women of informal sector in Batticaloa, Sri Lanka during the period of March and April, 2017. Stratified random sampling was applied to select working women for this study.

Survey Instrument

Primary data are collected through structured questionnaires with closed statements measured with Likert's scale (1= strongly disagree and 5= strongly agree). The questionnaire was consisting with three main section; impulse buying behaviour, urge to buy on impulse and situational factors.

Statistical tool used

The collected data was analyzed using descriptive, one way ANOVA and correlation analysis and regression analysis.

Results and Discussions

Table 1: Level of Situational Factors in Informal sector

Level	Money Availability		Family Influence		Time Availability	
	No. of Respondents	Percentage	No. of Respondents	Percentage	No. of Respondents	Percentage
Low	54	23.5	34	14.8	110	47.8
Medium	81	35.2	92	40.0	95	41.3
High	95	41.3	104	45.2	25	10.9
Total	230	100	230	100	230	100

Table 1 explains the level perceived by the respondents about the situational dimensions. It is found that 41.3 percent of the respondents have high level in Money Availability, 23.5 percent of the respondents have low level in Money Availability and 35.2 percent of respondents have medium level in Money Availability. This indicate that majority of the respondents are falling in the high level of money availability.

It is also denoted by this Table 1 that Family influences are 45.2 percent and falls in higher level whereas 40.0 percent falls in moderate level influences and 14.8 percent falls in the lower level of family influences. This indicates that high percent of the respondents are expressing higher family influences.

Time availability is 47.8 percent in low level among the respondents and 41.3 percent of the respondents have moderate level of time availability and 10.9 percent of the respondents have high level in time availability. This indicates that high percent of the respondents are expressing lower time availability.

Table 2: Level of urge to buy on impulse in Informal sector

Urge to buy on impulse	No. of Respondents	Percentage
Low	65	28.3
Medium	71	30.9
High	94	40.9
Total	230	100

Table 2 depicts that 40.9 percent of respondents have high level of urge to buy on impulse, 30.9 percent of respondents have medium level of urge to buy on impulse and only 28.3 percent of working women in informal sector have low level of urge to buy on impulse.

Table 3: Level of Impulse Buying Behaviour in Informal sector

Impulse Buying Behaviour	No. of Respondents	Percentage
Low	59	25.7
Medium	80	34.8
High	91	39.6

Total	230	100

Table 3 stipulates that 39.6 percent of respondents have high level of Impulse Buying Behaviour, 34.8 percent of respondents have medium level of Impulse Buying Behaviour and 25.7 percent of respondents have low level of Impulse Buying Behaviour.

Table 4: Situational Factors and Urge to buy on Impulse of working women in informal sector

Variables	**Money Availability**		**Family Influence**		**Time Availability**	
	r-value	P-value	r-value	P-value	r-value	P-value
Urge to buy	0.320	0.000	0.276	0.000	-0.042	0.527

Table 4 reveals the relationship between the urge to buy on impulse and situational factors of working women in informal sector. It shows there is positive relationship between money availability (r-value 0.320) and family influence (r-value 0.276) on urge to buy on impulse. The r-value is -0.042 between Time availability and urge to buy on impulse in informal sector working women.

Table 5: Situational factors and Impulse Buying Behaviour of working women in informal sector.

Variables	**Money Availability**		**Time Availability**		**Family Influence**	
	r-value	P-value	r-value	P-value	r-value	P-value
Impulse Buying Behaviour	0.485	0.000	0.134	0.042	0.231	0.000

Table 5 signifies that the relationship between Money availability, Time availability and Family Influences are positively influencing Impulse Buying Behaviour. The r-value for these variables are 0.485, 0.134 and 0.231 respectively.

In order to test the hypothesis Regression test is applied.

Table 6: Correlation between Urge to buy on Impulse and Impulse Buying Behaviour of working women in informal sector.

Sector	**Variables**	**Impulse Buying Behaviour**	
Informal	**Urge to buy**	0.711	0.000

Table 6 signifies that the relationship between Urge to buy on Impulse and Impulse Buying Behaviour of working women in informal sector. The r-value 0.711 at the significant level and therefore there is a strong positive relationship between these two variables.

Regression Analysis

Table 7: Multiple Linear Regressions between Situational Variables and Urge to buy on impulse

Model Summary			**ANOVA**	
Model	R Square	Std. Error of the Estimate	F	Sig.
1	0.157	1.009	14.052	0.000

Coefficients

Model		**B**	**Std. Error**	**t**	**Sig**
1	Constant	1.132	0.403	2.808	0.005

Money Availability	0.361	0.289	4.646	0.000
Family Influence	0.286	0.227	3.659	0.000
Time Availability	-0.059	-0.047	-0.766	0.445

Above table 7 summarizes the results of multiple linear regressions and it confirms that specified regression model explains 15.7% (R square) of the total variation in Urge. And P value for F-statistics 0.000, which is less than 0.05, suggests that overall, the model applied can statistically significantly predict the dependent variable. However, when looking into individual significance of the independent variables, Money availability and Family influence have significant influence on Urge (p-value is 0.000). Time availability does not have significant influence on Urge to buy on impulse. Thus, the estimated model can be established as follows:

Urge = 1.132 + 0.361 Money availability +0.286 Family influence + Ɛ

Table 8: Multiple Linear Regressions between Situational Variables and Impulse Buying Behaviour

Model Summary			**ANOVA**	
Model	R Square	Std. Error of the Estimate	F	Sig.
1	0.272	0.755	28.178	0.000

Coefficients

Model		**B**	**Std. Error**	**t**	**Sig**
1	Constant	0.930	0.302	3.082	0.002
	Money Availability	0.453	0.058	7.776	0.000
	Family Influence	0.174	0.059	2.965	0.003
	Time Availability	0.110	0.057	1.913	0.047

Above table 8 summarizes the results of multiple linear regressions and it confirms that specified regression model explains 27.2% (R square) of the total variation in Impulse Buying Behviour. And P value for F-statistics 0.000, which is less than 0.05, suggests that overall, the model applied can statistically significantly predict the dependent variable. However, when looking into individual significance of the independent variables, only Money Availability has significant influence on Impulse Buying Behaviour (p-value is 0.000). Both Family Influence and Time Availability do not have significant influence on Impulse Buying Behaviour. Thus, the estimated model can be established as follows:
Impulse buying behaviour = 0.930 + 0.453 Money availability + 0.174 Family influence + 0.110 Time availability + Ɛ

Accordingly, one unit increase in Money Availability will increase Impulse Buying Behaviour by 0.453 when the other variables are constant. And one unit increase in Family influence will increase Impulse Buying Behaviour by 0.174 whereas the other variables are constant. Further, one unit increase in Time availability will increase Impulse Buying Behaviour by 0.110 where other variables are not changing.

Table 9: Simple Linear Regression between Urge and Impulse Buying Behaviour of working women in informal sector

Model Summary			**ANOVA**	
Model	R Square	Std. Error of the Estimate	F	Sig.
1	0.505	0.620	232.705	0.000

Coefficients

Model		**B**	**Std. Error**	**t**	**Sig**
1	Constant	1.483	0.124	11.954	0.000
	Urge	0.573	0.038	15.255	0.000

Above table 9 summarizes the results of simple linear regressions and it confirms that specified regression model explains 50.5% (R square) of the total variation in Impulse Buying Behviour. And P value for F-statistics 0.000, which is less than 0.05, suggests that overall, the model applied can statistically significantly predict the dependent variable. Thus, the estimated model can be established as follows:

Impulse buying behaviour = 1.483 + 0.573 Urge + Ɛ

Accordingly, one unit increase in urge will increase Impulse buying Behaviour by 0.573 when other variables are not changing.

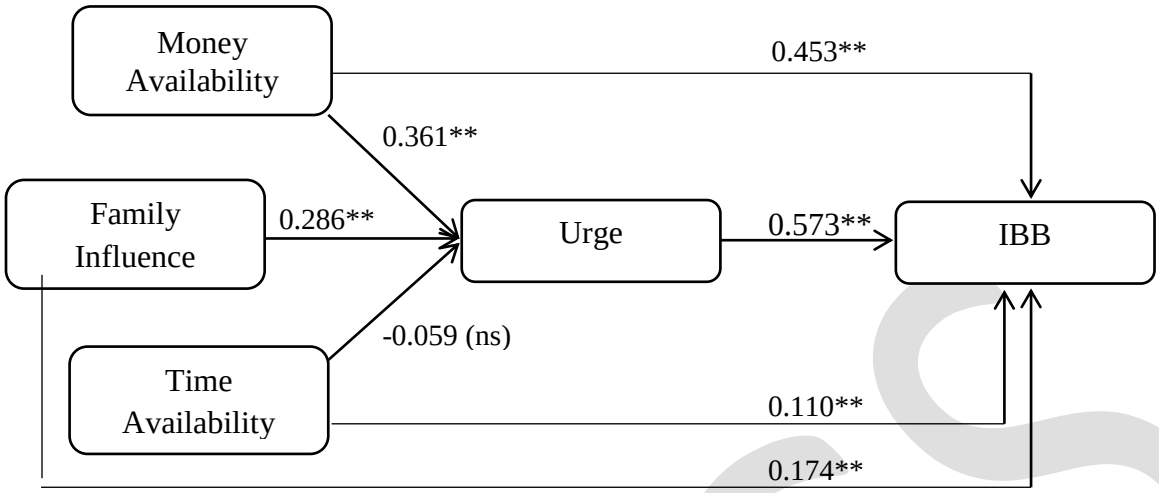

Figure 1:

CONCLUSION:

It is concluded that situational factors as money availability and family influences influencing the impulse buying behaviour through urge to buy on impulse in informal sector working women. But Time availability is not influencing on urge to buy on impulse, but influencing Impulse Buying Behaviour directly. Therefore, hypotheses H1a, H1b, H2a, H2b, H3a, H4 are accepted and H3b only not accepted in this study.

REFERENCES:

1. Anić, I., & Radas, S. (2006). The impact of situational factors on purchasing outcomes in the Croatian hypermarket retailer. *Ekonomski pregled*, *57*(11), 730-752.
2. Badgaiyan, A. J., & Verma, A. (2015). Does urge to buy impulsively differ from impulsive buying behaviour? Assessing the impact of situational factors. *Journal of Retailing and Consumer Services*, *22*, 145-157
3. Beatty, S. E., & Ferrell, M. E. (1998). Impulse buying: Modeling its precursors. *Journal of retailing*, *74*(2), 169-191.
4. Beatty, S.E. & Ferrell, M.E. (1998). Impulsive buying: modelling its precursors. Journal of Retailing, Vol.74 No. 2, pp. 169-191. *Journal of Advertising Research* Vol. 18 No. 6, pp. 15-18
5. Buttle, F. (1988). Merchandising. *European Journal of Marketing*, 18 (5), 4-25.
6. Dittmar, H., Beattie, J., & Friese, S. (1995). Gender identity and material symbols: Objects and decision considerations in impulse purchases. *Journal of economic psychology*, *16*(3), 491-511.
7. Hausman, A. (2000). A multi-method investigation of consumer motivations in impulse buying behavior. *Journal of consumer marketing*, *17*(5), 403-426.
8. Hirschman, E. C. (1979). Differences in consumer purchase behavior by credit card payment system. *Journal of Consumer Research*, *6*(1), 58-66.
9. Lin, Y. H., & Chen, C. Y. (2012). Adolescents' impulse buying: susceptibility to interpersonal influence and fear of negative evaluation. *Social Behavior and Personality: an international journal*, *40*(3), 353-358.
10. Pattipeilohy, V. R. (2013). Rofiaty, & Idrus, MS (2013). The influence of the availability of money and time, fashion involvement, hedonic consumption tendency and positive emotions towards impulsive buying behavior in Ambon City. *Journal of Business and Behavioral Sciences*, *3*(8), 36-49.
11. Ramanathan, S., & Menon, G. (2002). Don't Know Why but I Had This Craving: Goal Dependent Automaticity in Impulsive Decisions. In New York University Working paper.
12. Roberts, J. A., & Jones, E. (2001). Money attitudes, credit card use, and compulsive buying among American college students. *Journal of Consumer Affairs*, *35*(2), 213-240.
13. Rook, D. W. (1987). The buying impulse. *Journal of Consumer Research*, *14*, 189-199.

14. Rook, D. W., & Fisher, R. J. (1995). Normative influences on impulsive buying behavior. *Journal of consumer research*, *22*(3), 305-313.
15. Russell, J. A., & Yik, M. S. (1996). Emotion among the Chinese.
16. Verplanken, B., & Herabadi, A. (2001). Individual differences in impulse buying tendency: Feeling and no thinking. *European Journal of personality*, *15*(S1).

International Journal of Engineering Research and General Science Volume 5, Issue 4, July-August, 2017
ISSN 2091-2730

Densitometric and Viscometric studies of 2, 4 dioxo pyrimidine carbonitrile and 4-oxo-2-thioxo pyrimidine carbonitrile in 60 % aqueous DMSO at 298.15 K

Jayraj S. Aher[1*], Manoj R. Gaware[2], Dnyaneshwar D. Lokhande[3]

[1*]Department of Chemistry, K. T. H. M College, Nashik, (M.S), India.

[2]Department of Chemistry, Arts, Commerce and Science College, Nandgaon, Nashik, (M.S), India.

[3]Department of Chemistry, KPG Arts, Commerce and Science College, Igatpuri, Nashik, (M.S), India.

Email: js_aher@rediff.com

Abstract: Density, Viscosity of 2, 4 dioxo pyrimidine carbonitrile and 4-oxo-2-thioxo pyrimidine carbonitrile have been measured in 60% aqueous dimethyl sulphoxide (DMSO) at 298.15 K. From the experimental data the related parameters such as apparent molar volume, limiting apparent molar volume, semi-empirical parameter, Falkenhagen coefficient and Jones Dole coefficient were evaluated. Such parameters gives identification of molecular interactions such as ion-ion, ion-solvent and solvent-solvent.

Keywords: 2, 4 dioxo pyrimidine carbonitrile, 4-oxo-2-thioxo pyrimidine carbonitrile, density, viscosity, aqueous DMSO.

INTRODUCTION: Heterocyclic compounds contains heteroatoms such as oxygen, nitrogen and sulphur. These compounds may be aliphatic or aromatic in nature. Pyrimidine ring system belongs to the most important heterocycles in nature due to many biological significant compounds including nucleosides, nucleotides and biological activity[1-3] such as antiviral, antibacterial, anticancer, antifungal, antioxidant, antimalarial, anti HIV, sedatives, anticonvulsant, antihistamic agent, antihypertensive, anti-inflammatory, anticancer and calcium channel blockers. They are important component of nucleic acids and have been used as building blocks in pharmaceuticals. The study of ion-solvent interactions is very important to understand the nature of different solvents. The parameters like apparent molar volume, density, viscosity, 'A' and 'B' parameters of Jones Dole equation are useful to focus the solute solvent interactions and to understand different biochemical aspects at 298.15 K. The results are interpreted in terms of solute-solvent and solute-solute molecular interactions in these systems. Dimethyl sulphoxide (DMSO) is aprotic and is strongly associated due to highly polar S=O group. It has high miscibility in water and used for dissolving many organic as well as inorganic compounds. The study of DMSO is important because of its application in medicine.[4] It easily penetrates the biological membrane, facilitates chemical transport into biological tissues and is well known to have protective effects in biological systems.[5] It is also used as an inflammatory agent and for cancer treatment.[6] Therefore the unique property of DMSO gives rise to wide use as solvent. Also the drug water molecule interactions and its temperature dependence plays an important role in understanding

drug action[7] i.e. drug reaching the blood stream, its extend of distribution, its binding to the receptor and producing the physiological action.

MATERIAL: 2,4 dioxopyrimidine carbonitrile and 4-oxo-2-thioxo pyrimidine carbonitrile were synthesized and purified by recrystallization technique in laboratory.[8-10] Triple distilled deionised water was used for preparation of solution at room temperature in a molar range of 2 x 10^{-3} to 1 x 10^{-3} mol L^{-1}. DMSO used is of analytical reagent grade (AR) of minimum assay of 99.9% obtained from SD Fine Chemicals, Mumbai.

Density measurements: The pycknometer was calibrated by measuring the densities of triple distilled water. The densities of distilled organic liquids like acetone, toluene and carbon tetrachloride were evaluated with respect to density of water.

Viscosity measurement: The solution viscosities were measured by using Ubbelohde viscometer at 298.15 K. The temperature of thermostat was maintained to desired temperature by using demerstat. The flow time was recorded by using digital stop watch. The different concentrations of solution were prepared in 60 % aqueous DMSO.

Data evaluation: The apparent molar volumes, $Ø_v$ were obtained from the following equation[11-14]

$$\Phi V = \frac{1000\ (\rho_0 - \rho)}{C\ \rho_0} + \frac{M2}{\rho_0}$$

where M_2, C, , ρ_0 and ρ are the molar mass of 2, 4 dioxo pyrimidine carbonitrile and 4-oxo-2-thioxo pyrimidine carbonitrile derivatives, concentration (mol. L^{-1}) and densities of the solvent and the solution respectively.

The apparent molar volumes Φv were plotted against the square root of concentration ($C^{1/2}$) in accordance with the Masson's equation[15]

$$\Phi V = \Phi^o{}_V + S_v\ C^{1/2}$$

where $\Phi^o{}_V$ is the limiting apparent molar volume and S_v is semi empirical parameter or associated constant which depends on the nature of solvent, solute and temperature.

The viscosity results for the aqueous solutions of 2, 4 dioxo pyrimidine carbonitrile and 4-oxo-2-thioxo pyrimidine carbonitrile were plotted in accordance with John Dole equation[16]

$$\frac{\eta_r - 1}{C^{1/2}} = A + B\ C^{1/2}$$

Where $\eta_r = (\eta/\eta_o)$ and η, η_o are viscosities of the solution and solvent respectively. C is the molar concentration. The linear plot for $(\eta_r-1)/C^{1/2}$ vs $C^{1/2}$ were obtained. The intercept (A) coefficient shows solute-solute interaction and the slope (B) reflect the solute-solvent interaction.

Table 1: Densities, molar volumes, viscosities and relative viscosities of 2,4 dioxopyrimidine carbonitrile and 4-oxo-2-thioxo pyrimidine carbonitrile in 60 % aqueous DMSO solution at 298.15 K temperature

Densities (ρ) ($g.cm^{-3}$), Apparent molar volumes (Φv) ($cm^3.mol^{-1}$), Viscosities (η) (cP) and Relative Viscosities (η_r)

Compound	Conc mol L^{-1}	ρ	Φv	η	η_r
A-1	**0.002**	1.08925	-2907.7287	3.73009	1.106657
	0.004	1.08968	-1207.8968	3.72981	1.106576
	0.006	1.08978	-898.4166	3.74318	1.110542
	0.008	1.08982	-621.2701	3.74777	1.111902
	0.010	1.08994	-462.3727	3.75297	1.113446
A-2	**0.002**	1.08736	-2112.3182	3.70793	1.100084
	0.004	1.08772	-971.3985	3.71368	1.101791
	0.006	1.08815	-632.6639	3.72071	1.103874
	0.008	1.08893	-503.7138	3.7255	1.105296
	0.010	1.08912	-371.8382	3.73232	1.10732

Table 2: $(\eta_r-1)/C^{1/2}$ and $C^{1/2}$ values of 2,4 dioxopyrimidine carbonitrile and 4-oxo-2-thioxo pyrimidine carbonitrile in 60 % aqueous DMSO solution at 298.15 K temperature.

Compound	$C^{1/2}$ mol L^{-1}	$(\eta_r-1)/C^{1/2}$
A-1	**0.04472**	2.38493
	0.06325	1.68513
	0.07746	1.42709
	0.08944	1.25110
	0.10000	1.13446
A-2	**0.04472**	2.23794
	0.06325	1.60945
	0.07746	1.34100
	0.08944	1.17725

	0.10000	1.07320

Table 3: Masson's and Jones-Dole parameters of 2,4 dioxopyrimidine carbonitrile and 4-oxo-2-thioxo pyrimidine carbonitrile in 60 % aqueous DMSO solution at 298.15 K temperature.

Compound	Φ^o_V	S_v	A ($dm^{3/2}mole^{-1/2}$)	B (dm^3mole^{-1})
A-1	-4359.2	41876	3.2336	-22.101
A-2	-3179.1	30154	3.0451	-20.772

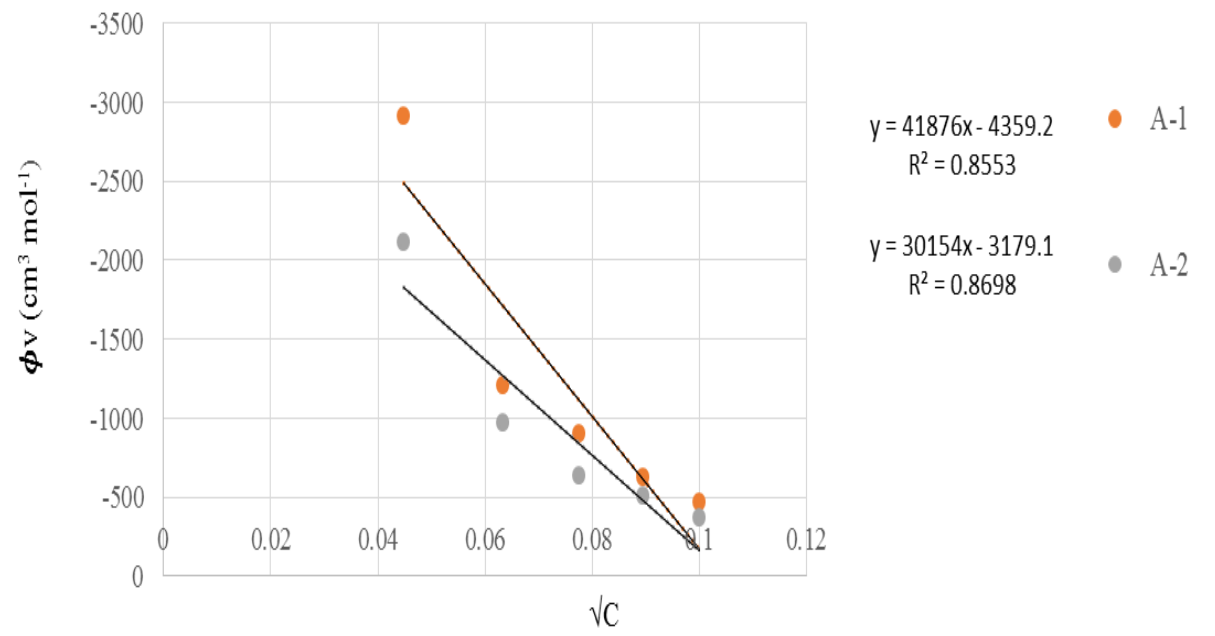

Figure:Plot of √C Vs ϕv for dihydropyrimidine carbonitrile A-1and A-2 at 298.15 K

Figure 1: Plot of ϕ_v versus C½ of 2,4 dioxopyrimidine carbonitrile and 4-oxo-2-thioxo pyrimidine carbonitrile in 60 % aqueous DMSO solution at 298.15 K temperature.

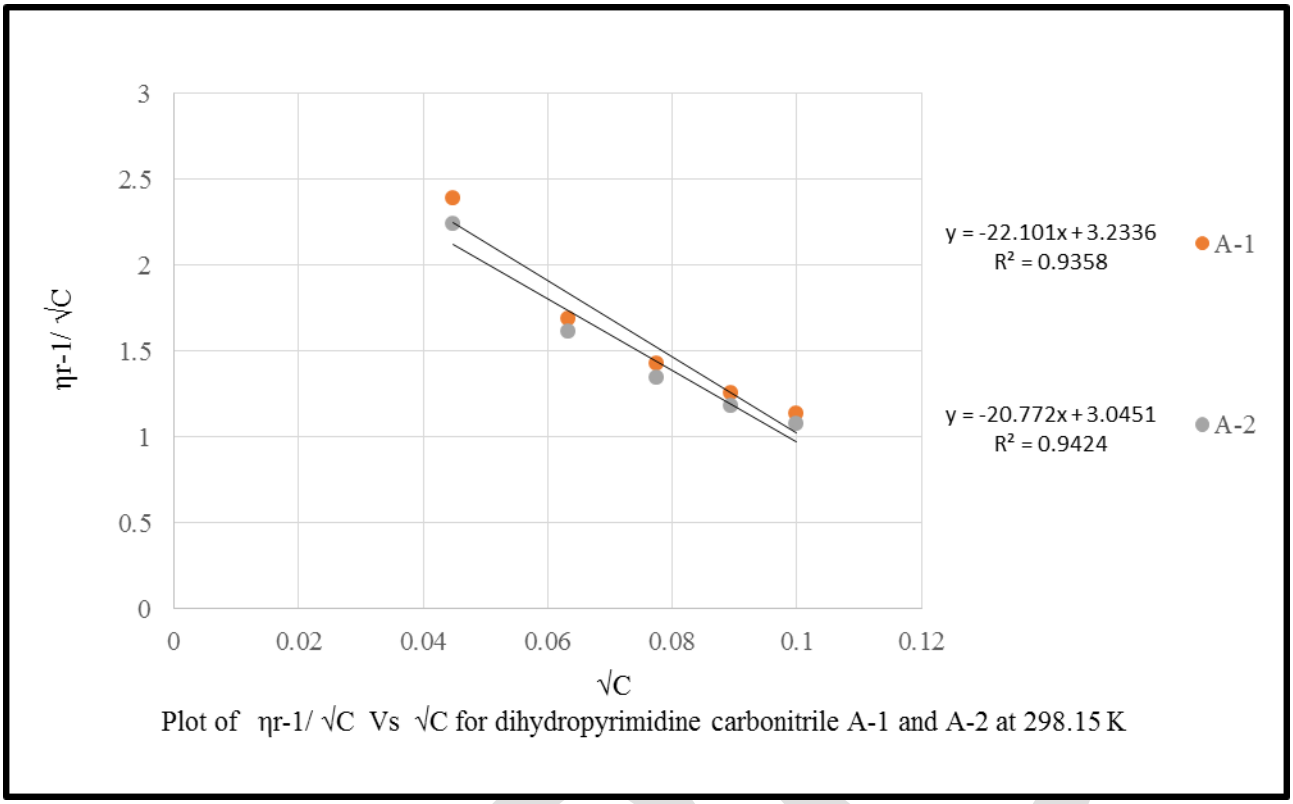

Figure 2: Plot of $(\eta_r-1)/C^{½}$ versus $C^{½}$ of 2,4 dioxopyrimidine carbonitrile and 4-oxo-2-thioxo pyrimidine carbonitrile in 60 % aqueous DMSO solution at 298.15 K temperature.

Structure:

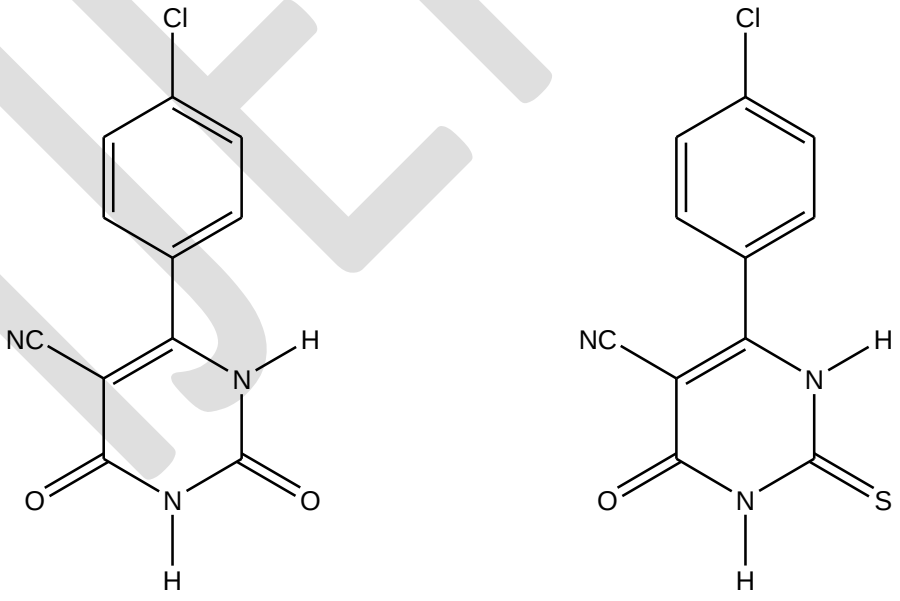

A-1 **A-2**

RESULT AND DISCUSSION: The values of the densities, molar volumes, viscosities and relative viscosities of 2,4 dioxopyrimidine carbonitrile and 4-oxo-2-thioxo pyrimidine carbonitrile in 60 % aqueous DMSO solution at 298.15 K

temperature are shown in Table 1. For A-1 and A-2 the densities increases slightly with increase in concentration, Similarly Φv values also increases with increase in concentration. The negative value indicate the electrostrictive salvation of ions. The Φv values are more negative in A-1 as compared to A-2 which suggest that there is strong molecular association in A-2 than A-1 i.e. presence of electrostriction and hydrophilic interaction (solute solvent interactions).

Figure 1 shows linear plots of Φv vs $C^{1/2}$ of 2,4 dioxopyrimidine carbonitrile and 4-oxo-2-thioxo pyrimidine carbonitrile in 60 % aqueous DMSO solution at 298.15 K temperature. Masson's parameter Φ^o_V (limiting apparent molar volume) and S_v (experimental slope or semi empirical parameter or associated constant) were obtained from linear plots in Table 3. The values of Φ^o_V are negative shows weak or absence of ion solvent interactions. In other words hydrophobic-hydrophobic group interactions are present. The values of Φ^o_V follow the trend A-1 > A-2. The positive value of S_v indicates the presence of solute-solute interactions. A-1 has high solute-solute interactions than A-2. The viscosities of solution increases with increase in concentration of solution. The value of $(\eta_r-1)/C^{1/2}$ vs $C^{1/2}$ studied at 298.15 K. is shown in Table 2. Figure 2 shows variation of $(\eta_r-1)/C^{1/2}$ against $C^{1/}2$ at 298.15 K. 'A' is constant independent of concentration and represent Falkenhagen coefficient (solute-solute interactions) while 'B' is Jones-Dole coefficient representing measure of order and disorder introduced by solute in solvent (solute-solvent interactions). Positive 'A' coefficient shows strong solute-solute interactions. The Jones-Dole parameters are shown in Table 3. The negative values of 'B' shows weak solute-solvent interactions. The value of 'A' in A-1 are high than A-2 indicates presence of strong solute-solute interactions in A-1 and focuses high electronegativity of oxygen in A-1 which gives rise to strong molecular association as compared to A-2.

CONCLUSIONS: From the present studies we have systematically reported densitometric and viscometric study of 2,4 dioxopyrimidine carbonitrile and 4-oxo-2-thioxo pyrimidine carbonitrile in 60 % aqueous DMSO solution at 298.15 K temperature. It has been observed that negative values of (Φv) indicates strong molecular associations. in A-2 as compared to A-1. The values of Φ^o_V are negative which are high in A-1 suggests weak ion-solvent interactions. The value of Jones-Dole coefficient 'B' in A-2 indicates strong interactions between solute and solvent while Falkenhagen coefficient 'A' indicates strong solute-solute interaction in A-1 pointing presence of high electronegativity in oxygen than sulphur. The Jones Dole and Masson's equations are found to be obeyed for study of 2,4 dioxopyrimidine carbonitrile and 4-oxo-2-thioxo pyrimidine carbonitrile in 60 % aqueous DMSO solution system at 298.15 K temperature.

ACKNOWLEDGEMENT: The authors are thankful to UGC WRO, Pune and BCUD Savitribai Phule Pune University, Maratha Vidya Prasarak Samaj Nashik for providing infrastructure and Principal, K. R. T. Arts B. H. Commerce and A. M. Science College, Gangapur Road, Nashik-422 002, (MS), India for providing the research facilities.

REFERENCES:

1 Clark J., Shahhet M. Korakas D., Varvounis G., 1193. Synthesis of thieno[2,3-D] pyrimidines from 4,6-Dichloropyrimidine-5-carbaldehydes. Heterocyclic Chem., 30, 1065-1072.

2 Ogowva K., Yamawaki I., Matsusita Y., Nomura N., Kador P., Kinoshita J., 1993. Syntheses of substituted 2,4-dioxo-thienopyrimidin-1-acetic acids and their evaluation as aldose reductase inhibitors. Eur. J Med Chem., 28, 769-781.

3 Tozkoparan B., Ertan M., Kelicen P., Demirdar R., 1999. Synthesis and anti-inflammatory

activities of some thiazolo[3,2-a]pyrimidine derivatives. Farmaco, 54, 588-593.

4 Jacob S., Rosenbanm E., Wood D., 1971. Dimethyl Sulphoxide, Marcel Dukker, New York.

5 Lal J., 1995. Exess partial molar enthalpies, entropies, Gibbs energies and volumes in aqueous dimethyl sulphoxide. J. Sol. Chem., 24(1), 89–102.

6 Scaduto R., 1995. Oxidation of DMSO and methanesulfinic acid by hydroxyl radical Free Radical. Biol. Med., 18(2), 271–277.

7 Muhammad J, Chaudhry M., 2009. Thermodynamic study of three pharmacologically significant drugs: density, viscosity and refractive index measurements at different temperatures. J. Chem. Therm., 41, 221-226.

8 Kambe S., Satio K., Kishi H., 1979. A one step synthesis of 4-oxo-2-thioxopyrimidine derivatives by the ternary Condensation of ethyl cyanoacetate, aldehydes and thiourea. Synthesis, 287-289.

9 Patel A., Pasha T., Modi A., 2015. Synthesis and biological evaluation of 4-aryl substituted -2-(5-carboxylicacid-1, 6-dihydro)-2-thiophenylethylene-6-oxo-Pyrimidine as protein tyrosine phosphatase PTP-1B) inhibitors. Inter. J. Phar Tech Res, 8, 136-143.

10 Murthy Y., Saveri L., Parimi A., Naresh S., 2013. $Mg(OMe)_2$ as a versatile catalyst for one po synthesis of 6-aryl-5-cyano-2-(oxo/thio) uracil derivatives and their antimicrobial evaluations. Org Commun., 6(1), 47-54.

11 Das M., Das S. Patnaik A., 2013. Molecular interionic interaction studies of benzimidazolium dichromate and 2 methyl imidazolium dichromate in water and DMSO + Water at different temperatures. J. Phy. Sci., 24(1), 37-50.

12 Sumathi T., Varalakshmi M., 2010. Ultrasonic velocity, density and viscosity measurement of methionine in aqueous Electrolytic solutions at 303k. Rasayan. J. Chem., 3(3), 550-555.

13 Sikarwar S., . Chourey V., Ansari A., 2015. Apparent molar volume and Viscometric study of alcohols in aqueous solution. Inter. J. Chem. Phy. Sci., 4(1), 115-120.

14 Das M., Pradhan S., Das S. Patnaik A., 2015. Density, viscosity and excess parameters of nicotinium dichromate in protic and aprotic solvent media. Der Pharma Chemica., 7(2), 315–322.

15 Chauhan S., Syal V., Chauhan M., Sharma P., 2007. Viscosity studies of some narcotic analgesic drugs in aqueous-alcoholic mixtures at 25ºC. J. Mol. Liqs., 136, 161-164

16 Jones G., Dole M., 1929. The viscosity of aqueous solutions of strong electrolytes with special reference to Barium Chloride. J. Am. Chem. Soc., 51, 2950-2964.

International Journal of Engineering Research and General Science Volume 5, Issue 4, July-August, 2017
ISSN 2091-2730

Investigation on Membrane Cured Geopolymer Concrete- Review

Pradeep D. Chimane[1], Dr. Sandeep L. Hake [1], Mohan N. Shirsath [2]

[1]PG Student, Depatment of Civil Engineering,
G.H. Raisoni College of Engineering & Management, Chas, Ahmednagar, Maharashtra, India
[1,2]Assistant Professor, Depatment of Civil Engineering,
G.H. Raisoni College of Engineering & Management ,Chas, Ahmednagar, Maharashtra, India

Abstract- Cement concrete is widely used material in civil engineering construction. However emission of carbon dioxide during the production of cement is hampering the image of concrete as a sustainable material. Therefore efforts are being made to reduce the consumptions of cement by using cementitious material such as fly ash as a partial replacement. Large amount of fly ash produced in thermal power station is creating environmental pollution, if not disposed properly. Geopolymer concrete is a new development in concrete technology in which cementitious material, rich in silica and alumina, is activated using alkaline solution.

In this report the investigation is carried to check the various parameters of geopolymer concrete. For this research work M30 grade of geopolymer concrete is designed. Sodium silicate and sodium hydroxide was used as alkaline liquid with the ratio of 2.5. Fly ash to solution ratio is 0.35. For each test three cubes, cylinders or beams were casted as per requirement of test procedure. All these specimens are wraped with plastic bag for curing in an oven for different temperature for analyzing effect of membrane. These cubes were examine by the membrane cured for the polymerisation. Due to membrane cured the moisture losses were entrapped.

Keywords- Geopolymer Concrete, Fly Ash, Membrane Cured, Alkaline solution.

INTRODUCTION

Cement industries releases CO2 in the atmosphere, which is one of cause of global warming. Also, in Most of the fly ash is disposed of as a waste material that coves several hectors of valuable land. So, efforts are needed to make concrete more environmental friendly by using fly ash which helps in reduce global warming as well as fly ash disposal problem. (Satpute Manesh B,2012). Thermal Power Plant are the two major issues concern with the environmental pollution and human health. Both these issue can be solve partially by utilizing fly ash in concrete by partial or full replacement of cement. Geopolymer concrete is a new cementitious material which is produced by chemically activation of fly ash with highly alkaline solutions like sodium hydroxide and sodium silicate. Subhash V. Patankar,et al. (2012).

We conducted study on the effects of sodium hydroxide concentration on the compressive strength of fly ash-based geo-polymer mortar. The authors have reported that alkaline concentration was proportionate to the compressive strength of geo-polymer mortar. They have claimed that higher concentration of sodium hydroxide solution result in a higher compressive strength of geo-polymer mortar. Hong ling Wang in their study on synthesis and mechanical properties of meta kaolinite-based geo-polymer have reported that higher concentration of sodium hydroxide solution provides better dissolving ability to meta kaolinite and produces more reactive bond for the monomer, consequently increase inter-molecular bonding strength of the geo-polymer. They have revealed that mechanical properties of the meta kaolinite-based geo-polymer activating meta kaolinite with sodium hydroxide and sodium silicate solution were greatly dependent on the concentration of sodium hydroxide solution. With the increase of sodium hydroxide concentration, the compressive strength, flexural strength and apparent density of the resulting geo-polymer were increased.

LITERATURE REVIEW

S. S. Jamkar et al [1] have highlighted on the effect of fly ash fineness on the compressive strength of geopolymer concrete. The specimens were cured in an oven for 4, 8, 12, 16, 20 and 24 hours at 90°C. The compressive strength results show that the fly ash fineness plays a vital role in the activation of geopolymer concrete. An increase in the fineness increased both workability and compressive strength. It was also observed that finer particles resulted in increasing the rate of reaction needing less heating time to achieve a given strength..

Subhash Patankar et.al [2] recommended that effect of concentration of sodium hydroxide, temperature, duration of heating, and test period on the development of geopolymer mortar. It is observed that the workability as well as compressive strength of geopolymer mortar increases with increase in concentration of sodium hydroxide solution in terms of molarity. It is also observed that the compressive strength of geopolymer concrete increases with increase in test period up to three days. The suitable preparation of geopolymer mortar, 13-molar solution of sodium hydroxide is recommended on the basis of workability and compressive strength.

Prakash R. Vora et.al [3], have described the experimental work conducted by casting 20 geopolymer concrete mixes to evaluate the effect of various parameters affecting its the compressive strength in order to enhance its overall performance. Various parameters i.e. ratio of alkaline liquid to fly ash, concentration of sodium hydroxide, ratio of sodium silicate to sodium hydroxide, curing time, curing temperature, dosage of super plasticiser, rest period and additional water content in the mix have been investigated. The test results show that compressive strength increases with increase in the curing time, curing temperature, rest period, concentration of sodium hydroxide solution and decreases with increase in the ratio of water to geopolymer solids by mass & admixture dosage, respectively. The addition of naphthalene based superplasticiser improves the workability of fresh geopolymer concrete. It was further observed that the water content in the geopolymer concrete mix plays significant role in achieving the desired compressive strength.

Satpute Manesh B et.al[4] have studied of effect of duration and temperature curing on compressive strength of geopolymer concrete. Geopolymer concrete is manufactured by cement fully replacing with processed fly ash which is activated by alkaline solutions like Na2Sio3 and NaoH. Cubes of size 150mm X 150mm X 150mm were made at solution to fly ash ratio of 0.35 with 16 Mole concentrated sodium hydroxide solution. The specimens were cured in oven at 60°C, 90°C and 120°C for 6, 12, 16, 20 and 24 hour's duration. Test results show that the compressive strength increases with increase in duration and temperature of oven curing up to 24 hrs.

Subhash Patankar et.al [5] studied that the flow of geopolymer concrete increases with increase in water-to-geopolymer binder ratio after changing the quantity of water. Geopolymer concrete becomes more viscous with decrease in water-to-geopolymer binder ratios because of the less quantity of water in the mixture. The compressive strength of geopolymer concrete is inversely proportional to the water-to-geopolymer binder ratio. Suitable range of this binder ratio is in the range of 0.25 to 0.35.

Sandeep Hake, et al [6], the oven heat curing of geopolymer concrete has been attempted by various researchers, but for curing of geopolymer concrete is quite difficult on site by using oven, so there is scope on types of curing which makes geopolymer concrete cure easily. The oven heat curing for geopolymer concrete is mostly used. The researchers studied only for different curing temperature in oven curing, but only few of them work on steam, membrane curing and no one work on accelerated curing, as well as comparison on steam, accelerated, membrane, natural and oven curing. So there is scope on method of curing of geopolymer concrete. Also researchers studied for different curing time like 6,12,18,24 and the optimum strength obtained at 18 Hrs of Curing. The different curing temperatures like 60°C, 90°C, 120°C and 150°C. The different type of curing like Oven, Accelerated, Membrane and Steam curing are need to be Study. The effect on compressive strength of Geopolymer concrete by using these parameter need to be study.

Davidovits introduced the term geopolymer in 1978 to represent the mineral polymers resulting from geochemistry [7]. Geopolymer are a class of inorganic polymer formed by the reaction between the alkaline solution, silica and alumina present in source material. The hardened material has an amorphous 3-dimensional structure similar to that of an alumino silicate glass. However unlike a glass these materials are formed at low temperature and as a result can incorporate an aggregate skeleton and a reinforcing system if required, during the forming process. The most common activator is a mixture of water, sodium hydroxide and sodium silicate but other alkali metal systems or mixtures of different alkalis can be used.

Djwantoro Hardjito and etal. [8] studied the influence of curing temperature, curing time and alkaline solution-to-fly ash ratio on the compressive strength. It was reported that both the curing temperature and the curing time influenced the compressive strength. The authors confirmed that the temperature and curing time significantly improves the compressive strength, although the increase in strength may not be significant for curing at more than 60°C. In addition, the compressive strength decreases when the water-to-geopolymer solids ratio by mass increased. The drying shrinkage strains of fly ash based geopolymer concretes were found to be significant.

Subhash V. Patankar et al. [9] studied the effect of quantity of water, temperature duration of heating on compressive strength of fly ash based geopolymer concrete. Na2Sio3 solution containing Na2O of 16.45%, SiO2 of 34.35% and H2O of 49.20% and sodium hydroxide solution with concentration of 13 Molar were used in geopolymer concrete as alkaline activators. Geopolymer concrete mixes were prepared with 0.35 solutions to processed fly ash ratio. Workability was measure by flow table apparatus. Geopolymer concrete cubes of 150 mm X 150 mm X 150 mm were cast. The temperature of curing was varied as 40°C, 60°C, 90°C, and 120°C for each period of 8, 12 and 24 hours of oven heating and tested after a rest period of 1,2,3,7and 28 days after demoulding the concrete cube. Test results show that the quantity of water plays important role in balancing workability but not effect on strength. While higher temperature requires less duration of heating to achieve desired strength and vice versa. Author says that the rest period of 3 days is sufficient after heating at and above 90°C temperature.

V.M. Malhotra [10] uses the fly ash in 1930 as a workability-improving admixture. Later on its application increases as people are aware about pozzolanic reactivity of fly ash. It is used in the manufacture of Portland Pozzolana Cement (P.P.C.), partial replacement of cement and workability-improving admixture in concrete. But its utilization is limited to 20% throughout the world.

An important achievement in this regard is the development of high volume fly ash (HVFA) concrete that utilizes up to 60 percent of fly ash, and yet possesses excellent mechanical properties with enhanced durability performance.

Prabir K. Sarker et al (2013) geopolymer as an alternative binder can help reduce CO2 emission of concrete. The binder of geopolymer concrete (GPC) is different from that of ordinary Portland cement (OPC) concrete. Thus, it is necessary to study the effects of the geopolymer binder on the behavior of concrete. In this study, the effect of the geopolymer binder on fracture characteristics of concrete has been investigated by three point bending test of RILEM TC 50 – FMC type notched beam specimens. The peak load was generally higher in the GPC specimens than the OPC concrete specimens of similar compressive strength. The failure modes of the GPC specimens were found to be more brittle with relatively smooth fracture planes as compared to the OPC concrete specimens. The post-peak parts of the load–detection curves of GPC specimens were steeper than that of OPC concrete specimens. Fracture energy calculated by the work of fracture method was found to be similar in both types of concrete.

Vaibhav A. Kalmegh, et al. [12] shows Cement is the important material for the constructions. But, ordinary Portland cement concrete structure emits large amounts of carbon dioxide, which results the global warming. Global warming is a big challenge for earth. Portland cement industry is one of the largest producers of carbon dioxide. The production of one ton of Portland clinker produces approximately one ton of carbon dioxide. A need of present status is to find alternative binder system to make concrete. On the other scenario huge quantity of fly ash generated around the globe from thermal power plants and generally used as a filler material in low level areas. The main constituent of geo-polymer concrete is fly ash and alkaline solutions. Fly ash is the main by product created from thecombustion of coal in coal-fired power plants. Geo-polymer is an inorganic alumina-Hydroxide polymer synthesized from predominantly silicon (Si) and aluminum (Al) materials of geological origin or byproduct materials such as fly ash. Geo-polymer is a type of alumino-hydroxide product having ideal properties of rock-forming elements. The main advantage of geo-polymer concrete is that it is eco-friendly.

CONCLUSION

In this research review paper, membrane curing of geopolymer concrete is discussed in brief. Oven heat curing of geopolymer concrete has been attempted by various researchers. But for curing of geopolymer concrete is quite difficult on site by using oven, so there is scope to work on types of curing which makes geopolymer concrete cure easily. Most of researcher used only oven heat curing for geopolymer concrete. For the polymerization the heat is required to the geopolymer concrete .They studied only for different curing temperature in oven curing, but only few researcher work on membrane, so there is scope on method of curing of geopolymer concrete. So there is scope to study the mechanical properties like short term as well as long term property of geopolymer concrete. Also researchers studied for different curing time like 6,12,18,24 hours and also for different curing temperature but few researchers worked on different rest period, so there is scope for work.

REFERENCES

1. Subhash v. Patankar, Sanjay s. Jamkar, Yuwaraj m. Ghugal, “Effect of fly ash fineness on workability and compressive strength of geopolymer concrete” The Indian Concrete Journal, April 2013.
2. Subhash V. Patankar, Yuwaraj M. Ghugaland Sanjay S.Jamkar, “Effect of Concentration of Sodium Hydroxide and Degree of Heat Curing on Fly Ash-Based Geopolymer Mortar” Hindawi Publishing Corporation Indian Journal of Materials Science, Volume 2014.
3. Prakash R. Vora, Urmil V. Dave, “Parametric Studies on Compressive Strength of Geopolymer Concrete”, Procedia Engineering 51 (2013) 210 – 219, Published by Elsevier Ltd.
4. Satpute Manesh B., Wakchaure Madhukar R., Patankar Subhash V. “Effect of Duration and Temperature of Curing on Compressive Strength of Geopolymer Concrete” International Journal of Engineering and Innovative Technology (IJEIT) Volume 1, Issue 5, May 2012.
5. Subhash V. Patankar, Sanjay S. Jamkar, Yuwaraj M.Ghugal, “Effect of Water-to-Geopolymer Binder Ratio on the Production of Fly ash Based Geopolymer Concrete” International Conference on Recent Trends in engineering & Technology - 2013(ICRTET' 2013).
6. Sandeep L. Hake, Dr R. M. Damgir, Dr S.V. Patankar “State of Art- Investigation of method of curing on geopolymer concrete” IOSR Journal of Mechanical and Civil Engineering (IOSR-JMCE), Volume 12, Issue 3 Ver. I (May. - Jun. 2015).
7. Djwantoro Hardjito, Steenie E. Wallah, D. M. J. Sumjouw and B.V. Rangan, “Properties of Geopolymer Concrete with Fly Ash as Source Material: Effect of Mixture Composition”, Seventh CANMET/ACI International Conference on Recent Advances in Concrete Technology, Las Vegas, USA, 26-29 May, 2004.
8. Djwantoro Hardjito, Steenie E. Wallah, D. M. J. Sumjouw and B.V. Rangan, “Fly ash-Based Geopolymer Concrete, Construction Material for Sustainable Development”, Invited paper, Concrete World: Engineering and Materials, American Concrete Institute, India Chapter, Mumbai, India, 9-12 December 2004

9. Subhash V. Patankar, Yuwaraj M. Ghugal, Sanjay S. Jamkar "Selection of Suitable Quantity of Water, Degree and Duration of Heat Curing for Geopolymer Concrete Production" Proceedings of 3rd International Conference on Recent Trends in Engineering & Technology (ICRTET'2014).
10. Sandeep L. Hake, Dr R. M. Damgir," Effect of lime added fly ash based Geopolymer Concrete" International Journal of Engineering Education and Technology, ISSN 2320-8821, Volume 5, Issue 1, Jan-2017.
11. N. N. Jain ,Sandeep L. Hake, M. N. Shirsath, "Geopolymer concrete with lime addition at normal room temperature" International Journal of Research Publication in Engineering and Technology (IJRPET), ISSN 2454-7875, Volume-2, Issue-8, August 2016, PP 13-16.
12. V. V. Yewale ,Sandeep L. Hake, M. N. Shirsath, "Effect on geopolymer concrete for different types of Curing Method" International Journal of Research Publication in Engineering and Technology (IJRPET), ISSN 2454-7875, Volume-2, Issue-8, August 2016, PP 17-20.
13. S. S. Satpute , M. N. Shirsath, Sandeep L. Hake, "Investigation of Alkaline Activators for fly ash based geopolymer concrete" International Journal of Advance Research and innovative Ideas in Education (IJARIIE), ISSN 2395-4396, Volume-2, Issue-5, 2016, PP 22-28.
14. N. N. Jain , M. N. Shirsath, Sandeep L. Hake, "Percentage Replacement of Cement in Geopolymer Concrete" International Journal of New Technologies in Science and Engineering, ISSN 2349-0780, Volume-3, Issue- 8, August 2016, PP 6-9.
15. V. V. Yewale , M. N. Shirsath, Sandeep L. Hake, "Evaluation of Efficient Type of Curing for Geopolymer Concrete" International Journal of New Technologies in Science and Engineering, ISSN 2349-0780, Volume-3, Issue- 8, August 2016, PP 10-14.

International Journal of Engineering Research and General Science Volume 5, Issue 4, July-August, 2017
ISSN 2091-2730

Effect of Infill Walls in Performance of Reinforced Concrete Building Structures

Prakash Paudel

MTech Structural Engineering, Graphic Era University, Dehradun, India

Paudel257@gmail.com

Abstract: In open ground story buildings, sudden change of stiffness takes place along the building height which makes the story more flexible than the adjacent story. Hence columns and beams in those storeys got heavily stressed. Presence of infill walls in the frame alters the behavior of the building under lateral loads. However, it is a common industry practice to ignore the stiffness of infill wall for analysis of framed building. Engineers believe that analysis without considering infill stiffness leads to a conservative design. But this may not be always true, especially for vertically irregular buildings with discontinuous infill walls. Hence, the modelling of infill walls in the seismic analysis of framed buildings is imperative. Indian Standard IS 1893: 2002 allows analysis of open ground story buildings without considering infill stiffness but with a multiplication factor 2.5 in compensation for the stiffness discontinuity. However, as experienced by the engineers at design offices, the multiplication factor of 2.5 is not realistic for low rise buildings. This calls for an assessment and review of the code recommended multiplication factor for low rise open ground story buildings.

Keywords- Stiffness, Story, infill, multiplication factor, Strut, Drift, Ductility, Model

INTRODUCTION

The building in which the ground story consists of open space is known as stilt building or soft story building. That open story is called as stilt Floor or Soft-Story and such space is used for recreational use such as parking or for retail and commercial purpose. In these buildings, sudden change of stiffness takes place along the building height which makes the story more flexible than the adjacent story. In other words, story of which significant reduction of stiffness is observed is known as soft story. Hence columns and beams in those storeys got heavily stressed. Therefore, it is required that the ground story columns must have sufficient strength and adequate ductility. These types of buildings are commonly used in the urban area nowadays since they provide parking area which is most required. Performance of these buildings is found to be poor in the recent earthquakes. Under earthquake load their deformations are greater than other floors so design of these stories should be different from upper storeys. Soft story can be existing at any story level but generally exist at the ground story. major type of failures that occurred during past earthquake in soft story building are snapping of lateral ties, crushing of core concrete, buckling of longitudinal reinforcement bars etc. As per IS-1893:2002 (part I), A Soft Story is one in which the lateral stiffness is less than 70 percent of that in the story above or less than 80 percent of the average lateral stiffness of the three storeys above. An extreme soft story is one in which the lateral stiffness is less than 60 percent of that in the story above or less than70 percent of the average stiffness of the three storeys above. After the Bhuj earthquake, the IS 1893 code was revised in 2002, incorporating new design recommendations for soft story buildings. Clause 7.10.3(a) states: "The columns and beams of the soft story are to be designed for 2.5 times the story shears and moments calculated under seismic loads of bare frames." The factor 2.5 is a multiplication factor (MF). This multiplication factor (MF) is used in the compensation for the stiffness discontinuity.

An appropriate way to analyze the soft story buildings is to model the infill walls. But due to lack of guidelines in IS 1893: 2002 (Part-1) for modeling the infill walls it is difficult to model. Alternatively, bare frame analysis is widely used that ignores the strength and stiffness of the infill walls. Since we are dealing with lateral loading, ductility of the structural members should be considered such that structure can sustain lateral load by its ductile behavior. structures are designed on the basis of strength and serviceability criteria. The strength is related to ultimate limit state, which assures that the forces developed in the structure remain in elastic range. The serviceability limit state stiffness is related to stiffness which assures that the structural displacements remains within the permissible limits.

In case of lateral forces the demand is for ductility. Ductility is an essential attribute of a structure that must respond to strong ground motions. Ductility is the ability of the structure to undergo distortion or deformation without damage or failure which results in dissipation of energy. Larger is the capacity of the structure to deform plastically without collapse, more is the resulting ductility and the energy dissipation. This causes reduction in effective forces. The seismic force generated at each floor levels are transferred through the various structural members to the ground. The building components need to be made ductile. The failure of a column can affect the stability of the whole building, but the failure of a beam causes localized effect. Therefore, strong column weak beam combination is desirable. In soft

story buildings, energy developed during earthquake is transferred through columns which are of reduced stiffness due to lack of infill walls. The bare frame is much less stiff than a fully infilled frame; it resists the applied lateral load through frame action and shows well-distributed plastic hinges at failure condition.

MODELLING

Beams and columns in this study are modelled by using 3D frame element by creating rectangular cross section in SAP2000. The floor slabs were assumed to act as diaphragms, which ensure integral action of all the vertical lateral load-resisting elements. Building is considered to be in isolated foundation. Column ends are fixed at the top of the isolated foundation. Three different models are used to study the effect of infill wall in RC framed building structure. First is without infills, another with open ground story and third is completely infilled. Infill walls are modelled by using diagonal struts pinned at the both ends. As self-weight of wall is considered already in the model, density of the strut material is taken as 0.so diagonal struts are modelled to provide stiffness only.

The geometric properties are of effective width and thickness of the strut. The thickness and material properties of strut are similar to the infill wall. many investigators have proposed various approximations for the width of equivalent diagonal strut. Originally proposed by polyakov and subsequently developed by many investigators, the width of strut depends on the length of contact between the walls and columns,α_h, and between the wall and beams , α_l.The proposed range of contact length is between one forth and one tenth of the length of the panel. Stafford Smith developed the formulations for α_h and α_l on the basis of beam on an elastic foundation. The following equations are proposed to determine $\alpha_h$and α_l,which depends on the relative stiffness of the frame and infill, and on the geometry of the panel.

$$\alpha_h = \frac{\pi}{2}\sqrt[4]{\frac{4E_f I_c h}{E_m t sin2\theta}}$$

$$\alpha_l = \pi\sqrt[4]{\frac{4E_f I_b h}{E_m t sin2\theta}}$$

Where,

E_m and E_f = Elastic modulus of the masonry wall and frame material, respectively

t, h, L = Thickness, height and length of the infill wall, respectively

I_c, I_b = moment of inertia of the column and the beam of the frame, respectively

$\theta = \tan^{-1}\frac{h}{L}$

Hendry has proposed the following equation to determine the equivalent strut width w, where the strut is assumed to be subjected to uniform compressive stress

$$W=\frac{1}{2}\sqrt{\alpha_h{}^2 + \alpha_l{}^2}$$

Holmes recommended a width of the diagonal strut equal to one third of the diagonal length of the panel, whereas New Zealand Code (NZS 4230) specifies a width equal to one quarter of its length.

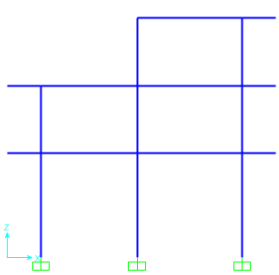

Figure 1. Model 1.

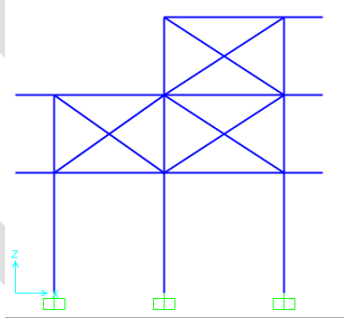

Figure 2. Model 2.

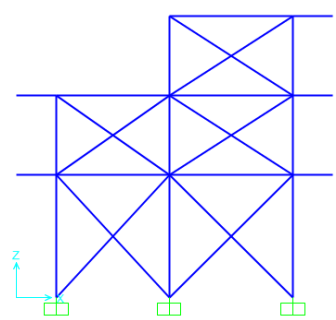

Figure 3. Model 3.

LOADING AND ANALYSIS

Nominal dead load and live loads are provided as static loads. Equivalent lateral load method is used to apply seismic loads in both the directions. Analysis of the three different models is carried out by using SAP2000 software.

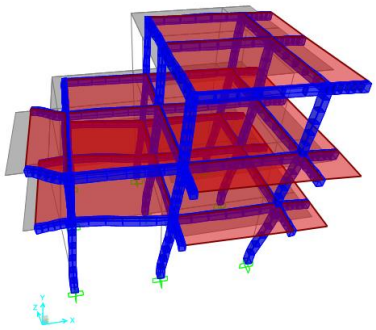

Figure 4. Deflected shape of model 2 building after analysis

4. Results

Time period is maximum in first model, decreases slightly in the second model which then decreases drastically in the third model. Reduction in time period means increase in earthquake response. So, structure should be designed for that increased earthquake force.

Table 1. Comparison of time periods of three models.

Modes	Model 1 (sec)	Model 2 (sec)	Model 3 (sec)
1st	0.885119	0.763663	0.088502
2nd	0.809937	0.701948	0.076088
3rd	0.670112	0.596686	0.067101
4th	0.271312	0.074745	0.059711
5th	0.248055	0.066062	0.058058
6th	0.208171	0.064401	0.056126
7th	0.171019	0.060411	0.053035
8th	0.160291	0.059215	0.05267
9th	0.153167	0.053573	0.051351
10th	0.075578	0.052887	0.050584
11th	0.069347	0.05249	0.049208
12th	0.061464	0.050801	0.048532

Story drift decreases as amount of infill increases in the building. We can also see that ground story drift in 2nd model is larger, it is because upper storeys with higher stiffness causes the ground story to be flexible one so that its displacement is larger than that of the upper storeys. Also drifts in ground floor of 3rd models are negligible due to increased stiffness by the infill walls.

Table 2. Drifts along x direction

Story	Model 1 (mm)	Model 2 (mm)	Model 3 (mm)
1st story	2.1	2.2	0.0486
2nd story	1.68	0.109	0.039
3rd story	0.99	0.1	0.073

Table 3. Drifts along Y direction

Story	Model 1 (mm)	Model 2 (mm)	Model 3 (mm)
1st story	2.13	3.22	0.014
2nd story	1.66	0.036	0.036
3rd story	0.7	0.062	0.058

Comparing the element forces, it is found that there is no significant change in moments in beams but every column of the infilled model is subjected to larger moments than that of the previous analysis. So, some modification should be applied for the moments obtained from the model without infills in the design procedure.

5. Conclusion

Analysis result shows that Column forces at the ground story increases for the presence of infills in upper storeys, but design load multiplication factor 2.5 is found to be much higher, it is actually found to be 1.15. Not significant change in beam forces of the first-floor beams was obtained after the consideration of infills too. Time periods decreases with the increase of amount of infill in the buildings (highest for without infills and lowest for the fully infilled case). This results in the attraction of more earthquake force for the lower time periods. Story drift is found to be lowest for fully infilled and highest for without infills but drift of first story is highest for the building with infills above ground floor (i.e. open ground story).

REFERENCES:

[1] Agarwal P. and Shrikhande M, “Earthquake resistant design of structures”, PHI Learning Pvt. Ltd., New Delhi, 2006.

[2] Chopra A. K, Earthquake resistance of buildings with a soft first story. “Earthquake and Structural Dynamics”, 1. 347-355, 1973.

[3] Das S, “Seismic design of vertically irregular reinforced concrete structures”. Ph.D. Thesis. North Carolina State University. Raleigh. NC, 2000.

[4] Deodhar S. V. and A. N. Patel, “Ultimate strength of masonry infilled steel frames under horizontal load”. Journal of Structural Engineering. Structural Engineering Research Centre, 24. 237, 1998.

[5] Dhansekar M. and A.W. Page “The influence of brick masonry infill properties on the behavior of infilled frames”. Proceedings of Institution of Civil Engineers, Part 2. 81. 593-605,1986.

[6] Dolsek M and P. Fajfar, “Soft story effects in uniformly infilled reinforced concrete frames”. Journal of Earthquake Engineering, 5(1). 1-12, 2001.

[7] Holmes M. “Steel frames with brick and concrete infilling”. Proceedings of Institution of Civil Engineers, 19. 473-478, 1961.

[8] I.S 13920, “Ductile Detailing of Reinforced Concrete Structures Subjected to Seismic Forces-Code of Practice”, Bureau of Indian Standards, 1993.

[9] Mehrabi A. B.; P. B. Shing; M. P. Schuller and J. L. Noland “Experimental evaluation of masonry – infilled RC frames”. ASCE Journal of Structural Engineering, 122. 228-237,1996.

[10] Murthy C.V.R. and S.K. Jain. “Beneficial influence of masonry infill on Seismic performance of RC frames buildings”. Proceedings of 12th World Conference on Earthquake Engineering, New Zealand, Paper No. 1790, 2000.

[11] Rahman, S. S. Influence of openings on the behavior of infilled frames. Ph. D. Thesis. Indian Institute of Technology Madras. Chennai, 1988.

[12] Sattar S and Abbie B. L “Seismic Performance of Reinforced Concrete Frame Structures with and without Masonry Infill Walls”, 9th U.S. National and 10th Canadian Conference on Earthquake Engineering, Toronto, Canada, July 2010.

International Journal of Engineering Research and General Science Volume 5, Issue 4, July-August, 2017
ISSN 2091-2730

CASE STUDY ON WHITE BOARD DUSTER

Ashiq Mohamed M,

Student of SASTRA University,

Tirumalaisamudram,Thanjavur- 613401,

E mail: ashiqtaheer@gmail.com

Abstract- This case study is related to a white board duster (also called as marker board duster). In this case study, the usage of the existing white board duster and its pros and cons were studied and its design was analyzed. Then the better design that could overcome the limitations of the existing duster was prepared, analyzed and validated theoretically. Then the redesigned duster was fabricated by rapid prototyping process and tested manually. The material of both the existing duster and the redesigned duster was acrylonitrile butadiene styrene (ABS) and the software used for analysis was CATIA V5.

Keywords-White board duster, Impressions, Principal stress, Displacement, Von mises stress, Paint thinner or Water, Ultimate tensile strength, Maximum principal stress theory, 3 D printing.

INTRODUCTION-

In today's scenario though the science and technologies are updated, the use of marker boards in educational institutions, offices and in various other places are unavoidable. Though the automatic board erasing robots have been already developed, their installation and maintenance are uneconomical in certain places like government schools, public notice boards etc. In such cases, it is necessary to use manual duster for erasing purpose. In this case study one of the major problems of this duster was studied and the solution is depicted.

CASE PRESENTATION-

The actual existing white board dusters are shown below. Some organization even uses the black board duster for erasing the marker board.

(*Figure 1)*

(Figure 2)

Here the Omega manufacturer's duster (Figure1) is taken as a reference. Usually these duster is of plastic material (preferably ABS) which would cost about INR 35 to INR 50. Inevitably these duster are integrated with foam material for the ease of erasing. The foam employed is of hard type which has high resistance to water absorption compared with soft foam.

Apart from this certain marker board duster have pocket on its top surface in order to hold the marker. These are the secondary functions of the duster whereas, the primary intended function is to erase the impressions on the board. Below table shows the function analysis of the existing marker board duster as similar to the function analysis of the application taken from the reference paper [1].

PART NAME	QUANTITY	FUNCTION		PART	
		VERB	NOUN	PRIMARY	SECONDARY
Gripper (plastic)	1	Provide	Grip	X	
		Hold	Marker pen		X
Sponge (Hard foam)	1	Erase	Impressions	X	

(Table 1: Function analysis of marker board duster)

For the purpose of case study, the duster that incorporates only the primary function is considered.

METHODOLOGY-

The methodology behind analyzing the duster is that, the type and nature of the material of the duster is noted initially. Then the properties of the material are taken from standard books. Then the type of load that act on the duster upon erasing action is identified and its magnitude is approximated. Then the duster is designed and analyzed from the obtained datum. Depending upon the nature (ductile or brittle) of the material, the appropriate theory of failure is selected and the results obtained from the analysis are cross-checked according to the selected theory of failure in order to prove for a safer design.

DISCUSSION-

The main advantage of using these manual duster for erasing purpose is that, they are economical, portable and there is no maintenance cost. They are reliable maximum up to the period of 6 months. But there are also certain limitations such as they have to be replaced frequently once in 6 months, and could not effectively erase the impressions on the white board after 3 days. In such cases, additional liquid substance like paint thinner or water is applied on the board and then they are erased off.

The reference plastic duster (ABS material) is approximated to design by Reverse Engineering process in CATIA V5. Reverse Engineering is a very important tool and this technique has been widely recognized as an important step toward developing improved products as well as reducing time and costs in order to achieve profitable production of the new product [2].

After the design is made the static analysis is performed on the design, which predicts the maximum normal stress that could be withstand by the duster, von mises stress and the deflection of the duster under loading condition. Usually the type of load, that acts upon the duster while erasing off the impressions on the board, is of shear type loading. The overall dimension of the duster (only plastic part) exist up to 10x3x3 cm with hallow surface on its top (as shown in figure 1) and the shear force of 1N is assumed to act upon the duster while erasing relatively with the board. The properties of the ABS material are given in the table below.

PROPERTY	VALUE
Technical Name	Acrylonitrile Butadiene Styrene
Softening Temperature	128 °C
Tensile Strength	55.2 MPa
Yield Strength	51 MPa
Specific Gravity	1.06
Typical Injection Moulding Temperature	204 – 238 °C
Shrink Rate	0.5 – 0.7 %

(Table 2: Material properties)

ABS resins are thermoplastic resins composed of three kinds of monomers- acrylonitrile, butadiene, and styrene[3]. The design is analyzed and the principal stress induced in the duster is shown below in figure 3. The principal stress that could be withstand by the duster is 2763.48 N/m^2 and it is constant irrespective of the magnitude of the load.

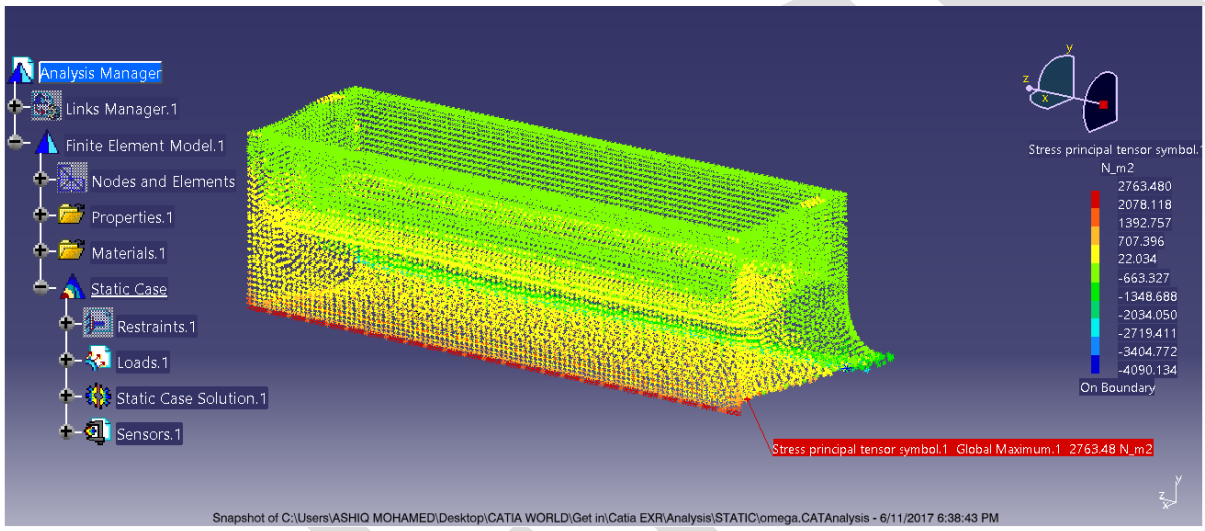

(Figure 3 : Principal stress)

From the table (2), it could be noted that the softening temperature is 128 °C [4], up to which the ABS material will behave as a brittle material. The appropriate theory of failure for brittle material is maximum principal stress theory which states that the material fails, when the principal stress induced in a material under complex loading condition exceeds the ultimate tensile strength of the material [5,6]. The obtained value of principal stress is lesser than ultimate tensile stress of the ABS material which is 55.2 Mpa (i.e. 5.5 x 10^7 N/m^2). So the design is safe according to maximum principal stress theory.

The maximum displacement of the duster, shown in figure 4, when acted upon by a force of 1N, under constrained condition is found to be 0.00000294 mm which is negligible. And the von mises stress due to the application of load is found to be 2481.14 N/m^2 which is shown in the figure 5. Since ABS is a brittle material, it is sufficient to validate only the maximum principal stress theory in order to prove for a safe design.

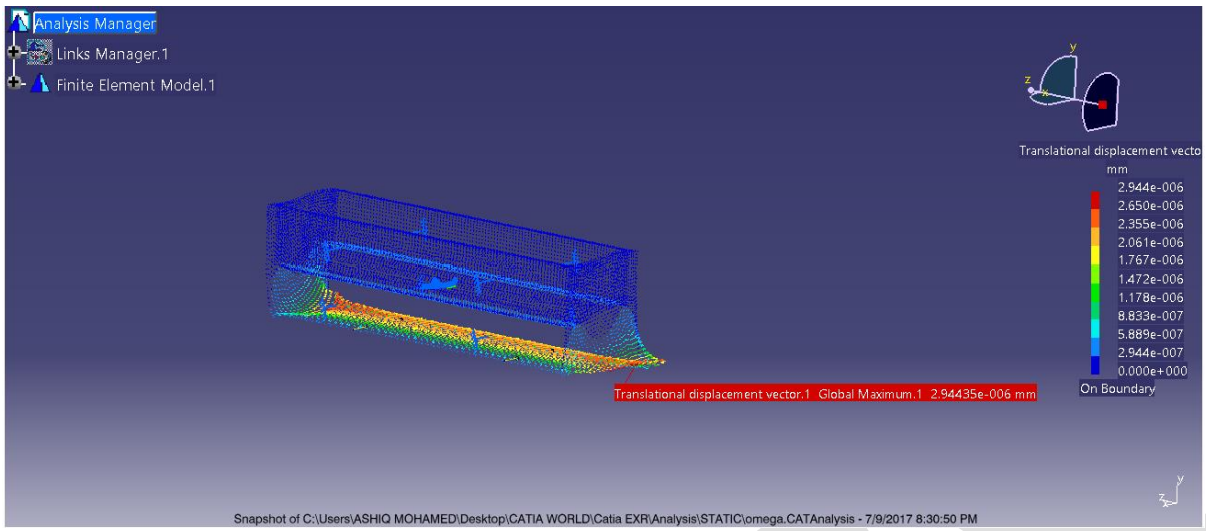

(Figure 4 : Displacement)

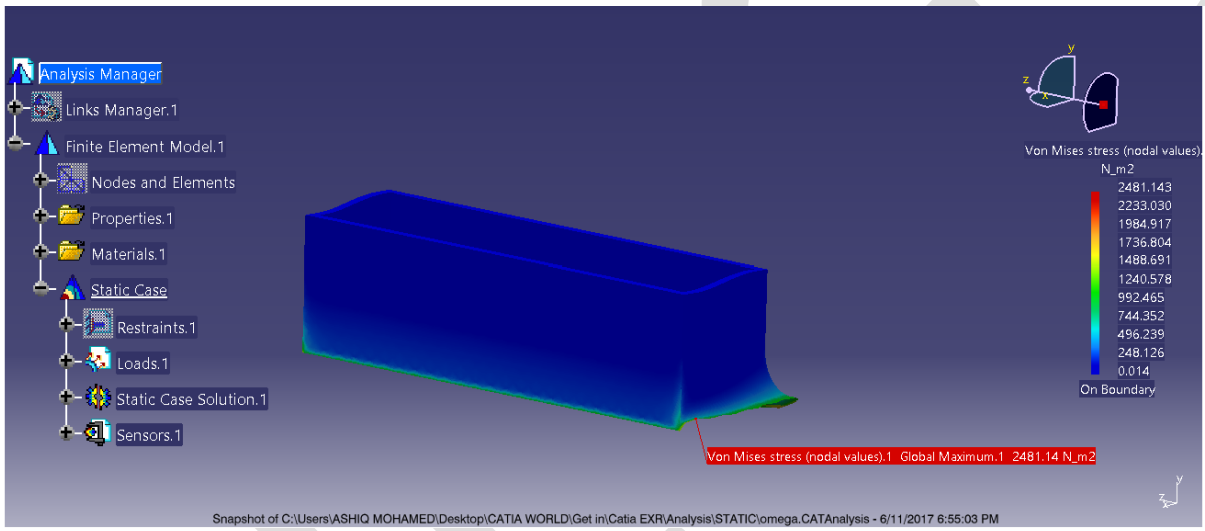

(Figure 5 : Von mises stress)

After such analysis, the modified design which could overcome the limitation of the existing duster is made and its drafting diagram is shown in figure 6. The final step of designing a part or assembly is communicating it in a medium other than the computer monitor's display. For some operations this means plotting out design drawings [7,8].

The dimensional details of the main body is given below in figure 7. Here the inner capsule which is a foam material is dipped in the liquid (water or paint thinner) used for cleaning, and then it is placed inside the main body along with the plunger. The lid is used to close these arrangements. Outer surface of the main body consist of dry foam. This duster can be used as a default duster while erasing the impressions instantaneously after writing it in the marker board.

If there is a need to erase the impressions after few days, here comes the use of liquid inevitable. In such cases the lid has to be opened, then the plunger has to be pulled out. Due to this action, the wet inner capsule will be compressed due to which the liquid from this inner capsule travels to the dry foam through the capillary holes present in the main body. Now the impressions can be easily erased off without taking effort separately as such in usual existing dusters.

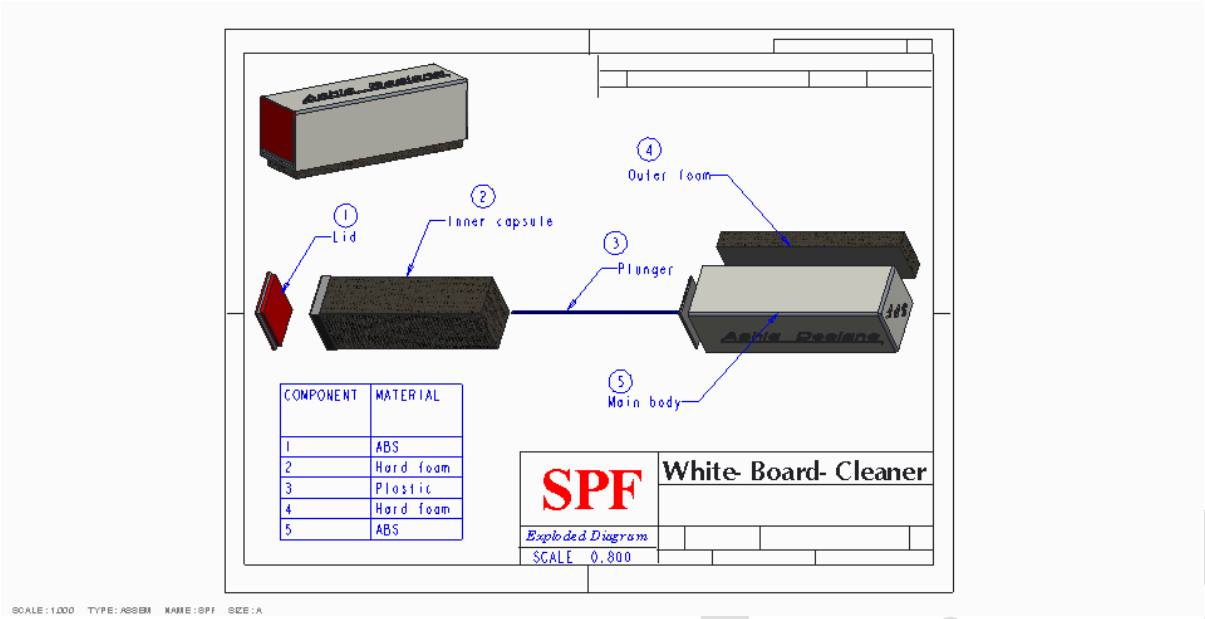

(Figure 6 : Exploded view of redesigned duster)

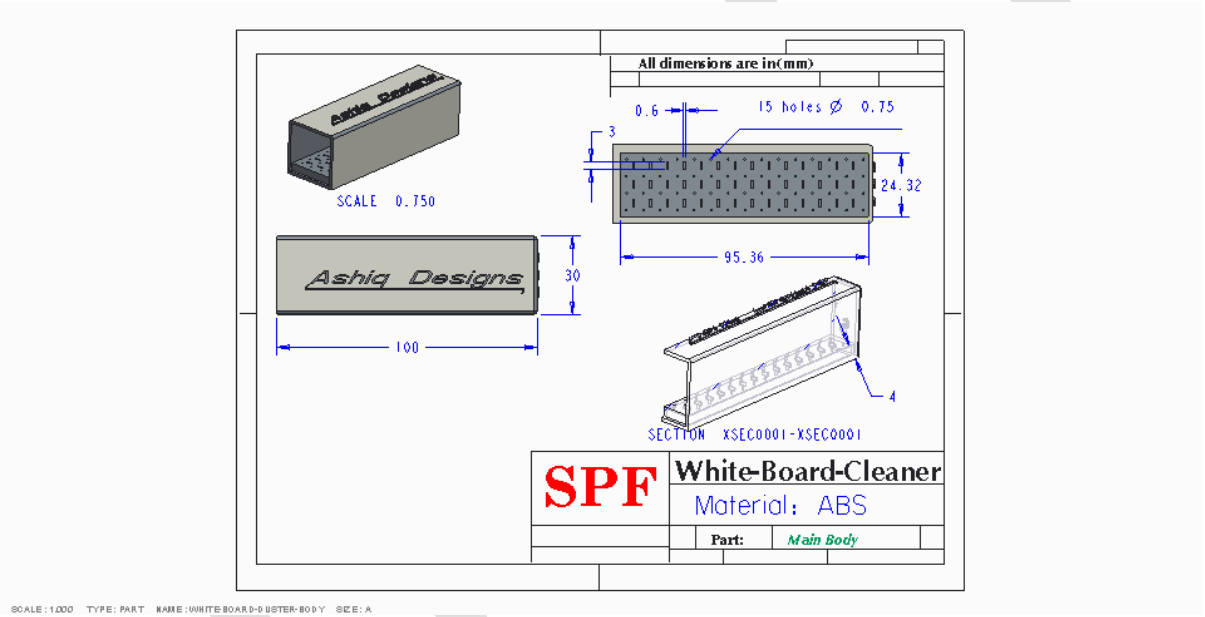

(Figure 7 : Dimensional details of main body)

The modified design is also proved to be safe according to maximum principal stress theory of failure for brittle materials [5,6]. The principal stress, when acted upon by the same shear load of 1N was found to be 10104.3 N/m^2 and it is lesser than ultimate tensile strength of ABS material.

The displacement of the redesigned duster was found to be 0.0000133 mm which is negligible and von mises stress was found to be 8620.25 N/m^2. And they are shown below in the corresponding figures below.

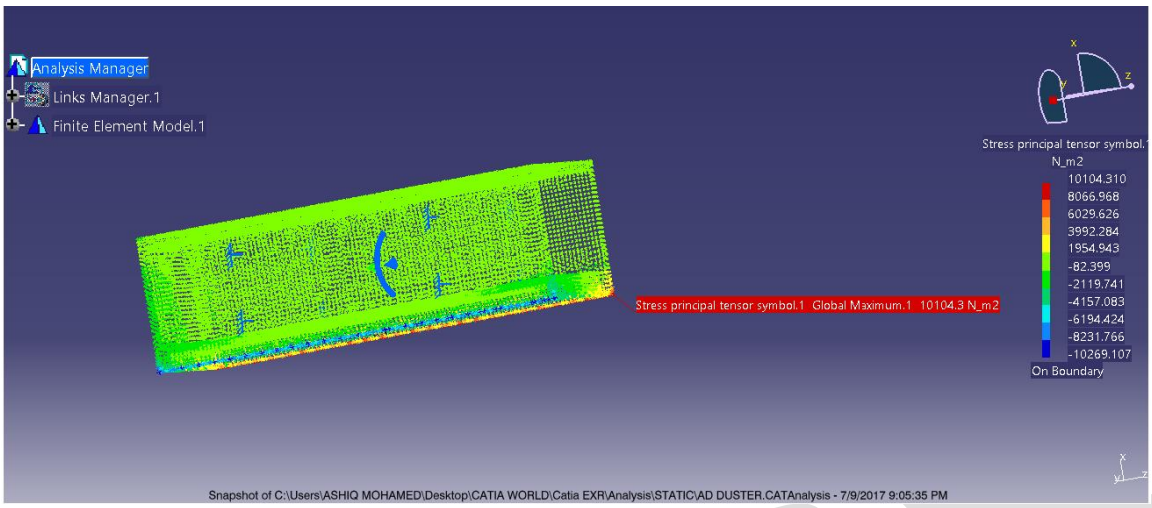

(Figure 8 : Principal stress of redesigned duster)

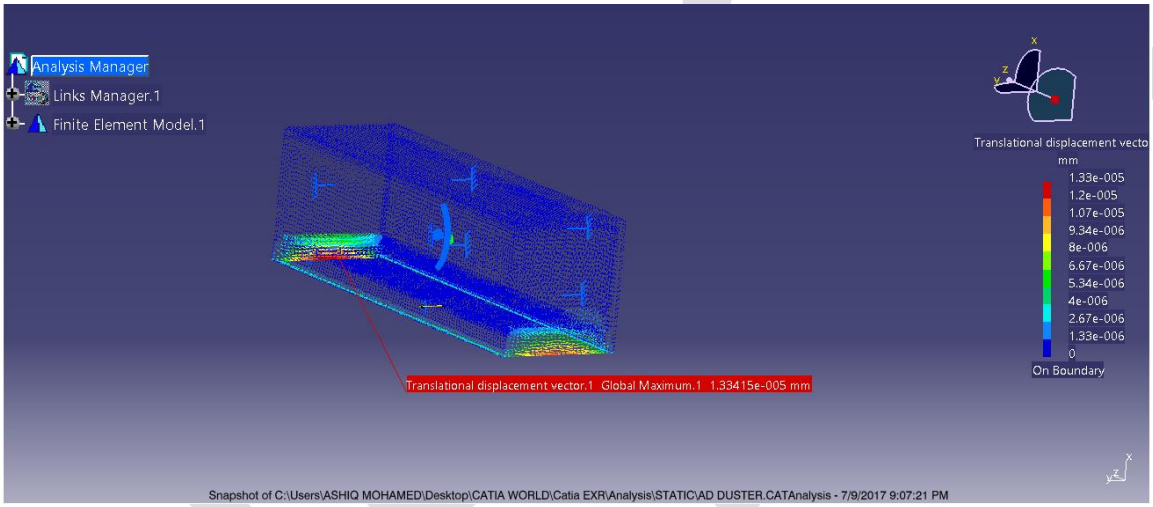

(Figure 9 : Displacement of redesigned duster)

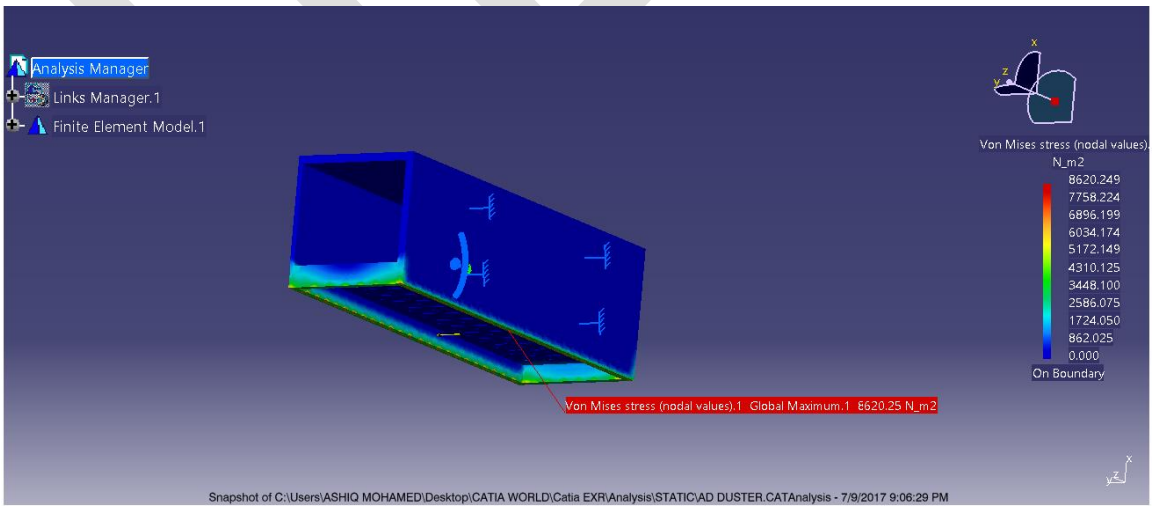

(Figure 10 : Von mises stress of redesigned duster)

This design was prototyped with the help of 3D printing by employing FDM method. In Fused Deposition Modeling method, the parts are build layer-by layer from the bottom to top by heating and extruding thermoplastic filament. Initially the build-assistance software like Cura, slices the 3D CAD file and predicts a path to extrude thermoplastic Then the 3D printer heats the thermoplastic and deposits it along the extrusion path [9,10].

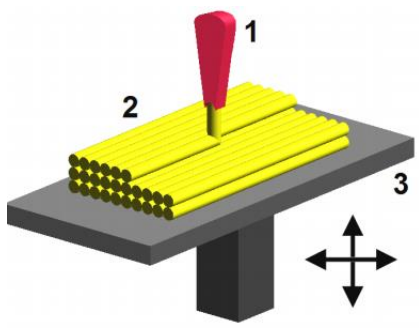

(Figure 11 : FDM principle. 1-nozzle, 2-building material, 3-moving table) [11]

Thus obtained duster was tested manually by erasing the impressions that were made few days before on the marker board and better improvements were noted. The details of the prototype is given below.

PARTICULARS	VALUE
Layer Thickness	200 microns
Infill Percentage	25 %
Shell	3

(Table 3 : Prototype details)

Infill refers to the amount of plastic to be used for the bulk of the object, it goes normally from 0% (hollow objects) to 50% (solid, very strong parts) [12].

The below table shows the function analysis of the redesigned marker board duster.

PART	FUNCTION	PRIMARY FUNCTION	SECONDARY FUNCTION
Main body	1. Grip for holding 2. supports lid and encloses plunger and wet foam	1	2
Lid	1. Covers the plunger and wet foam and gives aesthetic value		1
Dry foam	1. Erase the marking on the board 2. Absorbs the water/ paint thinner for better erasing of impressions	1	2

Plunger	1. Compress the wet foam		1
Wet foam	1. Used for holding the liquid.		1

(Table 4 : Function analysis of redesigned duster)

The image of the exact prototype of the redesigned white board duster is shown below in an exploded view. It consist of the main body attached to the dry foam, plunger and wet foam arrangement and finally a lid to enclose these parts

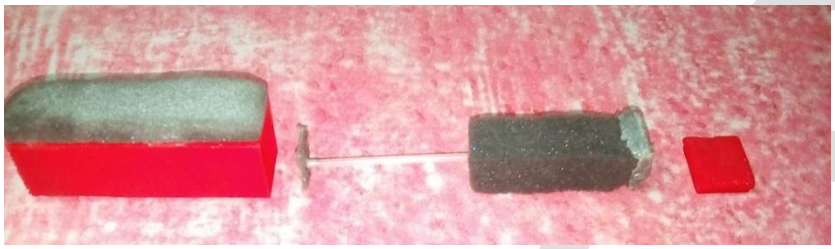

(Figure 12 : Prototype image)

CONCLUSION-

Thus this case study illustrated the major demerits of the existing marker board duster and its necessity to be redesigned. Also from the above discussion, we can conclude that the usual existing duster could be effectively replaced by this modified duster in order to make the erasing purpose easier and with the surface roughness of 200 microns which facilitates for good ergonomical effect to use the duster. This modified design of the duster has better significant than the existing design of the usual duster and it is theoretically proved to be safe from the following key aspects.

- Material of the duster is brittle in nature, so the maximum principal stress theory has to be validated in order to prove for a safer design.
- The principal stress in the duster under loading condition is lesser than the ultimate tensile strength of the material.
- The displacement of the duster under constrained condition is negligible.

So it is suggested to switch over from the existing marker board duster to this redesigned duster in order to make the erasing process in an ease approach.

REFERENCES:

[1] Chougule Mahadeo Annappa, “Application of Value Engineering for Cost Reduction of Household Furniture Product - A Case Study”, International Journal of Innovative Research in Science, Engineering and Technology, volume 3, issue 4, 2014.

[2] Alexandru C. Telea, “Reverse Engineering – Recent Advances and Applications”,ISBN 978-953-51-0158-1, 2012.

[3]James M. Margolis, ”Engineering Plastics Handbook”, Acrylonitrile-Butadiene-Styrene (ABS) Resin Chapter (McGraw-Hill Professional, 2006), Access Engineering

[4]Cambridge University Engineering Department, “Materials Data Book”, 2003, http://www-mdp.eng.cam.ac.uk/web/library/enginfo/cueddatabooks/materials.pdf

[5]Dr. R K Bansal, “A textbook of strength of materials”, Laxmi publications (p) ltd, 2009, https://docs.google.com/file/d/0B0U1_eNEi1r-bG1MMFVWckRiTk0/edit

[6] Er. R K Rajput, “Strength of material (Mechanics of solid)”, S. Chand Publishing, ISBN 9789385401367, 2015.

[7] P Radhakrishnan, S Subramanyan, V Raju, "CAD/CAM/CIM", New Age International (P) Ltd., Publishers, Third edition, ISBN (13) : 978-81-224-2711-0, 2008.

[8] P N Rao, " CAD/CAM Principles and Applications", Tata McGraw Hill Education Pvt. Ltd, ISBN(10) 0-07-068193-7, 2010.

[9] Vinod G. Surange, Punit V. Gharat, " 3D Printing Process Using Fused Deposition Modelling (FDM)", International Research Journal of Engineering and Technology (IRJET), Volume: 03 Issue: 03, March 2016.

[10] Deepa yagnik, " Fused Deposition Modeling – A Rapid Prototyping technique for Product Cycle Time Reduction cost effectively in Aerospace Applications", IOSR Journal of Mechanical and Civil Engineering (IOSR-JMCE), International Conference on Advances in Engineering & Technology – 2014

[11] Ludmila Novakova-Marcincinova, Ivan Kuric, " Basic and Advanced Materials for Fused Deposition Modeling Rapid Prototyping Technology", Manuf. and Ind. Eng., 11(1), 2012, ISSN 1338-6549

[12] Enrique Canessa, Carlo Fonda and Marco Zennaro, "Low-cost 3D Printing for Science, Education & Sustainable Development", ISBN 92-95003-48-9, May 2013.

International Journal of Engineering Research and General Science Volume 5, Issue 4, July-August, 2017
ISSN 2091-2730

SEISMIC ANALYSES OF SHELL SUPPORTED BRIDGE

Akshai K Sugathan [1], Dr. Syed Jalaludeen Shah[2]

[1] PG Scholar, Dept of Civil Engineering, Universal Engineering College, Vallivattom, Thrissur, Kerala, India.

[2] Professor and Head, Dept of Civil Engineering, Universal Engineering College, Vallivattom, Thrissur, Kerala, India.

[1]akshaiksugathan@gmail.com

[2] syedjshah@gmail.com

Abstract— This paper demonstrates the performance of shell supported bridge structure resting on different soil conditions when subjected to seismic analysis using ANSYS 15. As a part of the bridge, shells use all the modes of structural action available to beams, struts, arches, cables and plates. This paper provides a comparative study on the effects of structural configuration on static and seismic analyses of pedestrian shell supported bridge resting on pile foundation. The modelling of bridge is prepared on Auto cad 3D software and was analysed as FEM model using static structural analyses, Modal Analyses and response spectrum analyses. The parameters considered in the study are thickness of the shell, different soil and contact conditions and their effect on stress as well as deformation behaviour of structure under static and seismic loading.

Keywords— Shell supported Bridge, Anticlastic Shell, ANSYS 15, Response spectrum analyses, Pile Foundation

INTRODUCTION

The introductions of the concrete shell have made tremendous change in the field of construction. Shells are most commonly seen as domes, but may also the form of ellipsoid or cylindrical sections or a combination. The shells are commonly used are roots, nowadays for sports buildings or storage facilities. Anticlastic shells or hyper shells are shell capable of taking large compressive loads. The advantage of shell structures is that they bring down the dead load and material cost and that it has higher load carrying capacity. The disadvantage lies in higher cost of foam work and labour.

The confidence in shell structures over the years has led to shells being used to support bridge deck. The Musmeci Shell supported bridge in Potenza, Italy is an example of a shell supported bridge of an anticlastic shell. Even though shell sections are thin they have great strength derived from the shape rather than the mass. During earthquakes great damage is known to occur. Though shell type bridges are very promising due to their overall performances, use of shell supported bridges with confidence requires an detailed investigation of its performance.

SHELLS BRIDGES AND EARTHQUAKES

The concept of shell supported bridge is a recent innovation. The improved building terminology in structural concrete and steel work has led designers to use different topology of steel supported bridges. In shell supported bridges the bridge deck slab is supported by the concrete shell with beam stillness provided below the bridge deck slab. Such bridges have generally been found satisfactory under the usual loading.

When the soil conditions are not suitable for providing foundation, deep foundations such as piles, piers etc are adopted as foundations for bridges. Bridges supported on deep foundation need to be analyzed for soil structure interaction effects. Such shell supported bridges as mentioned above needs studies to ascertain their safety during an earthquake. Earthquakes such as The Great Hanshin earthquake is an example of the destructive force of an earthquake. The bridge has to be safe from damage, if it is to be adopted.

A. Scope of the Work

The scope of the research work conducted as a part of this project work is as follows;

1. To studying the role of stillness of bridge support by shell structure under static, Modal and seismic analyses by conducting analyses of three different thickness of shells.
2. To evaluate the effects of soil structure interaction on the pile supported Shell supported bridge by conducting different analyses in two types of soils with smooth and bonded contact condition.

3. To understand the behavior of a shell supported bridge resting on pile foundation and to evaluate the relative influence of each component the following analyses were performed separately.

- Static structural analyses shell supported bridge structure
- Static structural analyses shell supported bridge and pile foundation
- Model analyses – shell supported bridge structure
- Model analyses – shell supported bridge and pile foundation
- R S A of shell supported bridge structure along x, y and z axis.
- R S A of shell supported bridge and pile foundation.

B. Objective of the Work

This project work aims at considering the static and dynamic response of a Shell supported bridge. Shells of different stiffness are considered in the analyses. The seismic analyses of a shell supporting bridge structure resting on pile foundation considering the soil structure interaction is envisaged. The static analyses, model analyses and response spectrum in different soil condition and the influence of all these on the structural behaviour of a shell supported bridge resting on the pile is planned.

C. Methodology

This work studies the seismic performance of shell supported bridge using Finite Element Methods (FEM). In order to understand the relative role of this shell supported bridge deck, pile and soil structure interaction, each part is modelled separately and analysed statically and dynamically. The investigation is conducted using the FEM Software ANSYS version 15. The response spectrum of Savannah River Site Disaggregated Seismic Spectra is used for the seismic analyses. The Shell supported bridge was modelled using AUTOCAD, modal, static and response spectrum analyses were conducted to obtain the response of various parameters studied.

FINITE ELEMENT MODELLING OF SHELL SUPPORTED BRIDGE

In this project a finite element model of a shell supported bridge resting on pile foundation and surrounding soil is subjected in to static, modal and dynamic analyses. Details of geometry a finite model of Shell supported bridge, foundation and soil, material models, material properties, contact options and seismic data adopted are elaborated.

A. Shell Supported Bridge Model

The Shell supported bridge consists of an anticlastic shell which supports the deck slab of the bridge. The dimensions of the Shell supported bridge considered in this study were fixed with reference to the design of [13]. Figure 1. shows typical Shell supported bridge geometry.

Fig..1 Shell-supported bridges [13]

The shell supported bridge of a typical type was modelled as a part of optimisation technique by [13]. It consists of different boundary conditions and the following data as given below.

- Uniformly distributed load of 4 kN/m2
- Dimension the deck slab = 40 m x 6 m
- Height of 7 m from the bottom level which supports the deck and 5.5 m to the bottom shell.
- Thickness of deck = 0.15 m
- The thickness of the shell varies from 150 mm to 400 mm

As a part of this project 3 different models are developed for the different analyses. The 3 different models having shell thickness of 150 mm, 200 mm, and 320 mm with a deck slab of thickness 150 mm each. The shell structure was modelled using the Solid works and Auto Cad 2015 software's with appropriate boundary conditions provided by [13]. Meshing was carried out using quadrilateral and mapped mesh elements. The concrete element used here is solid 186. Figure 2 show the three model of bridge used

in this study. The different models were prepared for analysis in ANSYS. The concrete element type used in these analyses is solid186.

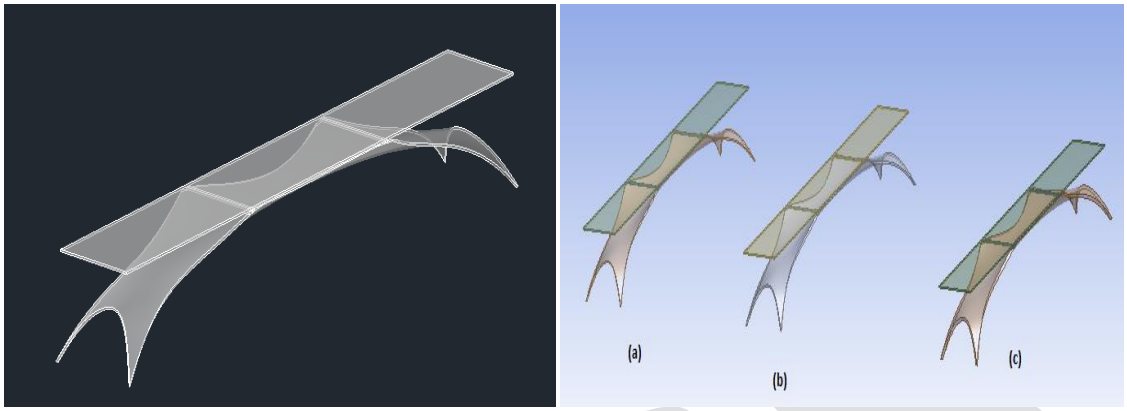

Fig. 2 Shell supported bridge of shell thickness (a) 150 mm, (b) 200 mm, (c) 320 mm

The details of the Shell supported bridge used in this study are given in table I. For seismic analyses of bridge the entire structure has to be considered. A combination of 3 piles with soil block is modelled with the Shell supported bridge.

Table I Dimension Details of Shell supported bridge

Thickness of the shell (m)	Span of bridge (m)	Width of bridge (m)	Height of bridge from bottom level (m)	Head level from the bottom portion of shell (m)	Size of beam stiffeners along the width
0.15	40	6	7	5.5	0.15 x 0.25
0.2	40	6	7	5.5	0.15 x 0.25
0.32	40	6	7	5.5	0.15 x 0.25

MODELLING OF PILE FOUNDATION AND SOIL GEOMETRY

The report of soil investigation carried out for design of pile foundation for the pedestrian bridge by [2] is taken. The end bearing piles are selected from the corresponding bore-log given in the same reference. From the data a group of 3 pile was designed using IS 2911 and IS 456. Figure 3 shows the shell supported bridge with piles. Figure 4 shows the shell supported bridge with piles and soil. Table II gives details of the pile foundation.

Fig. 3 Shell supported bridge with pile foundation modelled in Autocad 2015

Table II Dimension Details of pile

Diameter of pile	0.85m
Length of pile	8.8m
Depth including pile cap	10.2m

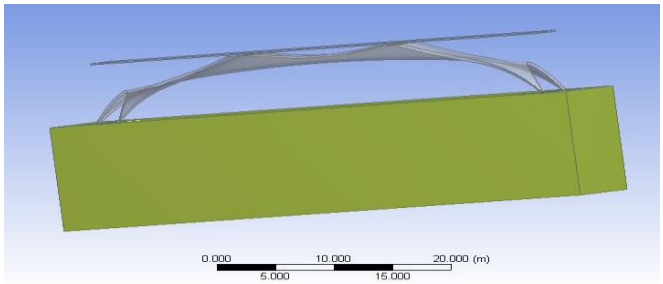

Fig. 4 Shell supported bridge with soil block modelled in AUTOCAD 2015

The thickness of soil below the pile tip is ten times the pile diameter from the pile tip and five times pile diameter from pile cap end [21]. The size of soil was restricted to small size in order to control number of nodes or elements**.** Since the structure is large in size, so the system needs more time and it requires more memory space. In order to overcome this issue an inflation layer was created between the pile and soil layer. Thus increasing the mesh size of the soil block and providing an inflation layer at the contact region enhances better soil structure interaction.

PROPERTIES USED FOR SHELL STRUCTURES AND SOIL.

Concrete is defined as multi-linear isotropic material. The plasticity model for concrete is based on the flow theory of plasticity, Von Mises yield criterion, isotropic hardening and associated flow rule. For concrete in compression, the ANSYS program requires the yield and ultimate strength of the material property to properly model concrete. The multi-linier isotropic material uses the Von Mises failure criterion to define the failure of the concrete [5]. The structures assigned for M30 grade concrete properties as tabulated in table III. The material properties adopted for soil in the present study are given in table IV

Table III Properties of concrete

SI No.	Concrete properties	Value
1	Modulus of Elasticity, E_c	2.238×10^7 kN/m^2
2	Poisson's Ratio, υ	0.17
3	Density	24 kN/m^3
4	Tensile ultimate strength	2.9×10^3 2.9kN/m^2
5	Compressive ultimate strength	3×10^4 kN/m^2

Table IV Properties of Soil

SI No.	Properties	Homogeneous soil condition	
		Loose sand	Medium clay
1	Modulus of Elasticity, E_s, (kN/m^2)	24×10^3	15×10^3
2	Poisson's Ratio, υ	0.3	0.45
3	Density (kN/m^3)	18	20
4	Cohesion(kN/m^2)	0	35
5	Angle of Internal Friction	30°	0

SEISMIC SPECTRUM ANALYSIS

For engineering design of earthquake-resistant structures, response spectra serve the function of characterizing ground motions as a function of period or frequency. These motions then provide the input parameters that are used in the analyses of structural response. Because they use the maximum response, the response spectra are an inherently conservative design tool. Response spectra are described in terms of amplitude, duration, and frequency content, and these are related to source parameters, travel path, and site conditions. Studies by a number of investigators have shown by statistical analyses that for different magnitudes the response spectrum values are different for differing periods. The spectrum analysis is mainly done in bridges. The savannah river site disaggregated seismic spectrum was mainly done in shantou bay bridge and tiger gate bridge. This response spectrum analyses can

bring out the dynamic behaviour of the structure [22]. The data consist of a maximum acceleration of 0.358 m/s^2 with a maximum frequency up to 50 hz (figure 5).

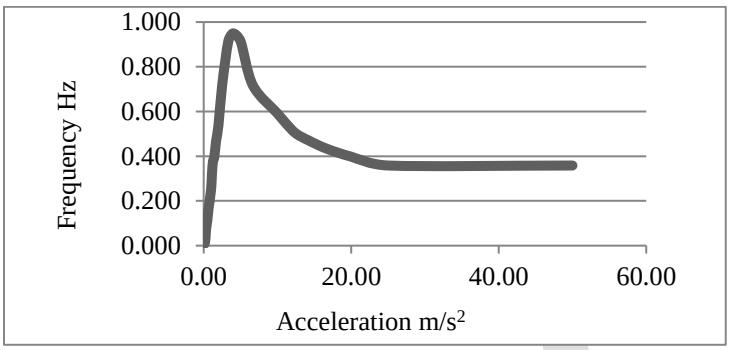

Fig. 5 Acceleration frequency spectrum of Savannah River site disaggregated seismic spectrum.

RESULTS AND DISCUSSIONS

The result of static analyses, modal analyses and dynamic analyses of Shell supported bridge are discussed. The static analysis is done in order to determine the deformation characteristics and stress generated on the Shell supported bridge. In this, static analyses is done on varying the thickness of the shells of thickness of 150 mm, 200 mm, and 320 mm. Modal analyses is the study of the dynamic properties of structures under vibration excitation. The modal analysis is done in order to determine the natural frequency of the particular structure. Dynamic characteristic of the bridge are investigated by using the response spectrum analyses. The seismic behaviour of the Shell supported bridge is conducted to check whether any possibilities for resonance conditions and to determine the strength and performance of anticlastic shells. Also the analyses were done based on the varying soil properties such as cohesive and cohesion-less soil and the varying interface roughness such as bonded and smooth contact to simulate the two extreme possibilities of contact. The following five cases were subjected to static, modal and dynamic analyses.

1) Shell supported bridge, 2) Shell supported bridge with pile foundation with bonded contact in loose sand, 3) Shell supported bridge with pile foundation with smooth contact in loose sand, 4) Shell supported bridge with pile foundation with bonded contact in medium clay, 5) Shell supported bridge with pile foundation with smooth contact in medium clay.

A. Static Analyses Of Shell Supported Bridge

Nonlinear static analyses were done on the Shell supported bridge. The analysis was performed on the bridge without soil, and the structure with pile foundation in different soil conditions. This was done in order to determine the behaviour of the structure. The load was applied on to the top of the deck surface. The standard earth gravity was also considered in the case of bridge with soil block. The boundary conditions were appropriately provided. The X, Y, Z directions in analysis is such that Y is vertical and X and Z are horizontal.

- Deformation of Shell supported bridge

The analyses were done under the static load of 4 kN/m^2 throughout the deck surface. The load from the deck slab is directly transferred through the beam stiffeners provided on the upper support of the shell. Static analyses of Shell supported bridge along with pile foundation in soil block were also done. The static load of 4 kN/m^2 along with the standard gravity load is applied. The analyses were done based on the varying soil properties such as cohesive and cohesion-less soil and the varying interface roughness such as bonded and smooth contact. The entire structure (i.e., bridge, pile foundation) is merged to a single body. The deformation of shell supported bridge under static analysis is given in table V

Table V deformation of Shell supported bridge under static analyses

Thickness of Shell supported bridge (m)	Deformation (m)
0.15	0.01002
0.2	0.00928
0.32	0.00455

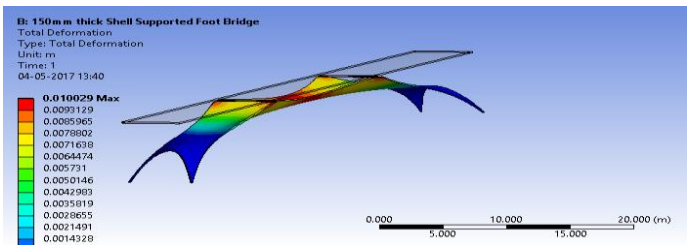

Fig. 6 Maximum deformation in Shell supported bridge of thickness 0.15m

- Deformation of shell supported bridge resting in soil**.**

From the above result it is found that the deformations of the shells are within the permissible deformation in the case of Shell supported bridge without foundation and soil. When the shell thickness increase the deformation decreases. The deformation of 0.15 m thick shell is within the permissible limit. Table VI shows the deformation of shell supported footbridge with pile foundation in different soil conditions while figure 6 shows the deformation on the structure.

Table VI Deformation of Shell supported bridge with pile foundation in different soil conditions

Thickness of Shell supported bridge shell (m)	Deformation under static load (m)			
	Loose sand		Medium clay	
	Bonded	Smooth	Bonded	Smooth
0.15	0.001214	0.0187	0.001581	0.02382
0.2	0.001242	0.01771	0.00161	0.02219
0.32	0.001298	0.01739	0.00165	0.02333

The result obtained in the bridge along with the pile foundation in different soil condition shows that the deformation is more in soil with smooth contact than the soil with bonded contact. In Fig.ure 7 the deformation of the entire structure is represented. The deformation occuring is the settlement of the soil. Deformation obtained in different soil is shown in the figure 8.

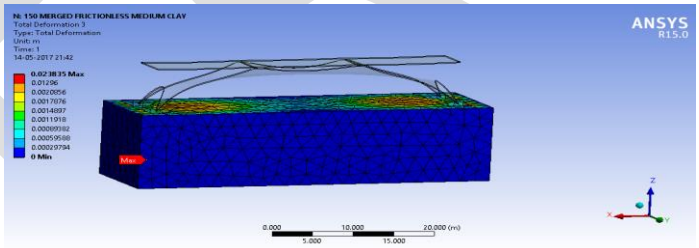

Fig. 7 Maximum deformation in Shell supported bridge with pile foundation of thickness 0.15m

The deformation of shell supported bridge obtained in soil and that without soil is plotted on a graph of deformation vs thickness (Fig 8). It is found that the maximum deformation is shown in medium clay with smooth contact. The soil with smooth contact shows maximum deformation than with bonded contact. In the case of shell supported bridge without soil the maximum deformation is obtained in shell supported bridge with thickness 0.15 m.

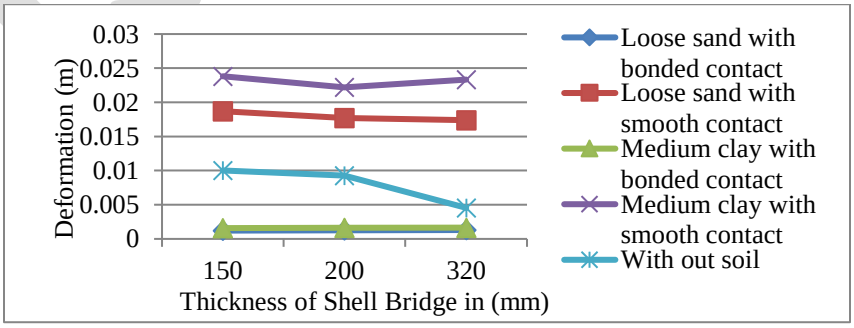

Fig. 8 Deformation of Shell supported bridge with soil and without soil

- Stress in Shell supported bridge

The stresses that developed due to the same static load of 4 kN/m^2 on the Shell supported bridge are shown in the table VII. This study is to determine the stress developed in the shell. The characteristic cylindrical strength was 30000 kN/m^2. The structure will be safe if the stresses developed are within this range. The table VII shows the stress developed on the shell supported bridge.

Table VII Stress on shell supported bridge

Thickness of Shell supported bridge (m)	Stress (kN/m^2)
0.15	25292
0.2	19200
0.32	17628

From the above result the stress is found to be more in bridge with 0.15 m thick shell. The maximum stress is obtained at the upper support of the shell. It can be seen that the stress obtained here does not exceeded the actual strength of the concrete. So the structure is safe.

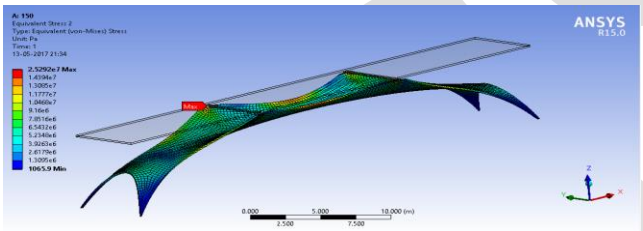

Fig 9 Maximum stress developed in Shell supported bridge of thickness 0.15m

- Shell supported bridge resting in soil

The case of the Shell supported bridge with pile and soil block standard earth gravity is considered. The table VIII shows the result of Stresses on shell supported bridge with pile foundation in different soil block. The table VIII shows the static analyses result of bridge with pile foundation embedded in the soil block. The above result shows the variation of stress in soil with bonded and smooth contact.. From the above result it is found that the stresses obtained in smooth contact are greater than that of stresses obtained in bonded contact. The stress is found to be more in the shell with thickness 0.15 m. The maximum stress is found to be at the centre of the shell. These stresses are developed due to the settlement of the supports or foundation.

Table VIII Stress on shell supported bridge with pile foundation in different soil

Thickness of Shell supported bridge shell.	Stress under static load (kN/m^2)			
	Loose sand		Medium clay	
	Bonded	Smooth	Bonded	Smooth
0.15	8510.9	8926.6	8516.2	9287.1
0.2	7038	7341.76	7189.3	7541.55
0.32	5446.2	6681.4	5217.2	6121.2

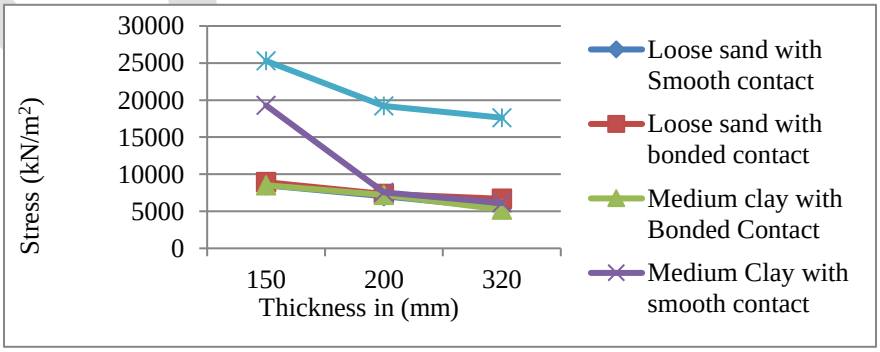

Fig. 10 Stress in Shell supported bridge with pile foundation in different soil and that with shell supported bridge only.

The maximum stress is obtained in the shell supported bridge without soil. The maximum stress is obtained in 0.15 m thick shell. From the figure 12 the stresses are found to be less in shell supported bridge with soil. In the case of shell supported bridge with soil, maximum stress is obtained in the soil with smooth contact than that with the bonded contact. It is because the less amount of friction between the soil and concrete.

B. Modal analyses of shell supported bridge

The modal analysis of Shell supported bridge is performed in order to determine the natural frequency of the bridge. The modal analysis is carried out on bridge only and with bridge cum foundation-soil system. The result of the analyses is shown in the table IX. This analysis was conducted to check the possibility of resonance which will occur when the natural frequency of the system is equal to the exciting frequency of the earthquake.

Table IX Frequency of Shell supported bridge

Thickness of Shell supported bridge (m)	Frequency (hz) of Shell supported bridge	Frequency (hz) of Shell supported bridge with pile foundation in soil block			
		Loose sand		Medium clay	
		Bonded	Smooth	Bonded	Smooth
0.15	1.6321	0.68677	0.68644	0.68647	0.6863
0.2	1.6601	0.89584	0.89353	0.89585	0.89341
0.32	1.8394	1.2958	1.2889	1.2936	1.2873

The results of modal analyses showed that the frequency of structure with bonded contact is having higher frequency than that of smooth contact. The frequency of the 0.2 m thick shell is taken for the validation purpose. The frequency value obtained from the modal analyses is not within the range of excited frequency. Hence there is no possibility for resonance conditions. So the structure is safe.

C. Seismic analyses of shell supported bridge

The response spectrum analyses (RSA) of the Shell supported bridge is done using the details of Savannah river site disaggregated seismic spectrum explained in previous section. The analyses are done with bridge without soil and bridge with pile foundation embedded in a soil block with the parameters bonded and smooth contact in loose sand and medium clay. The deformation and the stress developed due to this excited vibration on the structure are discussed in this section.

- Deformation of Shell supported bridge from response spectrum analyses

The maximum deformation obtained from the response spectrum analyses is shown in the table X. The response spectrum analyses is performed in x, y and z axis. The standard earth gravity is considered.

Table X Deformation of Shell supported bridge

Thickness of shell (m)	Deformation of the Shell supported bridge (m)		
	Along X-axis	Along Y-axis	Along Z-axis
0.15	0.02905	0.06831	0.01516
0.2	0.00702	0.03414	0.00969
0.32	0.00335	0.00909	0.00729

The above result shows the response spectrum analyses of shell supported bridge only. The maximum deformation s obtained along the Y-axis. Figure 11 illustrate the typical deformed contour plots of shell supported bridge for shell thickness 0.15 m.

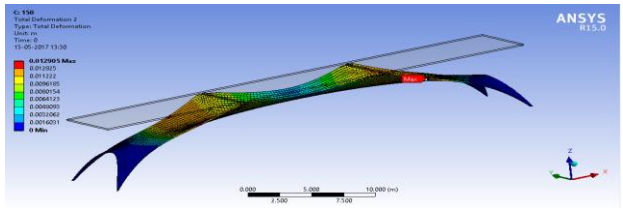

Fig. 11 Deformation of bridge with 0.15 m thickness obtained from RSA along X-axis

The maximum deformations along X-axis and Y-axis are found to be at the edges and curves of the shell. In the case of Z-axis the deformation is found to be at the centre of the anticlastic shell. These deformations are within the limit. Hence the structure is safe. The table XI shows the result for bridge with the combination of foundation and soil. The foundation is consists of three piles.

Table XI Deformation of Shell supported bridge with pile foundation and soil

Thickness of shell (m)	Deformation (m) in loose sand		Deformation (m) in medium clay	
	Bonded contact	Smooth contact	Bonded contact	Smooth contact
0.15	0.012835	0.013289	0.049361	0.04943
0.2	0.013308	0.013808	0.014554	0.014638
0.32	0.014274	0.014974	0.01415	0.01425

From the results it can be seen that with bonded contact and smooth contact in sand, the settlement is low, but with bonded and smooth contact in clay the settlement is high. It is also clear that the smooth contact show poor performance than bonded contact.

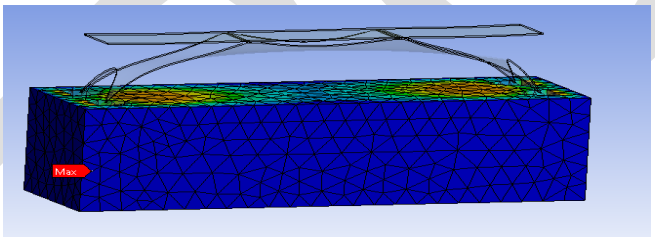

Fig. 12 The visualization of deformation in soil under RSA

The settlement is more found to be in soil with smooth contact than the bonded contact. This happens as the bridge can undergo settlement easily under smooth condition without any resistances. The maximum deformation is found to be in bridge with shell thickness 0.15 in medium clay with smooth contact. While comparing the deformations with shell supported bridge alone and shell supported bridge with soil, the maximum deformation is found to be at medium clay soil and thickness of 0.15 m shows maximum deformation. The deformation is more in smooth contact than in bonded contact cases.

- Stress in Shell supported bridge from response spectrum analyses

The maximum stress obtained from the response spectrum analyses is shown in the table XII and XIV. The response spectrum analysis of Shell supported bridge alone is done in X, Y and Z axis. The result shows that RSA along Z-axis shows higher stress than the other axis except in the case of 0.15 m thick shell. The stress is found to be more in Y-axis than Z-axis.

Table XII Stress developed in Shell supported bridge

Thickness of shell (m)	Stress developed on the Shell supported bridge (kN/m^2)		
	Along X-axis	Along Y-axis	Along Z-axis
0.15	9864.5	22034	21606
0.2	6135	15883	17868
0.32	2957	6251.6	7848.4

The other two models show better result than the 0.15 m. The stress is found to be more in Y-axis than Z-axis. The other two models show better result than the 0.15 m. The figure 13 shows the stress developed in 0.15m from response spectrum analyses along X, Y and Z-axis. Figure14 shows the stresses on the shell structure and the piles.

Table XIV Stress in Shell supported bridge along with foundation and soil

Thickness of shell (m)	Stress in loose sand (kN/m^2)		Stress in medium clay (kN/m^2)	
	Bonded contact	Smooth contact	Bonded contact	Smooth contact
0.15	1664.5	1222.2	1933.6	1648.3
0.2	1158.9	1039.7	1680.2	1439.7
0.32	8459.6	6397.2	4380.3	1811.4

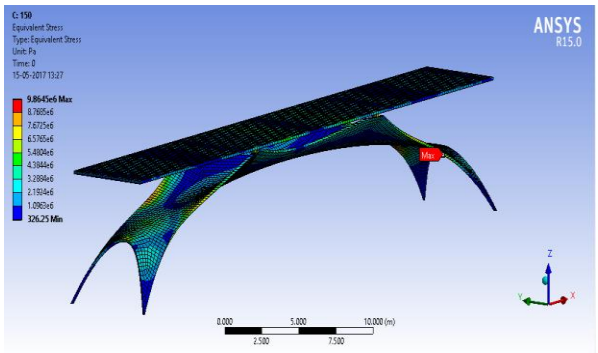

Fig. 13 Stress developed in 0.15m thick shell from RSA along X-axis

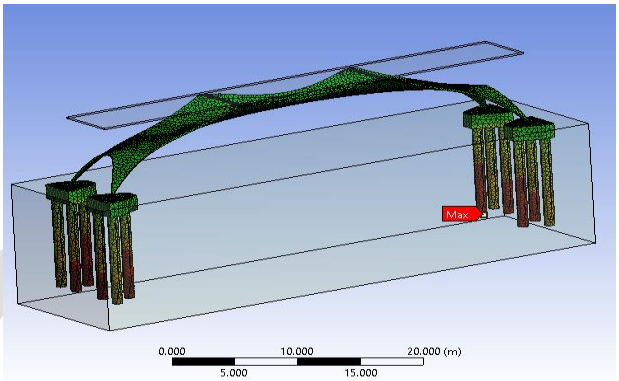

Fig. 14 Stress developed on the pile supporting bridge

From the table XIV it is found that the stress is more in the bonded contact than in the smooth contact. Among the shell of three thicknesses, 0.32 m thick shell show greater stress in bonded contact. The stress developed in 0.2 m thick shell is lesser than that of 0.15 m. from this it can be conclude that the performance of 0.2 m thick shell is comparatively better than the other two. The figure 15 shows a comparison of stress obtained from response spectrum analyses of shell supported bridge with and without soil. The maximum stress is obtained on 0.15 m thick shell supported bridge without soil. On the other hand shell supported bridge with soil, 0.32 m thick shell supported bridge shows higher stress. The stress is more in soil with bonded contact.

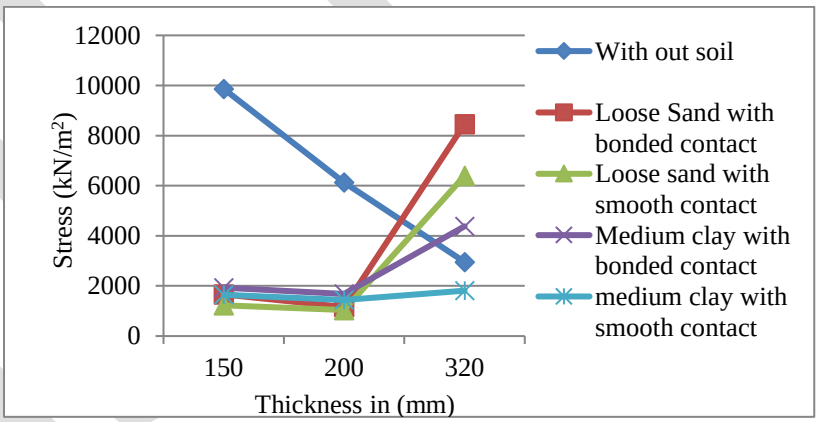

Fig. 15 Stress developed in Shell supported bridge with and without soil.

This projects the importance of the soil structure interaction analysis in estimating the deformation and stress behaviour of shell supported bridge structures.

CONCLUSION

The conclusions of this study cannot be generalised as they are applicable only to the specific data used in this study. Modal analyses of shell supported bridge is done in order to determine the natural frequency, and to compare it with the Savannah River site earthquake data. It can be concluded that no resonance take place in the shell supported bridge. From the static analysis of shell supported bridge without the foundation or soil shows that as the thickness of the shell increased the deformation or settlement of the bridge decreased. However when foundation and soil are taken in to account this is not always true. In shell supported bridge without soil, the maximum deformation is seen in shell supported bridge of shell thickness 0.15 m. In shell supported bridge with foundation cum soil system with different contact interface (bonded and smooth), maximum deformation is found to be in soil with smooth contact. 14. In shell supported bridge without soil, the maximum stress is seen in shell supported bridge of shell thickness 0.15 m. In case of Shell Bridge without soil as the shell thickness increase 0.15 m to 0.2 m (25 % increased) stress decreased by 24%. When the shell thickness increased from 0.2 m to 0.32 m (37.5 % increased), the deformation decreased by 8.1 %. In shell supported bridge with foundation cum soil system with different contact interface (bonded and smooth), maximum stress is seen in soil with smooth contact than that of bonded. From seismic analysis (response spectrum analysis) it is found that the deformation is in shell supported bridge with shell thickness 0.15 m. The deformation decrease with increase in the shell thickness. By varying the thickness of the shell of shell supported bridge 0.15 m, 0.2 m, 0.32 m the percentage difference in stresses between bonded and smooth contact in loose sand are 26.57 %, 10.28 %, 24.3 % respectively. By varying the thickness of the shell of shell supported bridge 0.15 m, 0.2 m, 0.32 m the percentage difference in stresses between bonded and smooth contact in medium clay are 14.7 %, 14.3 %, 58.6 % respectively. The following are the common conclusions,

- The bonded contact shows good soil structure interaction
- The deformation decrease with increase in the thickness of shell.
- Stresses are more in shell supported bridge with shell thickness 0.15 m

REFERENCES:

[1] Alireza, R. (2004), "Effect of earthquake vertical motion on rc bridge piers." *13th World Conference on Earthquake Engineering Vancouver, B.C, Canada August 1-6*, Paper No. 3192

[2] Ancy, J., Abhishek, D., Ajith, K. R., Anju, K. S. (2014), "Design of prestressed pedestrian bridge at Aluva." *Transaction on engineering and sciences*, 2(4).

[3] ANSYS (2014), ANSYS Theory Manual, ANSYS User's Manual, Version 15.0.

[4] ANSYS (2015), Release 15., *Theory Reference for the Mechanical workbench and Mechanical applications.*

[5] Anu, S. (2016), "Seismic behaviour of hyperbolic paraboloid shell footings." *M.Tech. Thesis*, University of Calicut, India.

[6] Asha, J., and Glory, J. (2013), "Influence of Vertical Acceleration on Seismic Response of End-bearing Pile Foundations.".*American Journal of Engineering Research*., *10*(4), 1-11.

[7] Briseghella B., Fenu, L. (2004), "Topology Optimization of Bridges Supported by a Concrete Shell." *J. Struct. Eng*, 130(6): 961-968

[8] Briseghella, B., Fenu, L., (2016), "Optimization Indexes to Identify the Optimal Design Solution of Shell-Supported Bridges." *J. Bridge Eng*, ASCE, 10.1061.1943-5592.0000838

[9] Briseghella, B., Fenu, L., Feng, Y., Mazzarolo, E., and Zordan, T. (2013a). "Topology optimization of bridges supported by a concrete shell." Struct. Eng. Int., 23(3), 285–294.

[10] Briseghella, B., Fenu, L., Lan, C., Mazzarolo, E., and Zordan Z. (2013b) "Application of Topological Optimization to Bridge Design." *J. Bridge Eng*, ASCE 2013, 18(8), 790-800

[11] Duggal, S. K. (2013), "Earthquake Resistant Design of Structures", *Oxford University Press*.

[12] Fatahi, B., and Samali, B. (2014), "Seismic performance based design for tall buildings considering soil- pile-structure interaction." *J. Advances in Soil Dynamics and Foundation Eng.*, (ASCE), 333-342. Available from, https://opus.lib.uts.edu.au/handle/10453/34637, (Accessed on 5 May 2017)

[13] Fenu, L., Briseghella, B., Congiu1, E. (2016), "Curved footbridges supported by a shell obtained as an envelope of thrust-lines." *IABSE Conference – Structural Engineering: Providing Solutions to Global Challenges, Geneva, Switzerland.*

[14] IS: 2911 Part IV (1989), Indian Standard for Design and construction of Pile foundations – Code of Practice, *Bureau of Indian Standards*, New Delhi.

[15] IS: 456 (2000), Indian Standard for Plain and Reinforced Concrete – Code of Practice, *Bureau of Indian Standards*, New Delhi.

[16] Kobe earthquake (1995). Available from, http://si.wsj.net/public/resources/images/BN-GM006_0116J__H_20150116014614.jpg

[17] Nayak, A. N., and Bandyopadhyay, J. N. (2005), "Free vibration analysis of laminated stiffened shells." *Journal of Engineering Mechanics*, ASCE, 131(1), 100-105.

[18] Potts, D. M. and Zdravkivic, L. (1999). "Finite element analysis in geotechnical engineering." *Thomas Telford Limited*.

[19] Sameena, K. (2015), "Seismic behavior of inverted spherical shell foundations." *M. Tech. Thesis*, University of Calicut, India.

[20] Shahbas, A. (2014), "Seismic investigation of conical shell footings." *M. Tech. Thesis*, University of Calicut, India.

[21] Sreerag, M. R. (2016), "Assesment of soil structutre interaction and vibration analysis of a tower structure." *M. Tech. Thesis*, University of Calicut, India.

[22] Yang, W. (1996), "Response analysis of Suspension bridges." *Eleventh World Conference on Earthquake Engineering, New Zealand.*

International Journal of Engineering Research and General Science Volume 5, Issue 4, July-August, 2017
ISSN 2091-2730

APPLICATION OF INVENTORY CONTROL TECHNIQUE IN CONSTRUCTION

Miss. Monika Ramdas Nanaware, Prof. U. R. Saharkar.

PG -Civil (Construction & Management) Students, nanawaremonika9@gmail.com

ABSTRACT— Paper provides details of basic elements of construction material management, role of inventory management in material management including inventory terminologies & classification, Inventory process, inventory control systems, key performance indicators of inventory management systems, inventory models and optimization of inventory with importance of material resources planning to keep just in time inventory. This paper deals with ABC and EOQ Analysis of Construction Company and finally concluding section, project provides detail of financial analysis of effective utilization of inventory models in material management for cost reduction. The concept of inventory management has been one of the many analytical aspects of management. It involves optimization of resources available for holding stock of various materials. Lack of inventory can lead to stock-outs, causing stoppage of production, but a very high inventory on the other hand can result in increased cost of production due to high cost of carrying inventory. Thus optimization of inventory should ensure that stocks are neither too low nor too high. Inventories like finished products, work-in-progress, components, raw materials, stores, spares, etc. account for 80 per cent or more of working capital in some of the representative industries studied in the past. It would appear that any effort put in towards rationalization of inventories can bring about an appreciable saving.

KEYWORDS— Inventory Management, Inventory Process, Inventory Control Systems, ABC and EOQ Analysis, optimization of inventory.

INTRODUCTION

One of the most important aspects of any business is inventory management. Those who have never worked in the business sector may not understand the importance of efficient inventory management. But, the reality of it is if we don't have control of our inventory, we will be unable to ascertain you will have enough inventories on hand to handle the needs of our customers. Even worse than that, we will not have enough supplies on hand to produce the products we need to meet the needs of our customers. This requires the inventory.

Without inventory management it would be difficult for any company to maintain control and be able to handle the needs of their customers. Whether you use a fulfilment company or ship products yourself you need to know where your inventory is and where it's going. Unless you can meet the needs of your customers you will soon lose all of them to competitors who are able to meet their requirements, no matter how stringent. While inventory management has always been important, it has become more important over the past several decades. As the needs of companies increase, they must in turn increase demands on their suppliers. In order for suppliers to have the goods their customers need, it is necessary for them to maintain excellent and accurate inventory management.

Inventory management is defined as the function responsible for the coordination of planning, sourcing, purchasing, moving, storing and controlling inventories in an optimum manner so as to provide a pre-decided service to the customer at a minimum cost.

NEED OF THE PROJECT WORK

Importance of materials management in construction can be accessed through the fact that about 50% to 60% of the total project cost goes the materials and its management. Survey shows that average material cost is 64% (50% to 65%) of the sales value and only 36% cost goes towards wages & salaries, overheads and profit etc.

Thus the importance of materials management lies in the fact that any significant contribution made by the materials manager in reducing materials cost will go a long way in improving the profitability and the rate of return on investment**.**

OBJECTIVE OF THE WORK

i) Study and analysis various inventory control systems, inventory models useful for day to day material management.
ii) Application of inventory management systems for case study to control the cost of a construction project.

LITERATURE REVIEW

The author suggested that the total cost of material may be 50% of total cost; so that it is important for contractor to consider that timely availability of material. Material Manager should maintain reports such as material to order between two dates, material assignments, waste control, when to purchase construction material, when material must be on site, and purchase order between two dates.“Material management is defined as the process to provide right material at right place at right time in right quantity so as to minimize the cost of project”. They had mention that the efficient procurement of material represents a key role in the successful completion of the work. Poor planning and control of material, lack of material when needed, poor identification of material, remanding and inadequate storage cause losses in labour productivity and overall delays that can indirectly increase total project cost. Construction delay is considered to be one of the recurring problems in the construction industry and it has an adverse effect on project success in terms of time, cost and quality. The time and cost for performance of a project are usually important to the employer and contractor. The authors highlight the types of construction delays due to which project suffer time and cost overrun. Also give external and internal factors that influence the construction process and outline the effect of delay in large construction projects. [1]

As per author, Inventory Classification is very important to manage inventory efficiently. For inventory optimization and Inventory Forecasting, products need to be classified appropriately. There are several methods used for categorization of products and items in inventory. In any industry today inventory optimization is such a vital function. Excess and Shortage of inventory in all levels of the supply chain can affect the availability of products and/or services to consumers. Several monitoring systems and processes can be employed to check inventory imbalances to minimize the supply and demand dynamics. Most common classification used is the Pareto Analysis. ABC Analysis is based on Pareto Analysis which says 20% of the items contribute to 80% of sales. It implies that a small portion of items in Inventory contribute to maximum sales. Typically less than 20% of items classified as A, contribute as much as 80% of the revenue. The next 15% (80% - 95%) contribution to revenue is done by B class Items. The last 5 % revenue is generated by items classified as C’. As the classification is done according to the importance of their relative value, this approach is also known as Proportional Value Analysis. [8]

As per author, if the material management is not properly managed it will create a project cost variance. Project cost can be controlled by taking corrective actions towards the cost variance. Material management deals with principles and practices which effectively optimizes cost of materials used in the project. Material management is the line of responsibility which begins with the selection of suppliers and ends when the material is delivered to its point.ABC analysis helps in rationalizing the number of orders and reduces the overall inventory even though overall purchase orders are the same, the average inventory can be reduced substantially. The Cost Variance values for the Class A materials is a tool to measure the profit and it has a positive value. It indicates the project has a cost

under run i.e. the cost incurred is less than the planned or budgeted cost. This S Curve analysis recognizes that there is too much increase in material cost during actual execution. [10]

METHODOLOGY

1. Study evolves importance of inventory cost & its relation with project cost. Further it provides detail study of inventory control systems, inventory models & effective utilization of it for reduction of inventory cost.
2. After going through all reference document and literature project lead ahead with typical case study of construction project inventory management.
3. Analysis is carried analyzing planned and actual material consumption through techniques.

ANALYSIS OF CASE STUDY

Based on the methodology above the case study is carried out and outputs are drawn. Case study is of construction of building in in Maharashtra state.

MECHANICS OF ABC ANALYSIS

The mechanics of classifying the items into 'A', 'B' and 'C' categories is described in the following steps:

i) Calculate rupee annual issues for each item in inventory by multiplying the unit cost by the number of units issued in a year. It is assumed that the issues and consumption are the same.
ii) Sort all items by rupee annual issues in descending sequence.
iii) Prepare a list from these ranked items showing item no. , unit cost, annual units issued and annual rupee value of units issued.
iv) Starting at the top of the list, compute a running total, item-by-item issue value and the rupee consumption value.
v) Compute and print for each item the cumulative percentages for the item count and cumulative annual issue value.

The normal items in most organizations show the following pattern:

i) 5 per cent to 10 per cent of the top number of items account for about 70 per cent of the total consumption value. These items are called 'A' items.
ii) 15 per cent to 20 per cent of the number of items account for 20 per cent of the total consumption value. These items are called 'B' items.
iii) The remaining number of items account for the balance 15 per cent of the total issue value. These items are called 'C' items.

ABC Analysis for a Building

Table 1. Showing Distribution of materials on the basis of ABC

Sr. No.	Item Description	Unit of Material	Annual usage	Usage %	Cumulative Item %	Rate/ Unit	Value	% Usage Value	Cumulative % Usage Value	Material Type
1	Cement	Bags	30177.39	4.411	4.411	300.0	9053217	19.141	19.141	A Type Material
2	Steel	Ton	401.691	0.059	4.470	45500.0	18276940.5	38.642	57.783	
3	Flooring	Sq. Feet	5144	0.752	5.222	951.8	4895900	10.351	68.134	
4	6" fly ash bricks	Nos	641040	93.700	98.921	7.0	4487280	9.487	77.621	B Type Material
Sr. No.	**Item Description**	**Unit of Materi**	**Annual usage**	**Usage %**	**Cumulative Item %**	**Rate/ Unit**	**Value**	**% Usage**	**Cumulative % Usage**	

		al						Value	Value	
5	Paint	Liter	1520.27	0.222	99.144	1661.6	2526134	5.341	82.962	
6	Crush Sand	Brass	945.88	0.138	99.282	2400.0	2270112	4.800	87.762	
7	Window	Nos	497	0.073	99.355	4328.0	2151038.5	4.548	92.310	
8	River Sand	Brass	355.96	0.052	99.407	2600.0	925496	1.957	94.266	C Type Material
9	Sanitary Fittings & Plumbing	Nos	1707	0.250	99.656	534.9	913015	1.930	96.197	
10	Aggregate	Brass	449.32	0.066	99.722	2000.0	898640	1.900	98.097	
11	Door	Nos	163	0.024	99.746	2595.5	423059.55	0.894	98.991	
12	Murum	Brass	903.08	0.132	99.878	420.0	379293.6	0.802	99.793	
13	Plinth filling (with outside murum)	Brass	169.62	0.025	99.902	420.0	71240.4	0.151	99.944	
14	Anti-termite liquid	Liter	586.79	0.086	99.988	40.0	23471.6	0.050	99.993	
15	Box type waterproofing – lift	Sq. Feet	80.96	0.012	100.000	40.0	3238.4	0.007	100.000	
	Total in Rs. =		**684142**				**47298077**			

Graph 1. Showing Distribution of materials on the basis of ABC

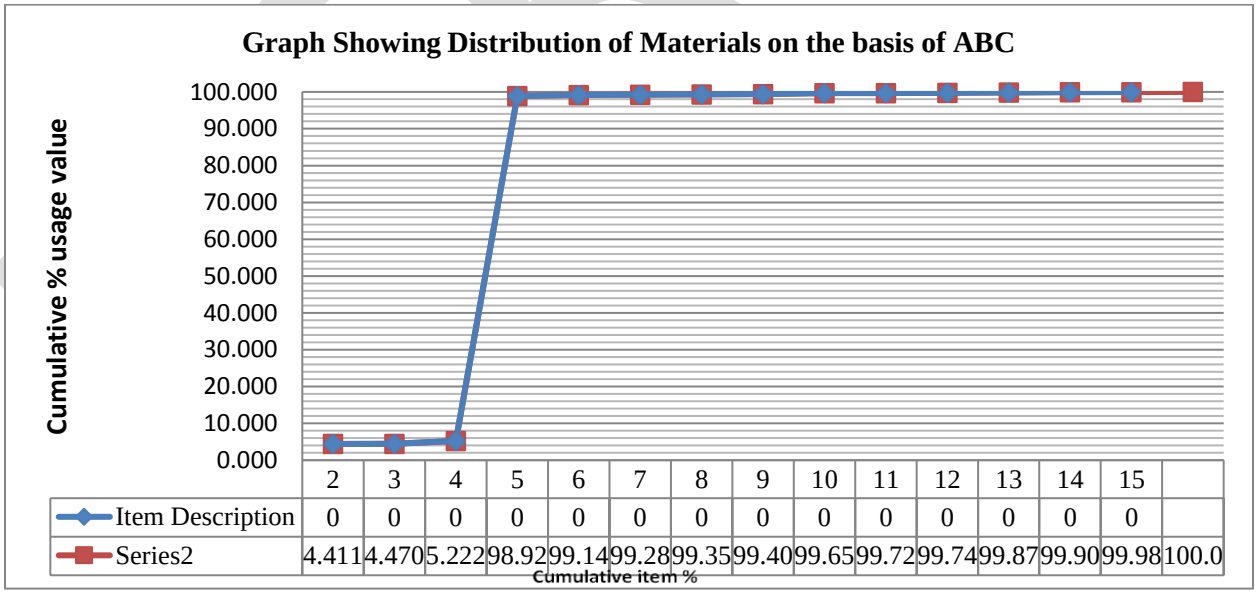

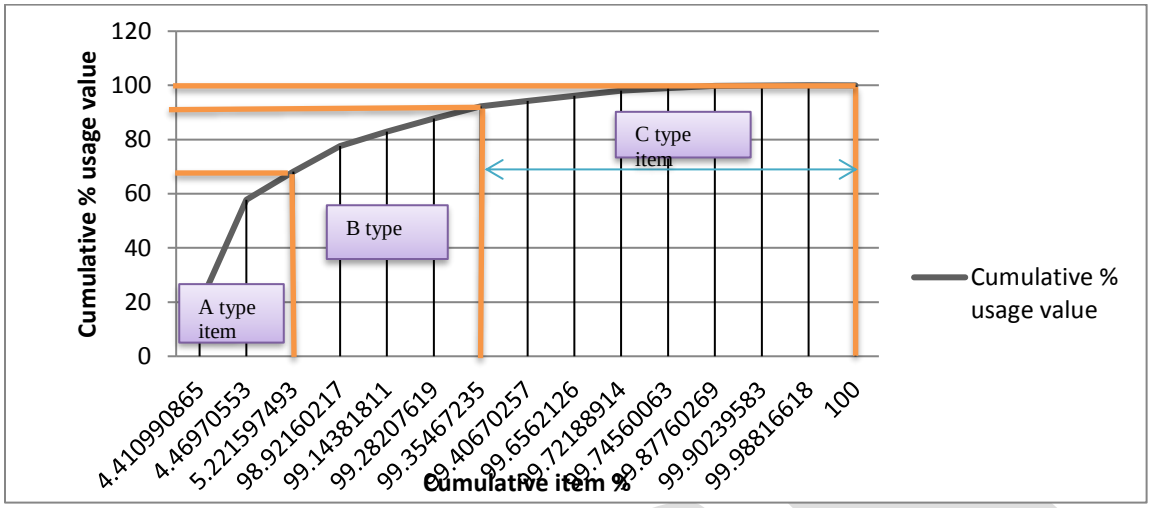

EOQ analysis for a Building

Economic order quantity is the order quantity of inventory that minimizes the total cost of inventory management. Two most important categories of inventory cost are ordering costs and carrying costs. Ordering costs are costs that are incurred on obtaining, additional inventories. They include costs incurred on communicating the order, transportation cost, etc. Carrying costs incurred on holding inventory in hand. This includes Cost of Storage, Insurance taxes, Deterioration & obsolescence this calculates in %. Inventory Carrying Cost = 20%

Economic Ordering Quantity $=\sqrt{(2DS/H)}$

D= Annual Demand (units)

S=Cost per Order

H=Annual Carrying cost per unit.

Table 2. EOQ Analysis of cement bags at Construction SiteNasik.

Sr No	Item	Unit	Annual Demand (units) (D)	Cost per Order (S)	No of Order	Quantity/ Order	Annual Carrying cost per unit (H)	EOQ
1	Cement	Bags	30177	71500	110	275	5200	**911**

From the data collection of the construction site, gives the 275 cement Bags per order for construction. Due to this order carrying cost & inventory cost are increases. But when we applied EOQ analysis on cement bags. Then we got the optimal quantity of cement bags. After EOQ Analysis we got Optimal Order Quantity of cement bags are 911 units. At this order we minimise the ordering and carrying costs.

Annual demand of Cement bags are 30177 units so the construction site to place 33 orders (= annual demand of 30177 divided of order size 911)

No of order for cement bags = D/EOQ

=30177/911

No of order for cement bags = 33.

No of frequency for cement bags=1/33*425=13 days.

CONCLUSION

1. As per analysis it can be conclude that the inventory control very useful to control the cost of a any construction project.
2. Inventory management can be done effectively by using ABC analysis and EOQ.
3. The implementation of ABC analysis gives the distribution of A, B, C type materials. This distribution of materials gives the Economical importance of materials.
4. EOQ gives the results of right quantity of orders at right time. It avoids the delays in material supply and also avoids wastage of materials.
5. From analysis it can be conclude that if there is saving of materials by implementing ABCS analysis and EOQ methods to project then this will give huge money savings in large projects.
6. Inventory control system minimizes the wastage of materials which ultimately saves the cost of a project.

REFERENCES:

[1] Ashwini R. Patil, Smita V. Pataska , "Analyzing Material Management Techniques on Construction Project" International Journal of Engineering and Innovative Technology Volume 3, Issue 4, October 2013.

[2] AdityaPande, "Material Management For Construction Site –A Review" Master Student, (M.E.Const.Engg. & Management) P.R.M.C.E.A.M Badnera, Assistant Professor, Civil Engg.Deptt. P.R.M.C.E.A.M Badnera. Volume 1 Issue 5, PP 1-7

[3] T. PhaniMadhavi, "Material Management In Construction – A Case Study" International Journal Of Research In Engineering And Technology, Nov-2013.

[4] L.C. Bell, G. Stukhart "Attributes of material management systems", ASCE, Vol.112, No. 1, March 1986

[5] Carlos H. Caldas,"Materials Management Practices in the Construction Industry" Practice Periodical on Structural Design and Construction, © ASCE, ISSN 1084-0680/04014039(2008).

[6] AshwiniArunSalunkhe, Rahul S. Patil, "EFFECT OF CONSTRUCTION DELAYS ON PROJECT TIME OVERRUN INDIAN SCENARIO" : International Journal of Research in Engineering and Technology Volume: 03 Issue: 01, Jan-2014

[7] G.Kanimozhi, P.Latha, "Material Management In Constuction Industry" Indian Journal Of Applied Research X 1 Volume : 4 , Issue : 4 , Special Apr Issue 2014

[8] D. Dhoka and Y. Lokeswara, " ABC Classification for Inventory Optimization," IOSR Journal of Business and Management (IOSR-JBM), Volume 15, Issue 1 Nov. - Dec. 2013), PP 38-41.

[9] Dr.G.Brindha, "Inventory Management", International Journal of Innovative Research in Science, Engineering and TechnologyVol. 3, Issue 1, January 2014 PP 8163-8176

[10] Prof. Anup Wilfred, "AN EMPIRICAL CASE STUDY OF MATERIAL MANAGEMENT IN RESIDENTIAL PROJECT", International Research Journal of Engineering and Technology, Volume: 02 Issue: 04 | July-2015 PP 1116-1119

[11] RakeshNayak , Rakesh Gupta, MukeshPandey, "Management of Construction Materials on Project Site", IJEDR Volume 4, Issue 2, 2016 PP 1062-1066

International Journal of Engineering Research and General Science Volume 5, Issue 4, July-August, 2017
ISSN 2091-2730

PREDICTION OF ROAD TRAFFIC NOISE LEVELS BY USING REGRESSION ANALYSIS AND ARTIFICIAL NEURAL NETWORK IN TIRUPATI TOWN

Gollamandla Sukeerth[1*] , Dr.N.Munilakshmi[2*] , Chammireddy Anilkumarreddy[3*]

([1] M.Tech Student, Department of Civil Engineering, SV University College of Engineering, SVU, Tirupati, AP, India.)
([2] Assistant Professor, Department of Civil Engineering, SV University College of Engineering, SVU, Tirupati, AP, India.)
([3] M.Tech Student, Department of Civil Engineering, SV University College of Engineering, SVU, Tirupati, AP, India.)

Abstract*:* Traffic Noise pollution is an interfering air-pollutant which possesses both auditory and a host of non-auditory effects on the exposed population. Since there is no medicine to cure hearing loss, prevention to over exposure is the only alternative left. Noise pollution not only effects the human beings but also the animals. Hypertension, sleeplessness, mental stress, etc. are the implications of noise pollution. Due to this adverse effect of noise level, it is essential to assess the impact of traffic noise on residents and road users.

The present study measures traffic volume and noise levels during the peak traffic flow in the selected areas of Tirupati town. The traffic volume studies are carried out by means of manual methods prescribed by Indian Standards and noise levels are measured following standard procedure using Sound Pressure Level Meter. The obtaining results are used to validate the developed model by using regression analysis and artificial neural networks for the prediction of road noise levels of Tirupati town.

Keywords: Traffic noise pollution, Traffic volume, octave band analyzer, regression analysis , Neural networks

I. INTRODUCTION

Fast growing vehicle population in town in the recent years, has resulted in considerable increase in traffic on roads causing alarming noise pollution and air pollution. Transportation operators are major contributors to noise in modern urban areas. Noise is generated by the engine and exhaust system of vehicles by aerodynamic friction and by interaction between the vehicle and its supporting system (Example: tyre pavements and rail wheel interaction). Noise diminishes with distance from the source. The vehicle by virtue of the movement are not only polluting the atmosphere by emission of poisonous gases but also grabbing off peace from mankind by generating high noise levels that are annoying of irritating to the inhabitants to such an extent that noise pollution caused by the highway traffic has to be studied at great depth, analyzed and has to be controlled. Noise levels increases with traffic volume in an exponential manner. In India like many other developing countries traffic noise is major continents of environmental pollution and now it has become a permanent part of urban and sub-urban life. It is very harmful to human beings. In the new millennium, for protection environmental degradation it is imperative to pay greater attention towards measuring noise pollution, enforcing regulation for noise emission limits, elimination and control noise pollution. Taking a step in this direction, Noise pollution level was measured in Tirupati town.

II. METHODOLOGY

The traffic volume study was conducted in Tirupati town at different Junctions. To measure the potential effects of traffic noise at different Junction, data on traffic volume, including types of vehicles were measured and roadside sound levels, are measured and

interpreted using various models. Sound level meters, a manual hand counter, and portable measurement instruments were used to obtain the required data. Data analysis was conducted using Microsoft Excel and SLM(Sound Level Meter).Traffic volume (composition and flow) and traffic noise were measured at three time periods per day at different Junctions. These time periods were the morning peak hour (08:00–10:00 AM), the daytime peak hour (02:00–03:00 PM), and the evening peak hour (05:00–07:00 PM). The volume and composition of traffic were measured for 60 min during each peak period. Traffic composition was determined on the basis of the presence of two wheelers, three wheelers, four wheelers and Heavy vehicles (Buses, Lorries).

Data on the geometric dimensions of road sections, as well as the number of lanes and their widths, were also measured. Sound level measurements were performed using a sound level meter (Real Time Octave Band Analyzer Model No: 407790). Traffic noise was measured using Sound Level Meter in1/3 Octave- band mode index with an A-weighted scale expressed as Leq, in decibel units at an interval of 3 seconds throughout the peak period.

III. MEASUREMENT PROCEDURE:

Volume studies have been undertaken in this junction at different hours i.e., morning 8 am to 10 am, afternoon 2:00 pm to 3:00 pm and in the evening at 5:00 to 7:00 pm. For traffic volume studies manual method is being used. In this process enumerators count the number of vehicles moving over that section during the peak hours. The vehicles are categorized in to Two Wheelers (2W), Three Wheelers (3W), Four Wheelers (4W) including cars and school buses, and Heavy Vehicles (HV) including buses and lorries as the prediction of traffic noise levels at the intersection total number of vehicles per hour data is required. Since the intersection consist of three roads, the traffic volume is carried out on each side for a time interval of 20mins such that the total intersection is covered in one hour of time.

The sound level meter was placed closest to the noise source, and the microphone was positioned 70 m from the traffic light, at a height of 1.2 m above the ground level corresponding to the ear level of an individual of average height (Onnu, 2000) and 70 m was adopted with the assumption that most vehicles in the traffic stream had already reached steady speed (Burgess, 1997). Measurements were taken at a time interval of 3seconds for about 20mins on each side of the three road intersection in 1/3 octave band frequency mode and L_{eq} values also measured.

IV. REGRESSION ANALYSIS

Excel’s regression analysis tool performs linear regression analysis, which fits a line through a set of observations using the "least squares" method. Regression is used in a wide variety of applications in finance and accounting to analyze how the value of a single dependent variable is affected by the values of one or more independent variables. You can then use the regression results to predict the value of the dependent variable based on values of the independent variable(s).

The standard formula for multiple regression with two independent variables is :

$$Y = a + b1X1 + b2X2$$

Y = Predicted value of the dependent variable

a = Y-intercept

b1 = Coefficient of Weight of Materials (first independent variable)

X1 = Any value of Weight of Materials (first independent variable)

b2 = Coefficient of the second independent variable

X2 = Any value of Dollar Value of Materials (second independent variable)

As noted previously, the Y-intercept can be found in cell B17, the coefficient b1 of X1 can be found in cell B18, and the coefficient b2 of X2 can be found in cell B19.

Thus, using Excel terminology, the regression formula in this example could be written as:

=B17+B18*X1 +B19*X2

$$Leq = 83.3711-0.28435(Q)-0.64327(P)+0.285084(Nc)+0.000245(Nm)-0.01837(Nb)$$

Where

Leq =Equivalent Continuous Noise Level (dBA),

P =Percentage of heavy vehicles (%),

Q = Total number of vehicles per hour,

Nc = Number of light vehicles per hour,

Nm = Number of motorcycles per hour,

Nb =Number of buses per hour

Table 1 : Traffic Parameters

Balaji Colony

DATE	Time	Q	P	N_c	N_m	N_{hv}	N_b
DAY-1							
18/02/15	8 to 9am	4039	0.297103	4027	2820	12	55
18/02/15	9 to 10am	4150	0.216867	4141	3029	9	66
18/02/15	2 to 3pm	3693	0.324939	3681	2572	12	46
18/02/15	5 to 6pm	4067	0.245881	4057	2927	10	60
18/02/15	6 to 7pm	4081	0.269542	4070	2804	11	66
DAY-2							
19/02/15	8 to 9am	4122	0.291121	4110	2990	12	74
19/02/15	9 to 10am	4126	0.15	4120	2967	6	75
19/02/15	2 to 3pm	3685	0.35	3672	2560	13	48
19/02/15	5 to 6pm	4164	0.17	4157	2989	7	65
19/02/15	6 to 7pm	3984	0.28	3973	2769	11	71
DAY-3							
21/02/15	8 to 9am	4173	0.19	4165	2981	8	81
21/02/15	9 to 10am	4372	0.21	4363	3101	9	76
21/02/15	2 to 3pm	3175	0.28	3166	2110	9	49
21/02/15	5 to 6pm	4323	0.16	4316	3134	7	77
21/02/15	6 to 7pm	4363	0.16	4356	3169	7	87
DAY-4							
22/02/15	8 to 9am	2522	0.317209	2514	1618	8	61
22/02/15	9 to 10am	2847	0.175623	2842	1821	5	77
22/02/15	2 to 3pm	2712	0.184366	2707	1898	5	61
22/02/15	5 to 6pm	4243	0.141409	4237	3075	6	75
22/02/15	6 to 7pm	3765	0.185923	3758	2767	7	76

Table 2 : Traffic Parameters

Annamayya Circle

No.Days	Date	Time	Q	P	N_c	N_m	N_{hv}	N_b
DAY-1								
	23/02/15	8 to 9 AM	3163	0.189693	3157	1804	6	48
	23/02/15	9 to10AM	3530	0.1983	3523	2258	7	60
	23/02/15	2 to 3 PM	2680	0.223881	2674	1540	6	13
	23/02/15	5 to 6 PM	3015	0.099502	3012	2055	3	35
	23/02/15	6 to 7 PM	4092	0.146628	4086	2747	6	38
DAY-2								
	24/02/15	8 to 9 AM	3066	0.163079	3061	1714	5	52
	24/02/15	9 to10AM	3419	0.116993	3415	2124	4	43
	24/02/15	2 to 3 PM	2599	0.153905	2595	1489	4	10
	24/02/15	5 to 6 PM	2909	0.068752	2907	1984	2	31
	24/02/15	6 to 7 PM	4170	0.143885	4164	2712	6	57
DAY-3								
	07/03/15	8 to 9 AM	3368	0.356295	3356	1816	12	59
	07/03/15	9 to10AM	4584	0.283595	4571	2411	13	83
	07/03/15	2 to 3 PM	2840	0.56338	2824	1601	16	17
	07/03/15	5 to 6 PM	3276	0.3663	3264	2194	12	43
	07/03/15	6 to 7 PM	4252	0.211665	4243	2844	9	41
DAY-4								
	08/03/15	8 to 9 AM	2160	0.32	2153	989	7	28
	08/03/15	9 to10AM	2858	0.17	2853	1727	5	21
	08/03/15	2 to 3 PM	2530	0.32	2522	1379	8	20
	08/03/15	5 to 6 PM	2565	0.19	2560	1702	5	21
	08/03/15	6 to 7 PM	3867	0.13	3862	2619	5	18

Table 3: Traffic Parameters

Bliss Circle

No.Days	Date	Time	Q	P	N_c	N_m	N_{hv}	N_b
DAY1	9/3/2015	8 to 9 AM	5919	0.135158	5911	3790	8	256
	9/3/2015	9 to 10AM	6010	0.366057	5988	3608	22	251
	9/3/2015	2 to 3 PM	4540	0.528634	4516	2543	24	266
	9/3/2015	5 to 6 PM	5620	0.24911	5606	3351	14	258
	9/3/2015	6 to 7 PM	6083	0.21371	6070	3832	13	295
DAY-2								
	10/3/2015	8 to 9 AM	5711	0.262651	5696	3428	15	268
	10/3/2015	9 to 10AM	5750	0.365217	5729	3425	21	297
	10/3/2015	2 to 3 PM	4850	0.391753	4831	2711	19	296
	10/3/2015	5 to 6 PM	5654	0.371418	5633	3207	21	278
	10/3/2015	6 to 7 PM	6083	0.21371	6070	3832	13	295
DAY-3								
	14/03/2015	8 to 9 AM	5103	0.293945	5088	3022	15	288
	14/03/2015	9 to 10AM	5226	0.267891	5212	2923	14	299
	14/03/2015	2 to 3 PM	4400	0.568182	4375	2382	25	268
	14/03/2015	5 to 6 PM	5594	0.375402	5573	3387	21	259
	14/03/2015	6 to 7 PM	6257	0.287678	6239	3894	18	316
DAY-4	15/03/2015	8 to 9 AM	3716	0.32	3704	2051	12	246
	15/03/2015	9 to 10AM	4060	0.39	4044	2228	16	289
	15/03/2015	2 to 3 PM	3465	0.61	3444	1681	21	291
	15/03/2015	5 to 6 PM	5212	0.21	5201	3073	11	269
	15/03/2015	6 to 7 PM	5353	0.28	5338	3172	15	288

Table 4: Traffic Parameters

Leelamahal Junction

No.DAYS	DATE	TIME	Q	P	N_c	N_m	N_{hv}	N_b
DAY-1								
	17/03/15	8 to 9 AM	4420	0.135747	4414	2896	6	143
	17/03/15	9 to 10AM	4320	0.115741	4315	2846	5	137
	17/03/15	2 to 3 PM	3151	0	3151	1933	0	152
	17/03/15	5 to 6 PM	3706	0.269833	3696	2236	10	180
	17/03/15	6 to 7 PM	2583	0.038715	2582	1610	1	71
DAY-2								
	18/03/15	8 to 9 AM	4000	0	4000	2509	0	169
	18/03/15	9 to 10AM	3618	0	3618	2216	0	144
	18/03/15	2 to 3 PM	2832	0	2832	1607	0	173
	18/03/15	5 to 6 PM	3351	0.268577	3342	2006	9	183
	18/03/15	6 to 7 PM	2583	0.038715	2582	1610	1	71
DAY-3								
	21/03/15	8 to 9 AM	4142	0.12	4137	2696	5	124
	21/03/15	9 to 10AM	3995	0.10	3991	2557	4	145
	21/03/15	2 to 3 PM	2807	0.04	2806	1607	1	159
	21/03/15	5 to 6 PM	3411	0.21	3404	1949	7	175
	21/03/15	6 to 7 PM	4428	0.07	4425	2887	3	165
DAY-4								
	22/03/15	8 to 9 AM	2821	0.248139	2814	1573	7	140
	22/03/15	9 to 10AM	2931	0.102354	2928	1643	3	140
	22/03/15	2 to 3 PM	2511	0	2511	1345	0	147
	22/03/15	5 to 6 PM	2901	0.241296	2894	1544	7	192
	22/03/15	6 to 7 PM	3829	0.026116	3828	2310	1	169

Statistical Performance Measure Of Regression Analysis

BALAJI COLONY

Predicted	Measured
82.40	82
83.24	82.7
82.23	82.35
82.96	82.5
82.53	82.1
82.16	82.17
83.94	84.18
81.88	81
83.86	83.65
82.35	81.65
83.27	82.98
83.24	83.45
82.57	82.19
83.79	83.67
83.65	83.4
82.01	81.44
82.95	82.31
83.16	82.98
84.05	84.01
83.30	83.05

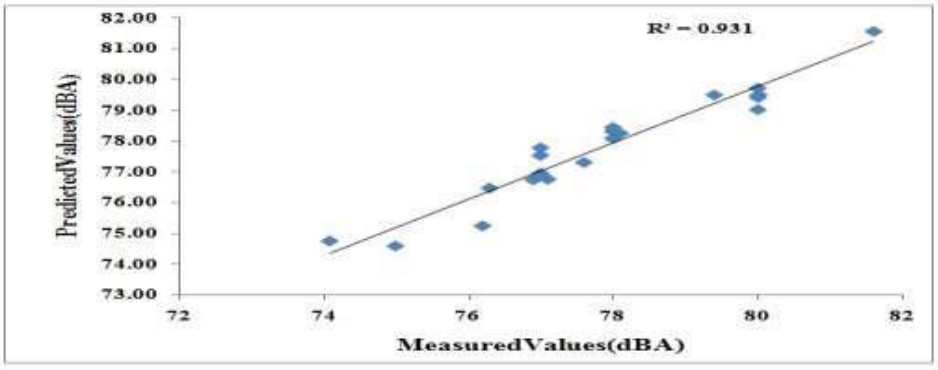

ANNAMAYA CIRCLE

Measured	Predicted
81.6	81.5668
78.1	77.54096
76.2	75.25269
80.1	79.41958
80.1	79.50496
81.01	79.02765
77	76.74635
76.3	76.48344
77	76.96756
80.1	79.50496
79.3	78.09522
79	78.26086
75.1	74.7634
77.6	77.31416
78.3	77.78891
79	78.44911
78.7	76.7686
77	74.60009
80	79.73022
79	78.32398

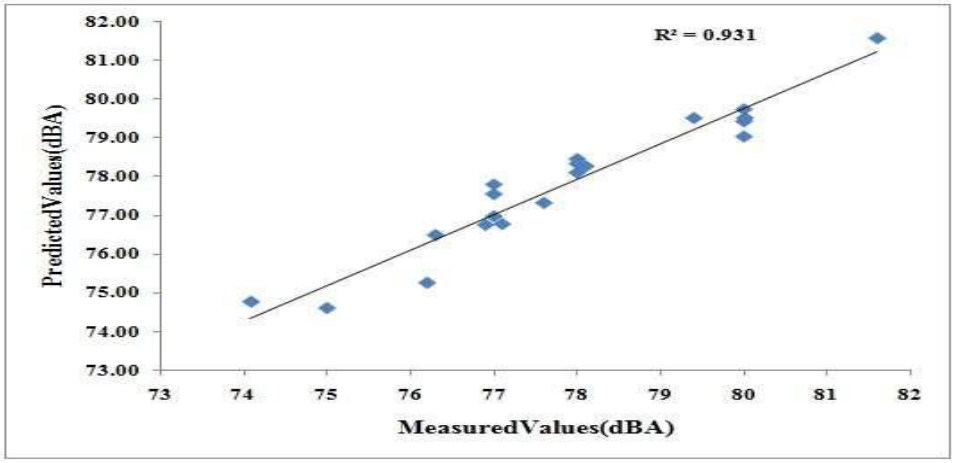

BLISS CIRCLE

Measured	Predicted
81.6	81.5668
78.1	77.54096
76.2	75.25269
80.1	79.41958
80.1	79.50496
81.01	79.02765
77	76.74635
76.3	76.48344
77	76.96756
80.1	79.50496
79.3	78.09522
79	78.26086
75.1	74.7634
77.6	77.31416
78.3	77.78891
79	78.44911
78.7	76.7686
77	74.60009
80	79.73022
79	78.32398

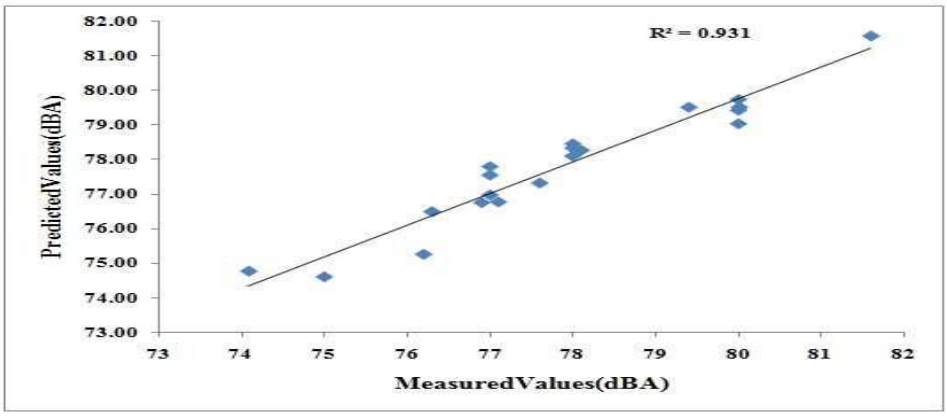

LEELA MAHAL JUNCTION

Measured	Predicted
83	82.89477
83.2	83.21742
83	83.36154
80.1	80.30371
84	84.04402
83.6	83.81248
83.4	83.91998
82	82.66221
79.9	80.21804
84	84.04402
83.1	83.28582
83.06	83.05666
82	82.59304
81	81.00589
83.01	83.39334
81	81.09673
82.3	82.42859
82.4	82.84036
80.09	80.19752
83.1	83.33653

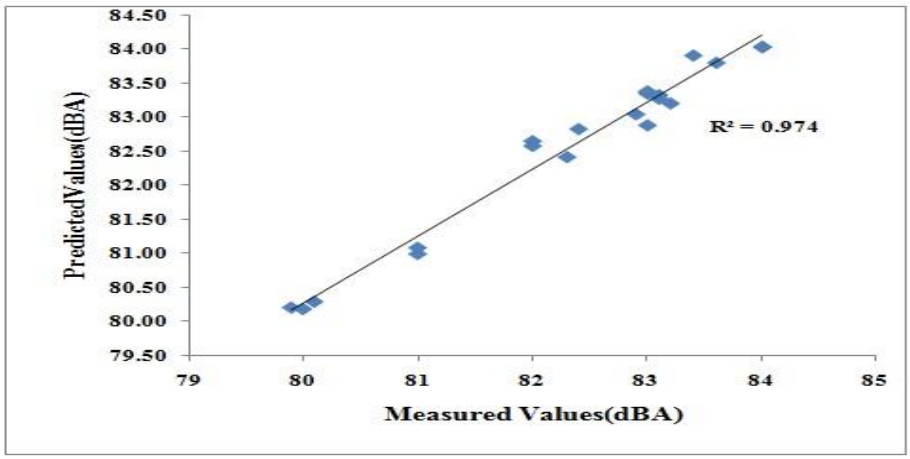

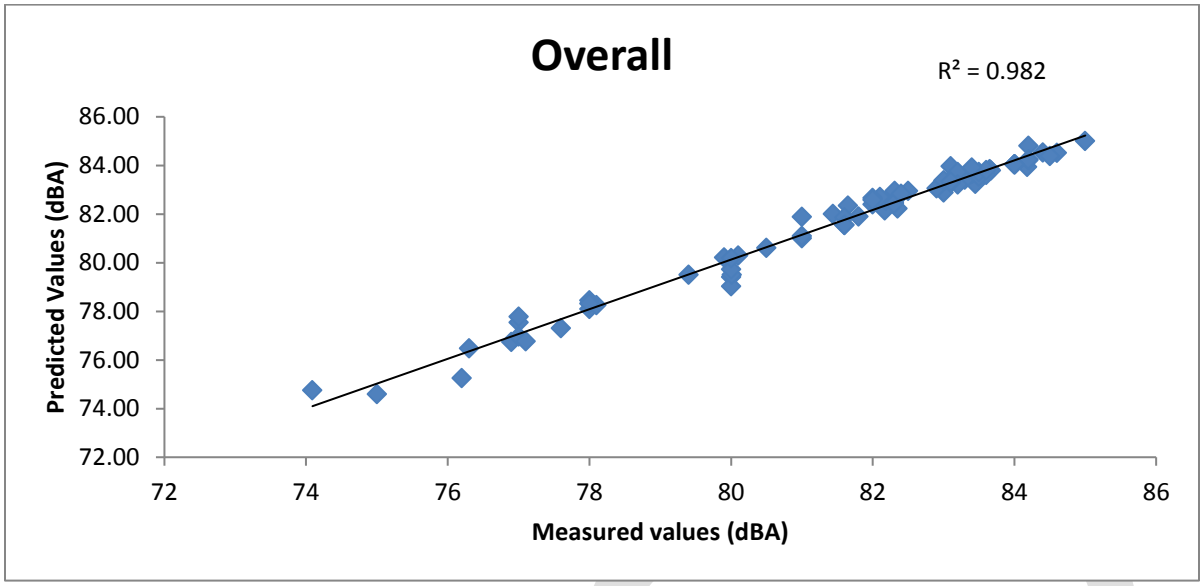

IV Neural Network

An artificial neural network is a computational tool inspired by biological neural systems. It is a massively parallel distributed processor with the ability to learn and generalize, i.e. ability to model complex relationships between inputs and outputs or find patterns in data. The proposed ANN model is developed using "Graphical User Interface(GUI)" using NN tool in MATLAB software. In this a neural network will be developed with different number of inputs, outputs, hidden layers and hidden neurons

The whole dataset was divided in to three parts:

Data points for training

Data points for validation

Data points for testing

Neural networks predict equivalent sound level (Leq) according to the input data set which contains a number of two wheelers, three wheelers, four vehicles, buses and heavy vehicles. A network has been developed by taking the traffic volume studies as input and the Leq values are taken as output value. Eighty data sets were used for training, testing and validation of the neural Network. Data sets are collected by systematic noise measurement in urban areas of Tirupati. The training set is used to adjust the values of the connections weights, the validation set to prevent over fitting problem and the test set to evaluate the performance of the developed neural network.

In neural networks, mainly four types of networks are used:

Feed- Forward Neural Network

Radial Basis Function (RBF) Network

Kohonen Self – Organizing Network.

Feed- Forward Back propagation.

A few applications of ANN are: Aerospace ,Financial, Automotive Manufacturing, Defense, Medical, Electronics, Oil and Gas **,**Engineering etc.,

Development of a ANN model with Feed- Forward Back Propagation:

Normalize the inputs and outputs with respect to their maximum values.

Normalization can be done by using the formula:

$$X=0.1+0.8*(x_i / x_{max})$$

where

X= Normalized Value

Choose a neural network, configure its architecture and set its parameters. The network will choose randomly the training data and will train the network with the training-set data. The network itself evaluate its performance by using the validation-set data. Repeat steps 2 and 3 with different architectures and training parameters. Select the best network by identifying the smallest error found with validation set.

In this study an architecture have been developed for the prediction of Leq values at the four junctions by taking traffic volumes studies of the study area under consideration.. The no. of neurons assumed for the present study are 1 to 5. It is based on trial and error basis.

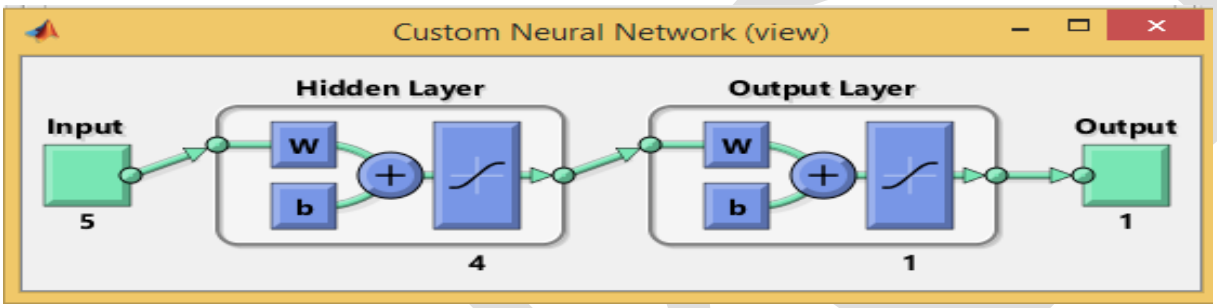

Architecture for the prediction of Leq values by using traffic volume studies as inputs

S.No	Network	No. of Hidden Neurons	R(CORRELATION)			
			Training	Validation	Testing	Overall
1	5-1-1	1	0.981	0.955	0.969	0.977
2	5-2-1	2	0.983	0.980	0.982	0.982
3	5-3-1	3	0.981	0.986	0.981	0.981
4	**5-4-1**	**4**	**0.984**	**0.986**	**0.993**	**0.986**
5	5-5-1	5	0.973	0.979	0.987	0.975

Performance statistics of a Neural network models for the prediction of Leq values

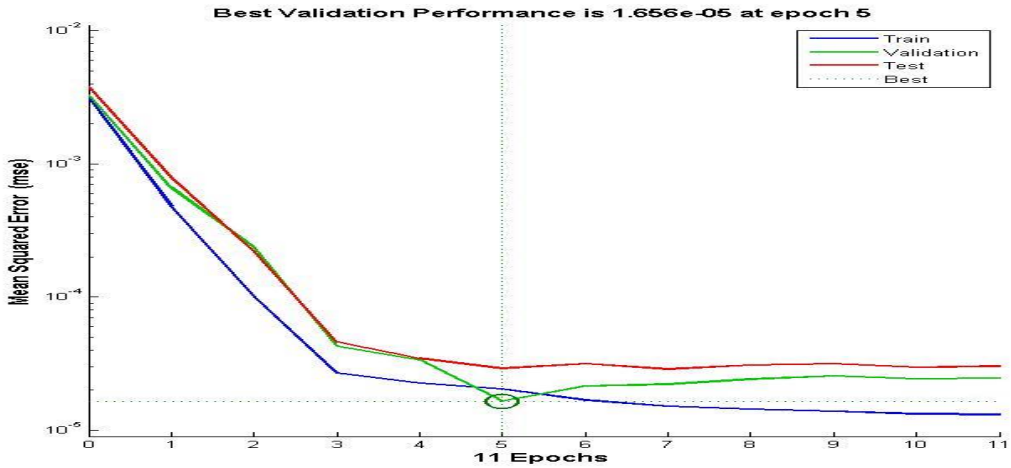
Best Validation Performance is 1.656e-05 at epoch 5
Train
Validation
Test
Best
Mean Squared Error (mse)
11 Epochs

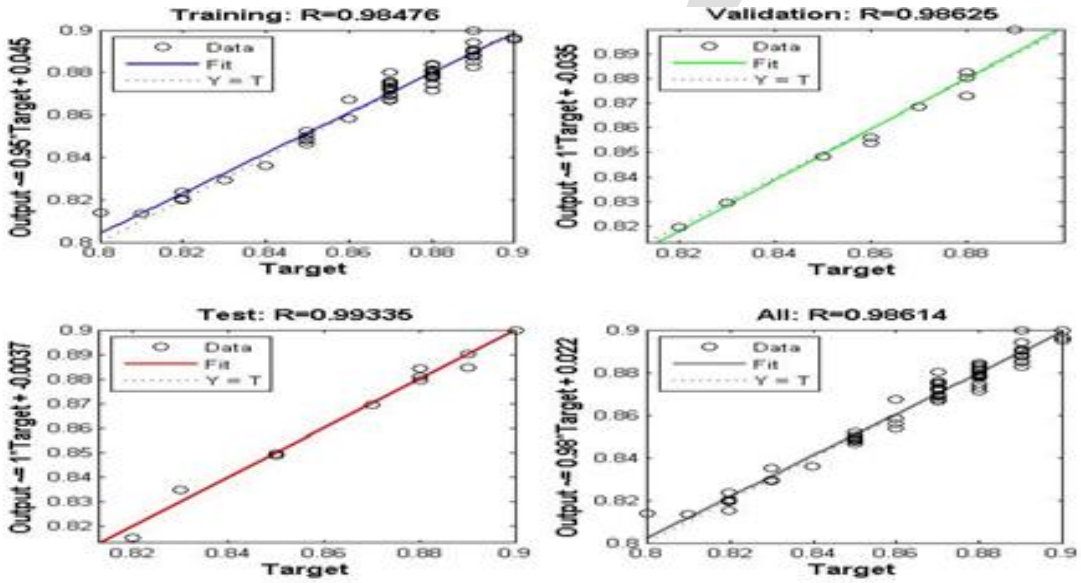
Training: R=0.98476
Validation: R=0.98625
Test: R=0.99335
All: R=0.98614
Data
Fit
Y = T
Output ~= 0.95*Target + 0.045
Output ~= 1*Target + -0.035
Output ~= 1*Target + -0.0037
Output ~= 0.98*Target + 0.022
Target

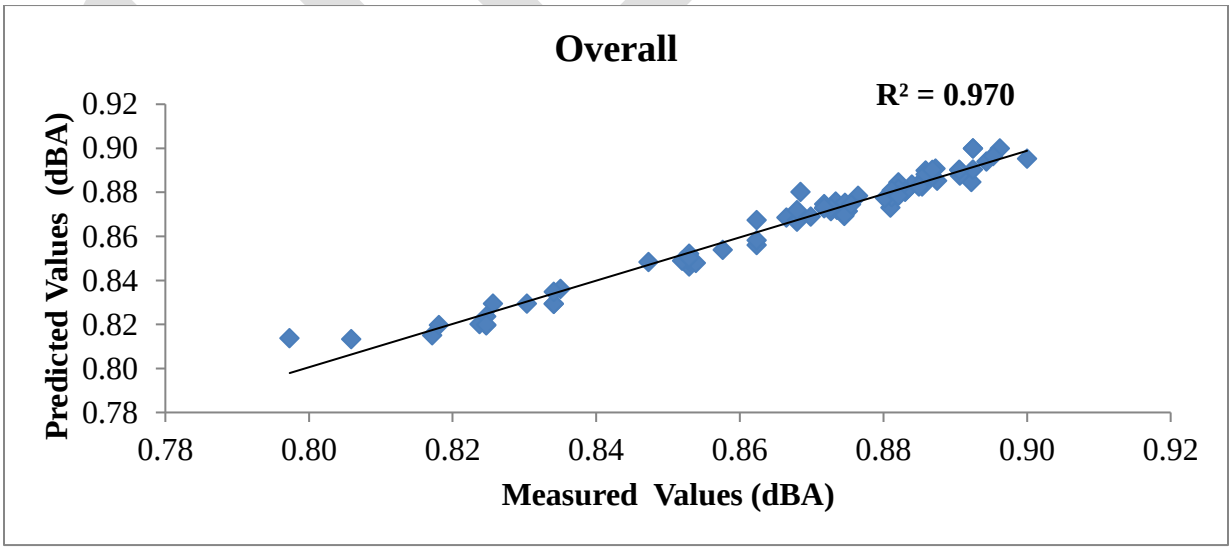
Overall
R² = 0.970
Predicted Values (dBA)
Measured Values (dBA)

Overall regression for Developed mathematical equation	Overall regression for Artificial Neural Network (NN tool)

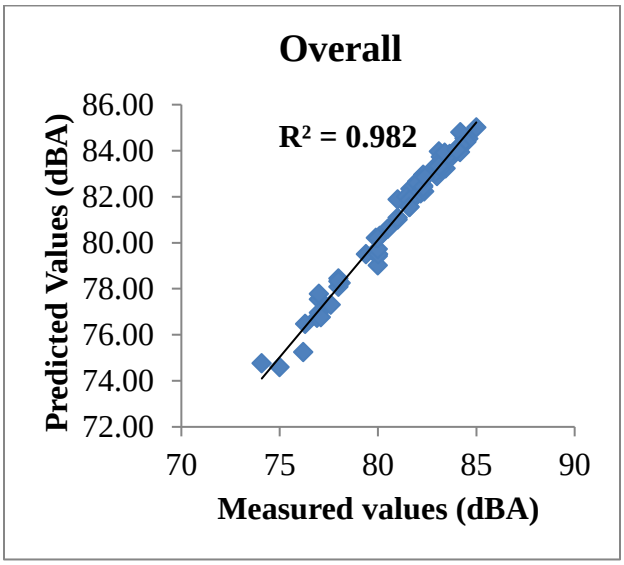

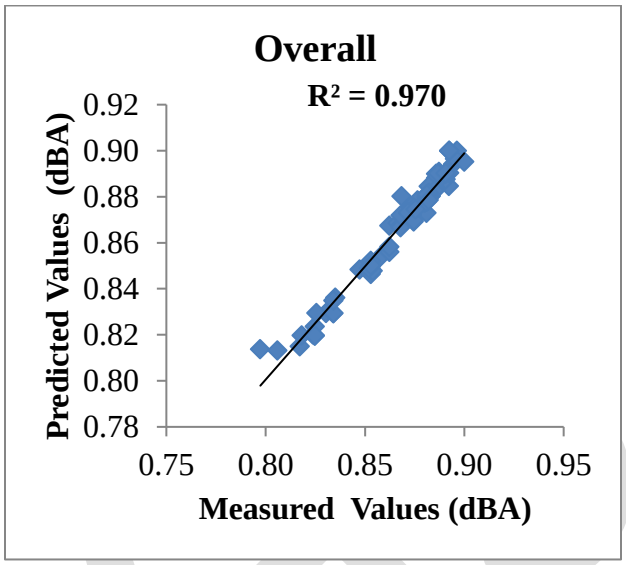

Comparison of regression values between developed Mathematical equation and Artificial neural network (NN tool) .

CONCLUSION

The traffic flow and volume were high during the peak periods, and the highest volume was recorded during both morning and evening timings. The measured noise level in Leq for the studied locations varied between 74 and 85 dB(A), which exceeds Indian guidelines of Noise Pollution Act (1972) of range 70 dB(A). A slight decrease was observed during the early afternoons followed by a gradual increase during the evening times from 4 PM due to increase in the traffic flow. It was observed that the highest and lowest sound pressure levels witnessed in an octave band analysis in the present study were25 Hz and 3150 Hz, respectively. It was observed from the spectral analysis, the lowest Sound Pressure Level recorded was in the range of 17.5 dBA at 25 Hz during the afternoon due to decrease in the traffic volume and the highest value recorded was in the range of 78.1dBA at 3.15 KHz due to the more number of traffic volume during the evening timings and at the same time more or less almost equal sound pressure level was recorded during the morning time also.

From the spectral analysis, it was observed that for all the study period the maximum Sound Pressure Level was recorded at 3.15 KHz frequency which was beyond the permissible limits for the human being which is usually 1 KHz. An equation has been developed by using regression analysis for the prediction of Leq values at the four junctions by taking traffic volumes studies of the study area under consideration. The predicted values from the developed mathematical model was then compared with the measured values to know the validity of the model.

From the graphs it was observed that the R^2 value between the measured values and predicted values at all the four junctions is > 0.9. A neural network had also developed for the prediction of noise levels L_{eq} and the best network 5-4-1 had been proposed. The Regression(R^2) values for Developed Mathematical equation and for Artificial neural network are 0.982 and 0.970. Among the two models (i.e., developed Mathematical equation and Artificial neural network) the developed Mathematical equation given accurate predicted Noise levels. Finally it can be concluded that the suggested Two models could nicely predict the road traffic noise in Tirupati town.

REFERENCES:

[1] Chammireddy AnilKumarReddy et al (2016). Verification of mathematical models for road traffic noise prediction of Tirupati town at leelamahal circle. IJSER.

[2] Gollamandla Sukeerth et al prediction of road traffic noise levels in Tirupati town using analytical models and neural networks. June 2017 | IJIRT | Volume 4 Issue 1 | ISSN: 2349-6002.

[3] John O. Mason performing regression analysis using Microsoft excel International Journal of Arts and Commerce Vol. 1 No.5 PP192-208.

[4] F. Cirianni and G. Leonardi Environmental modeling for traffic noise in urban area, American Journal of Environmental Science, 2012, 8 (4), 345-351

[5] Gollamandala sukeerth et al, (2017) Mathematical Modeling For The Prediction Of Road Traffic Noise Levels In Tirupati Town. 2017 IJEDR | Volume 5, Issue 2 | ISSN: 2321-9939.

[6]. Zoran Petrović1 et al, Application of Neural Networks for Calculation of Intensity of Traffic Noise Sources AIA-DAGA 2013 Merano

International Journal of Engineering Research and General Science Volume 5, Issue 4, July-August, 2017
ISSN 2091-2730

Study of the effect of varying the concentration of zinc sulphate in the PEM on the morphological features of the 1.531211 BMJ24 Jeewanu (both PUOC and PUAC)

Deepa Srivastava

Assistant Professor, Department of Chemistry, S.S.Khanna Girls' P.G. College, Constituent College of Allahabad University, Allahabad 211003, Uttar Pradesh, India

srivastava.deepa@ymail.com

Abstract— The present form of cell as we see it today has undergone evolution of 3.2 billions of years. According to Bahadur and Ranganayaki the earliest living cells was very simple in structure and were full of the properties of biological order. Bahadur in 1967 suggested that the way in which the systems organize themselves with properties of biological order is very important feature of the study of origin of life. Jeewanu, the autopoetic eukaryotes were prepared by Bahadur in 1967.It was observed that when a mixture of Jeewanu and water is exposed to sunlight, water is split up into H_2 and O_2.But due to the nitrogenase like activity of Jeewanu, the produced hydrogen is utilized in the fixation of nitrogen.

The hydrogen produced by the splitting of water is also utilized in the reduction of inorganic carbon. Khare prepared boron molybdenum Jeewanu in 1989 which showed significant water splitting. The presence of certain transitional metal ions e.g. Mn, Co, Zn, Cu and Fe individually in the parental environmental medium of molybdenum Jeewanu activated the water splitting ability of molybdenum Jeewanu. An attempt has been made in this paper to study the effect of addition varying concentrations of $ZnSO_4$ to the PEM on the morphological properties of BMJ24 Jeewanu prepared both under oxygenic (PUOC) and anoxygenic conditions (PUAC).

Keywords— Jeewanu, BMJ24, PEM, $ZnSO_4$, autopoetic, eukaryotes, exposure, Mineral solution, sunlight, PUOC, PUAC, morphology, pyrogallol.

Introduction

INTRODUCTION

The present form of cell as we see it today has undergone evolution of 3.2 billions of years. According to Bahadur and Ranganayaki the earliest living cells was very simple in structure and were full of the properties of biological order. (Bahadur, K and Ranganayaki, S, 1964). [1] To tackle the problem of origin of life, it is essential to know how this earliest cells were synthesized under natural conditions. The molecular or the Chemical Evolution Theory given by Haldane (1929) [2] and Oparin (1924) [3] is the basis of the modern approach to the problem of 'Origin of life'. Bahadur in 1967 suggested that the way in which the systems organize themselves with properties of biological order is very important feature of the study of origin of life. (Bahadur, 1967). [4] The problem of origin of life in investigated basically in order to find out the natural condition under which the replicating, self-sustaining systems were produced. (Blum, 1961, Bahadur and Ranganayaki, 1966). [5,6]

The origin of life can be approached the best way if life and the living systems are considered in the light of functional properties. (Bahadur and Ranganayaki, 1980). [7]

It was observed that when a mixture of Jeewanu and water is exposed to sunlight, water is split up into H_2 and O_2.But due to the nitrogenase like activity of Jeewanu, the produced hydrogen is utilized in the fixation of nitrogen. Kumar in 1982 estimated the fixed nitrogen of the exposed mixture and thus confirmed the fixation of nitrogen by Jeewanu chemically. (Kumar, 1982). [8] The hydrogen produced by the splitting of water is also utilized in the reduction of inorganic carbon. (Smith et al, 1981). [9] They observed that on exposure to light from a mercury lamp, the aqueous mixture of Jeewanu, $NaHCO_3$ and water shows the appearance of ^{14}C in the organic material.

It was observed that the presence of certain transitional metal ions e.g. Mn, Co, Zn, Cu and Fe individually in the parental environmental medium of molybdenum Jeewanu activated the water splitting ability of molybdenum Jeewanu. (Bhattacharya, 1982). [10]

Khare, Y, (1989) studied the effect of addition of zinc to the PEM of 1. ½: 3: 1: 2: 1:1: ¼ BMJ24 Boron Molybdenum Jeewanu and reported that that the PEM having 10 mg of zinc sulphate per 107.5 ml of PEM showed maximum number as well as maximum size of the particles formed. He further observed that the particles produced are less efficient in the splitting of water but more efficient in the fixation of nitrogen. (Khare, Y, 1989). [11]

Bahadur and Ranganayaki (1970) have observed that the organo- molybdenum microstructures are able to split water into hydrogen and oxygen in presence of sunlight and fix molecular nitrogen. [12]

It was observed that addition of sodium chloride in the PEM of BMJ24 Jeewanu, produced particles of larger size and the hydrogen ion formation increased with period of exposure. (Srivastava, D., 1991) [13].

Effect of variation in the concentration of mineral solution, formaldehyde and ammonium molybdate on pH and colour intensity of the PEM of 1.531211 SMJ38 Jeewanu before and after exposure to sunlight was studied by Srivastava, D. [14] - [18]

Effect of irradiation of 1.5312211SMJ29 Silicon Molybdenum Jeewanu PEM with clinical mercury lamp and sunlight on the morphology of the silicon molybdenum Jeewanu was studied by Srivastava. [19]

Effect of addition of Methanol and Ammonium Molybdate to(0+15):30:10:20:10:10 SMJ8 Jeewanu on the morphology, pH and colour intensity of the PEM of the Jeewanu both before and after Exposure to Sunlight up to a Total of 32 Hours was studied by Srivastava, D. [20,21]

Variation in the blue colour intensity and the pH of the PEM of 1.531211SMJ29 silicon molybdenum Jeewanu when the PEM is irradiated with clinical mercury lamp and sunlight" was studied by Srivastava, D. [22]

Srivastava, D., "Study of the effect of addition of Sodium Chloride on the pH and blue colour intensity of the PEM of the BMJ24 Jeewanu" was studied by Srivastava, D. [23]

Study of the effect of NaCl addition on the functional properties of BMJ24 (PUOC) in water and in phosphate buffer of pH 6, 7 and 8 under oxygenic conditions was studied by Srivastava, D. [24]

Study of the effect of NaCl addition to the PEM on the functional properties of BMJ24 Jeewanu prepared under oxygenic conditions (PUOC) in water and in phosphate buffer of pH 6, 7 and 8 under anoxygenic conditions was studied by Srivastava, D. [25]

Study of the effect of NaCl addition to the PEM on the functional properties of BMJ24 Jeewanu prepared under anoxygenic conditions (PUAC) in water and in phosphate buffer of pH 6, 7 and 8 under anoxygenic conditions was studied by Srivastava, D. [26]

This paper deals with the study of the effect of addition of different concentrations of $ZnSO_4$ on the morphological properties of BMJ24 Jeewanu prepared under oxygenic conditions (PUOC) and anoxygenic conditions (PUAC).

EXPERIMENTAL

PROCEDURE:

The following solutions were prepared:

1) 4% (w/v) ammonium molybdate
2) 3% (w/v) diammonium hydrogen phosphate
3) **Mineral solution:** It was prepared by mixing appropriate proportions of different minerals.
4) 36% formaldehyde
5) 3% (w/v) sodium chloride solution,
6) 5% (w/v) sodium borate solution
7) In order to study the effect of zinc on the properties of the BMJ24 Jeewanu a solution of 100 mg of zinc sulphate in 100 ml of distilled water was prepared in addition to the other usual solutions.

Each solution, except formaldehyde, was sterilized in an autoclave at 15 lbs for 15 minutes.

Preparation of alkaline pyrogallol

0.15 ml of 30% aqueous solution of sodium hydroxide and 0.15 ml of 20% aqueous solution of pyrogallol were mixed and thus the alkaline pyrogallol was prepared.

Eight clean, sterilized, dry corning conical flasks of 250 ml capacity were taken and marked from 1 to 8. In each of them, 30 ml of ammonium molybdate solution, 60 ml of diammonium hydrogen phosphate solution, 20 ml of mineral solution, 40 ml of 36% formaldehyde solution, 20 ml of sodium chloride solution and 20 ml of sodium borate were taken. Then the zinc sulphate was added to each flask as follows:

Flask number	1	2	3	4	5	6	7	8
Volume of $ZnSO_4$	0	5	10	20	0	5	10	20

Then in each of the flask labeled 5,6,7 and 8 a test tube half filled with alkaline pyrogallol was kept in such a manner that it stands erect and the solution within the test tube and outside the test tube do not get mixed up. The total volumes of flask number 1, 2, 3, 4, 5, 6, 7 and 8 were 190 ml, 195 ml, 200 ml, 210 ml, 190 ml, 195 ml, 200 ml and 210 ml respectively. The percentage by weight of $ZnSO_4$ in flasks 1 to 8 were 0%, 0.26%, 0.5%, 0.95%, 0%, 0.26%, 0.5%, 0.95% respectively. Then flask numbers 1 to 4 were cotton plugged and flask number 5 to 8 were plugged tightly with rubber cork. Each flask was shaken gently by whirling motion and exposed to sunlight for a total of 24 hours giving four hours exposure daily.

After4hours, 8 hours, 12 hours, 16 hours, 20 hours and 24 hours of exposure, the microscopic observations were done simultaneously. But for flask number 5 to 8, observations were made only after24 hours of exposure to maintain the anoxygenic condition within the flasks.

OBSERVATIONS

TABLE – 1

Effect of different concentrations of $ZnSO_4$ in the PEM of 1.531211 BMJ24 Jeewanu on the yield of the solid material formed in g.

Condition	Yield of the solid material formed in the PEM in g			
	Percentage of $ZnSO_4$ added to the PEM			
	0	0.20	0.50	0.95
Oxygenic	1.0386	0.3880	0.2846	1.0528
anoxygenic	1.0752	0.9354	0.9070	1.1910

TABLE – 2

Effect of addition of different concentrations of $ZnSO_4$ to the PEM of 1.531211 BMJ24 Jeewanu on the number of the particles (SA/View) with increasing period of exposure.

Period of exposure in hours	Oxygenic set			
	Percentage of $ZnSO_4$ added to the PEM			
	0.00	0.26	0.50	0.95
4	50.4± 0.66	21.6± 0.46	31.4± 0.97	61.4± 0.67
8	71.0± 0.63	30.4± 0.24	44.0± 1.37	84.0± 1.09
12	111.0± 0.80	20.6± 0.40	35.2± 2.13	71.0± 0.54
16	131.0± 0.54	51.6± 0.60	61.4± 1.12	96.8± 1.77
20	143.0± 0.73	99.4± 0.40	51.6± 0.87	306.8± 1.77
24	152.6± 1.02	121.2± 0.96	32.8± 1.01	159.4± 0.40
Period of exposure in hours	Anoxygenic Set			
	Percentage of $ZnSO_4$ in the PEM			

	0.00	0.26	0.50	0.95
24	108.6± 0.60	82.4± 1.12	5.2± 0.80	1.6±2.44

TABLE – 3

Effect of addition of different concentrations of $ZnSO_4$ to the PEM of 1.531211 BMJ24 Jeewanu on the size of the particles in µ (SA/View) with increasing period of exposure.

Period of exposure in hours	Oxygenic set			
	Percentage of $ZnSO_4$ added to the PEM			
	0	5	10	20
4	0.25±0.006	0.50±0.009	0.50±0.008	1.50±0.008
8	0.25±0.004	0.50±0.063	0.50±0.114	1.00±0.018
12	0.75±0.108	0.50±0.720	0.25±0.064	0.50±0.062
16	1.00±0.043	0.50±0.014	0.50±0.601	0.75±0.044
20	1.00±0.061	0.50±0.006	0.50±0.005	1.25±0.081
24	1.00±0.042	0.50±0.010	0.25±0.002	1.25±0.001
Period of exposure in hours	Anoxygenic Set			
	Percentage of $ZnSO_4$ in the PEM			
	0.00	0.26	0.50	0.95
24	1.00±0.006	0.75±0.001	0.25±0.004	0.50±0.008

CONCLUSION

The microscopic observations reveal that when 0.26% or 0.50% $ZnSO_4$ was added, the number as well as the average size of the particles decreased. But when the concentration of $ZnSO_4$ was increased to 0.95%, the number as well as average size of the particle increased. The maximum number was 306 and maximum size was 1.25µ which were observed in the BMJ24 (PUOC) having 0.95%$ZnSO_4$ in the PEM after 20 hours of exposure.

It was observed that in all the four cases of PEM with no additional $ZnSO_4$ and with 0.26%, 0.50% and 0.95% additional $ZnSO_4$ prepared under anoxygenic conditions yield was more as compared to the yield obtained under oxygenic conditions. It was further observed that both under oxygenic conditions and anoxygenic conditions the dry weight decreased gradually when 0.26% or 0.50% $ZnSO_4$ was added but when 0.95% additional $ZnSO_4$ was present, the dry weight increased to a large extent.

Further observation was that when 0.26% or 0.50% of additional $ZnSO_4$ was present the number of the particles decreased But when 0.95% $ZnSO_4$ was present the number of the particles

The average size of the particles was also observed to be maximum when 0.95% additional $ZnSO_4$ was present but their number was exceedingly small.

REFERENCES:

[1] Bahadur, K. and Ranganayaki, S., Zbl. Bakt. 117(2), pp 567, 574, 1964.
[2] Haldane, J.B.S., Rationalist Ann.: Science and Human Life, Harper Bros, New York and London, (1933), pp 148-49, 1929.
[3] Oparin, A.I., Proiskhozhdenie zhizni, Izd.Moskovskii Robochii, Moscow, 1924.
[4] Bahadur, K., Zbl. Bakt. 121(2), pp 291-319, 1967.
[5] Blum, H.F., American Scientist, 49(4), pp 474-479, 1961.
[6] Bahadur, K. and Ranganayaki, S., Vijanana Parishad Anusandhan Patrika, 9(4), pp 171-82, 1966.
[7] Bahadur K. and Ranganayaki S., "Origin of life, a functional approach", M/S Ram Narain Lal and Beni Prasad, Allahabad, India, 1980.
[8] Kumar, S., "Studies in the Photochemical Molecular Evolution in Aqueous Systems", D.Phil. Thesis, Dept. of Chem. Univ. of Allahabad, Allahabad, India, 1981.
[9] Smith A.E., Folsome C. and Bahadur K., Experientia, 37, pp 357, 1981.
[10] Bhattacharya, S., "The study of Cytology of the primitive autotrophs", D.Phil. Thesis, Dept. of Chem. Univ. of Allahabad, Allahabad, India, 1982.
[11] Khare, Y., "Photochemical Splitting of Water by Organo- Molybdenum Jeewanu", D.Phil. Thesis, Dept. of Chem. Univ. of Allahabad, Allahabad, India, 1989.
[12] Bahadur, K. and Ranganayaki, S. , J. Brit. Interplanetary Soc., Vol. 23(12), 813-829, 1970.
[13] Srivastava, D., "Study of the kinetics of Jeewanu the Autopoetic Eukaryote", D.Phil. Thesis, Dept. of Chemistry, Univ. of Allahabad, Allahabad, India, 1991.
[14] Srivastava. D., "Study of the Effect of Variation in the Concentration of Mineral Solution in the PEM of 1.531211SMJ 38 before and after Exposure to Sunlight, on Morphology of 1.531211 SMJ 38". Int J Recent Sci Res. 7(4), pp. 10648-10651, ISSN number: 0976-3031, 2016.
[15] Srivastava. D., " Effect of variation in the concentration of mineral solution on pH and colour intensity of the PEM of 1.531211 SMJ38 Jeewanu before and after exposure to sunlight" , International Journal of Innovative Research in Science, Engineering and Technology (An ISO 3297: 2007 Certified Organization), (IJIRSET), vol. 5, Issue 5, May 2016, pp 8065 8068. DOI: 10.15680/IJIRSET. 2016. 0505111, ISSN number: 2319-8753, 2016.
[16] Srivastava. D., "Effect of Addition of Higher Concentration of Mineral Solution in the PEM on the colour intensity and the pH of the PEM during the formation of the Silicon Molybdenum Jeewanu SMJ8", Journal of International Academy of Physical Sciences(IAPS), Vol. 14 No.1 (2010), pp. 131-136, ISSN number: 0974-9373, 2010.
[17] Srivastava. D., " Effect of increase of concentration of formaldehyde in the PEM of 1.531211 SMJ8 on the proton release and degree of Mo^{6+} reduction to Mo^{4+} during the exposure to sunlight", Journal of Natural science Research (JNSR) published by(IISTE), Vol 2, No.7, 2012, pp 56-59, ISSN number: 2225-0921, 2012.
[18] Srivastava. D., "Effect of variation in the concentration of ammonium molybdate in the parental environmental medium (PEM) on the pH and the photochemical reduction of Mo 6+ to Mo 4+ in the PEM of the Silicon Molybdenum Jeewanu 1.531211 SMJ8 both before and after exposure" , International Journal of Scientific and Engineering Research (IJSER), Vol 3, Issue 6, June-2012,pp750-754. DOI: 10. 14299/000000, ISSN number: 2229-5518, 2012.
[19] Srivastava, D., "Effect of irradiation of the PEM of 1.531211SMJ29 Jeewanu with clinical mercury lamp and sunlight of the morphological features of the silicon molybdenum Jeewanu" , International Journal of Engineering Research and General Science (IJERGS), Vol. 4,Issue 4, pp.372-376, ISSN number: 2091-2730, 2016.
[20] Srivastava, D., "Morphological changes in (0 +15):30:10:20:10:10 SMJ8 Jeewanu on adding methanol and ammonium molybdate to the PEM of the Jeewanu both before and after exposure to Sunlight up to a total of 32 hours" published in International Journal of Advanced Research (Int.J.Adv.Res.), vol.4, issue 8, 2016, pp1612-1614. DOI: 10.21474/IJAR01/1370, ISSN number: 2320-5407, 2016.
[21] Srivastava, D., "Effect of addition of Methanol and Ammonium Molybdate to (0+15):30:10:20:10:10 SMJ8 Jeewanu on the pH and colour intensity of the PEM of the Jeewanu both before and after Exposure to Sunlight up to a Total of 32 Hours", International Journal of Innovative Research in Science, Engineering and Technology (An ISO 3297: 2007 Certified Organization), (IJIRSET), vol. 5, Issue 8, August 2016, page15500-15504. DOI: 10.15680/IJIRSET. 2016. 0508201, ISSN number: 2319-8753, 2016.
[22] Srivastava, D., "Variation in the blue colour intensity and the pH of the PEM of 1.531211SMJ29 silicon molybdenum Jeewanu when the PEM is irradiated with clinical mercury lamp and sunlight" published in International Journal of Engineering Research and General Science (IJERGS), ISSN: 2091-2730, Vol. 4, Issue 5, pp.22-25, ISSN number: 2091-2730, 2016.
[23] Srivastava, D., "Study of the effect of addition of Sodium Chloride on the pH and blue colour intensity of the PEM of the BMJ24 Jeewanu" published in International Journal of Innovative Research in Science, Engineering and Technology (An ISO 3297: 2007 Certified Organization), (IJIRSET), vol. 5, Issue 9, September 2016, pp 16819-16824. DOI: 10.15680/IJIRSET. 2016.0509044, ISSN number: 2319-8753, 2016.
[24] Srivastava, D., "Effect of NaCl addition to the PEM on the functional properties of BMJ24 Jeewanu prepared under oxygenic conditions (PUOC) in water and in phosphate buffer of pH 6, 7 and 8 under oxygenic conditions." published in International Journal of Innovative Research in Science, Engineering and Technology (An ISO 3297: 2007 Certified

Organization), (IJIRSET), vol. 5, Issue 10, October 2016, pp 18666-1871. DOI: 10.15680/IJIRSET. 2016.0510088., ISSN number: 2319-8753, 2016.

[25] Srivastava, D., "Study of the effect of NaCl addition to the PEM on the functional properties of BMJ24 Jeewanu prepared under oxygenic conditions (PUOC) in water and in phosphate buffer of pH 6, 7 and 8 under anoxygenic conditions." published in International Journal of Innovative Research in Science, Engineering and Technology (An ISO 3297: 2007 Certified Organization), (IJIRSET), vol. 5, Issue 11, November 2016, pp 20046-20052. DOI: 10.15680/IJIRSET. 2016.0511081, ISSN number: 2319-8753, 2016.

[26] Srivastava, D., "Study of the effect of NaCl addition to the PEM on the functional properties of BMJ24 Jeewanu prepared under anoxygenic conditions (PUAC) in water and in phosphate buffer of pH 6, 7 and 8 under anoxygenic conditions." published in International Journal of Innovative Research in Science, Engineering and Technology (An ISO 3297: 2007 Certified Organization), (IJIRSET), vol. 5, Issue 12, December 2016, pp 21135-21140. DOI: 10.15680/IJIRSET. 2016.0512040, ISSN number: 2319-8753, 2016.

International Journal of Engineering Research and General Science Volume 5, Issue 4, July-August, 2017
ISSN 2091-2730

Flexural Behaviour of Concrete Beams Reinforced with Biaxial Geogrid

Rakendu K [1], Anagha Manoharan [2]

[1] PG Scholar, Dept of Civil Engineering, Universal Engineering College, Vallivattom, Thrissur, Kerala, India.

[2] Assistant professor, Dept of Civil Engineering, Universal Engineering College, Vallivattom, Thrissur, Kerala, India.

[1]krakendu6070@gmail.com

[2]anaghamanoharan99@gmail.com

Abstract— Geogrid is a new material used as reinforcement in structural members therefore it is necessary to identify the benefits and feasibility of using geogrids in concrete. This work deals with the flexural behaviour of plain cement concrete beams reinforced with biaxial geogrid in one, three and five layers for three different mixes. The experimental program consisted of testing thirty four geogrid concrete beams and six control beam specimens under two-point loading. The test results are presented in terms of ultimate load carrying capacity, flexural strength behaviour, load deflection behaviour and crack patterns. The two point bending test on geogrid beams reveals that strength of geogrid and number of layers plays a crucial role in enhancing load carrying capacity and flexural strength.

Keywords— Portland cement concrete, Geogrids, Biaxial Geogrid, Flexural strength, Load deflection, Crack pattern, Types of geogrid.

INTRODUCTION

Concrete is the most common and widely used structural material in the construction world. It is more versatile but modern day engineering structures require more demanding concrete owing to the huge applied load on smaller area and increasing adverse environmental conditions [13].

Geosynthetics is the term used to describe a range of generally polymeric products used to solve civil engineering problems. The term is generally regarded to encompass six main product categories: Geotextiles, Geogrids, Geonets, Geomembranes, Geofoam and Geocomposites. Geosynthetics are available in a wide range of forms and materials, each to suit a slightly different end use. These products have a wide range of applications and are currently used in many civil, geotechnical, transportation, hydraulic, and private development applications including roads, airfields, railroads, and embankments, retaining structures, reservoirs, canals, dams, erosion control, sediment control, landfill liners, landfill covers, mining, aquaculture and agriculture [12].

Geogrids can be categorized as geosynthetic materials that are used in the construction industry in the form of a reinforcing material. It can be used in the soil reinforcement or used in the reinforcement of retaining walls and even many applications of the material are on its way to being flourished. The high demand and application of geogrids in construction are due to the fact that it is good in tension and has a higher ability to distribute load across a large area.The geosynthetic material, geogrids, are polymeric products which are formed by means of intersecting grids. The polymeric materials like polyester, high density polyethylene and polypropylene are the main composition of geogrids [26].

These grids are formed by material ribs that are intersected by their manufacture in two directions: one in the machine direction (md), which is conducted in the direction of the manufacturing process. The other direction will be perpendicular to the machine direction ribs, which are called as the cross machine direction (cmd). These materials form matrix structured materials. The open spaces, as shown in the above figure, due to the intersection of perpendicular ribs are called as the apertures. This aperture varies from 2.5 to 15cm based on the longitudinal and transverse arrangement of the ribs. Among different types of geotextiles, geogrids are considered stiffer. In the case of geogrids, the strength at the junction is considered more important because the loads are transmitted from adjacent ribs through these junctions. The geogrid serves the function of holding or capturing the aggregates together. This method of interlocking the aggregates would help in an earthwork that is stabilized mechanically. The apertures in the geogrid help in interlocking the aggregates or the soil that are placed over them. A representation of this concept is shown below [17].

Fig. 1 Representation of geogrid confining the aggregates

SIGNIFICANCE OF THE WORK

A. Scope of the Work

The study reveals that using geosynthetic materials as reinforcement in concrete beams is a new promising technology that could enhance the flexural strength of beams. The main problem associated with the steel reinforcement is corrosion that will affect the life and durability of the concrete structures. Many materials act as a substitute to steel reinforcement in truculent environment. As a new innovation geogrids are used as reinforcement in concrete, but the studies using on these are very few. In addition, these studies did not include more number of layers of geogrid. Therefore the flexural behaviour of beams reinforced with more number of layers of geogrid are needed to be investigated for knowing the potential of using geogrids in structural members.

B. Objective of the Work

The objective is to introduce a new dimension in the employment of geosynthetics in structural engineering and to assess the feasibility and benefits of using geogrids in concrete.

C. Methodology

The methodology of the work consists of:

(1) Preliminary test on materials
(2) Mix design for M20, M30, M40 grade PCC
(3) Casting of control specimens and geogrid beams using one, three and five layers.
(4)Conducting two point loading test using 30t loading frame.
(5) Study on the obtained results

MIX DESIGN

Table 1 Concrete Mix Design

SI.No	Concrete Mix Design Quantities	
1	Grade of concrete	M20,M30,M40
2	Type of exposure	Moderate
3	Sp. Gravity of cement	3.15
4	Coarse aggregate (20mm)	2.95
5	Fine aggregate	2.67

Table 2 Result of mix proportions

Mix	Cement	Fine Aggregate	Coarse Aggregate	Water	Ratio
M20	383.16	591.54	1337.19	191.58	1:1.54:3.5:0.5

M30	348.33	873.81	989.32	191.58	1:2.5:2.84:0.55
M40	478.95	774.99	1080.99	191.58	1:1.62:2.25:0.4

Table 3 Properties of Geogrids

Parameters	100S
Minimum average tensile strength - longitudinal direction	100 kN/m
Tensile strength at 2% strain- longitudinal	20 kN/m
Tensile strength at 5% strain- longitudinal	40kN/m
Minimum average tensile strength- transverse direction	100 kN/m
Tensile strength at 2% strain- transverse	18 kN/m
Tensile strength at 5% strain- transverse	36 kN/m
Typical junction strength efficiency	95%

EXPERIMENTAL INVESTIGATION

A. Experimental Procedure

The experimental investigation of this project includes thirty eight (38) beams. Six (6) beams were cast as control specimens with traditional stirrups using PCC mix. The longitudinal reinforcement is calculated using IS 456-2000 code and is equal for all beams. The main bottom reinforcement was provided with 12 mm diameter bars and 6mm diameter bars were used as stirrups.

In case of geogrid beams the reinforcement are provided in layers, which are provided based on varying the u/B ratio,

Where, u = distance from the neutral axis to the top of the layer,
B = width of the beam.

The geogrid layers are placed throughout the beam, i.e. the width of the geogrid layer is taken same as the width of the beam. Geogrid layers are provided only below the neutral axis.

Table 4 Test matrix

Mix	Plain Concrete Cement	Geogrid Beam		
		100S		
		100G1	100G3	100G5
M20	2	2	2	-
M30	2	2	2	2
M40	2	2	2	2
Total	22Beams			

B. Test Procedure

Flexural strength is one measure of the tensile strength of concrete. It is measure of an unreinforced concrete beam or slab to resist failure in bending. It is measured by loading 150 x150 mm concrete beams with span length of at least three times the depth [13].

The flexural strength of the specimens was tested using a 30 ton loading frame. A dial gauge was attached at the bottom of the beam to determine the deflection at the centre of the beam. For the testing of the specimen the supports are provided at a distance of 130mm

from the edges of the beam. The effective span of the beam is taken as 990 mm in the case of 1250 mm beam. A proving ring of 500 kN isconnected at the top of the beam to determine the load applied. The following figure shows the schematic set up of testing.

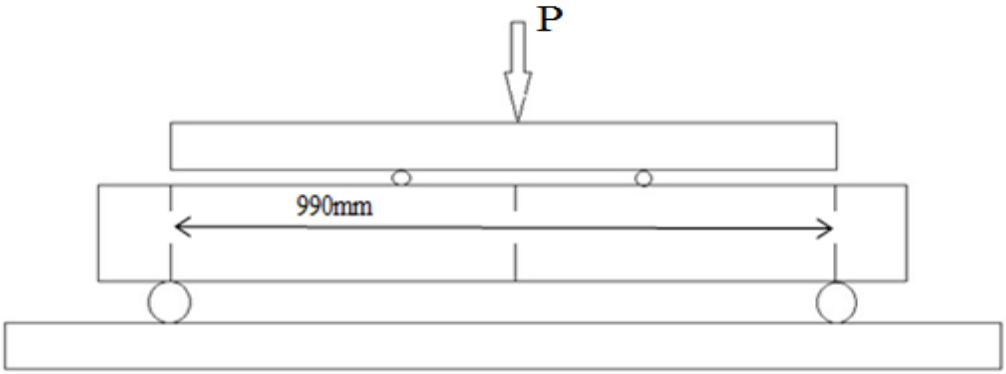

Fig.2 Schematic Set Up of Testing

The flexural strength of the beam is tested as two point loading system using a hydraulic jack attached to the loading frame. The behaviour of beam is keenly observed from beginning to the failure. The loading was stopped when the beam was just on the verge of collapse. The first crack propagation and its development and propagation are observed keenly. The values of load applied and deflection is noted directly and further the load vs. deflection is plotted. The load in kN is applied by uniformly increasing the value of the load and the deflection under the different applied loads is noted. The applied load is increased up to the breaking point or till the failure of the material [13].

Flexural strength of beams are calculated by using the formula; [11]

$$\sigma = \frac{3P(L - L_i)}{2bd^2} \qquad \text{(Eqn.1)}$$

Where, P is ultimate load (kN),
L is distance between the supports (mm),
L_i is distance between loads (mm),
b is width of beam (mm)
d is depth of beam (mm)

EXPERIMENTAL RESULTS

A. Ultimate Load Carrying Capacity

Ultimate strength of beams was the maximum load indicated by the proving ring at the time of loading. From the results it was found that the geogrid beam reinforcer with five layers exhibit more load carrying capacity than conventional beams. 100G1 and100G3 exhibits less load carrying capacity than the plain concrete beam in case of all the three mix.

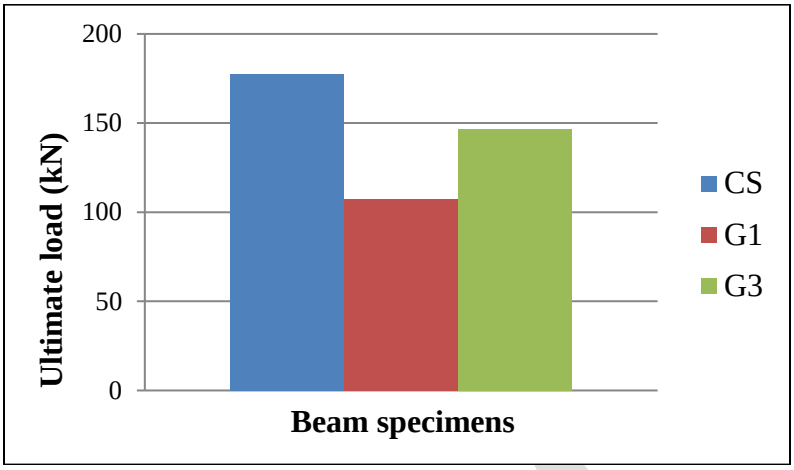

Fig.3 Ultimate Load of Beam with M20 mix

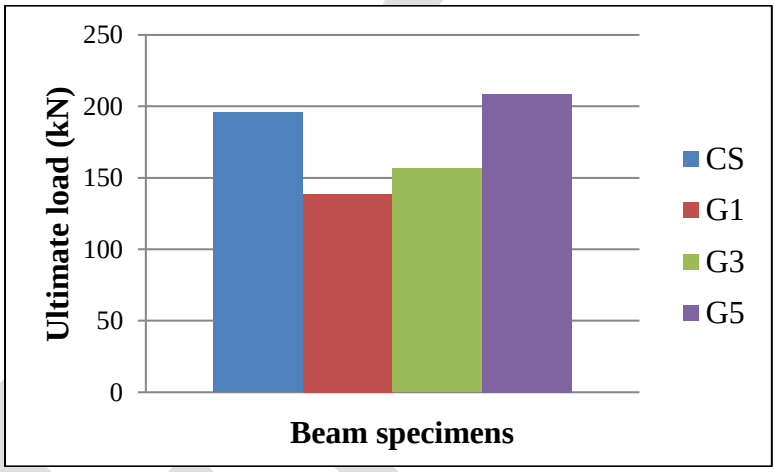

Fig.4 Ultimate Load of Beam with M30 mix

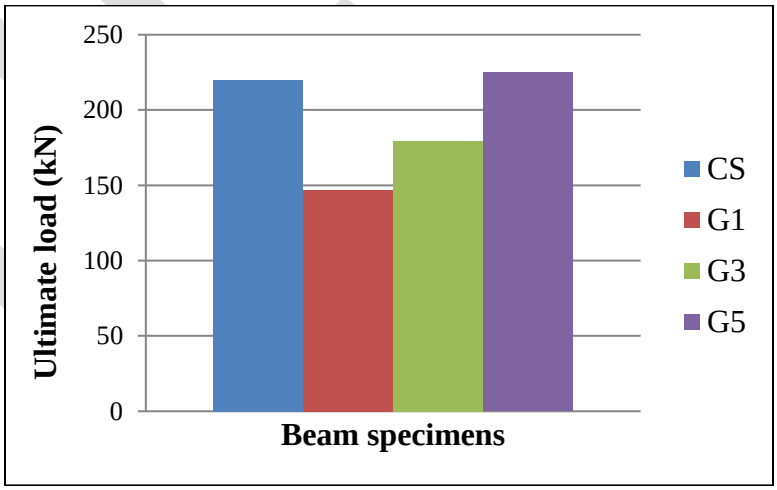

Fig.5 Ultimate Load of Beam with M40 mix

B. Flexural Strength Behaviour

The flexural strength of the beam under two point loading was calculated using Eqn.1. It was found that there is a slight difference in the flexural strength of solid control beam and geogrid reinforced beams. The flexural strength of the control beams and geogrid beams are given in Table 5. From the results it is observed that 100G1, 100G3 and 100G5 shows less flexural strength than the conventional beam.

Table 5 Flexural strength of beams

Mix	Plain Concrete Beam	Geogrid Beams		
		100G1	100G3	100G5
	Flexural strength in N/mm^2			
M20	41.05	23.18	31.6	-
M30	45.2	29.85	33.72	44.96
M40	50.85	31.61	38.64	48.47

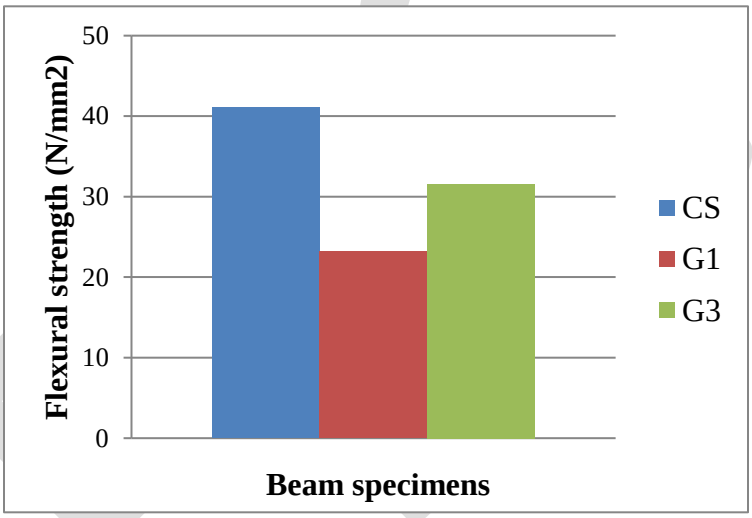

Fig.6 Flexural strength of geogrid and control beams for M20

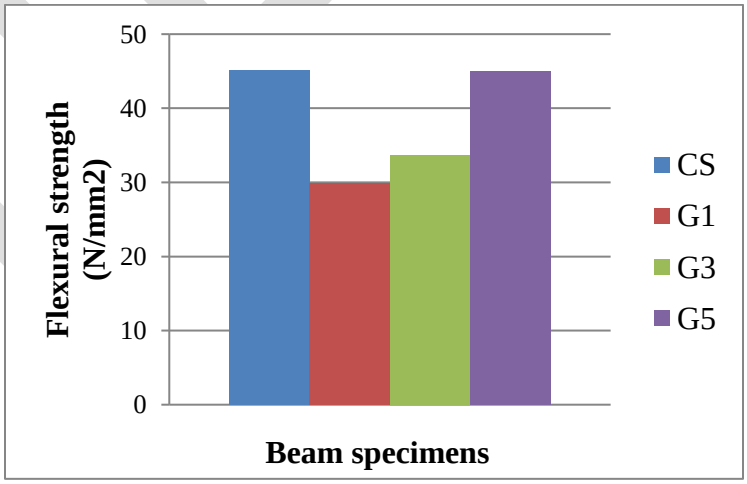

Fig.7 Flexural strength of geogrid and control beams for M30

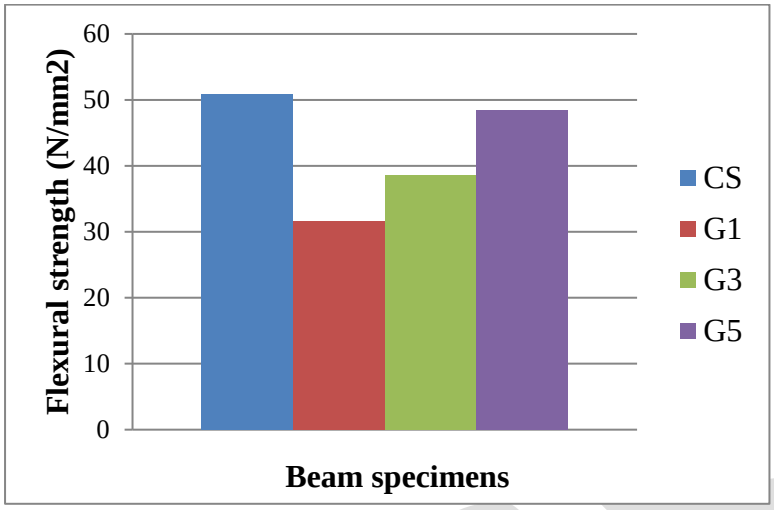

Fig.8 Flexural strength of geogrid and control beams for M40

C. Load Deflection Behaviour

Due to increase in the load, deflection of the beams starts, up to certain level the load vs. deflection graph will be linear ie. load will be directly proportional to deflection. Due to further increase in the load, the load value will not be proportional to deflection, since the deflection values increases as the strength of the materials goes on increasing material loses elasticity and undergoes plastic deformation. Fig. 9 to fig.12 shows the load deformation graph for contol and geogrid reinforced beams for various mix.

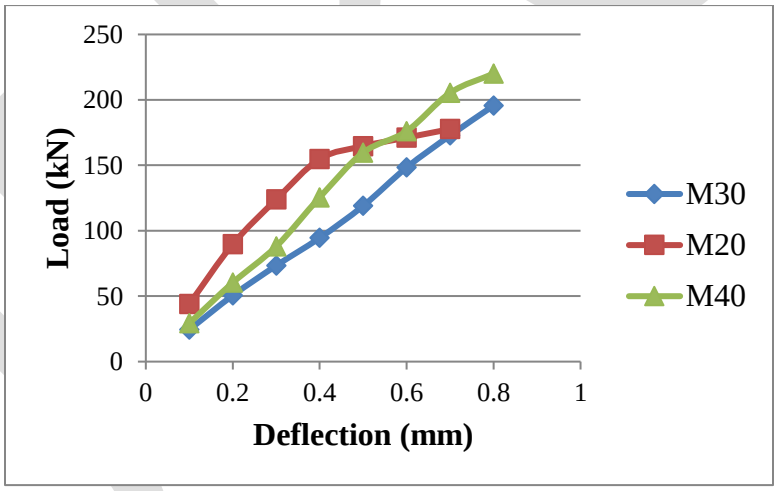

Fig.9 Load-deflection curve for control specimens

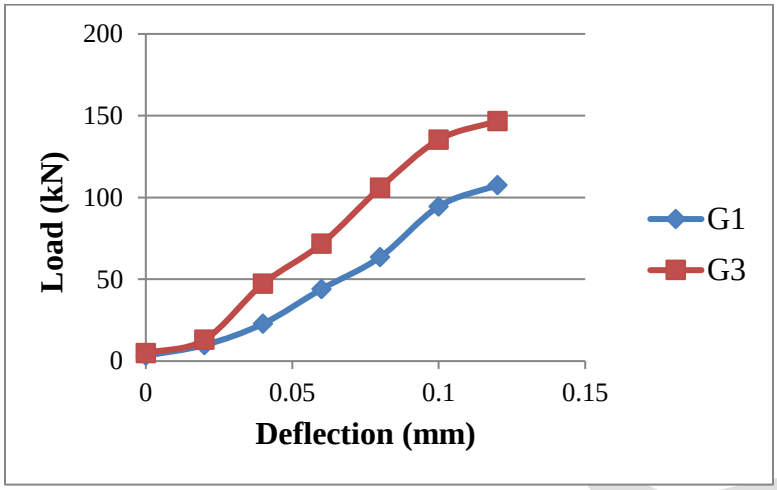

Fig.10 Load-deflection curve for M20 concrete

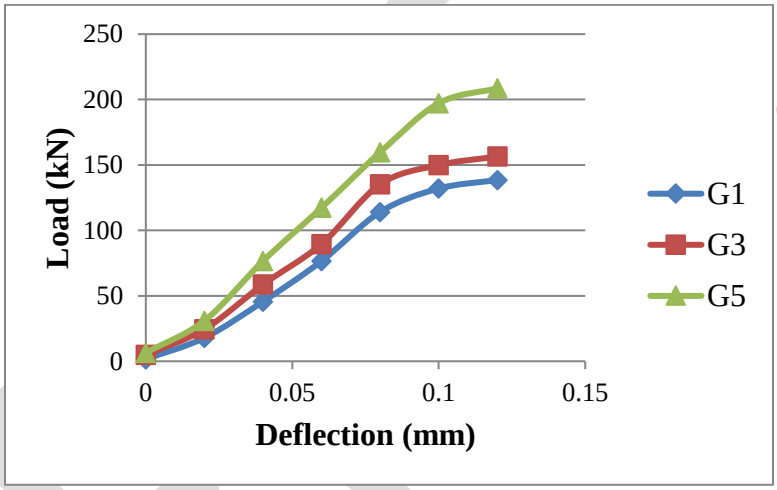

Fig.11 Load-deflection curve for M30 concrete

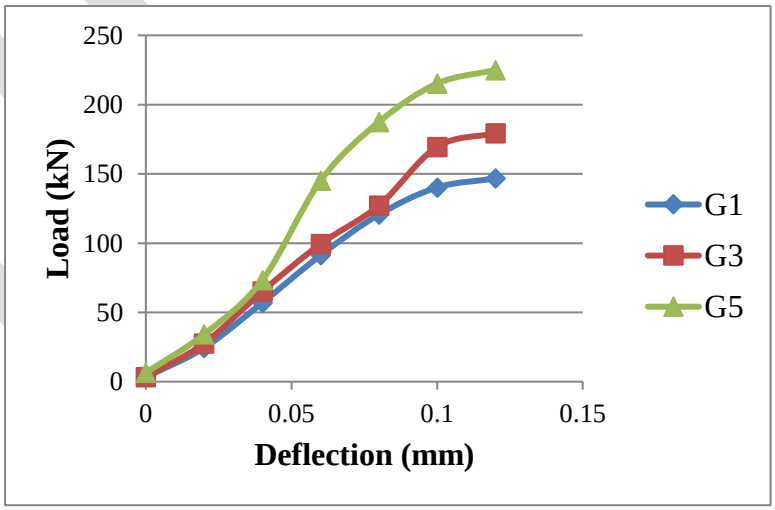

Fig.12 Load-deflection curve for M40 concrete

D. Crack Pattern

The crack pattern for all the geogrid beams and control beams are shown below. It is observed that only flexural cracks were formed in both control beams and in geogrid beams. In case of geogrid beams the cracks were initiated from the bottom of the beam and cracked all the way to the top of the specimen, these cracks appeared only in the middle section of the beam. It can be seen from Fig.14 and Fig.18 the geogrid beam reinforced with one layer separated into two parts directly upon failure of concrete, while the reinforced beam with more layers remained intact as the crack initiated and cracked all the way to the top of the specimen.

Fig.13 Crack pattern for M30 control beam

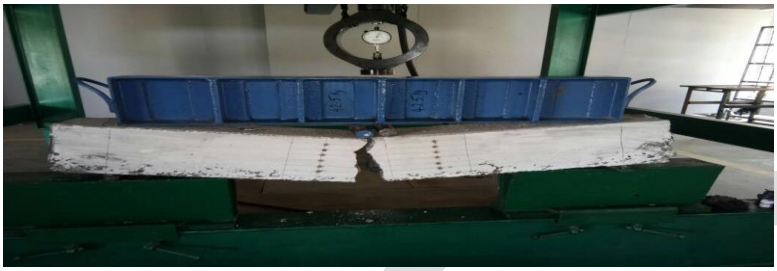

Fig.14 Crack pattern for 100G1 of M30

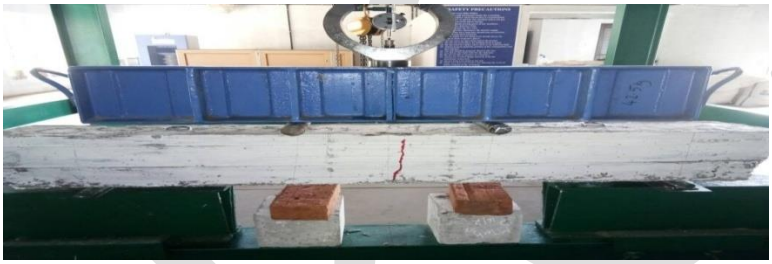

Fig.15 Crack pattrern for 100G3 of M30

Fig.16 Crack pattern for 100G5 of M30

Fig.17 Crack pattern for M40 control beam

Fig.18 Crack pattern for 100G1 of M40

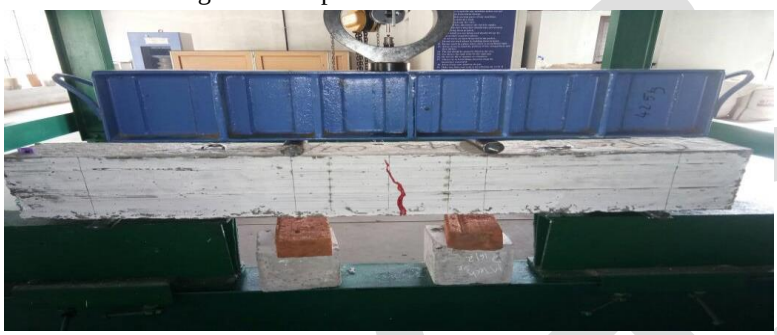

Fig.19 Crack pattern for 100G3 of M40

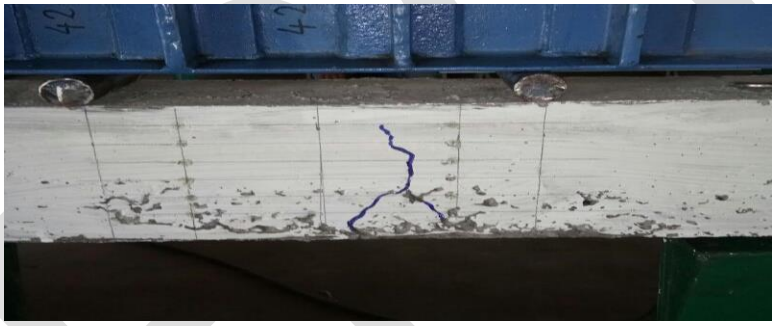

Fig.20 Crack pattern for 100G5 of M40

ACKNOWLEDGMENT

My whole hearted gratitude to Mrs. Anagha Manoharan, Assistant Professor who has believed in me since the beginning and accepted in undertaking my research work and for her constant guidance, support and encouragement throughout my research work.

Gracious gratitude to all teaching and non-teaching staffs of Department of Civil Engineering, Universal Engineering College for offering me the opportunity to do this research work.

Finally, deep thanks to God for his unconditional support and also honorable mention goes to my family and friends for their wholehearted support that help me greatly in completing my work.

CONCLUSIONS

Based on the findings from the beam flexure tests performed, the following conclusions can be drawn from the use of geogrid as reinforcement for concrete sections

1. The tensile strength of geogrid and number of layers used plays a major role in flexural behaviour and load carrying capacity of beams.

2. Beams reinforced with more number of layers of geogrid exhibits a good result in load carrying capacity and provide a flexural strength which is only 2.6% less than the control beams.
3. Load carrying capacity is more when five layers of geogrid is used in plain cement concrete beams.
4. In case of load carrying capacity an average of 4.4% increase is shown by the geogrid beams reinforced with 100G5.
5. Geogrid can take tensile forces when these are kept in plain cement concrete beams.
6. Deflection can be reduced by the use of geogrid in beams.
7. Cracks appeared only in the middle section of the beam i.e. only flexural cracks are formed for all the beams reinforced with geogrid.
8. The confining effect of geogrid plays a major role in the properties of concrete.
9. The variation in flexural strength may be due to experimental errors like improper compaction which might have lead to weak bonding between aggregate and geogrid.

REFERENCES:

[1] Aluri Anil Kumar, Y. Anand Babu, (2015), **"**A Complete Study On Behaviour Of Concrete Columns By Using Biaxial Geogrid Encasement " *International Journal of Civil Engineering*, Volume 2, Issue 9, September 2015.

[2] Binata Debbarma & Dr.Sujit Kumar Pal *(2015), "* Shear Strength of fly Ash Reinforced with Non- Woven and Woven Geotextiles*", International Journal of Engineering & Technology*, Vol. 4, 2015, pp. 951-958.

[3] Erol Tutumluer, Hai Huang, Xuecheng Bian, (2012), "Geogrid-Aggregate Interlock Mechanism Investigated through Aggregate Imaging-Based Discrete Element Modeling Approach" *International Journal Of Geomechanics* © Asce / July/August/ 2012 / 391.

[4] F. El Meski and G. R. Chehab (2014), "Flexural Behavior of Concrete Beams Reinforced with Different Types of Geogrids" *Journal of Materials in Civil Engineering*, © ASCE / AUGUST 2014.

[5] Ir. Zakaria Che Muda, Dr. Salah F. A. Sharif , Tan Yen Lun, (2012), " Impact Behavior Enhancement Of Oil Palm Shells Concrete Slab By Geogrid Reinforcement" *International Journal of Scientific & Engineering Research*, Volume 3, Issue 11, November-2012

[6] Khodaii A, Fallah.S, "Effects of geo-synthetic reinforcement on the propagation of reflection cracking in asphalt overlays", *International journal of Civil Engineering*, 2009, 7(2), 131–140.

[7] Manas Mohanty, Dr.C.R. Patra, (2007), " Behavior Of Strip Footing On Multi Layered Geogrid Reinforced Sand Bed" *Final Report*, Dept. of Civil Engineering National Institute of Technology ,Rourkela.

[8] Miguel A. Pando, Robert H. Swan, Youngjin Park, and Scott Sheridan (2014). "Experimental study of bottom coal ash geogrid interaction" *Geo-Congress 2014 Technical Papers.*

[9] Munir D. Nazzal, Murad Abu-Farsakh and Louay N.Mohammad (2007). " Evaluation of Geogrid benefits using monotonic and repeated load triaxial tests" *Journal of Materials in Civil Engineering* ,ASCE.

[10] R. Siva Chidambaram and Pankaj Agarwal (2014), "The confining effect of geo-grid on the mechanical properties of concrete specimens with steel fiber under compression and flexure*" Journal of Construction and Building Materials,* Elsevier Ltd, 71 (2014) 628–637.

[11] S.Shobana and G.Yalamesh (2015), "Experimental Study of Concrete Beams Reinforced with Uniaxial and Biaxial Geogrids" *International Journal of ChemTech Research* Vol.8, 2015, pp 1290-1295.

[12] Saranyadevi M, Suresh M and Sivaraja M (2016), "Strengthening of Concrete Beam by Reinforcing with Geosynthetic Materials*" International Journal of Advanced Research in Education & Technology* Vol.3, 2016, pp 2394-6814.

[13] Shetty, M. S. (2014), " Concrete Technology Theory and Practice" *S. CHAND & COMPANY LTD.*

[14] S. Soji and P. Anima, (2016) Experimental and Analytical Investigation on Partial Replacement of Concrete in the Tension Zone, *IJERGS*, Vol 4, Isssue 4, pages 23-32.

[15] Zakaria Che Muda.Ir, Dr. Salah F. A. Sharif and Ng Jun Honga, (2012), "Flexural Behavior Of Lightweight Oil Palm Shells Concrete Slab Reinforced With Geogrid*", International Journal of Scientific & Engineering Research*, Vol.3, 2012, pp 1-18.

[16] https://www.scribd.com-document-Secugrid.com

[17] https://theconstructor.org

International Journal of Engineering Research and General Science Volume 5, Issue 4, July-August, 2017
ISSN 2091-2730

OPTIMIZATION AND COMPUTATIONAL FLUID ANALYSIS OF RAMP IN SCRAMJET INLET TO INCREASE COMPRESSION EFFICIENCY

SAHAYA PRINCE.D, FAZLUDEEN.J, SUDHARSAN.S & UTHAYA KUMAR.N

Dept. of Aeronautical Engineering, Infant Jesus College Of Engineering,
Tuticorin, Tamilnadu, India.

ABSTRACT: In our project we have re-designed the rectangular type scramjet inlet in comparison of different ramp angles by making shock trains formed in isolator region for compression that happens inside the inlet has analysed through Computational Fluid Analysis with the airflow of high mach number passing over on it. Using CATIAV5 for designing the scramjet engine and by ANSYS-Workbench the followed designing of inlet through GEOMETRY (Design Modeler) and meshing by MESH (ICEM-CFD) & FLUENT analysis has been done for analyzing/checking the flow reactions. By re-designing an inlet which makes the compression that possibly efficient internally for such high mach number 10. The optimization of our project helps knowing all the aspects of and about ramp angle implementing to increase the compression efficiency.

Key Words: CATIAV5, ANSYS, Ramp Angle, K-ε Turbulence Model

Introduction:

A supersonic combustion ramjet (scramjet) is a variant of a ramjet air-breathing combustion jet engine. The definition of ramjet engine is first necessary, as a scramjet engine is a direct descendant of a ramjet engine. Ramjet engines have no moving parts, instead operating on compression to slow free stream supersonic air to subsonic speeds, thereby increasing temperature and pressure and then combusting the compressed air with fuel. Finally, a nozzle accelerates the exhaust to supersonic speeds, resulting in thrust.

Due to the deceleration of the free stream air, the pressure, temperature and density of the flow entering the burner are “considerably higher than in the free stream”. At flight Mach numbers of around Mach 6, these increases make it inefficient to \continue to slow the flow to subsonic speeds. Thus, if the flow is no longer slowed to subsonic speeds, but rather only slowed to acceptable supersonic speeds, the ramjet is then termed as supersonic combustion ramjet, resulting in the acronym scramjet. To study the inlet performance, multiple standard parameters need to be evaluated.

This study involves comparison of performance parameters for scramjet inlet which are evaluated as a result of FEM computation of 2-D turbulent flow field around six different scramjet inlet geometries. The salient geometrical parameters which are varied are; inlet ramp angle and length, cowl lip angle, leading edge and axisymmetric inlet. The 2-D computation of turbulent flow is obtained by implementing high Reynolds number k-omega compressible turbulent formulation.

The boundary and initial conditions are carefully selected to the free stream conditions that pertain to a cruise altitude of 25km. The simulations were performed for two free stream Mach number 8. Thus from the obtained result, comparative studies of performance parameters are carried out by parameterising geometrical variables and free stream Mach number.

It is necessary to simulate the inlet design to obtain the appropriate inlet performance. Computational Fluid Dynamics (CFD) is used to study flight simulations in both steady and un-steady flow. A time-averaged, viscous, two Dimensional, CFD scheme used to compute aero-thermodynamic quantities including boundary layer effects. A variety of turbulent models available ranging from one to three equations transport models. Oblique shock waves, expansion waves and shock wave interactions are mainly considered.

Accuracy of the solution is dependent on many parameters like size of the control volume, orientation of boundaries, discretization and its order of accuracy.

Scramjet Inlet:

Intake is the most vital component of the engine. It converts the K.E of the air flow into a static pressure rise that helps in deceleration of flow at lower speeds. This deceleration takes place as the flow passes through a series of oblique shocks that are formed due to the presence of ramps in the inlet, also called as staged compression. The internal inlet compression provides the final compression of the propulsion cycle.

The forebody along with the internal inlet is designed to provide the required mass capture and aerodynamic contraction ratio at maximum inlet efficiency. The air in the captured stream tube undergoes a reduction in Mach number with an attendant increase in pressure and temperature as it passes through the system of shock waves in the fore body and internal inlet. It typically contains non-uniformities, due to oblique reflecting shock waves, which can influence the combustion process.

A scramjet air induction phenomenon includes vehicle bow shock and isentropic turning Mach waves, shock boundary layer interaction, non-uniform flow conditions, and three-dimensional effects.

Ramp Angle:

An intake ramp is a rectangular plate-like device within the air intake of a jet engine designed to generate a number of shock waves to aid the inlet compression process at supersonic speeds. The ramp sits at an acute angle to deflect the intake air from the longitudinal direction.

At supersonic flight speeds, the deflection of air stream creates a number of oblique shock at each change of gradient along the ramp. Air crossing each shock wave suddenly slows to a lower mach number, thus increasing pressure.

Inlet Ramp

Ideally, the first oblique shock wave should intercept the air intake lip, thus avoiding air spillage and pre-entry drag on the outer boundary of the deflected streamtube. For a fixed geometry intake at zero incidence, this condition can only be achieved at one particular flight mach number, because the angle of the shock wave to the longitudinal direction becomes more acute with increasing aircraft speed.

More advanced supersonic intakes feature a ramp with a number of discrete changes of gradient in order to generate multiple oblique shock waves. For a fixed geometry it is feasible to use curved intakes without any shock before the final normal shock.

Variable geometry intakes, such as those on concorde, vary the ramp angle to focus the series of oblique shock waves onto the intake lip, control of which is accomplished by complex non-linear control laws using the ramp void pressure as a control input.

K-epsilon (k-ε) turbulence model:

It is the most common model used in Computational Fluid Dynamics (CFD) to simulate mean flow characteristics for turbulent flow conditions. It is a two equation model which gives a general description of turbulence by means of two transport equations (PDEs). The original impetus for the k-epsilon model was to improve the mixing length model, as well as to find an alternative to algebraically prescribing turbulent length scales in moderate to high complexity flows.

The first transported variable determines the energy in the turbulence and is called **turbulent kinetic energy (k)**.

The second transported variable is the **turbulent dissipation (ε)** which determines the rate of dissipation of the turbulent kinetic energy.

k-ε turbulence model derives two equations in CFD analysis and they were., Continuity and Momentum equation (u & v momentum eqn).

ANSYS-WORKBENCH:

ANSYS Workbench platform is the framework upon which the industry's broadest deepest suite of advanced engineering simulation technology is built. An innovative project schematic view ties together the entire simulation process, guiding the user through even complex multi-physics analyses with drag-and-drop simplicity.

With bi-directional CAD connectivity, powerful highly-automated meshing, a project-level update mechanism, pervasive parameter management and integrated optimization tools, the ANSYS Workbench platform delivers unprecedented productivity, enabling Simulation Driven Product Development.

The version of ANSYS software we used in our project designing and analyzing is ***ANSYS-Workbench 17.1***

Inlet Ramp Angle Selection:

A design of Ramp types selected in our project are draw through Graphical User Interface (GUI) in ANSYS-Workbench Design Model.

Methodology:

The design geometry we drawn in ANSYS Design Modeler are as follow.,

- ✓ Sharp Axi-symmetric Ramp Inlet.
- ✓ Sharp Four Ramp Angle Inlet.
- ✓ Sharp Five Ramp Angle Inlet.

The sketching of ramp design in ANSYS-Workbench has tools that to create the sketch that then by using constraints and dimensions the desirable geometry has drawn.

After completing the sketch, the boundary used for fixing the sketch that a body that influencing the sketch of ramp model. Through Surfaces from sketches, the sketch then formed as a surface for further consideration.

Selected Ramp Angle Parameters:

Leading edge	Sharp
No. of ramps	Three
Ramp angles	5.5º, 10.8º, 14.1º
Throat area	50mm

Table 1., Sharp axi-symmetric Inlet Specifications

Leading edge	Sharp
No. of ramps	Five
Ramp angles	5.5º, 6.05º, 8.14º, 9.60º, 11.5º
Cowl angle	11.5º
Throat area	60mm

Table 2., Five Ramp Angle Inlet Specifications

Leading edge	Sharp
No. of ramps	Four
Ramp angles	5.5º, 7.55º, 9.05º, 12.5º
Cowl angle	12.5º
Throat area	60mm

Table 3., Four Ramp Angle Inlet Specifications

Geometry and Grid Generation:

Computational Model:

This problem analyses the flow analysis of air along the inlet ramp angle. The mole fractions of each of the species are also shown in the analysis.

Procedure in the way of analysis were.,

1. Draw a Geometry of 2-Dimentional sketch in the Design Modeler.
2. Using Mesh the following mesh has to be carried out for further analyzing process.
3. Analysis in Fluent, the selection of inputs and Boundary Conditions are to be considered.
4. Select the k-ε Turbulence Model for analysis which solves two equations
5. Check On the Energy Equation.
6. Preferred Boundary Conditions are to be applied.
7. Results were taken.

Create Modeling:

Sharp Axi-Symmetric Inlet Geometry:

The sharp axi-symmetric model used to drawn in ANSYS-Workbench as.,

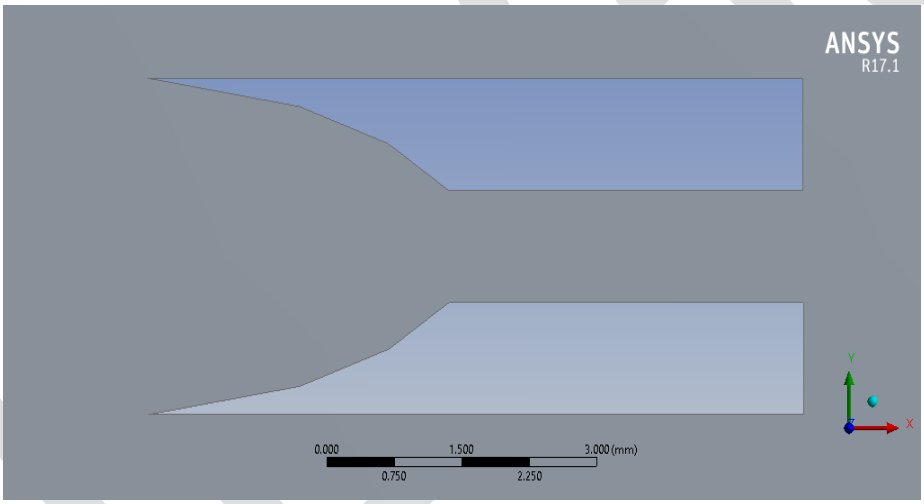

Geometry of Axi-symmetric Inlet

Five and Four Ramp Angle Inlet Geometry:

Five and Four ramp angle inlet model has drawn in ANSYS-Workbench as.,

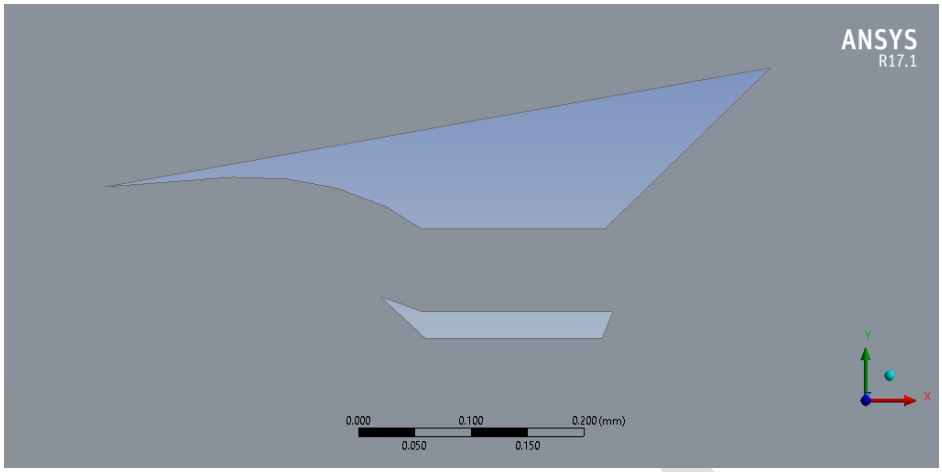

Five Ramp Angle Inlet Geometry

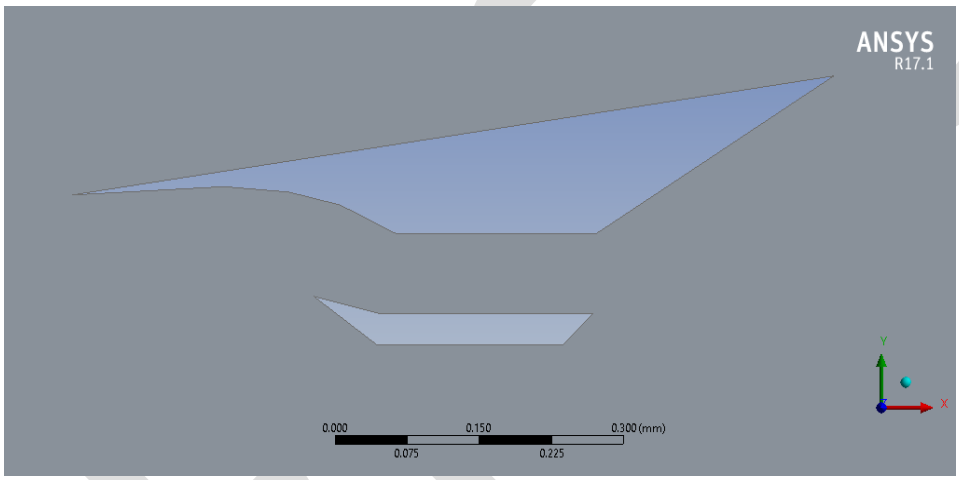

Four Ramp Angle Inlet Geometry

MESHING:

A mesh is the **Discretization** of the component into a number of small elements of defined size. Finite element analysis is dividing the geometry into various small numbers of elements. These elements are connected to each other at points called nodes. Each node may have two or more than that elements connected to it. A collection of these elements is called mesh.

Meshing is a very important part of pre-processing in any **FEA** software. In **ANSYS-Workbench** there are many tools and options available to help you create an effective mesh. And effective mesh is one that requires less computational time and gives maximum accuracy.

In ANSYS-Workbench, you can generate mesh with the default settings available when you start the software. You can also set parameters as per your requirements to generate the mesh.

Create Meshing:

Meshing Of Inlets:

Meshing of all the inlet type for the considered geometry will then draw through ANSYS-Mesh (ICEM-CFD) as follow.,

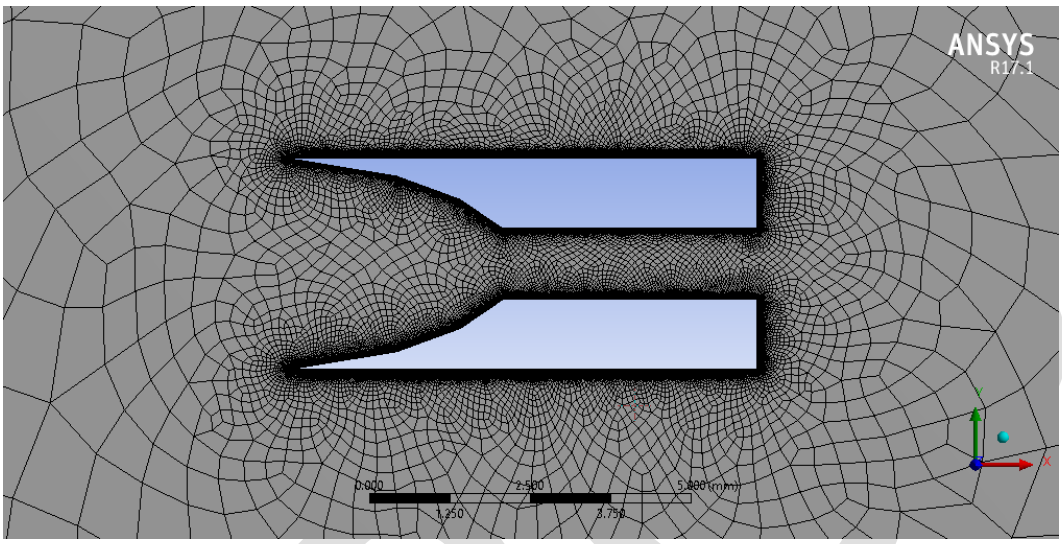

Mesh Of Axi-Symmetric Inlet Design

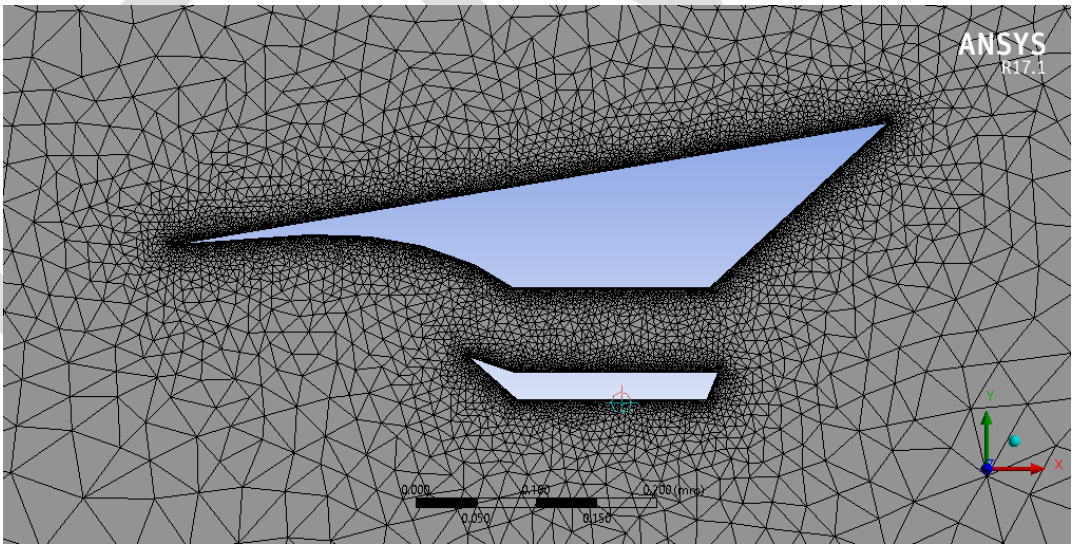

Mesh Of Five Ramp Angle Inlet Design

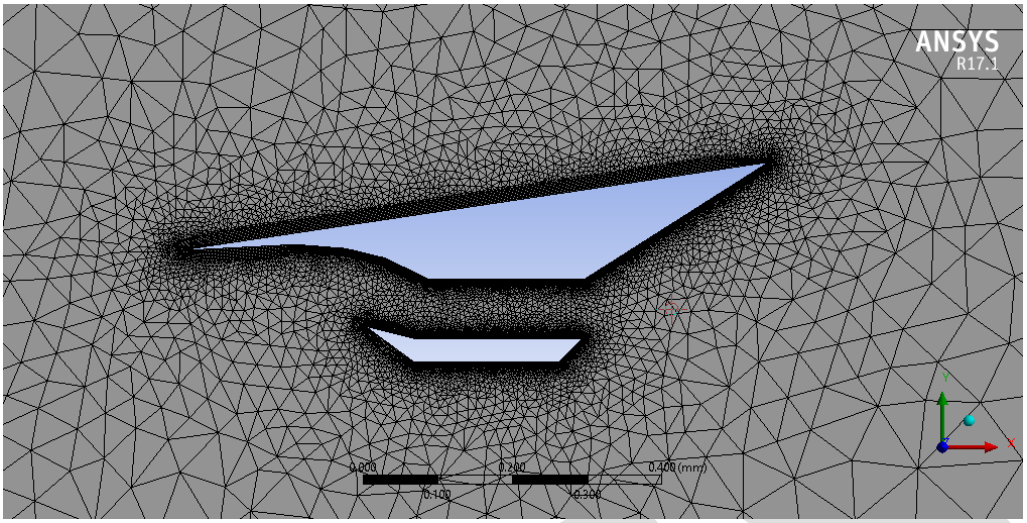

Mesh Of Four Ramp Angle Inlet Design

In global meshing, the mesh selected is for CFD analysis with fine mesh and the quality of hard smoothening.

In local meshing, the body sizing, edge sizing and inflamation has done to qualify the meshed model for better accurate results. By doing smaller divisions of elements assumed as minimum sizing of 0.02mm and number of elements as between 8 to 12.

Result and Analysis:

Two dimensional simulations of the flow field using FLUENT are to be made. Computations validated through the simulation of hypersonic inlet at desired mach number.

Boundary Conditions:

Inlet	Velocity inlet
Outlet	Pressure outlet
Upper boundary	Wall
Lower boundary	Wall
Body & Cowl	Farfield
Fluid	Air
Mach number	10
Gauge pressure	1197 pa
Reference temperature	226.5 k

Turbulent viscosity	0.01
Turbulent ratio	10

Table 4., Boundary conditions

Fabrication of Scramjet Engine

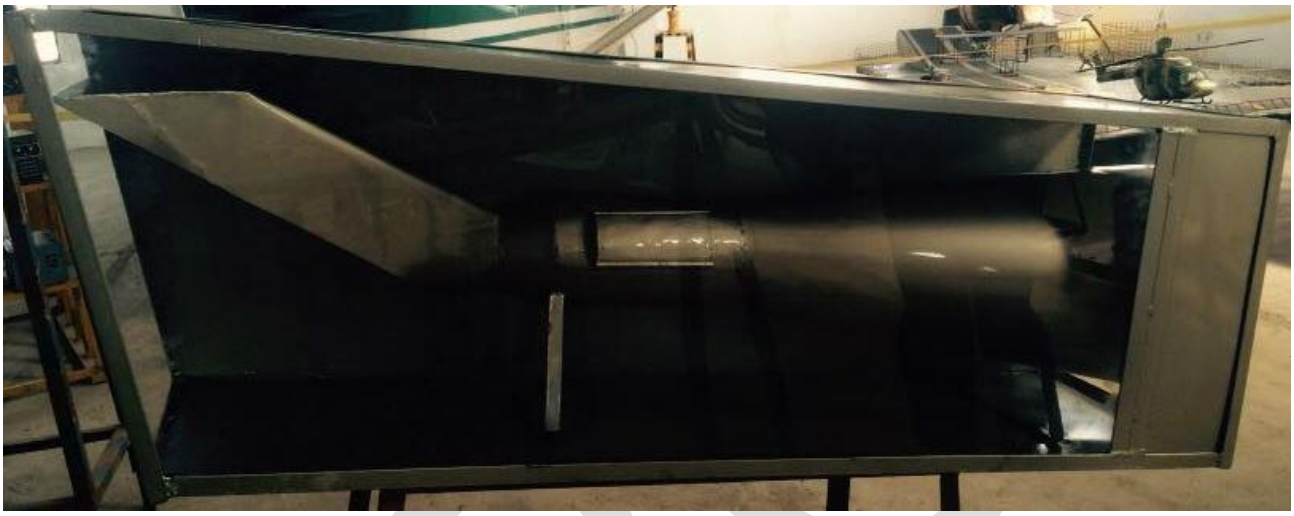

Fully Fabricated Scramjet Engine

ANALYSIS OF SCRAMJET INLET IN FLUENT

Case 1 – Sharp Axi-symmetric Inlet

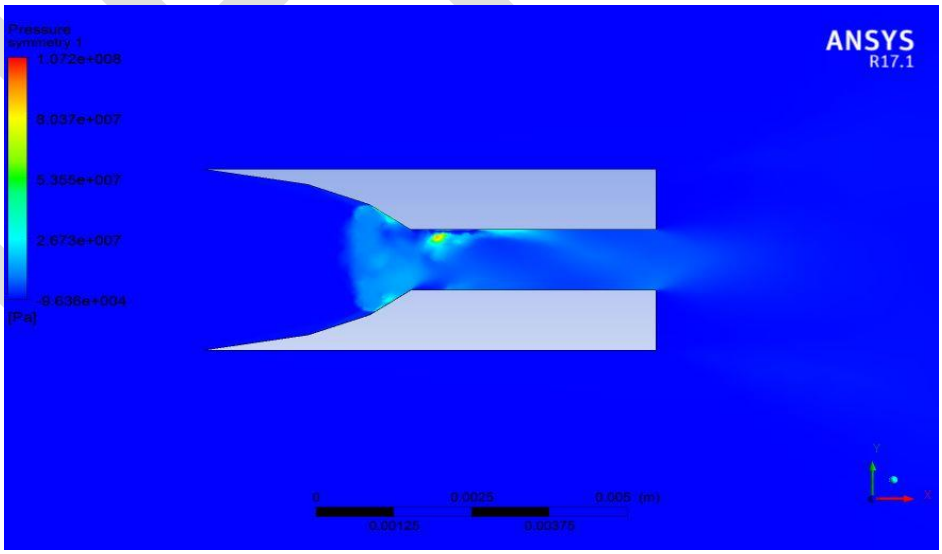

Axi-symmetric Pressure Contour

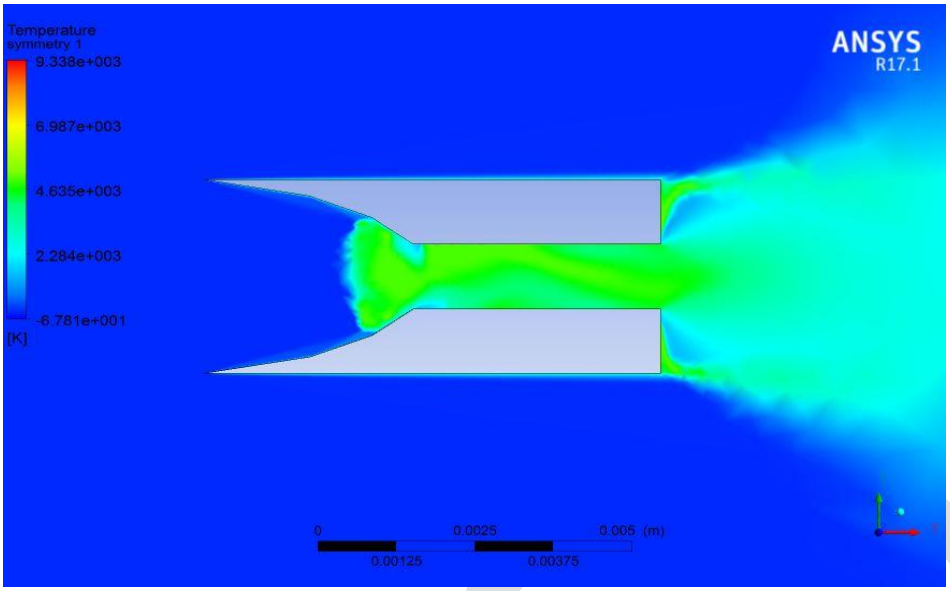

Axi-symmetric Temperature Contour

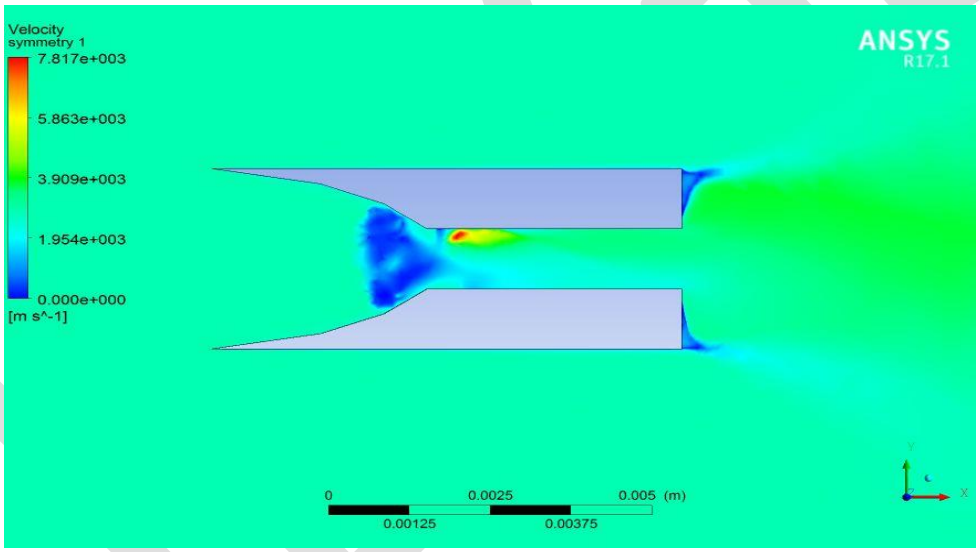

Axi-symmetric Velocity Contour

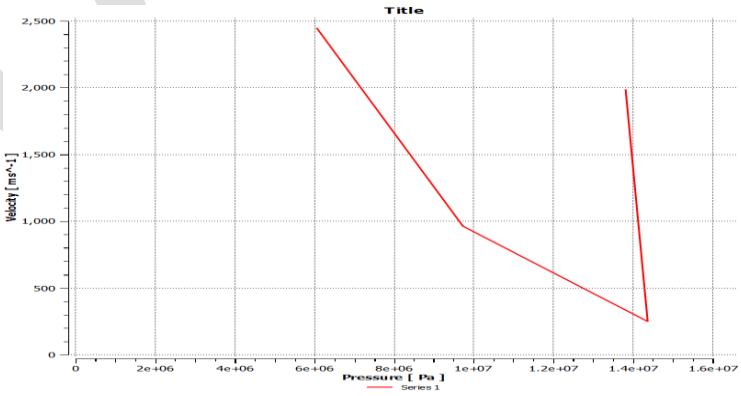

Pressure to Velocity at Inlet

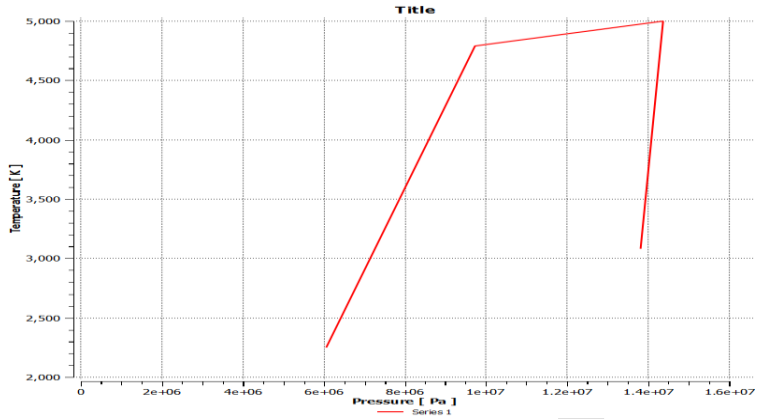

Pressure to Temperature at Inlet

Case 2 – Five Ramp Angle Inlet

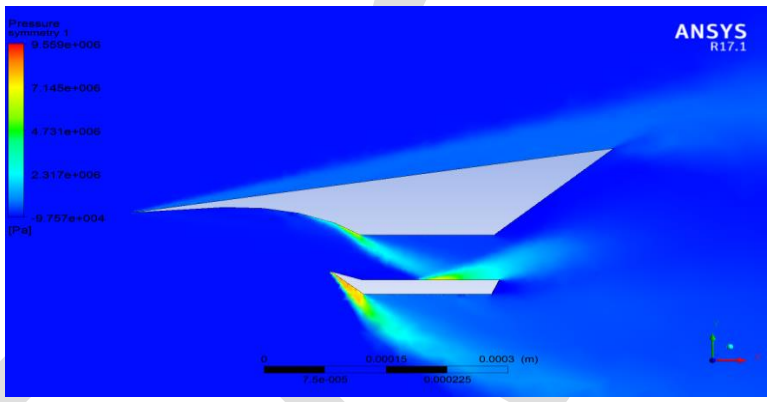

Five Ramp Pressure Contour

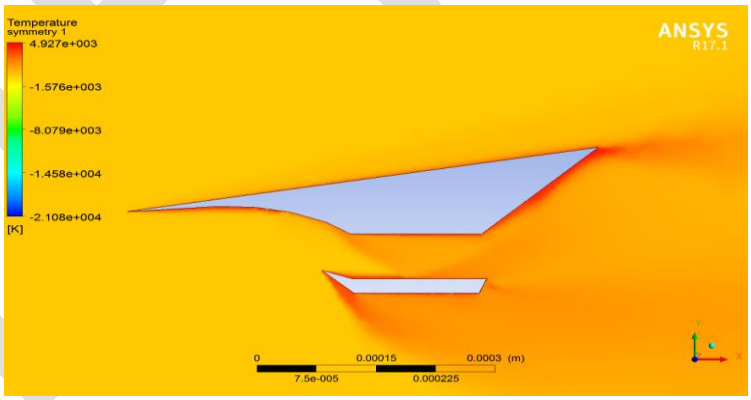

Five Ramp Temperature Contour

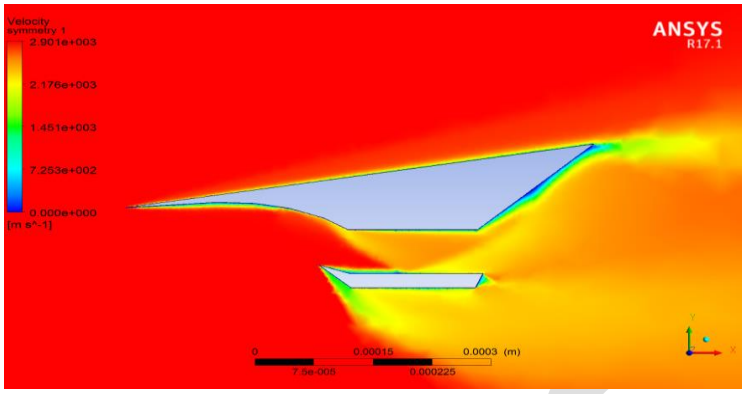

Five Ramp Velocity Contour

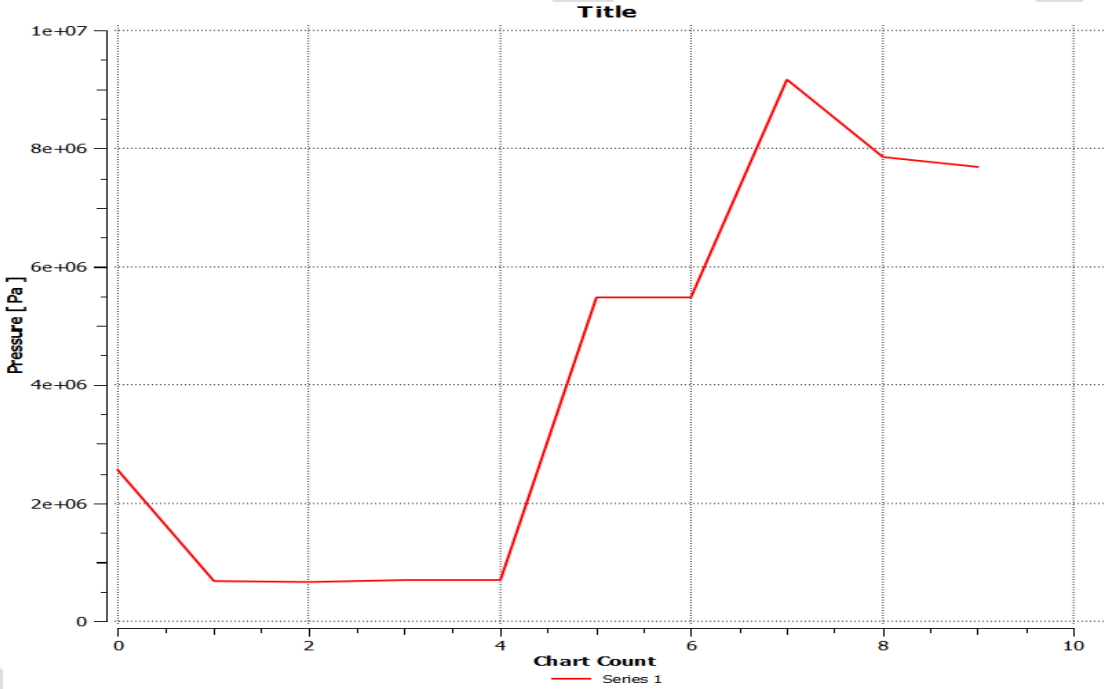

Pressure at inlet

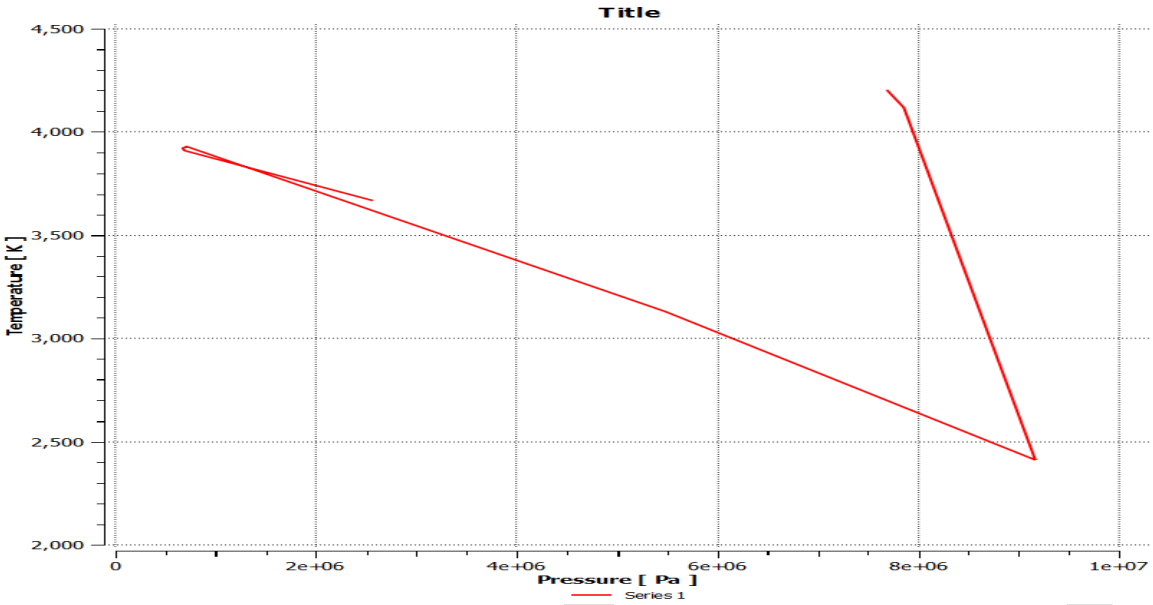

Pressure to Temperature at Inlet

Case 3 – Four Ramp Angle Inlet

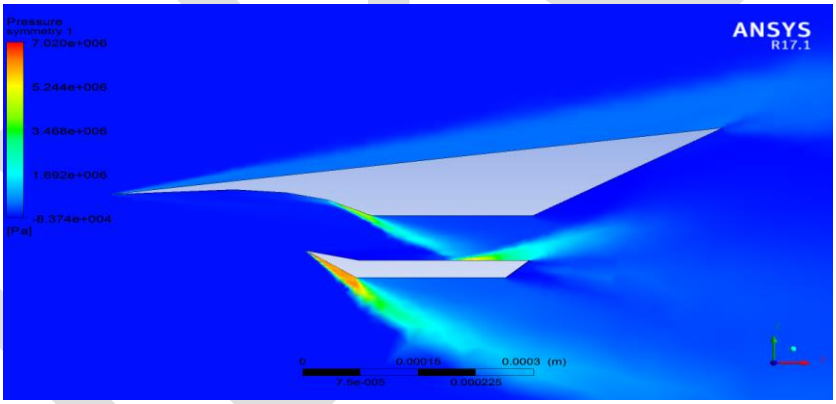

Four Ramp Pressure Contour

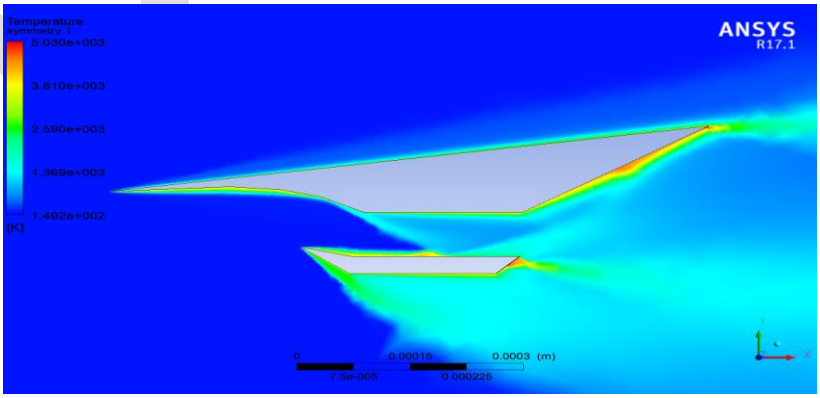

Four Ramp Temprature Contour

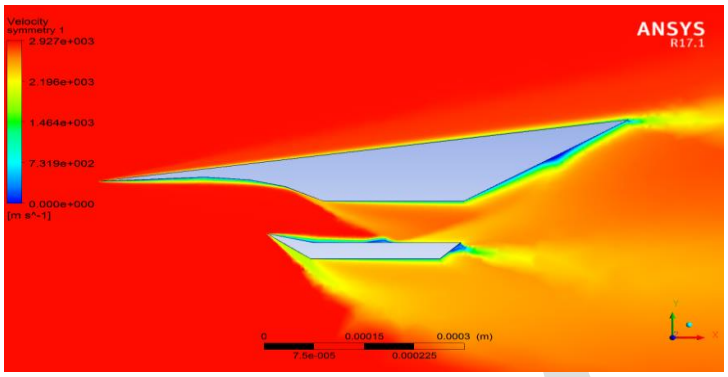

Four Ramp Velocity Contour

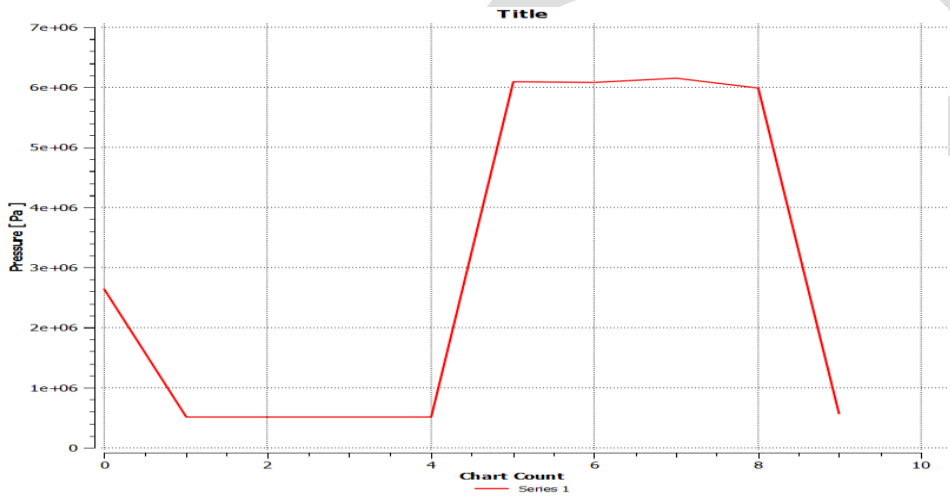

Pressure at Inlet

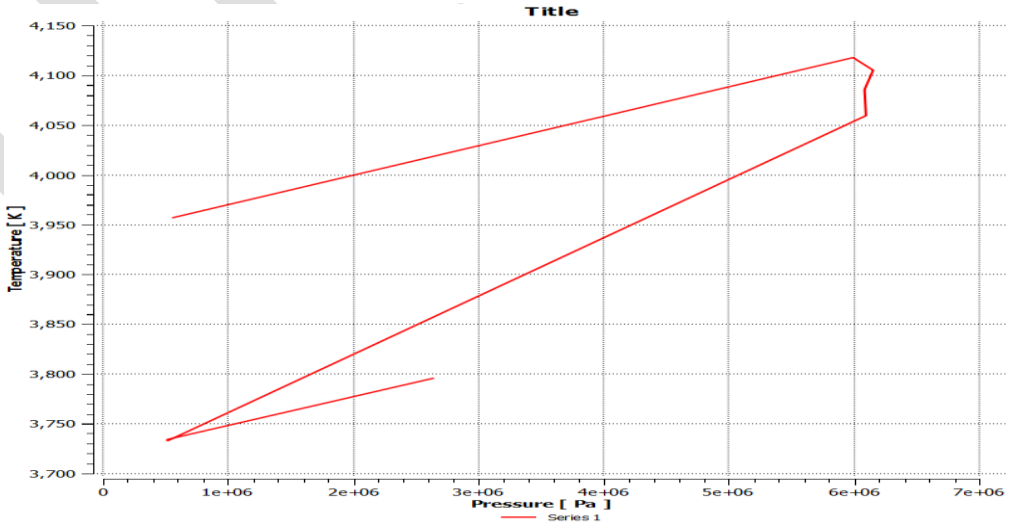

Pressure to Temperature at inlet

Parameters	Sharp Axi-symmetric Inlet		Five Ramp Angle Inlet		Four Ramp Angle Inlet	
	Min	Max	Min	Max	Min	Max
Static Pressure	-96355.5 pa	1.07e6 pa	-97569.1 pa	9.55e6 pa	-83744.6 pa	7.02e6 pa
Static Temperature	-67.81 k	9338.13 k	-21083.9 k	4926.75 k	149.2 k	5029.8 k
Velocity Magnitude	0 m/s	7817.36 m/s	0 m/s	2901.36 m/s	0 m/s	2927.4 m/s
Density	0.0035 kg/m3	74.76 kg/m3	0.0036 kg/m3	9.65 kg/m3	0.015 kg/m3	10.54 kg/m3
U Velocity	-1.202e3 m/s	5.21e3 m/s	-36.101 m/s	2901.26 m/s	-585.17 m/s	2925.95 m/s
V Velocity	-3.08e3 m/s	6.02e3 m/s	-1605.75 m/s	1893.95 m/s	-1427.4 m/s	1738.13 m/s

Table 5., CFD Result Comparison

Conclusion

In this project, the Computational Fluid Dynamics Analysis is performed by using ANSYS-Workbench and ANSYS-Fluent software`s. Analysis has compared to all these three cases of inlet types as.,

Case 1: Sharp Axi-symmetric Inlet.

Case 2: Sharp Five Ramp angle inlet.

Case 3: Sharp Four ramp angle inlet.

When the upcoming air that enters into the rectangular type inlet, through the ramp angle design the air that facing the inlet has distracted and the process of shock formation that possibly attain inside the inlet lip which then makes the flow of air be compressible that then helps the flow as pressurized to meet the combustion chamber of mach 1. The name supersonic combustion happens inside the chamber that possible if the pressurized air be so effectively compressed by shock waves that makes through ramp angle deflection. In this present work project, the simulation of ramp angle types that in the scramjet inlet rectangular type is analyzed. Optimization in ramp angle re-design has considered as effective and implementing that in inlet design were possibly analyzed as efficient in compression and make it more effective in pressure formation. Five ramp angle inlet simulation results as the most preferable one as it gives efficient in compression at the selected mach number and has better performances.

REFERENCES:

1. Luu Hong Qyan, Nguyen Phu Hung, Le Doan Quang, Vu Ngoc Long, "Analysis and Design of a Scramjet engine Inlet operating from mach 5 to 10" "Science Publishing Group" 2016.

2. Ajay kumar, S.N. Tiwari, "Analysis of Scramjet Inlet flow field using 2D Navier-Strokes equations" "NASA Contractor Report 3562", Langley Research Centre 1982.

3. Michael k. Smart, "Scramjet Inlets" Centre of Hypersonics, NATO OTAN & ORT Organization, Approved OMB No. 0704-D188, 2010.

4. B. Reinartz, "Performance Analysis of a 3D Scramjet Intake" AICES Technical Report, 2008-13.

5. V. Rajashree, P. Manivannan, G. Dinesh Kumar, "Computational Analysis of Scramjet Inlet" International Journal of Innovative Research in Science, Engineering and Technology, Volume 3, Issue 3, 2014.

6. Ramesh Kolluru and Vijay Gopal, "Comparative Numerical Studies of Scramjet Inlet Performance using k-ε Turbulence Model with Adaptive Grids" COMSOL Conference, 2012.

7. Yufeng Yao & Danial Rincon, Yao Zheng, "Shock Induced Separating Flows in Scramjet Intakes" International Journal of Modern Physics Conference Volume 19, 2012.

8. Bo Huang, Zhufei Li, Jiming Yang, Xisheng Luo, "An Experimental Observation of 3D Scramjet Inlet Flow in Shock Tunnel" 10th International Conference on Fluid Control, Measurements and Visualization, 2009.

9. Kristen Nicole Roberts, "Analysis and Design of a Hypersonic Scramjet Engine with a Starting Mach Number of 4" Project in University of Texas, 2008.

10. Richard J. Weber & John S. Mackay, "An Analysis of Ramjet Engine using Supersonic Combustion" Technical Note-4386, National Advisory Committee for Aeronautics, 1958.

International Journal of Engineering Research and General Science Volume 5, Issue 4, July-August, 2017
ISSN 2091-2730

Modelling and Optimization of Dressing Parameters of CNC Cylindrical Grinding Wheel for Minimum Surface Roughness

Dadaso D, Mohite[1], Neeraj Tiwari[2], Sandeep Sontakke[3], Udayshankar Mishra[4]

[1]Assistant Professor, Department of Mechanical Engineering, Keystone School of Engineering, Pune, Maharashtra, India

Email: dadasomohite@gmail.co

[2]Department of Mechanical Engineering, Bharati Vidyapeeth's College of Engineering, Lavale, Pune

[3]Department of Mechanical Engineering, Keystone School of Engineering, Pune

[4]Department of Mechanical Engineering, Keystone School of Engineering, Pune

Abstract— The dressing operation of a grinding wheel is a machining process involving re-sharpening and renewing the cutting face of the wheel by removing or severing dull grains with a diamond or other type of dressing tool. The four parameters of dressing operation are; dressing depth of cut, dressing cross feed rate, drag angle of dresser and number of passes. The effect of these parameters on grinding wheel surface topography is measured in terms of the surface roughness generated on work piece during subsequent grinding operation. A blade type multi point diamond dresser tool was used for dressing. The experiments were performed on EN19 steel bar using CNC cylindrical grinding machine. In this study, the design of experiment was done by Taguchi parametric optimization technique involving L9 orthogonal array. Experimental results were optimized by S/N ratio and Analyzed by ANOVA. Based on the experimental results, a mathematical model was developed using multiple regression method. The results were further confirmed by conducting a confirmation experiment and it was confirmed that dressing cross feed rate is the dominating parameter of dressing which shows a major impact on response surface roughness. Finally FEA was done to find stresses and deflections analysis of grinding wheel and work piece.

Keywords: CNC Cylindrical Grinding, Dressing, Taguchi Design, ANOVA, Modeling and Optimization, FEA.

INTRODUCTION

Dressing of grinding wheel is one of the important factors which determine that how efficiency a grinding wheel will cut, hence it becomes an extremely important prerequisite of the grinding process [1, 7]. The dressing operation of a grinding wheel is a process of re-sharpening and renewing the cutting face of the wheel by removing or severing dull grains with a diamond or other type of dressing tool. Generally, the grinding grits are made of hard abrasive materials like aluminum oxide or silicon carbide, hence dressing tools of greater hardness and durability are needed to ensure efficient dressing of wheel. The ability of a grinding wheel to perform is significantly affected by the way in which the wheel is dressed [1, 8]. The use of diamond as a dressing medium in the form of single point and cluster tool, multi point dressing tools and cluster tools, and more recently in the form of diamond rollers has increased significantly due to this. In this investigation, the dressing of grinding wheel is done by using a blade type multi point diamond dresser. The four important parameters of dressing operation are dressing depth of cut, dressing cross feed rate, drag angle of the dresser and numbers of passes were selected. These dressing parameters were influencing on grinding wheel performance and were measured in terms of the surface roughness generated on the work-piece.

In industries, the prime objective in grinding process is to get a better surface finish or to get high material removal rate (MRR) of the work piece. Better surface finish can be obtained by using fine grained grinding wheel whereas higher MRR can be obtained from the coarse grained grinding wheel. Fine grained topography is obtained by providing a lower dressing depth and dressing the wheel for a short period of time while coarse grained topography is obtained by providing a greater dressing depth and dressing the same wheel for more time duration (Pande and Lal, (1979)) [8]. Pacitti and Rubenstein (1972) reported the effect of dressing depth of cut on alumina grinding wheel using single point diamond dresser and had concluded that as dressing depth of cut increases up to specific range,the useful life of alumina grinding wheel could be increased [5]. Vickerstaff (1976)) has analyzed the effect of the wheel dressing condition on the distribution of metal removal rate over the wheel surface and on surface roughness of the work piece. A new model of dressing method was proposed which claims to have advantages of both fine dressing (good surface finish) and coarse dressing (increase metal removal rate and decrease thermal damage). His experiment also proved that the grinding wheel conditions and topography of the wheel surface were having significant effects on radial wheel wear [4].

In this study, four important parameter of grinding wheel dressing (i.e., dressing depth of cut, cross feed rate, drag angle of dresser and number of passes) were selected as variable parameters and other grinding process parameters were fixed. Taguchi design methodology has been applied to determine the optimum dressing parameters leading to minimum surface roughness in CNC cylindrical grinding machine on EN19 Steel bar. Also, mathematical model is developed for surface roughness by considering selected four parameters of dressing as control factors and using multiple regression analysis. In the present work, experimental results were optimized by S/N ratio and analyzed by analysis of variance (ANOVA) which explains the significance of the parameters on the responses. Conformation experiment was conducted at the optimum level to verify the effectiveness of the Taguchi approach. Finally, Finite Element Analysis is done to find stresses and deflections analysis of grinding wheel and work piece.

METHODOLOGY

In this present paper, efforts are made to find the most influencing dressing parameter on the grinding wheel surface topography and the result of which is measured in terms of minimum surface roughness (R_a) generated on the EN19 steel bar during the CNC cylindrical grinding operation. For this purpose, experiments were performed selecting various levels of a multi point diamond dressing tool parameters such as, dressing depth of cut, dressing cross feed rate, drag angle of dresser and number of passes of dresser on the wheel, in order to explore the effect of the dressing conditions. The design of experiment was done by Taguchi parametric optimization technique involving L9 orthogonal array, which is used to check the interactions between the factors of dressing conditions. Experimental results were optimized by S/N ratio and Analyzed by analysis of variance method (ANOVA). ANOVA explains the significance of the parameters on the responses. Based on the experimental results, a mathematical model was developed using multiple regression method. Finally, the predicted value is validated and compared with experimental result. Also, Finite element analysis (FEA) was done for analysis of stresses and deflections generated by grinding wheel on work piece. The software used for FEA is Hyper-mesh 12.0 for meshing and ANSYS 15.0 for static analysis to get stress and deflection.

EXPERIMENTAL DESIGN AND PROCEDURE

I. Design of Experiments

For improving the product design and solving production problems, the Design of Experiment (DoE) is an important statistical technique. Dr. Genichi Taguchi (1980) has prescribed a standard way to utilize the DoE so as to enhance the quality of product, process the design & manufacturing and also to reduce the cost [3].

In this present work, three levels at four factors has been employed to predict the optimal values as shown in Table I. Ranges of dressing parameters have been established based on review of literature and by performing the pilot experiments using one factor at a time (OFAT) approach. The number of experiments to be conducted can be reduced by using Taguchi optimization technique.

Factors	Parameters	levels		
		L1	L2	L3
A	Dressing Depth of Cut (µm)	20	25	30
B	Dressing cross feed rate (mm/min)	80	90	100
C	Drag Angle of dresser (^{0})	45	50	55
B	Number of passes	3	4	5

Table I. Parameters and their levels of Experiments

In the present work, Number of experiments used to design the orthogonal array (OA) for four factors and three levels is used.

$$\text{Minimum experiments} = [(L-1)*P]+1 = [(3-1)*4]+1 = 9 \approx L9$$

Table II shows Taguchi's orthogonal array to check the interactions between the parameters. On the basis of design of experiments concept L9 orthogonal array (OA) is selected for dressing parameters of grinding wheel.

Expt. No.	Depth Of Cut (μm) (d)	Feed Rate (mm/min) (f)	Drag Angle (°) (d_a)	Number of Passes (n)
1	1	1	1	1
2	1	2	2	2
3	1	3	3	3
4	2	1	2	3
5	2	2	3	1
6	2	3	1	2
7	3	1	3	2
8	3	2	1	3
9	3	3	2	1

Table II. Taguchi's L9 Standard Orthogonal Array

II. Work piece Material

In this work, EN19 steel bar of 40 mm diameter and 120 mm length has been selected as a work piece material. EN19 is a high quality carbon alloy steel which offers a good ductility and shock resistance. EN19 steel is widely used for manufacturing of Axles, Drive Shafts, Crankshafts, Connecting Rods, High Tensile Bolts, Studs, Propeller Shaft Joints, Rifle Barrels, Breech mechanisms for Small Arms, Induction Hardened Pins. EN19 is a good quality steel which have good wear resistance and is widely used for manufacturing power transmitting gears, pinions, spindles etc. The universal central lathe machine was used for turning operation which was done by holding the work piece between the two centers of the lathe machine. After the turning operation, heat treatment was done at 867^0C so as to increase the hardness of the material. The hardness of each job was maintained to 60HRC. After heat treatment, the specimens were ready for experiments. The close up view of the single job is shown in the fig. 1.

Fig. 1.Heat treated specimen

III. Experimental conditions:

Table III shows the experimental conditions of grinding operation.

Grinding Machine	CNC Cylindrical Grinding Machine (AHG 60X300 CNC)
Work piece	EN19 steel bar
Grinding Wheel	Aluminum oxide (Al2O3)
Grinding Condition	Wheel speed : 1000 rpm Spindle Speed : 100 rpm Depth of cut : 100 μm **Plunge and wet**
Coolant used	Soluble oil
Dressing	Dresser : Multi pointed diamond Depth of cut : 10-40 µm

Table III. Experimental Conditions

IV. Experimental Details

The experiments were accomplished using CNC Cylindrical Grinding Machine and EN19 steel bar as workpiece. To find out the effect of dressing on grinding wheel surface topography, four important dressing parameters were selected for experimentation namely

dressing depth of cut, dressing feed rate, drag angle of dresser and number of passes. The influence of these parameters was measured in terms of Surface roughness Ra (µm). In this work, the grinding wheel is used for the experimental work has Aluminum oxide (Al_2O_3) abrasives and vitrified bond. A blade type multi-point diamond dresser was used for dressing and soluble oil is used as coolant. Fig. 2 shows the dressing process and Fig. 3 shows the grinding operation on CNC Cylindrical grinding machine.

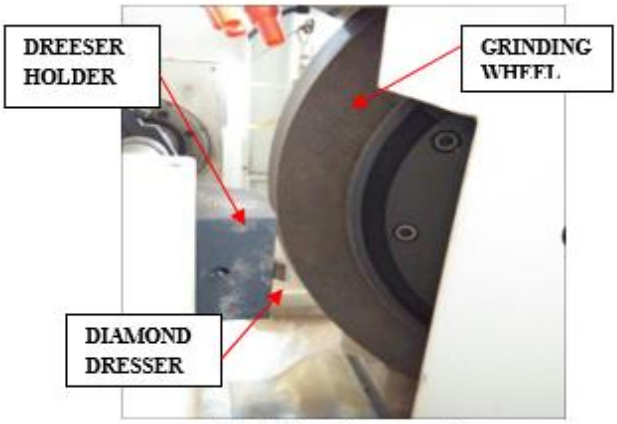

Fig. 2.Dressing operation

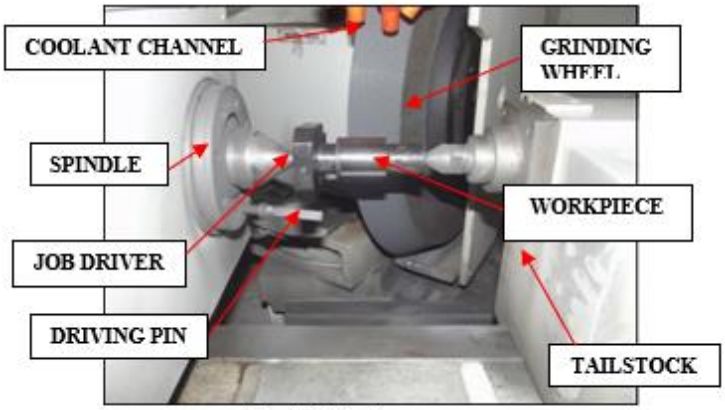

Fig. 3.Grinding process

MATHEMATICAL FORMULATION

The experimental results are used to develop a mathematical correlation between and response surface roughness and dressing variables using multiple regression analysis. Multiple regression analysis is used for modeling and analyzing experimental results, as it is practical, economical and relatively easy to use [3, 11]. The equations of mathematical correlation used for the grinding wheel dressing with the dressing variables under consideration are represented by:

$$Q = \phi\,(d, f, d_a, n) \tag{1}$$

Where Q is the dressing response, ϕ is the response function and d, f, d_a and n are dressing variables. Expressed in non-linear form, Eq. (1) becomes,

$$Q = C d^{w} f^{x} d_a^{y} n^{z} \tag{2}$$

Where, w, x, y and z are Dressing Depth of cut, dressing cross feed rate, drag angle and number of passes exponents in mathematical respectively.

The following mathematical models are formulated in this work:

Surface Roughness model:

$$R_a = C_1 d^{a_1} f^{a_2} d_a^{a_3} n^{a_4} \tag{3}$$

Where, a_1, a_2. a_3 and a_4 are Dressing Depth of cut, dressing cross feed rate, drag angle and number of passes exponents in Surface roughness Ra respectively.

These mathematical models are converted from non-linear to linear form by performing a logarithm transformation to determine values of constants and variables. The above function can be expressed in linear mathematical form is given by:

$$\ln \mathrm{Ra} = \ln \mathrm{C}_1 + a_1 \ln \mathrm{d} + a_2 \ln \mathrm{f} + a_3 \ln \mathrm{d_n} + a_4 \ln n \tag{4}$$

The constants and variables C_1, d, f, $d_a$and n can then are solved by using Multiple Regression Analysis with the help of experimental results. The error between experimental values and predicted values from the mathematical model can be calculated by the method of least square.

$$E_{least\ sq.} = (y_{1o} - y_{1c})^2 + (y_{2o} - y_{2c})^2 + \ldots\ldots\ldots\ldots\ldots\ldots + (y_{9o} - y_{9c})^2 \tag{5}$$

Equation (5) gives the least square error between observed values and computed values by model.

KINEMATICS OF GRINDING

The process of an external cylindrical grinding is carried out by the movement of the grinding wheel against a rotating cylindrical work piece. During this process, surface of a work piece comes in contact with abrasives grain of the grinding wheel and a certain amount of material is removed from it. For an external cylindrical grinding, a wheel of a diameter d_s rotating with a peripheral velocity v_s gives a wheel depth of cut 'a' on the work piece rotating with angular velocity v_w. The forces are developed between the wheel and the work piece owing to the grinding action. For the plunge grinding operations, as shown in fig.4 for external cylindrical grinding, the total force vector exerted by the work piece against the wheel can be resolved into a tangential component $F_t$and a normal component F_n[1].

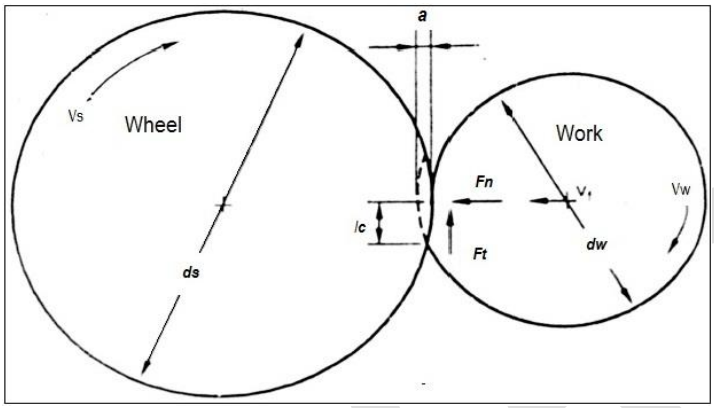

Fig. 4.Illustration of force components for cylindrical grinding

For this work, a three phase squirrel cage induction motor of 5 H.P was used to transmit power *(P)* to the CNC Angular grinding wheel. The angular velocity of grinding wheel (v_s) having radius (R) of 344 x 10^{-3} m was set up to 1000 rpm while the angular velocity of the work-piece (v_w) was set up to 100 rpm.

The grinding power P associated with the force components in above figure 4 and can be written as

$$P = F_t(v_s \pm v_w) \tag{6}$$

Where, F_t is the tangential force of wheel.

While performing the experiment, it was observed that there are some losses of power (Frictional loss, Hysteresis loss etc) generated while transmitting power from motor to the wheel. This loss of power is equal to 3% of the total power generated from the motor. And also, v_w is much smaller than v_s so the net power from equation (6) can be simplified to,

$$P_{net} = (P - 3\%P) = F_t v_s \tag{7}$$

Hence, tangential force obtained by equating the above values in equation (7) is 103.54 N

Now, the torque equation of the wheel is given by,

$$T = F_t R \tag{8}$$

Where, R is Radius of The Wheel.

Hence, the torque generated by the wheel on equating tangential force is 35.62 N-m.

EXPERIMENTAL RESULT AND DISCUSSION

The Grinding experiments were conducted to study the effect of dressing parameters on surface topography of grinding wheel and were measured in terms of the surface roughness generated on the work-piece. Total 9 experiments were conducted using Taguchi experimental design methodology as shown in TABLE II and each experiment was simply repeated three times for obtaining S/N values so as to minimize the errors. The experimental results for surface roughness and S/N ratios are given in TABLE IV. The design, plots and analysis have been carried out using MINITAB 17 statistical software.

A) Surface Roughness Measurement

Surface roughness values were obtained from MITUTOYO Surf test SJ-210 surface roughness tester for each experiment. Three trials of surface roughness value were taken for each experiment. The obtained values were used for the Taguchi optimization process.

Expt. No	Input parameters				Output	
	Depth of Cut (μm)	Feed rate (mm/min)	Drag angle (^{0})	Number of passes	Surface Roughness (Ra) (μm)	S/N Ratio
1	20	80	45	3	0.249667	12.0504
2	20	90	50	4	0.262667	11.6112
3	20	100	55	5	0.316333	9.9970
4	25	80	50	5	0.263667	11.5778
5	25	90	55	3	0.309667	10.1770
6	25	100	45	4	0.327333	9.6988
7	30	80	55	4	0.275000	11.2109
8	30	90	45	5	0.296000	10.5731
9	30	100	50	3	0.332000	9.5767

Table IV. Experimental values of Surface Roughness and S/N ratio

The Signal-to-noise ratio is found out in each case using the criteria of 'lower is better' for surface roughness as a factor of consideration.

$$\text{Lower is better, S/N= -10 log [1/n } (\sum y_i^2)] \quad (9)$$

Average S/N ratio for each parameter at each level is found out. Similarly, the values of average Surface roughness for each parameter at each level are also found out which is shown in Table IV.

B) Analysis of Variance

The experimental results were analysis of variance (ANOVA) by using MINITAB 17 statistical software. The ANOVA results for the response are shown in Table V.

a) Regression analysis : Ra (Mean) Vs Dressing Parameters

Source	DF	Adj SS	Adj MS	F-Value	P-Value
Regression	4	0.00694	0.00174	12.15	0.016
d	1	0.00092	0.00092	6.45	0.064
f	1	0.00585	0.00585	40.96	0.003
da	1	0.00013	0.00013	0.92	0.393
n	1	0.00004	0.00004	0.27	0.628
Error	4	0.00057	0.00014		
Total	8	0.00751			

DF–Degree of freedom, SS–sum of square, MS–mean square (variance), F-ratio of variance of source to variance of error, P< 0.05–determine significance of factors at 95% confidence level

Table V. Analysis of Variance of S/N Ratio of surface Roughness

Analysis of Variance (ANOVA) explains the significance of the parameters on the responses. In the present work, The R^2 value is about 0.9240, which is very high, close to one, it indicates that regression model is adequate to represent the dressing process parameters. The "Pred R-Square" of 0.7428 is in reasonable agreement with the "Adj R-squared" of 0.8479 in case of surface roughness. The P-Values of dressing cross feed rate is lower than 0.05 (at 95% confidence level) indicates that the it can be considered to be statistically significant parameter.

b) Regression Equation

ANOVA gives the linear regression equation for Surface roughness Mean, which indicates that all dressing parameters are significantly, affects on surface roughness.

$$Ra(mean) = -0.0869 + 0.002478\, d + 0.003122\, f + 0.000933\, da - 0.00256\, n \quad (10)$$

c) Main Effects Plots

The main effects plots for the experiments have been given in Fig. 5.

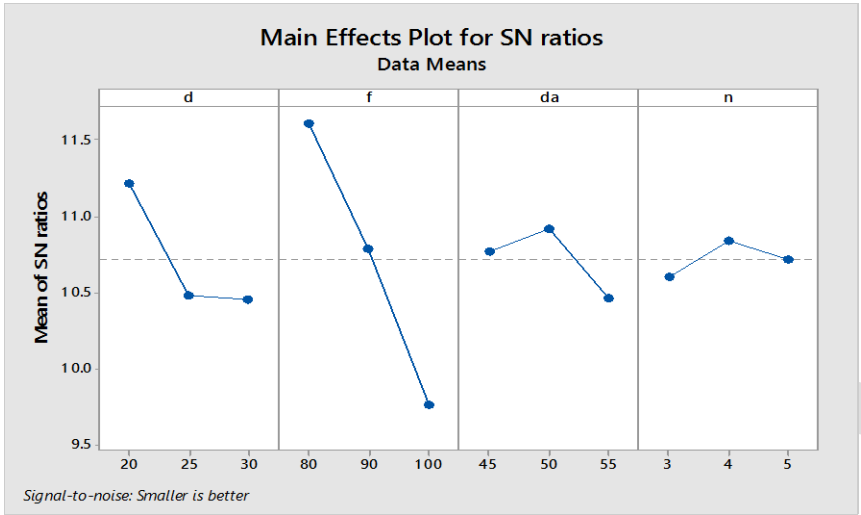

Fig.5.Main Effects plot for S/N ratio

The response graph shown in fig.5 for S/N values for surface roughness shows that level I of dressing depth of cut and dressing cross feed rate are d1=11.21dB and f1= 11.61dB respectively, indicated as the optimal situation in terms of S/N ratio. And level II of drag angle of dresser and number of passes are da2=10.92dB and n2= 1.84dB respectively, indicated as the optimal situation in terms of S/N ratio.

C) Mathematical Modeling of response

- **Surface Roughness (Ra) model:**

By the method of multiple regressions analysis equation (3) solved by using MATLAB software and found values of constants C1, a_1, a_2, a_3 and a_4. Hence, while developing the model for roughness, only the individual variables d, f, d_a and n are considered and the non-linear fit between response and dressing variables is given by:

$$Ra = (1.03 \times 10^{-3}) d^{0.2233} f^{0.9551} d_a^{0.1728} n^{-0.0287} \quad (11)$$

It is observed from the mathematical model of surface roughness that the roughness is increases with increase in dressing depth of cut, dressing cross feed rate and drag and angle of the dresser. But, roughness is decreases with increase in number of passes.

Expt. No.	Surface Roughness (µm)		
	Experimental value	Predictive Value	Least Square Error (%)
1	0.2497	0.2467	0.0055%
2	0.2627	0.2789	
3	0.3163	0.3115	
4	0.2637	0.2602	
5	0.3097	0.3004	
6	0.3273	0.3183	
7	0.2750	0.2773	
8	0.2960	0.2979	
9	0.3320	0.3404	

Table VI. Comparison of experimental values and predicted values

Table VI gives the comparison between the experimental values and predicted values. The least square error is obtained by equation (5).

D) Finite Element Model

Finite Element Analysis (FEA) is a computing technique that is used to obtain approx solutions of boundary value problems. It uses a numerical method called as Finite Element Method (FEM). FEA uses a computer model of a design that is loaded and analyzed for specific results. It is utilizable for quandary with perplexed geometry, loading, and material properties where exact analytical solution are arduous to obtain. Most often utilized for structural, thermal, fluid analysis, however wide applicable for other type of analysis and simulation.

In this work, static analysis is performed by FEA software using Hyper-mesh 12.0 for meshing and ANSYS 15.0 for static analysis to get stress and displacement. A three dimensional model of the mentioned dimensions of workpiece was made and further meshing is done with appropriate mesh size as shown in Fig. 6. Material properties like Young's modulus, Poisson ratio and density and support boundary condition are mentioned in the Table VII.

Material Properties	
Modulus of Elasticity (E)	2×10^5 N/mm^2
Yield strength	555 N/mm^2
Tensile strength	775-925 N/mm^2
Poisson's Ratio	0.3
Density of the work piece	7800×10^{-9} Kg/mm^3

Table VII. Material properties

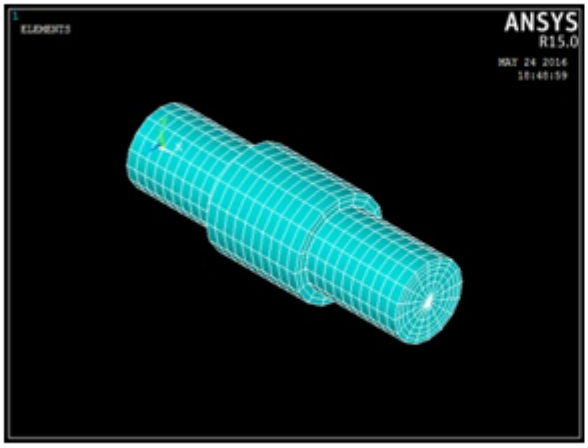

Fig.6. Mesh Model

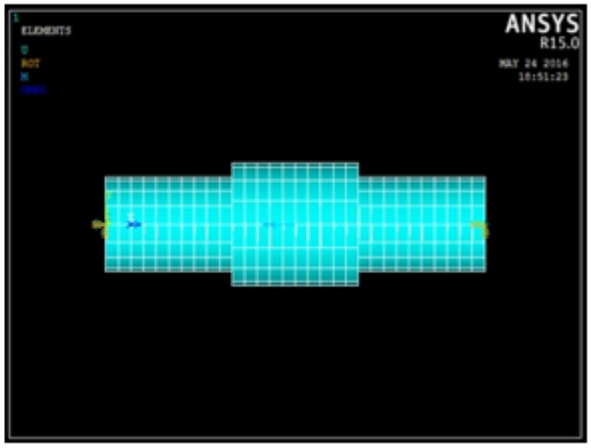

Fig.7. Boundary Conditions

Loading and Boundary conditions

The workpiece is considered as a simply supported beam of which one end is having a hinged support while other with a roller support as shown in fig.7. At a distance of 40 mm from hinged support, the grinding operation was performed through further distance of 40 mm. Hence the middle most section of 40 mm experienced a torque as mentioned in kinematics of grinding. This torque can be assumed to act at center.

Von-mises stresses

Fig.8. shows the distribution of Von-misses stresses induced within the beam. Initially when the workpiece was acted with no load conditions, stresses were zero. After initial start of grinding operation, stresses were induced at the center of the workpiece. Since the workpiece was supported by both the ends, stresses tend to develop more at the ends of the workpiece. The utmost maximum values of equivalent stresses goes up to 0.3307 N/mm^2 which were acted at the ends.

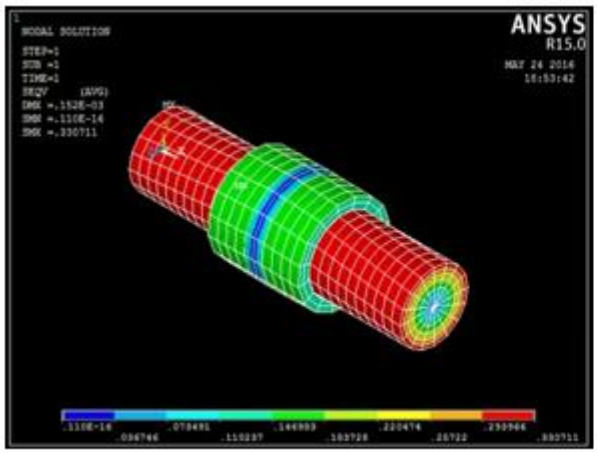

Fig.8. Stress Analysis

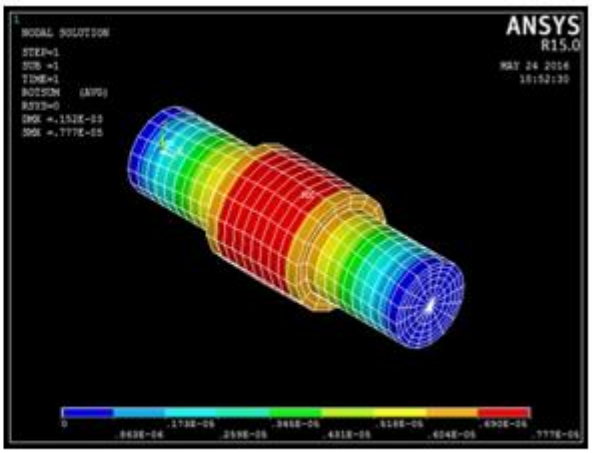

Fig.9. Displacement Analysis

Displacement

Fig.9. shows the deflection of beam from its axial position. Initially, when the workpiece was acted with no load conditions, displacements were zero. After initial start of grinding, displacement occurs at the center where the grinding wheel and workpiece are in contact with each other. The utmost maximum displacement of the beam goes up to 0.77 x 10^{-5} mm which was acted at the center.

CONCLUSION

On the basis of this investigation, the following conclusion can be drawn

1. This paper has presented application of Taguchi method to determine the optimal process parameters for grinding wheel dressing process. The concept of ANOVA and S/N ratio has been used to determine the effect and influence of process parameters namely dressing depth of cut, cross feed rate, drag angle of dresser and number of passes that were studied on output responses. MINITAB 17, software has been used for analysis of response graphs of average values and S/N ratios.
2. It was found that, for Surface Roughness (Ra), out of four dressing parameters dressing cross feed rate is the most influencing factor for EN19 work material followed by dressing depth of cut, drag angle of dresser and number of passes were having lower influence.
3. In this work, mathematical model is generated for Surface roughness by using multiple regression analysis which shows that the roughness is increases with increase in dressing depth of cut, dressing cross feed rate and drag and angle of the dresser, and decreases with increase in number of passes.
4. The optimal set of dressing parameters obtained for surface roughness using Taguchi design of experiment methodology is dressing depth of cut: 20 µm, dressing cross feed rate: 80 mm/min, drag angle: 50^0 and number of passes : 4.
5. It was found that, by finite element analysis the maximum stress of 0.3307 N/mm^2 was induced at both the ends of work piece and maximum displacement of 0.77 x 10^{-5} mm was at the contact surface of the grinding wheel and work piece

REFERENCES:

[1] Malkin S. and Guo C. (2008), "Grinding Technology: Theory and Applications of Machining with Abrasives", Second edition, *Industrial Press*, Inc. 989, *New York*, NY 10018.
[2] W. Brian Rowe (2009), "Principle of Modern Grinding Technology", William Andrew, Second Edition, *The Boulevard, Langford Lane, Kidlington, Oxford* OX5 1GB, UK.
[3] Douglas C. Montgomery, (1991), "Design and Analysis of Experiments", 7th edition, Wiley, Singapur.
[4] T. J. Vickerstaff (1970), "The Influence of Wheel Dressing on the Surface Generated in the Grinding Process", *International Journal of Machine Tools Design*, Res. Vol. 16, pp. 260-267.
[5] Pacitti, V. and Rubenstein, C. (1972), "The influence of the dressing depth of cut on the performance of a single point diamond dressed alumina grinding wheel", *International Journal of Machine Tool Design and Research*, Vol. 12, pp. 267-279.
[6] P. Ramchandran and S. Vaidyanathan (1976), "Statistical Evaluation of Parameters in Grinding", *Wear*, Vol. 36, pp. 119-125.
[7] N.P. Fletcher (1978), "Single Point Diamond Dressing of Aluminium Oxide Grinding Wheel and its Influence in Cylindrical Transverse Grinding", *International Journal of Machine Tools Design*, Res. Vol. 20, pp. 55-65.

[8] S.J. Pande and G.K. Lal, (1979), "Effect of Dressing on Grinding Wheel Performance", *International Journal of Machine Tools Design*, Res. Vol. 19, pp. 171-179.

[9] Buttery, T.C., Statham, A., Percival, J. B. and Hamed, M. S. (1979), "Some Effects of Dressing on Grinding Performance", *Wear*, Vol. 55, pp. 195-219.

[10] Andrzej Koziasrski and Andrze Golabczak (1985), "The Assessment of the Grinding Wheel Cutting Surface Condition after Dressing with Single Point Diamond Dresser", *International Journal of Machine Tools Design*, Res. Vol. 25, No.4, pp. 313-325.

[11] Xun Chen, W. Brian Rowe (1996), "Analysis and Simulation of Grinding Process. Part I: Generation of Grinding Wheel Surface", *International Journal of Machine Tools & Manufacture*, vol.36, No. 8, pp 871-882.

[12] B.Linke (2008), "Dressing Process Model for Vitrified Bonded Grinding Wheel", *CIRP Annals - Manufacturing Technology*, Vol. 57, pp. 345-348.

[13] Thiagarajan, R. Sivarama krishnan and S. Somasundaram (2011), "Modeling and Optimization of Cylindrical grinding of Al/SiC composites Using Genetic Algorithms", *ABCM Journal of Braz. Soc. Of Mechanical Sciences and Engineering*, Vol. 34, No. 1, 32-40.

[14] M. Janardhan and Dr. A. Gopala Krishna (2011), "Determination and optimization of cylindrical grinding process parameters using Taguchi method and regression analysis", *International Journal of Engineering Science and Technology*, Vol. 3, No. 7, pp. 5659-5665

International Journal of Engineering Research and General Science Volume 5, Issue 4, July-August, 2017
ISSN 2091-2730

Strategies: To Defeat Ransomware Attacks

REETA MISHRA
Department of Information Technology
K. J. Institute of engineering & Technology, Savli
Vadodara, Gujarat, India
Email id- reeta.mishra@kjit.org

Abstract— Ransomware is a malware software design in order to extract or collect a huge amount of money from victims, whose system got infected by this attack. It leads to deny access to a user's (or organization's) data, usually by encrypting the data with a secret key. After the data is encrypted, the malware /hacker instruct the user to pay the ransom amount to the hacker (usually in a digital currency such as Bitcoin) in order to receive a decryption key. The amount of ransom requested typically increases, if the hacker determines the data has substantial value. Normally Financial transaction, Medical details and personal identity theft are the soft target for these attack because of the quantity and value of their data. The objective of this paper is to create awareness among less skilled computer users by providing cyber safeguard knowledge and regular updating practice of prevention techniques.
Keywords- Ransomware Attack, Families, Crypto wall, Tesla Crypto, Locker, Prevention method, Bitcoin.

INTRODUCTION

Ransomware Attacks are one of the most notorious malware floating around the internet. These are a piece of software that locks down your files in your or victims PC or smartphone behind an encrypted paywall. In order to overcome this problem victim need to pay ransom to get back there valuable files. But attacker normally prefer to get the ransom payment through bitcoin. . Even after full payment — there's no guarantee to get that decryption key to unlock victim encrypted files.

Bitcoin is digital currency that lets you anonymously buy goods and services. The victims can send bitcoins digitally using a mobile phone app or computer. It's as easy as swiping a credit card. Each bitcoin transaction is on a public log. Names of buyers and sellers are anonymous – only their wallets IDs are exposed. And it allows buyers or sellers do business without easily tracing it back to them. As a result, it's become a popular choice for cybercriminals to choose bitcoin as a form of payment

Ransomware attacks are typically carried out using a Trojan, entering a system through a downloaded file or a vulnerability in a network service [1][2].

I. TOP FAMOUS RANSOMWARE FAMILIES-

A) Locky- The malware gets spread using spam in the form of an email messages containing malicious links and it is disguised as an invoice. When user opens it, the invoice is scrambled, and the victim is instructed to enable macros to read the document. When macros are enabled, Locky Ransomware begins to encrypt a large array of file types using AES encryption. Bitcoin ransom is demanded when encryption is complete.

B) Tesla Crypt – This type of Ransomware, it uses an AES Algorithm to encrypt files. It is typically disseminated via the Angler exploit kit specifically attacking Adobe vulnerabilities. Once vulnerability is exploited, Tesla Crypt installs itself in the Microsoft temp folder. The ransom money is paid in terms of bitcoins.

C) Crypto Ransomware (Data Locker)- prevents access to files or data via encryption.

D) Locker Ransomware (Computer Locker)- Denies access to a computer / device by disabling the user interface.

E) Crypto Wall- After the downfall of Crypto Locker, the Crypto Wall had gained its importance. It including Crypto bit, Crypto Defense, Crypto Wall 2.0 and Crypto Wall 3.0, among others .Crypto Wall is distributed via spam or exploit kits.

II. CAUSES OF ATTACK

1) Traffic distribution system –Improper distribution of traffic through the data transfer from one network to other in case of distribution system.
2) Mal advertisement .or Data breach-Unnecessary advertisement and add on can be the reason.
3) Spam Email-Frequently usage or checking spam email is one important cause of this attack.
4) Auto downloader & botnet- Never allow auto downloader application to get install if in case it happened then turn off/ disconnect the device from internet.
5) Social engineering & self-propagation-Social media is the most important cause of these attacks.

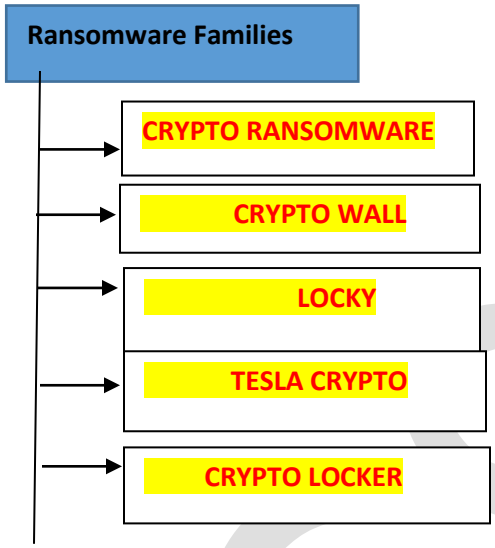

Fig 1. Top Ransomware families

IV.RELATED WORK-In the paper "automatic test packet generation" proposed by Hongyi Zeng, Peyman Kazemian,, George Varghese, ,Fellow, ACM, and Nick McKeown, proposed about the working of the ATPG techniques[5] for testing and debugging networks This method generates a minimum number of dummy nodes or test packets to check every link in the network. Our implementation also augments testing with a simple fault localization scheme also constructed using the header space framework. Thus the liveness of the network is tested.

The work by Nolen Scaife, Henry Carter, Patrick Traynor, Kevin R.B.Butler "Crypto lock (drop it): Stopping Ransomware attacks on user data" explains about the Crypto Drop,[6] an early warning detection system that alerts user during suspicious file activity. It focuses on detecting Ransomware through monitoring the real time change of user data. Indicators have been used to track the suspiciousness. By tracking these, they develop a reputation score, which alerts the user and suspends the suspicious process.

Analysis:- In this paper we main focus on the top 3 Ransomware threads, which is now-a-days at its fame. we try to have a comparative study between these three threads for that we collect 18 affected countries data of April-May 2016 for crypto wall , locky and Tesla as given below-

Country	Crypto wall	Locky	Tesla Crypto
US	43	53	14
FR	2	18	NA
JP	8	8	3.5
SK	NA	5	NA
CA	2.5	4	11
MX	4.5	3	1
CL	NA	2.5	NA
GB	NA	2.5	NA
ZA	NA	1.5	NA
IL	3.5	1.5	NA
TR	NA	NA	13

ES	**5**	**NA**	**2**
IT	**3**	**NA**	**3.5**
CO	**2**	**NA**	**NA**
KR	**NA**	**NA**	**39**
TR	**7**	**NA**	**NA**
IN	**NA**	**NA**	**2**
DE	**NA**	**NA**	**2**

Table 1. Data to measure effect of this attack

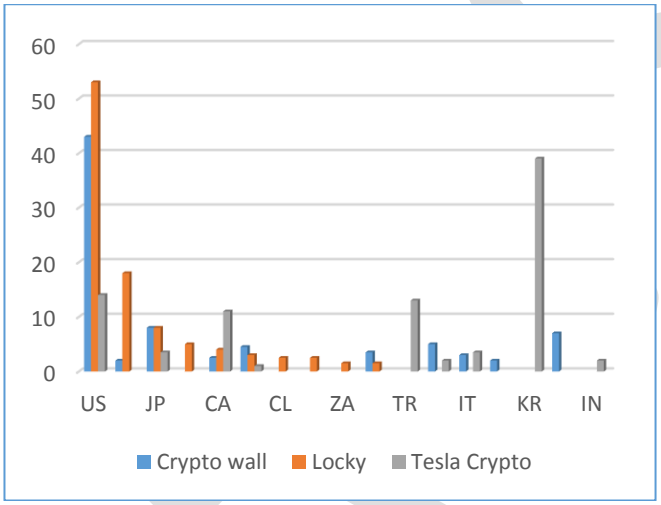

Fig 3. Attack effect show through graph

In case of crypto wall top two most hit countries are US & JP

In case of locky top two most hit countries are US & FR

In case of Tesla crypto top two most hit countries are KR **& US**

V. IMPACT OF ATTACK

1) Shutdown Cost: Organization may be forced to shut down systems to deal with the infection. Customers may be affected as target not achieved on time or may have financial loss, which can't be repay. It surely damage organization goodwill in market.

2) Data or Information loss: Loss of data due to files being encrypted and stolen can have a huge impact on businesses. The loss of company records, personally identifiable information, or intellectual property can significantly impact the organization. On other side those personal data can be mishandle by attacker. The aim behind the attack may threaten to publish stolen data online and attempt to extort more money from victim.

3) Financial Cost: Companies may have to pay for the incident response and other security related solutions in response to ransomware. Organizations could also be hit with large legal bills if customers are affected. Fines and other penalties may also apply.

4) Loss of life: In the case of a hospital or other medical organization, patients' lives may put at risk as essential medical equipment may be affected. Patient record including medical history may be inaccessible, leading to delays in treatment or even incorrect medication.

VI. PREVENTION FROM RANSOMWARE ATTACK

1. Install a good & license antivirus: First tip is to install a top-notch antivirus that often scans your online activity and applications in your PC.

2. Secure back up of your data: We need to create secure backups of data on a regular basis to USBs or an external hard drive and always remember to disconnect your external memory devices from computer after backing up otherwise they will also infect with ransomware. We can also use a Cloud storage with high-level encryption and multiple-factor authentication features to store confidential files.

3. Download files from trusted sources: Always try to download files from trusted sources or websites. Be alert and check file description before downloading from torrents. Try to avoid websites that have too many pop ups.

4. Scan email attachments before download: So always double-check email attachments before downloading even if it is came from your relatives/friends or office. Also never open email attachments from strangers. And check thoroughly email details like sender name and email address, company logo, spelling — because potential scammers forge emails that looks like coming from official source. And in Gmail make sure you scan attachments before open.

5. Update operating system and other applications: Using Windows or Android always update your operating system and other applications.

6. Browser Protection- Apart from antivirus it is also important to use firewall or other secure measure to provide protection to the browser

7. Use a sandboxing solution

8. Block risky file extension- End user must avoid from opening risky files extension with .wsf, .chm, .jscript,. vbscript etc.

9 Use URL filtering-It means block the access of C&C Server so the system get protected.

10. Use HTTPS filters-Instead of using simple HTTP it is recommended to use a secure HTTPS filters

11. Use HIPS or other signature less technologies -User must use host HOST INTRUSION PREVENTION SERVICE, these will help the user to protect from attack.

12. Encrypt data-As security point the user must keep all his confidential data in encrypted form.

13. Use security analysis tool and whitelisting solution-User must use whitelisted (trustful) solution and security tool as well as have a periodic check on the functioning of system.

VII. CONCLUSION & FUTURE SCOPE- In this complete paper try to explain overview, causes of ransomware attack, to show the effect of these attack through comparative study, its impact and the preventive measure for those people who are not much aware of these type of computer related attack threads .In continuation of this paper in my next paper , basically focus on the proposed model in order to fetch ransomware code and eliminated it without delay by using multilevel filtration techniques.

REFERENCES:

[1] G. Eason, B. Noble, and I. N. Sneddon, “On certain integrals of Lipschitz-Hankel type involving products of Bessel functions,” Phil. Trans. Roy. Soc. London, vol. A247, pp. 529–551, April 1955. *(references)*

[2] J. Clerk Maxwell, A Treatise on Electricity and Magnetism, 3rd ed., vol. 2. Oxford: Clarendon, 1892, pp.68–73.

[3] I. S. Jacobs and C. P. Bean, “Fine particles, thin films and exchange anisotropy,” in Magnetism, vol. III, G. T. Rado and H. Suhl, Eds. New York: Academic, 1963, pp. 271–350.

[4] K. Elissa, “Title of paper if known,” unpublished.

[5] R. Nicole, "Title of paper with only first word capitalized," J. Name Stand. Abbrev., in press.

[6] Y. Yorozu, M. Hirano, K. Oka, and Y. Tagawa, "Electron spectroscopy studies on magneto-optical media and plastic substrate interface," IEEE Transl. J. Magn. Japan, vol. 2, pp. 740–741, August 1987 [Digests 9th Annual Conf. Magnetics Japan, p. 301, 1982].

International Journal of Engineering Research and General Science Volume 5, Issue 4, July-August, 2017
ISSN 2091-2730

Some Fixed Point Results For Multivalued Operators In Vector Valued Spaces

Kumari Sarita, Mamta Kamra, Renu Chugh

mkhaneja15@gmail.com

Abstract : The aim of this paper is to prove some fixed point theorems for multivalued operators in E-b-metric space which is a Riesz space valued b-metric space.

Keywords : b-metric space, contraction mapping theorem, dedekind complete, E-b-metric space, multivalued operator, Riesz space, vector metric space.

Introduction : F. Riesz [7] introduced the concept of Riesz space. For a more extensive treatment of the theory of Riesz space we refer C. D. Aliprantis and K. C. Border [1], W. A. J.Luxemburg and A.C. Zannen [7].

Riesz space (or vector lattice) is an ordered vector space and at the same time a lattice also. Let E be a Riesz space with the positive cone $E_+ = \{x \in E : x \geq 0\}$ for an element $x \in E$, the absolute value $|x|$, the positive part x^+, the negative part x^- are defined as $|x| = x \vee (-x)$, $x^+ = x \vee 0$, $x^- = (-x) \vee 0$ respectively.

If every non−empty subset of E which is bounded above has a supremum, then E is called Dedekind complete or order complete. The Riesz space E is said to be Archimedean if $\frac{1}{n} a \downarrow 0$ holds for every $a \in E_+$.

Example 1 ([1]). Let $R^n (n \geq 1)$ be the real linear space of all real n−tuples $x = (x_1, x_2, x_3, \ldots, x_n)$ and $y = (y_1, y_2, y_3, \ldots\ldots, y_n)$ with coordinatewise addition and multiplication by real numbers. If we define that $x \leq y$ means that $x_k \leq y_k$ holds for $1 \leq k \leq n$, then R^n is a Riesz space with respect to this partial ordering.

Definition 1.1 ([1]). Let E be a Riesz space. A sequence (b_n) is said to be order convergent or o−convergent to b if there is a sequence (a_n) in E satisfying $a_n \downarrow 0$ and $|b_n - b| \leq a_n$ for all n, written as $b_n \xrightarrow{0} b$ or $o.\lim b_n = b$.

Definition 1.2 ([1]). A sequence (b_n) is said to be order Cauchy (o−Cauchy) if there exists a sequence (a_n) in E such that $a_n \downarrow 0$ and $|b_n - b_{n+p}| \leq a_n$ holds for all n and p.

Definition 1.3 ([1]). A Riesz space E is said to be o−Cauchy complete if every o−Cauchy sequence is o−convergent.

If range space of a metric space is Riesz space then it becomes a vector metric space.

Definition 1.4 ([2]). Let X be a non−empty set and E be a Riesz space. Then function $d : X \times X \to E$ is said to be a vector metric (or E−metric) if it satisfies the following properties :

(a) $d(x, y) = o$ if and only if $x = y$

(b) $d(x, y) \leq d(x, z) + d(y, z)$ for all $x, y, z \in X$.

Also the triple (X, d, E) is said to be a vector metric space. Vector metric space is generalization of metric space. For arbitrary elements x, y, z, w of a vector metric space, the following statements are satisfied :

(i) $0 \leq d(x, y)$ (ii) $d(x, y) = d(y, x)$

(iii) $|d(x, z) - d(y, z)| \leq d(x, y)$

(iv) $|d(x, z) - d(y, w)| \leq d(x, y) + d(z, w)$

Example 2 ([2]). A Riesz space is a vector metric space $d : E \times E \to E$ defined by $d(x, y) = | x - y|$. This vector metric is said to be the absolute valued metric on E.

Definition 1.5 ([2]). A sequence (x_n) in a vector metric space (X, d, E) vectorial converges (E−converges) to some $x \in E$, written as $x_n \xrightarrow{d.E} x$ if there is a sequence (a_n) in E satisfying $a_n \downarrow 0$ and $d(x_n, x) \le a_n$ for all n.

Definition 1.6 ([2]). A sequence (x_n) is called E−cauchy sequence whenever there exists a sequence (a_n) in E such that $a_n \downarrow 0$ and $d(x_n, x_{n+p}) \le a_n$ holds for all n and p.

Definition 1.7 ([3]). A vector metric space X is called E−complete if each E−cauchy sequence in X, E converges to a limit in X.

For more details and results regarding vector metric spaces we refer to [3], [5].

When E = R, the concepts of vectorial convergence and metric convergence, E−cauchy sequence and Cauchy sequence in metric are same.

When also X = E and d is the absolute valued vector metric on X, then the concept of vectorial convergence and convergence in order are the same.

I.A. Bakhtin [14] defined the concept of b-metric space in 1989.

Definition 1.8 ([6]) : Let X be a non−empty set and let $s \ge 1$ be a given real number. A function $d : X \times X \to R_+$ is called a b−metric provided that, for all $x, y, z \in X$

(i) $d(x, y) = 0$ if and only if $x = y$

(ii) $d(x, y) = d(y, x)$

(iii) $d(x, z) \le s[d(y, x) + d(y, z)]$

A pair (X, d) is called a b−metric space. It is clear from definition that b−metric space is an extension of usual metric space .

Example 3 ([3]) : The space $L_p(0 < p < 1)$ of all real functions x(t), $t \in [0, 1]$ such that $\int_0^1 | f(t) |^p dt < \infty$, is b−metric space if we take

$$d(f, g) = \left(\int_0^1 | f(t) - g(t) |^p \, dt \right)^{1/p} \quad \text{for each } f, g \in L_p$$

Several authors have investigated fixed point theorems on b−metric spaces, one can see [6], [8]

Combining the concept of vector metric space (E-metric space) and b-metric space I. R. Petre [5] defined E−b−metric space as follows:

Definition 1.9 ([5]). Let X be a non−empty set of $s \ge 1$, A functional $d : X \times X \to E_+$ is called an E−b−metric if for any $x, y, z \in X$, the following conditions are satisfied :

(a) $d(x, y) = 0$ if and only if $x = y$

(b) $d(x, y) = d(y, x)$

(c) $d(x, z) \le s[d(x, y) + d(y, z)]$

The triple (X, d, E) is called an E−b−metric space.

Example 4. Let $d: [0,1]\times [0,1]\to R^2$ defined by $d(x,y) = (\alpha |x-y|^2, \beta |x-y|^2)$ then (X,d,R^2) is an E-b-metric space where $\alpha, \beta > 0$ and $x,y \in [0,1]$.

Example 5 . The space $l_p(0 < p < 1)$, $l_p = \left\{ x = (x_i) : x_i \in R, \sum_{i=1}^{\infty} |x_i|^p < \infty \right\}$ and $x = \{x_i\}$, $y = \{y_i\} \in l_p$ define $\rho(x, y) = (\alpha_1 \|x - y\|_p, \alpha_2\|x - y\|_p, \ldots \alpha_n\|x - y\|_p)$ then (l_p, ρ, R^n) is an E-b-metric space.

For more facts regarding vector metric space see [11], [12].

Let X is a non empty set and $T: X \to P(X)$ is a multivalued operator, we denote by $F_T = \{x \in X : x \in T(x)\}$, where

$p(X) = \{Y : Y \subseteq X\}$;

$P(X) = \{Y \in P(X) : Y \neq \phi\}$

And in the context of a vector metric space (X, d, E), we denote by

$P_{cl}(X) = \{Y \in P(X) : Y \text{ is E- closed}\}$;

$P_b(X) = \{Y \in P(X) : Y \text{ is E- bounded}\}$;

$\text{Graph}(T) = \{(x,y) \in X : y \in T(X)\}$.

Definition 1.10 ([4]). Let (X, d, E) be a vector metric space. The operator $T: X \to P_{cl}(X)$ is said to be a multivalued k- contraction, if and only if $k \in [0,1)$ and for any $x, y \in X$ and any $u \in T(x)$, there exists $v \in T(y)$ such that

$$d(u,v) \leq k\, d(x, y) \qquad \text{..... (*)}$$

Definition 1.11 ([4]). Let (X, d, E) be a vector metric space. The operator $T: X \to P(X)$ be a multivalued operator. The sequence $(x_n)_{n\in N} \subset X$, recursively defined by

$$\{x_0 = x, x_1 = y;$$
$$\{x_{n+1} \in T(x_n),\ for all n \in N$$

is called the sequence of successive approximations of T starting from $(x,y) \in \text{Graph}(T)$.

Definition. Let (X, d, E) be an E-complete E-b-metric space. The operator $T : X \to P_{cl}(X)$ is said to be a multivalued (a,b,c,e,f)-contraction if and only if $a,b,c,e,f \in R_+$ with $a+b+c+e+f < 1$ and for any $x,y \in X$ and any $u \in T(x)$, there exists $v \in T(y)$ such that

$d(u,v) \leq ad(x,y) + bd(x,u) + cd(y,v) + e\, d(x,v) + f\, d(y,u)$

Main Results :

Theorem 1. Let (X, d, E) be a complete E-b-metric space with $s \geq 1$ and E-Archimedean and let $T : X \to P_{cl}(X)$ be a multivalued k-contraction with $sk < 1$ and $k \in (0,1]$. Then T has a fixed point in X and for any $x \in X$, there exists a sequence of successive approximations of T starting from $(x,y) \in \text{Graph}(T)$ for $n \in N$ which E-converges in (X, d, E) to the fixed point of T.

Proof : Let $x_0 \in X$ and $x_1 \in Tx_0$ then there exists $x_2 \in Tx_1$ such that

$d(x_1,x_2) \leq k\, d(x_0,x_1)$

Thus, define the sequence $(x_n) \in X$ by $x_{n+1} \in Tx_n$ and

$d(x_n,x_{n+1}) \leq k\, d(x_{n-1},x_n)$ for $n \in N$.

Inductively, we obtain,

$d(x_n,x_{n+1}) \leq k\, d(x_{n-1},x_n) \leq k^2\, d(x_{n-2},x_{n-1}) \leq \ldots\ldots \leq k^n\, d(x_0,x_1)$ for $n \in N$.

Now, for all n and p, we have

$d(x_n,x_{n+P}) \leq sd(x_n,x_{n+1}) + s^2 d(x_{n+1},x_{n+2}) + \ldots\ldots\ldots\ldots + s^p\, d(x_{n+p-1},x_{n+p})$ for any $n \in N$

$d(x_n,x_{n+P}) \leq sk^n\, d(x_0,x_1) + s^2 k^{n+1}\, d(x_0,x_1) + \ldots\ldots\ldots\ldots + s^p k^{n+p-1}\, d(x_0,x_1)$ for any $n \in N$

$$= \frac{sk^n\left(1-(sk)^p\right)}{(1-sk)} \; d(x_0,x_1) \;\leq\; \frac{sk^n}{1-sk} \; d(x_0,x_1) \;= a_n.a = b_n \text{ for any } n \in N,\ p \in N$$

Where $a_n = \dfrac{sk^n}{1-sk} \downarrow 0$ and $a = d(x_0, x_1) \in E^+$

Now, since E-Archimedean property, we get $b_n \downarrow 0$. So, the sequence $\{x_n\}$ is E-cauchy sequence in X. By the E- completeness of X, there is $z \in X$ such that $d(x_n,z) \leq a_n$.

We know that $x_{n+1} \in Tx_n$ for any $n \in N$ and by the multivalued k-contraction condition it follows that there exists $u \in Tz$ such that $d(x_{n+1},u) \leq k\, d(x_n,z)$ for any $n \in N$.

Then the following estimation holds:

Since $d(z,u) \leq sd(z,x_{n+1}) + sd(u,x_{n+1}) = sd(x_{n+1},z) + sd(x_{n+1},u)$

$\leq skd(x_n,z) + sa_{n+1}$

$\leq ska_n + sa_{n+1} \leq s(k+1)a_n \downarrow 0$

Thus, there exists $z = u \in Tz$ i.e. T has a fixed point in X.

Example 6. Let $E = R^2$ with componentwise ordering and let $X = [0,1]$

The mapping $d : X \to E$ is defined by

$$d(x, y) = \left(\frac{4}{3}|x-y|^2, |x-y|^2\right)$$

Then X is E-b-metric space. Let $T: X \to P_{cl}(X)$ with $T(x) = \{u(x), v(x)\}$, where $u,v : X \to X$ are defined by $u(x) = \dfrac{x}{2}$, $v(x) = \dfrac{x}{3}$

We have the following possibilities:

Case 1: for any $(x,y) \in X$ and any $\dfrac{x}{2} \in T(x)$, there exists $\dfrac{y}{2} \in T(y)$ such that

$$d\left(\frac{x}{2},\frac{y}{2}\right) \leq kd(x,y)$$

$$\Rightarrow \left(\frac{4}{3}\left|\frac{x}{2}-\frac{y}{2}\right|^2, \left|\frac{x}{2}-\frac{y}{2}\right|^2\right) \leq k\left(\frac{4}{3}|x-y|^2, |x-y|^2\right)$$

Case 2: for any $(x,y) \in X$ and any $\dfrac{x}{3} \in T(x)$, there exists $\dfrac{y}{3} \in T(y)$ such that

$$d\left(\frac{x}{3},\frac{y}{3}\right) \leq kd(x,y)$$

$$\Rightarrow \left(\frac{4}{3}\left|\frac{x}{3}-\frac{y}{3}\right|^2, \left|\frac{x}{3}-\frac{y}{3}\right|^2\right) \leq k\left(\frac{4}{3}|x-y|^2, |x-y|^2\right)$$

For all of these cases, the condition $d(u,v) \leq k\, d(x, y)$ holds for $k = \dfrac{1}{2}$. From theorem 1, it follows that T has a fixed point in X.

Theorem 2. Let (X, d, E) be an E- complete E-b-metric space with $s \geq 1$ and E-Archimedean and let $T : X \to P_{cl}(X)$ be a multivalued (a,b,c,e,f)-contraction with $ks < 1$

Where $k = a + b + c + se + sf$

Then T has a fixed point in X and for any $x \in X$, there exists a sequence of successive approximations of T starting from $(x,y) \in Graph(T)$ which E-converges in (X, d, E) to the fixed point of T.

Proof : Let $x_0 \in X$ and $x_1 \in Tx_0$ then there exists $x_2 \in Tx_1$ such that

$d(x_1,x_2) \leq a\, d(x_0,x_1) + b\, d(x_0,x_1) + c\, d(x_1,x_2) + e\, d(x_0,x_2) + f\, d(x_1,x_1)$

$d(x_1,x_2) \leq ad(x_0,x_1) + bd(x_0,x_1) + cd(x_1,x_2) + e\, d(x_0,x_2)$,

Inductively, we define the sequence $(x_n) \in X$, $x_{n+1} \in Tx_n$ for $n \in N$.

$d(x_n,x_{n+1}) \leq a\, d(x_{n-1},x_n) + b\, d(x_{n-1},x_n) + c\, d(x_n,x_{n+1}) + e\, d(x_{n-1},x_{n+1}) + f\, d(x_n,x_n)$

$d(x_n,x_{n+1}) \leq a\, d(x_{n-1},x_n) + b\, d(x_{n-1},x_n) + c\, d(x_n,x_{n+1}) + e\, d(x_{n-1},x_{n+1})$

$d(x_n,x_{n+1}) \leq a\, d(x_{n-1},x_n) + b\, d(x_{n-1},x_n) + c\, d(x_n,x_{n+1}) + se\, d(x_{n-1},x_n) + se\, d(x_n, x_{n+1})$

$(1-c-se)\, d(x_n,x_{n+1}) \leq (a+b+se)\, d(x_{n-1},x_n)$ for any $n \in N$ ……..(1)

Further,

$d(x_{n+1},x_n) \leq a\, d(x_{n-1},x_n) + b\, d(x_{n+1},x_n) + c\, d(x_{n-1},x_n) + e\, d(x_n,x_n) + f\, d(x_{n-1},x_{n+1})$

$d(x_{n+1},x_n) \leq a\, d(x_{n-1},x_n) + b\, d(x_{n+1},x_n) + c\, d(x_{n-1},x_n) + sf\, d(x_{n-1},x_n) + sf\, d(x_n,x_{n+1})$

$(1-b-sf)\, d(x_{n+1},x_n) \leq (a+c+sf)\, d(x_{n-1},x_n)$ for any $n \in N$ ……..(2)

From (1) and (2) ,

$(1-b-c-se-sf)\, d(x_n, x_{n+1}) \leq (2a+b+c+se+sf)\, d(x_{n-1}, x_n)$

$$d(x_n, x_{n+1}) \leq \frac{2a+b+c+se+se}{1-(b-c-se-sf)}\, d(x_{n-1}, x_n)$$

$d(x_n, x_{n+1}) \leq \lambda\, d(x_{n-1}, x_n)$

where $\lambda = \dfrac{2a+b+c+sc+sf}{1-(b+c+se+sf)} < 1$

Now, $d(x_n, x_{n+1}) \leq \lambda\, d(x_{n-1}, x_n) + \lambda^2\, d(x_{n-2}, x_{n-1}) + \ldots\ldots\ldots\ldots + \lambda^n\, d(x_0, x_1)$ for any $n \in N$

We have

$d(x_n,x_{n+P}) \leq sd(x_n,x_{n+1}) + s^2 d(x_{n+1},x_{n+2}) + \ldots\ldots\ldots\ldots + s^p\, d(x_{n+p-1},x_{n+p})$ for any $n \in N$

$d(x_n,x_{n+P}) \leq s\lambda^n\, d(x_0,x_1) + s^2 \lambda^{n+1}\, d(x_0,x_1) + \ldots\ldots\ldots\ldots + s^p \lambda^{n+p-1}\, d(x_0,x_1)$ for any $n \in N$

$$= \frac{s\lambda^n\left(1-(s\lambda)^p\right)}{(1-s\lambda)}\, d(x_0,x_1) \leq \frac{s\lambda^n}{1-s\lambda}\, d(x_0,x_1) = a_n.a = b_n \text{ for any } n \in N, p \in N$$

Where $a_n = \dfrac{s\lambda^n}{1-s\lambda} \downarrow 0$ and $a = d(x_0, x_1) \in E^+$. Note that $s\lambda < 1$, since $sk < 1$.

On the other hand, by E-Archimedean property, we get $b_n \downarrow 0$. So, the sequence $\{x_n\}$ is E-cauchy sequence in X. By the E-completeness of X, there is $z \in X$ such that $d(x_n,z) \leq a_n$.

We know that $x_{n+1} \in Tx_n$ for any $n \in N$ and by the multivalued (a,b,c,e,f)-contraction condition it follows that there exists $u \in Tz$ such that

$d(x_{n+1},u) \leq a\, d(x_n,z) + b\, d(x_n, x_{n+1}) + c\, d(z,u) + e\, d(x_n,u) + f\, d(z, x_{n+1})$ for any $n \in N$.

Since $d(z,u) \le sd(x_{n+1},u) + sd(x_{n+1},z)$

$$\le sa\, d(x_n,z) + sb\, d(x_n, x_{n+1}) + sc\, d(z,u) + se\, d(x_n,u) + sf\, d(z, x_{n+1}) + sd(x_{n+1},z)$$

$$\le sa\, a_n + sb\, d(x_n, x_{n+1}) + sc\, d(z,u) + se\, [sd(x_n,z) + sd(u,z)] + sf\, a_{n+1} + sa_{n+1}$$

$$\le s(a+f+1)\, a_n + sb\, d(x_n, x_{n+1}) + sc\, d(z,u) + s^2e\, d(x_n,z) + s^2e\, d(z,u)$$

$(1-sc-s^2e)\, d(z,u) \le s(a+f+1)a_n + sb\, d(x_n, x_{n+1}) + s^2e\, a_n$

$$d(z,u) \le \frac{s(a+f+se+1)}{(1-sc-s^2e)}\, a_n + \frac{sbd(x_n, x_{n+1})}{(1-sc-s^2e)} \downarrow 0, \quad \text{note that } 1-sc-s^2e > 0.$$

Thus, we have there exists $z = u \in Tz$ i.e. T has a fixed point in X.

Theorem 3. Let (X, d, E) be a complete E−b−metric space with E-Archimedean and let $T : X \to P_{cl}(X)$ be a multivalued mapping and satisfies the following conditions :

(i) for any $x \in X$, $d(u,v) \le kL(x,y)$ where $u \in Tx$, $v \in Ty$, $ks<1$

and

$$L(x, y) \in \{d(x,y), d(x,u), d(y,v), \frac{1}{2}[d(x,v) + d(y,u)], \frac{1}{2}[d(x,u) + d(y,v)]\}$$

Then T has a fixed point in X and for any $x \in X$, there exists a sequence of successive approximations of T starting from $(x,y) \in Graph(T)$ which E-converges in (X, d, E) to the fixed point of T.

Proof : Let $x_0 \in X$ and $x_1 \in Tx_0$.

Inductively, we define the sequence $\{x_n\} \in X$, $x_{n+1} \in Tx_n$ for $n \in N$.

We first show that

$$d(x_n, x_{n+1}) \le kL(x_{n-1}, x_n) \text{ for all n.}$$

Now we have to consider the following cases :

Case 1 : $d(x_n, x_{n+1}) \le kd(x_{n-1}, x_n)$ for all n.

Case 2 : $d(x_n, x_{n+1}) \le kd(x_{n-1}, x_n)$ for all n.

Case 3 : $d(x_n,x_{n+1}) \le kd(x_n, x_{n+1})$

$\Rightarrow$ $d(x_n, x_{n+1}) = 0$ for all n.

Case 4 : $d(x_n,x_{n+1}) \le k\frac{1}{2}[d(x_{n-1}, x_{n+1}) + d(x_n, x_n)]$

$$d(x_n,x_{n+1}) \le \frac{k}{2}[d(x_{n-1},x_{n+1})]$$

$$\le \frac{k}{2}s\,[d(x_{n-1},x_n) + d(x_n,x_{n+1})]$$

$$\left(1-\frac{k}{2}s\right)d(x_n,x_{n+1}) \le \frac{k}{2}s\, d(x_{n-1},x_n)$$

$$d(x_n,x_{n+1}) \le \left(\frac{\frac{k}{2}s}{1-\frac{ks}{2}}\right)d(x_{n-1},x_n) \qquad \left\{\frac{ks}{2} < \frac{1}{2} \text{ i.e. } ks<1\right\}$$

Thus $d(x_n, x_{n+1}) \le \lambda_1 d(x_{n-1},x_n)$ where $\lambda_1 = \left(\dfrac{\frac{k}{2}s}{1-\frac{ks}{2}}\right) < 1$

Case 5 : $d(x_n,x_{n+1}) \le k\frac{1}{2}[d(x_{n-1}, x_n) + d(x_n, x_{n+1})]$

$$\le \frac{k}{2}[d(x_{n-1}, x_n) + d(x_n, x_{n+1})]$$

$$\left(1-\frac{k}{2}\right)d(x_n, x_{n+1}) \le \frac{k}{2}d(x_{n-1}, x_n)$$

$$d(x_n, x_{n+1}) \le \left(\frac{\frac{k}{2}}{1-\frac{k}{2}}\right)d(x_{n-1}, x_n) \quad \left\{\because \frac{k}{2} < \frac{1}{2}\right\}$$

$d(x_n,x_{n+1}) \le \lambda_2 d(x_{n-1},x_n)$ where $\lambda_2 = \dfrac{\frac{k}{2}}{1-\frac{k}{2}} < 1$

Thus for all n and p, we have

$$d(x_n,x_{n+p}) \le sd(x_n, x_{n+1}) + s^2 d(x_{n+1},x_{n+2}) + \ldots + s^p d(x_{n+p-1},x_{n+p})$$

$$\le s\lambda^n d(x_0, x_1) + s^2 \lambda^{n+1} d(x_0,x_1) + \ldots + s^p\lambda^{n+p-1} (x_0,x_1)$$

$$= \frac{s\lambda^n(1-(s\lambda)^p)}{(1-s\lambda)}d(x_0, x_1) \le \left(\frac{s\lambda^n}{1-s\lambda}\right)d(x_0, x_1)$$

$= a_n.a = b_n$ for any $n \in N$ and $p \in N$

Now, since E is Archimedean, we have $b_n \downarrow 0$. So the sequence $\{x_n\}$ is E–Cauchy in X. By the E–completeness of X, there is $z \in X$ such that $d(x_n, z) \le a_n$.

We know that $x_{n+1} \in Tx_n$ and $T : X \to P_{cl}(X)$ be a multivalued mapping so it follows that there exists $w \in Tz$ such that

$$d(x_{n+1},w) \le kL(x_n,z) \text{ for any } n \in N$$

Then the following estimation holds:

$d(z,w) \le sd(x_{n+1},z) + sd(x_{n+1},w)$

$\le ska_n + skL(x_n,z)$

Where $L(x_n,z) \in \{d(x_n,z), d(x_n,x_{n+1}), d(z,w), \frac{1}{2}[d(x_n,w) + d(z,x_{n+1})], \frac{1}{2}[d(x_n,x_{n+1}) + d(z,w)]\}$

Case 1 : $d(z,w) \le ska_n + skL(x_n,z) \le ska_n + ska_{n-1} \le 2ska_{n-1} \downarrow 0$

Case 2 : $d(z,w) \le ska_n + skd(x_n,x_{n+1}) \le ska_n + sk[sd(x_n,z) + sd(z,x_{n+1})]$

$\le ska_n + s^2ka_{n-1} + s^2ka_n \le ska_n + 2s^2ka_{n-1} \le sk(1 + 2s)a_{n-1}$ $(\because a_n \le a_{n-1})$

Case 3 : $d(z,w) \le ska_n + skd(z,w)$

$(1-sk)\, d(z,w) \le ska_n$

$$d(z,w) \leq \left(\frac{sk}{1-sk}\right) a_n \downarrow 0$$

$$d(z,w) = 0$$

Case 4 : $d(z,w) \leq ska_n + \frac{1}{2} sk[d(x_n,w) + d(z,x_{n+1})] \leq ska_n + \frac{sk}{2} [\{sd(x_n, z) + sd(z,w)\} + d(x_{n+1}, z)]$

$$\leq ska_n + \frac{s^2k}{2} d(x_n, z) + \frac{s^2k}{2} d(z,w) + \frac{sk}{2} d(x_{n+1}, z)$$

$$\leq ska_n + \frac{s^2k}{2} a_{n-1} + \frac{s^2k}{2} d(z,w) + \frac{sk}{2} a_n$$

$$\left(1-\frac{s^2k}{2}\right) d(z,w) \leq \left(\frac{s^2k}{2} + \frac{3sk}{2}\right) a_{n-1}$$

$$d(z,w) \leq \frac{\left(\frac{s^2k}{2} + \frac{3sk}{2}\right)}{\left(1-\frac{s^2k}{2}\right)} a_{n-1}$$

$$\Rightarrow d(z,w) = 0$$

Case 5 : $d(z,w) \leq ska_n + \frac{1}{2} sk[d(x_n, x_{n+1}) + d(z,w)] \leq ska_n + \frac{sk}{2} [\{sd(x_n, z) + sd(x_{n+1}, z)\} + d(z,w)]$

$$\left(1-\frac{sk}{2}\right) d(z,w) \leq ska_n + \frac{s^2k}{2} a_{n-1} + \frac{s^2k}{2} a_n$$

$$d(z,w) \leq \frac{sk(s+1)}{1-\frac{sk}{2}} a_{n-1} \downarrow 0$$

$$\Rightarrow d(z,w) = 0$$

Therefore T has a common fixed point in X.

REFERENCES:

[1] C.D.Aliprantis and K.C.Border, "Infinite Dimensional Analysis" Berlin: Springer-Verlag, 1999
[2] Cuneyt Cevik and Ishak Altun, "Vector Metric Spaces and Some Properties"Topological Methods in Nonlinear Analysis, Volume 34, 375-382,2009.
[3] Ishak Altun and Cuneyt Cevik "Some Common Fixed Point Theorems in Vector Metric Spaces"Faculty of Sciences and Mathematics, University of Nis. Serbia, Filomat 25:1,105-113,July5,2010.
[4] Ioan-Radu-Petre "Fixed Point Theorems In Vector Metric Spaces For Multivalued Operators" Miskolc Mathematical Notes,HU e-ISSN 1787-2413, Volume 16,391-406, 2015.
[5] Ioan-Radu-Petre "Fixed Point Theorems in E-b-Metric spaces" J.Non Linear Science 264-271, 2014.
[6] Pankaj Kumar Mishra, Sachdeva and Banrrjee, "Some Fixed Point Theorems in b-Metric Spaces" Turkish Journal of Analysis and Number Theory, Volume 2, No.1, 19-22,2014.
[7] Luxemburg and Zannen, "Riesz Spaces" North-Holland Publishing Company, Amsterdam,1971.
[8] Tania Lazer and Gabriela, "The Theory Of Reich's Fixed Point Theorem for Multivalued Operators" Fixed Point Theory and Applications, Volume 2010, Article ID 178421, 10 pages, 2010.

[9] Lakshmi Kant Dey, "Fixed Point Theorems in Vector Metric Spaces" International Journal of Mathematical Analysis, Volume 4, no. 48, 2395-2400, 2010.
[10] Sam Nadler Jr. "Multivalued Contraction Mapping" Pacific Journal Of Mathematics, Vol 30, No. 2, 1969.
[11] Renu Praveen Pathak and Ramakant Bhardwaj "Fixed Point and Common Fixed Theorems in Vector Metric Spaces" Mathematical Theory and Modeling, ISSN 2224-5804 Vol.3, No. 6, 2013.
[12] Bazine Safia, Abdelkrim Aliouche and Fateh Ellaggoune, "Common Fixed Point Theorems on Spaces With Vector –Valued Metrics" Congres des Mathematiciens Algeriens, 11-13, May 2014.
[13] Do Hong Tan and Nguyen Thi Thanh Ha " Nadler's Fixed Point Theorem in Cone Metric Spaces" Vietnam Journal Of Mathematics , 40:4 , 447-452, 2012.
[14] Bakhtin, "The Contraction Mapping Principle In Quasi - Metric Spaces" Functional Analysis Unianwisk Ges. Pwd. Inst 30, 26-37, 1989

International Journal of Engineering Research and General Science Volume 5, Issue 4, July-August, 2017
ISSN 2091-2730

VALUE ASSESSMENT OF HISTORIC FORT PRECINCTS OF MUMBAI

A user-centric approach to analyzing significance of forts

Vidhi K. Jobanputra [i]

[i] Assistant Professor, Balwant Sheth school of Architecture, NMIMS University – Mumbai

[i] Student(M.Arch), Sir J.J. College of Architecture,Fort, Mumbai

Abstract: The significance of a site is determined by multiple values.[1] These values are a combination of the '***tangible'*** ones held by experts- the art historians, archaeologists, architects, and other professionals-as well as '***intangible'*** values brought forth by '***new'*** stakeholders over the years – the citizens and local communities. These citizens have their own set of socio-cultural values which often '***differ***' from those of heritage specialists or experts. (*Torre 3*).Since the '***right to decide***' the fate of heritage sites through planning conservation strategies lies in the hands of experts who are expected to work within a fixed framework of rules and regulations laid down by the government, end up ***prioritizing historic or archaelogical significance*** of the site. In this context, the historical or archaeological significance which is more relevant to the ***'past'*** ends up being ***emphasized*** whereas the '***present'*** socio-cultural significance shaped by the citizens and the '***future potential***' of these sites is pushed to the ***periphery***.

There are two prime reasons determining such an approach :

Firstly, the methods of measuring these ***'intangible'*** values which are relevant to all stakeholders, experts and citizens in a diverse country like India is difficult.

Secondly, understanding the '***influence of underlying parameters'*** such as rules and regulations, potential and flexibility of the built form, infrastructure development and neighborhood characteristics of the precincts on the existing significance and future potential of these sites is a complex phenomenon.

The paper thus intends to discuss the identification of ways in these ***'intangible'*** values could be measured through the lenses of '***citizens as primary stakeholders'*** and then viewing it in context with the underlying parameters mentioned above to obtain a more holistic vision regarding conservation of historic sites.

The case of historic fort precincts in a metro city like Mumbai is used as a model to explain these ***'ways of seeing and measuring significance'***.

Keywords:
Measuring intangible values, holistic vision, citizens as primary stakeholders.

I. INTRODUCTION

Mumbai metropolitan region with its historical variety is home to at least 25 forts. *(Study of forts within the Mumbai Metropolitan Region -Volume 1 4*) The main city of Mumbai and its extended suburbs, itself has 10 British and Portuguese colonial forts enclosing an area of more than 115 acres. Caught between a time warp of functional redundancy and contemporary urban pressures of development, several of these gradually face extinction. *(Study of forts within the Mumbai Metropolitan Region -Volume 1 4)* The laws post-independence which remained unevolved since decades restricted their role to archeological monuments that are ***'forms freed of function***' with no defined purpose, apart from being viewed as museum exhibits rather than living architectural buildings. Mumbai, a city where every inch of space is a luxury, the ***'buffer spaces'*** around the enclosures of the forts which fall into ***prohibited*** (100 metres)[2] and ***regulated*** zones (200m)[3] as per laws, informally started serving as ***spillover*** spaces for the neighborhood especially the local communities with their activities flowing into these buffer areas and sometimes even into the enclosures of the fortifications serving either ***religious***, ***cultural***, ***recreational*** or ***livelihood*** purpose and thus compensating for the crunch of space in the growing city. This new land-usage gave birth to new values and significance to these precincts which now forms an integral part of the existing reality of fort precincts. This phenomenon, if viewed positively, can help us decode the future potential of these forts reincorporating them into the urban milieu as vital multifunctional spaces. To explore this new acquired significance of the forts further, the fort precincts of ***Sewri, Bassein, Sion and Worli*** are taken up for value assessment through lenses of citizens and local communities as

[1] Value can be defined simply as a set of positive characteristics or qualities perceived in cultural objects or sites by certain individuals or groups *(Torre 4)*

[2] Prohibition within the monument: Consumption or cooking of food, hawking, selling, begging, vehicular movement, official meetings, parties, conference or entertainment apart from the purpose of religious usage or customs except under and in accordance with a permission in writing granted by central government.*(AMASR Act-1958)*

[3] Regulated zone is the 200 m radius from the boundary of the prohibited zone (*AMASR rules, 1959-rule 32)*

primary stakeholders. Sewri fort precinct is chosen for its ecological significance and sudden rise in pace of development caused due to Mumbai Trans-harbour Link ;Bassein fort precinct for its scale and size (110 acres) and enormous future potential; Sion fort precinct for it being the only landlocked hill fort in the city; and Worli fort for its emerging socio-cultural importance in the ***koliwada*** surrounding it. Currently, Sion and Bassein fort are centrally protected monuments under the Archaeological Survey of India (ASI) whereas Sewri and Worli forts are state-protected monuments.

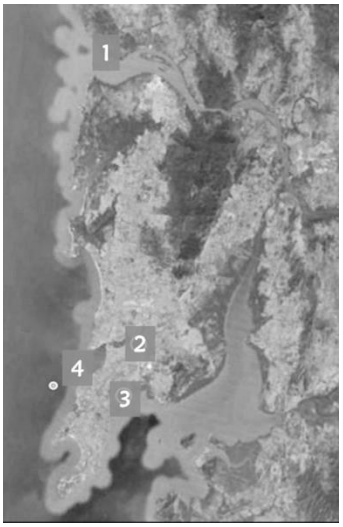

Figure 1 : Map of Mumbai showing Bassein fort (1), Sion fort(2), Sewri fort (3) and Worli fort (4)

Source: Google earth

II. EXISTING METHODOLOGIES

Since Riegl's (1902) distinction between memorial(past) and present-day values, several typologies of values have followed (*Labadi, 2007*), including in national and international heritage conservation guidelines. *(Candiracci 29)* . If one were to map these value schemata, there would be a great deal of overlap even between such different frameworks as Frey's (from economics) and Riegl's (from art history). The typology suggested in English Heritage's paper on sustainability is perhaps the most comprehensive and balanced *(English Heritage 1997)* This breakdown is well oriented to conservation practice because the value categories focus on how heritage is used and valued (contingently, and by people other than elites and experts), whereas many other typologies resonate more with connoisseurship and professional values and are strongly influenced by the notion of heritage's intrinsic value. *(Torre 10)*

For the value assessment of fort precincts, the English heritage value typologies are taken as reference with a few modifications to accommodate with the site context of Mumbai fort precincts. The value typologies of English heritage (cultural, educational

RIEGL(1902)	**UNESCO, World Heritage Convention (1972)**	**LIPE(1984)**	**BURRA CHARTER (1998)**	**FREY (1997)**	**ENGLISH HERITAGE (1997)**
▪ Age ▪ Use ▪ Commemorative ▪ Historical	Value for monuments (historical, artistic, scientific) Values for groups of buildings (historical, artistic, scientific) Values for sites (historical, aesthetic, ethnological, anthropological)	▪ Aesthetic ▪ Informatio nal ▪ Associativ e-symbolic ▪ Economic	▪ Aesthetic ▪ Historic ▪ Scientific ▪ Social (spiritual political national and cultural)	▪ Monetary ▪ Option ▪ Existence ▪ Bequest ▪ Prestige ▪ Educational	▪ Cultural ▪ Educational and academic ▪ Economic ▪ Resource ▪ Recreational ▪ Aesthetic

Table 1:Summary of heritage value typologies devised by various scholars and organizations (Reigl 1902; Lipe 1984; for the BurraCharter, UNESCO, World Heritage Convention (1972) Australia ICOMOS 1999; Frey 1997; English Heritage 1997 *(Torre 9) (Candiracci 29)*

economic, resource, recreational and aesthetic) are revised as ***socio-cultural, educational monetary, recreational*** and ***aesthetic*** values (economic and resource value are clubbed together as monetary value).

III. VALUE ASSESSMENT OF FORT PRECINCTS

a) METHODOLOGY

An on-field survey Questionnaire with a total of 23 statements was used for evaluating the significance of each precinct from the citizens perspective. The citizens on the site were expected to give their opinion on how strongly do they agree/disagree with these 23 statements on a rating scale of 0 to 3. All 23 statements were broadly classified into 4 categories with each one belonging to one of the categories[4]-Educational(6 statements), Socio-cultural (5 statements), recreational (8 statements)or Aesthetic (4 statements).

Each Statement in every category/value was framed with a purpose of measuring a specific important attribute of that particular value .(refer table 2 for list of attributes under each category of value).

For example, for measuring the *Recreational* value, a few statements were :

- This place is safe for me to spend time alone (*measuring safety/security*)
- I find it very easy to move around here without using google maps or asking other people about directions. (*measuring Legibility*)
- I find this place very comfortable to visit even in hot afternoon sun.(*measuring Physical Comfort*)

Similarly, for measuring educational value, a few statements were:

- This place offers knowledge that is not available through any other resources like internet,books,etc (*measuring rare source of knowledge*)
- This place offers something to learn for everyone irrespective of age, sex and occupation.(*Measuring relevance of knowledge to all age groups, gender and occupation*)

The survey was carried out multiple times with stratified random sampling for reliable results.

b) FINDINGS

Based on the scores obtained, a percentage value assessment was obtained for each fort (*refer Figure 2,3,4 and 5*). A detailed value assessment with attributes is given in *Figure 6* based on citizens opinions.

[4] Monetary value of land is assessed through interaction with experts. Since this paper deals with value assessment from citizen's perspective, results of monetary value are not a part of this paper.

Educational/ Academic value	Socio-cultural Value	Recreational Value	Aesthetic Value	Monetary Value
▪ Relevance of knowledge to all age groups, gender and occupation ▪ Authenticity ▪ Rare source of knowledge ▪ Knowledge from fort (built heritage) ▪ Knowledge from precinct and natural heritage ▪ Learning Environment	▪ Social Integration ▪ Sense of pride/belongingness ▪ Symbolic value/landmark ▪ Opportunities for sociability ▪ Religious and cultural events	▪ Safety/Security ▪ Legibility ▪ Physical Comfort ▪ Accessibility to all ▪ Variety in Recreation Activities ▪ Proximity ▪ Basic Facilities (drinking water, toilets,etc) ▪ Cleanliness	▪ Ambience ▪ Visual beauty-built heritage ▪ Visual beauty-unbuilt & natural heritage ▪ Vantage point for scenic views	▪ Land cost ▪ Monetary value of built heritage materials ▪ Resource value

Table 2 :List of attributes to be measured under each value for assessment purpose through questionnaire. Source : Author

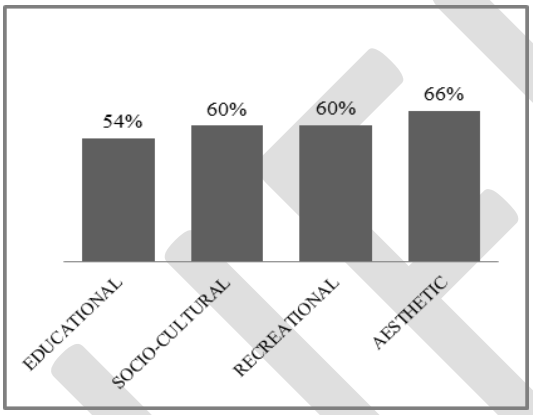

Figure 2 : Value Assessment results : Sion fort

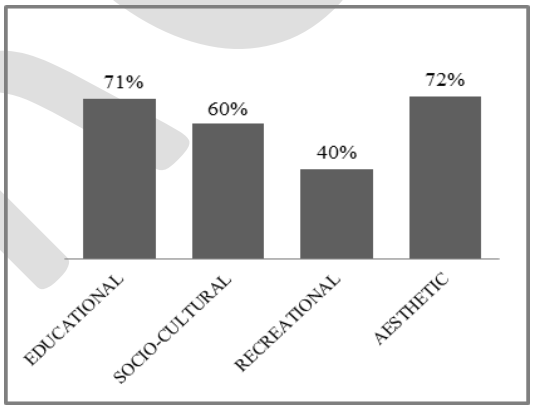

Figure 4: Value Assessment results :Vasai fort

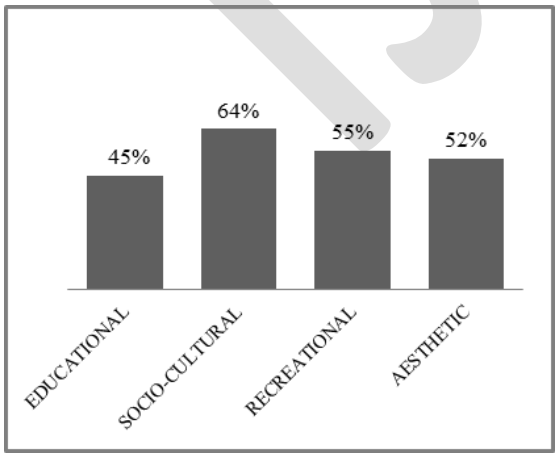

Figure3 : Value Assessment results :Worli fort

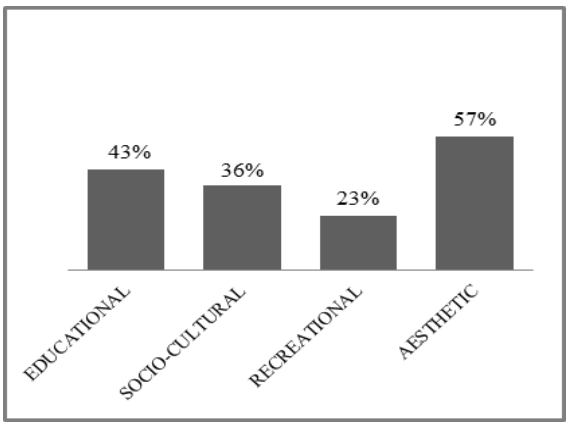

Figure 5: Value Assessment results : Sewri fort

Figure 6 : Value assessment with attributes : Sion fort *, source : Author*

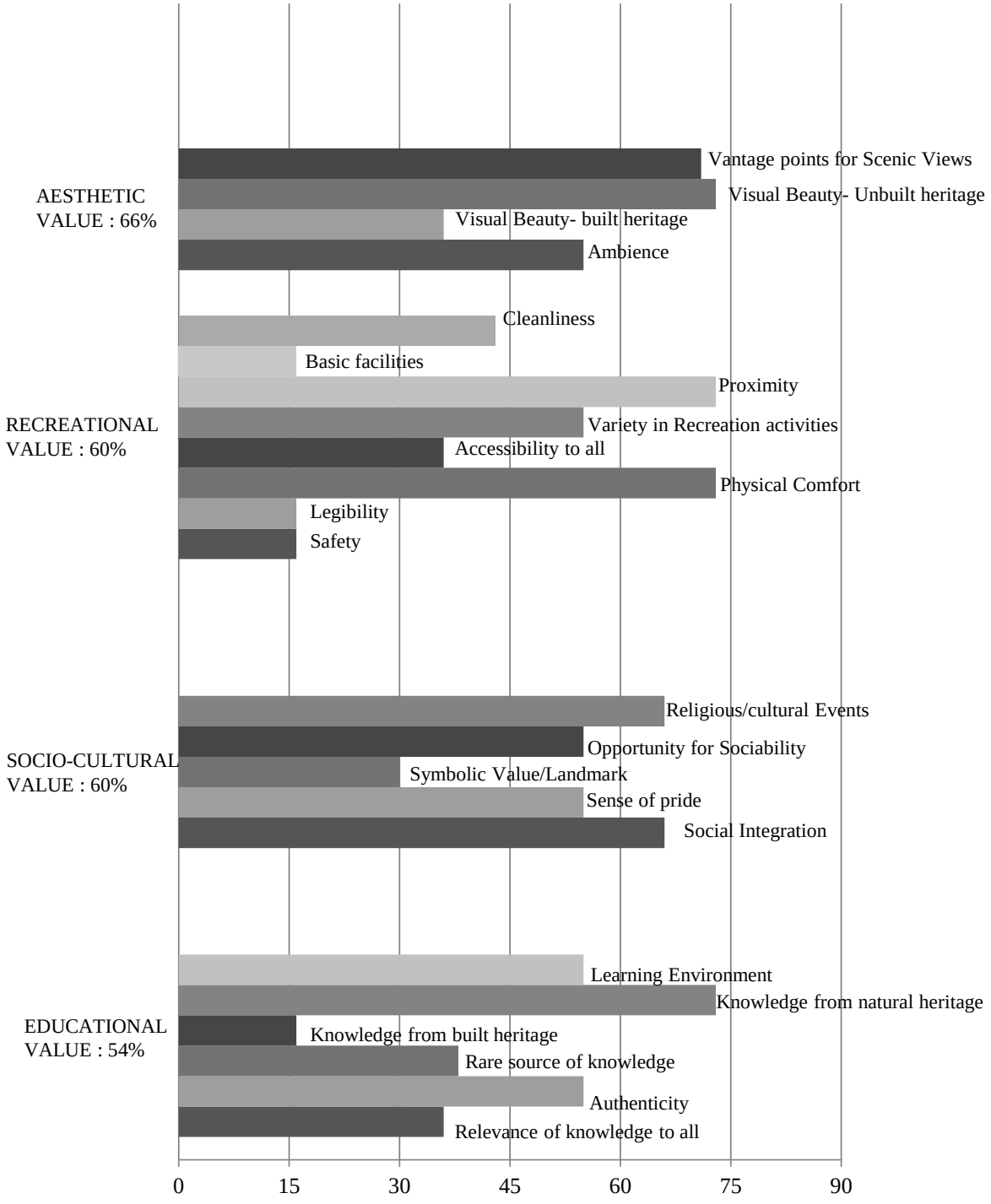

IV. THE HOLISTIC APPROACH:

After the value assessment, the following questions were explored in order to understand the cause and the effect to these existing values.

1) *What caused/allowed the emergence of these values?*
2) *Why do these values continue to thrive?*
3) *Are these values co-existent at a particular point in time?*
4) *Will they continue to thrive in future?*

The '***parameters'*** identified in a process to understand answers to these questions were then studied in detail. The parameters identified were as follows:

A. SPATIAL CONFIGURATION/BUILT FORM:

Figure 7 : Schematic Plan of Sion Fort

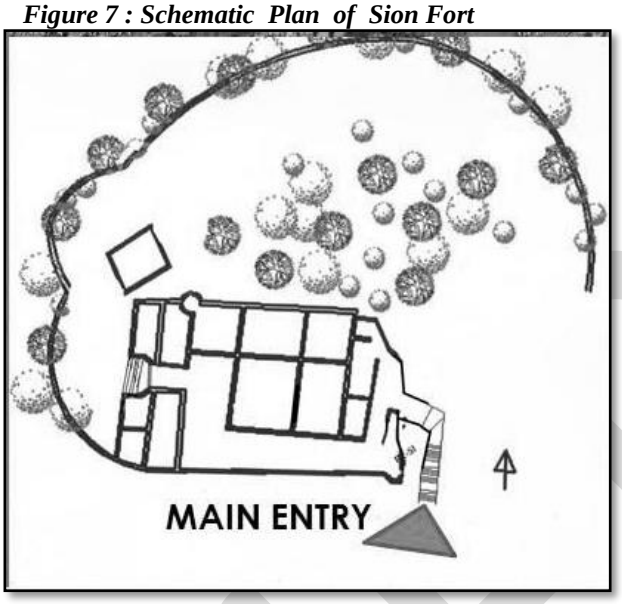

Source :

Abandoned Treasures-Forts of Mumbai (book)

The built form along with the shape of its enclosures determines the kind of function it can allow. For instance, In case of Sion hill fort, the built form comprises of a number of chambers-each chamber of the size and volume of a habitable room. The fort has more than 12 such chambers. The volume thus has a good potential for activities involving social interaction at a more personal level. Currently, the precinct being a home to many schools, the chambers are used for group study by students . the fort is also popular amongst youngsters as they hold dance and music rehersals in small groups.

Figure 8 : Dance rehearsals at Sion fort. Source :gettyimages.in

Figure 9 : Dance rehearsals at Sion fort. Source : tinydrops.org

These people mostly belong to the same neighborhood. The enclosures majorly act as a spillover space for students and neighborhood whose houses are too small to accommodate certain group activities. The fort being surrounded by Jawaharlal Nehru udyan forms a buffer space of around 100 meters in all directions from the boundary of the fort walls thus enhancing the potential of the site for open-air study.

The role of built form and spatial configurations in usage and future potential is also evident in case of the defining existing Vasai. coastal fort of

Figure 10 : Sion fort chambers. Source : trekshitiz.com

Spanning around 110 acres of land, it contains ruins of a number of churches and the citadel connected through internal pathways. Many of the walls of this fort are more than 10 meters which gives a sense of very strong enclosure creating visual disconnect between different built structures(churches, citadel, etc) within the fort boundaries. This visual disconnect in a way allows the development of each enclosure independently with different usage co-existing within the same precinct. Thus, in some spaces, one can see fishermen drying

their nets within the shade of high walls whereas at the same point in time, artists painting canvas in other spaces and a few meters away church prayers taking place in one of the ruined churches. Although the built structure of the fort isn't intact, the high walls itself create strong acoustical properties essential for religious prayers.

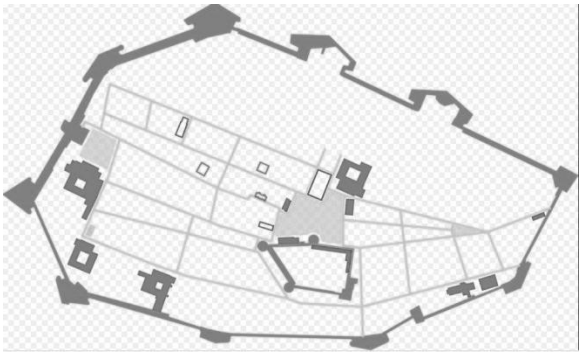

Figure 11 : Vasai fort map with built structures. Source : Heritage of Portuguese influence

Figure 12 : Vasai fort fishermen drying nets
Source : Author

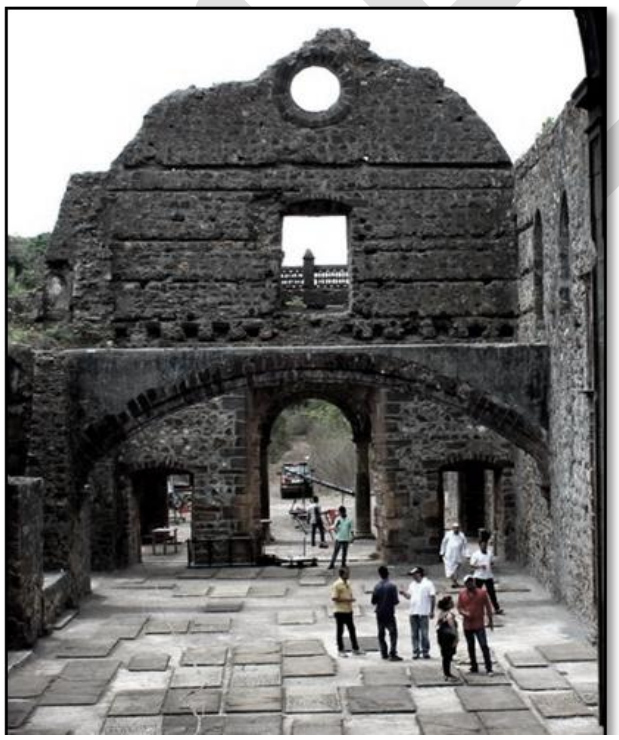

Figure 13 : Vasai fort church remains
Source : Author

B. TYPE OF NEIGHBORHOOD

Type of Neighborhood defines type, degree and pace of encroachment .In case of industrial neighborhood, the pace and degree of encroachment is very slow whereas in predominantly residential neighbourhood especially belonging to the low- income housing settlements, the pace and degree of encroachment is more. The dense residential neighbourhood of Worli fort consists of koliwada - the settlements of which extend till the fort boundaries thus leaving no buffer space around the fort. As a result of this, the historical context of the site is completely lost. In order to prevent this, the state government had proposed a buffer space extending 100 m on all sides of the fort. But since the people of the koliwada were using these areas(the only open space within these settlements) for drying of fishing nets as well as for leisure activities, the government had to drop the plan.

Figure 14 : Worli fort encroachment
Source : google earth

One peculiar characteristic observed in encroaching forts is through ***religious markers*** such as temples, dargahs or gates or in some cases, territorializing the precinct through ***religion-specific identity markers*** such as gates (refer figures 15,16 and 17) . In a country like India, controversial religious markers become a tool for permanent encroachments. In some cases, the communities justify these construction of temples within the forts as a way of protecting the fort from anti-social activities. In case of Worli fort, the justification is found to be true.

Figure 15 : Hanuman Temple in Premises of Worli fort . Source : Author

Figure 16 : Dargah touching the sewri fort wall . Source : Google earth

Figure 17 : Entry to Mahim fort (now completely encroached by slums) marked by gate of religious symbolism . Source : Google earth, Author

C. INFRASTRUCTURE DEVELOPMENT/FUTURE PROJECTS :

Study of infrastructure development and future projects determine the changing urban fabric of the precinct over the years.one way of studying this is through study development plans of the region. Any kind of infrastructure development has the power to dramatically change the pace of development in any precinct. Sometimes, the connectivity through infrastructure (railways,sealink,etc) brings in more people to the sites making them less derelict whereas in some cases , it makes the sites more vulnerable and is a threat to their existence. In case of Sewri fort precinct, the construction of Mumbai Trans-harbor link (refer figure 18,) may destroy the ecological importance of the site by intervening the natural habitat of mudflats for flamingos.In addition to this, it may also dramatically increase the pace of development in the zone. The fort precinct of Sewri thus calls for design interventions to save the context of the heritage on a priority basis.

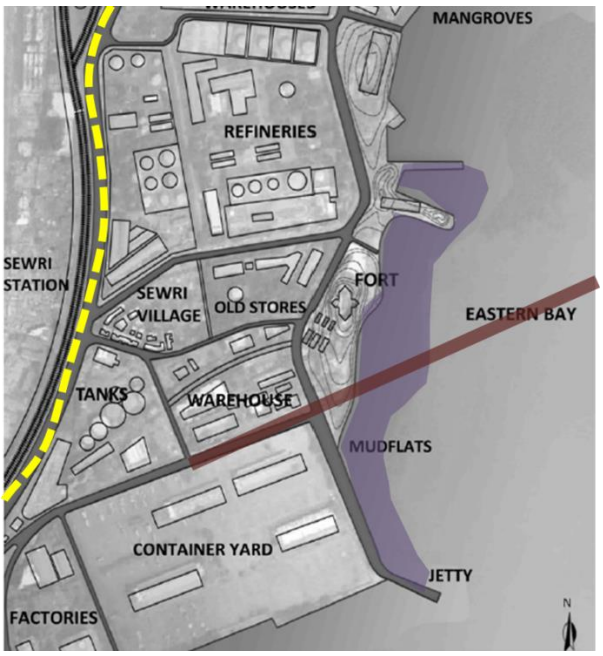

Figure 18 : Prroposed Mumbai Trans-harbour Link (red) connecting Eastern coast to Nhava Sena port passing through Sewri Mudflats (*Rane* 2)

D. OWNERSHIP AND THEIR APPROACH

Ownership determines the approach and the budget under which development takes place within the forts. Centrally protected monuments have strict rules of prohibiting and development within 100 m radius of the fort boundaries. As a result of which, site context is preserved. Whereas in case of state protected monuments such as Dharavi, Mahim and Worli forts, there are no such rules implemented. This leniency makes the sites vulnerable to encroachments.

E. SITE TOPOGRAPHY

Topography defines the microclimate as well as the accessibility factor. For instance, the hill fort of Sion is less accessible to senior Citizens.Thus ,the usage of the fort structure is restricted to youngsters and children for whom its easier to climb and access the hill fort.

V. CONCLUSION

The fort studies need a comprehensive study of ground realities, future infrastructure projects and most importantly the cultural significance of the site understand the current and future potential of forts in addition to the historical study. In the process, a wide range of heritage values need to be identified and characterized in a way that is relevant to all stakeholders involved. It is self-evident that no society makes an effort to conserve what it does not value. Until all the stakeholders don't value a place, all efforts to in will be futile *(Torre 3*)

To ensure public participation and economic sustenance of the sites, there is an urgent need for innovative strategies that ***monetize*** these precincts without disturbing the historical significance of the site. Adaptive reuse, strategically planned access roads and navigation patterns within the precinct, defining buffer spaces around forts with strong physical boundaries such as trees instead of mental boundaries of 100 m prohibited zones may be some of the strategies that can work for these forts.

The value assessment methodology mentioned in the paper have resulted from site context of selected sites. The methodology needs to be verified further for their pertinent applicability to other similar sites. This methodology showed difficulties in being implemented at a derelict site of restricted access like Sewri fort and its sparsely populated precinct.

VI. ACKNOWLEDGEMENT

I profoundly thank the institute of Sir J.J College of Architecture, especially professors Mustansir Dalvi, Sushma Joglekar and Parul Kumtha for their constant guidance and support during the research.

REFERENCES:

1. Academy of Architecture. Study of forts within the Mumbai Metropolitan Region -Volume 1. Mumbai: MMR- HCS, 2003.
2. Candiracci, Sara. Developing a methodology for a landscape-based approach to urban conservation in sub-saharan Africa. Thesis. Italy: University of Naples Federico II, 2016.
3. FOUNDATION, NAGAR. Abandoned Treasures- Forts of Mumbai. Mumbai, 2015.
4. India, Archaelogical Survey of. "The Ancient Monuments and Archaeological Sites and Remains Act." 1958.
5. Maharashtra, Government of. "The Maharashtra Ancient monuments and Archaelogical sites and remains act." 1960.
6. Manders Martijn R, Van Tilburg Hans K. , Staniforth Mark. Significance Assessment. Bangkok: UNESCO, 2012.
7. Mumbai, Muncipal Corporation of Greater. Development plan. Mumbai, 1981.
8. Mumbai, Municipal Corporation of Greater. Development plan . Mumbai, 2016.
9. Rane, Amol. "Sewri Ecological Park:A proposal for sustainable waterfront development at eastern bay of Mumbai." Thesis. 2012.
10. Roders, Ana Pereira. "Monitoring cultural significance and impact assessments." International Association for Impact Assessment (IAIA). 2013, n.d.
11. Torre, Marta De La. Assessing the values of cultural heritage. Los Angeles: The Getty Conservation Institute, 2002.

International Journal of Engineering Research and General Science Volume 5, Issue 4, July-August, 2017
ISSN 2091-2730

Biosorption of Cr, Ni & Cu from industrial dye effluents onto *Kappaphycus alvarezii*: assessment of sorption isotherms and kinetics

Krishna Y. Pandya[1,2], Rinku V. Patel[1,2], Rakesh T. Jasrai[3], Nayana Brahmbhatt[2*]

[1]Sophasticated Instrumentation Centre for Applied Research and Testing, Vallabh vidhyanagar-388120, Gujarat, India.

[2]Department of Biology, V. P. Science College, Sardar Patel University, Vallabh vidhyanagar-388120, Gujarat, India.

[3]Department of Chemistry, R. K. Parikh Arts & Science College, Sardar Patel University, Petlad-388450, Gujarat, India.

*Corresponding Author: naina_bbhatt@yahoo.co.in

Abstract— Biosorption is considered as one of the most effective treatment technology for the removal of toxic metals from the environment. Biosorption potential of *Kappaphycus alvarezii* was studied for removal of toxic heavy metals such as chromium (Cr), nickel (Ni) and copper (Cu) from industrial dye effluents in batch mode. The experiments were carried out at room temperature (25 ± 1°C) at pH 7. The equilibrium time was observed at 70 to 80 minutes. The study reveals maximum 90.22 % and 68.78 % of Ni and Cr removal respectively in E1 effluent and 81.53 % of Cu removal in E4 effluent. The Freundlich and Langmuir isotherm shows the favorable biosorption of metals and data are well fitted; kinetic study reveals the adsorption reaction follows pseudo-second order model and the data fitted well with the kinetic studies. The SEM and FTIR analysis represents strong cross linkage of the metals and functional groups variation which was occurred due to the potential biosorption capability of the biomass. Thus the red seaweed biomass of *Kappaphycus alvarezii* has considerable potential as biosorbent for the removal of heavy metals from effluent which is eco friendly and low cost material to apply on polluted water contaminated with toxic metals.

Keywords— Biosorption, Heavy metal, FTIR, SEM, Freundlich model, Langmuir model, Kinetics

INTRODUCTION

Presence of heavy metal in water is main concern of water pollution. Various industries contribute in environmental pollution by discharging loads of toxic substances and hazardous material which damages the environment [1]. There are more than 0.7 million tons of synthetic dyes are produced every year and more than 10,000 different types of dyes and pigments produced around the globe. India leads the production of reactive dyes due to accessibility of dyes intermediate such as vinyl sulphone in the country; the other countries such as Taiwan, China and Korea mainly produce scatter dyes [2]. Thus it resulted in increasing demands of dyes in various applications such as pulp & paper, ink & paint, food, cosmetics, pharmaceuticals, textile, electroplating, plastic, tannery & leather industries etc. This excessive demand of applications contributes release of hazardous chemicals and heavy metals in water systems which creates health hazardous for all living organisms [3][4]. During the processing operations approximately 10-20 % of the dye products lost in effluent streams [5]. There are various conventional methods to treat these effluents such as chemical coagulation and flocculation, trickling filter, ion-exchange methods, membrane separation, advanced oxidation process, electrolysis process, photo-degradation available [6][7][8][9][10][11][12] However these processes possess inherent astrictions such as generation of by products, high cost intense power requirements [13]. Biological treatments such as biosorption and biodegradation implied economically low cost and environment friendly methods to be proposed for its potential application in mitigation of dyes from dyes effluent [14][15][16][17]. Biosorption takes place on the surface of biomass. It can be considered that biosorption process indicates passive sorption of pollutants and metals which contributes in reduction of pollutant by allowing the recovery of the products from the effluent by utilizing living and non living biomass [18][19][20][21]. Biosorption acquired from dead microbial cells, seaweed biomass, agricultural waste [22], aquatic ferns, orange peels [23] are used as chelating and complexing biosorbents to appropriately remove metals to contemplate and dyes from effluent [24][25][26][27][28][29][30]. Seaweed biomass is reported to have a tremendous biosorptive performance [31][32]. Seaweeds can to be easily and speedily grown on rocky surface because of its vast abundance in oceanic shores, they are found suitable for the biosorption. Seaweeds have special surface properties to easily bind metallic and organic components from the effluent. They possess characteristic cell wall that binds with pollutants. The algal cell wall comprised of various functional groups such as sulphate, phosphate, amino, carboxylic acid, alginic acid, proteins [30]. Even though large abundance of seaweed species on the globe was found but there are very few reports available to study biosoption of metals and organic components removal application in effluent treatment. Various species of microalgae and macro algae are potential for the waste treatment systems but all the reports were found only on metal removal capabilities from effluents [33][34][35][36]. In the present study red seaweed biomass of *Kappaphycus alvarezii* was used for determination of heavy metal removal. The adsorption procedure studied through kinetics and isotherm perspectives.

MATERIAL AND METHODOLOGY

Effluent Collection with Heavy Metal Analysis

The effluent was collected from different industrial dyes units of Gujarat, India. The collected effluents were entitled as E1, E4 and E6 as they are the effluent of reactive red azo, reactive yellow azo dyes and reactive black azo dyes effluent respectively. These effluents contain mixture of chemical complex structures and heavy metals. The heavy metal concentration in effluents was studied by ICP-OES (Model-Optima 3300 RL, Make-Perkin Elmer) followed by standard methods of APHA-AWWA, 1985. The concentration of Cr, Ni and Cu is indicated in Table-1.

The effluent samples E1, E4 and E6 were digested by aqua-regia of HCL: HNO_3 (1:3 V/V) on hot plate in a beaker for an hour and then diluted with double distilled water. These light yellow colored effluent samples were analyzed for heavy metals Cr, Ni and Cu after digestion using Atomic Absorption Spectroscopy (Make-Shimadzu, Model-AA 7000).

Table-1 Heavy Metal Analysis of Effluent

Heavy Metal	Chromium (Cr) ppm	Nickel (Ni) ppm	Copper (Cu) ppm
E1	0.6573	0.174	-
E4	0.5179	0.2054	16.865
E6	0.1376	0.1754	16.048

(E1 is the effluent of reactive red azo dyes, E4 is the effluent of reactive yellow azo dye and E6 is the effluent of reactive black azo dyes; ppm is parts per million)

Biosorption Study by *Kappaphycus alvarezii*

The biosorption of heavy metal such as Cr, Ni and Cu was studied by using biomass of *Kappaphycus alvarezii*. The experiment was carried out in batch mode in which 2 g of seaweed biomass was inoculated in 200 ml of dye effluent in 500 ml conical flask. the constant agitation speed of 80 rpm was maintained throughout the experiment in flask shaker for better contact of biomass surface area at ambient condition. The samples were taken at every 10 minutes interval and immediately filtered the effluent with Whattman paper no. 40 to prepare the effluent adsorbent free. The filtered effluent samples were analyzed using atomic adsorption spectrophotometer (Make-Shimadzu, Model-AA 7000). The biosorption equilibrium was calculated by

$$q_e = \frac{(C\,o - C\,e)V}{W} \quad (1)$$

Co and Ce is the initial and equilibrium dye effluent respectively, W and V are the weight of the biomass (g) and V is the volume (ml). The concentration of adsorbed heavy metal at time t mentioned as qt was calculated according to equation (2) [37]

$$q_t = \frac{(C\,o - C\,t)V}{W} \quad (2)$$

Where Co is the initial concentration (ppm) and Ct is concentration of metal in filtrate effluent at time t; W is the weight of biomass (g) and V is the volume (ml). The percentage heavy metal removal was determined by equation as below:

$$\text{Biosorption yield (\%)} = \frac{Co - Ct}{Co} \times 100 \quad (3)$$

Scanning electron microscopy (SEM)

The morphological study of *Kappaphycus alvarezii* for before and after treatment of effluent E1, E4 and E6 was induced by Field emission gun- scanning electron microscopy (Make: FEI Ltd., Model: Nova NanoSEM 450)

Fourier Transform Infrared Analysis (FTIR)

The FTIR spectra was studied by FTIR spectrophotometer (Make: Perkin Elmer, U.S.A., Model: Spectrum GX) by analyzing treated and untreated seaweed biomass which is achieved by K-Br disk method. The 2 mg of biomass samples were crushed with 200 mg of K-Br (spectroscopic grade). It was analyzed and scanned under 4000 to 400 cm^{-1} range.

RESULT AND DISCUSSION

The heavy metal quantity absorbed by the *Kappaphycus alvarezii* as a function of contact time with the heavy metal Cr, Ni and Cu is shown in Fig-1. Biomass indicates slow adsorption initially and reaches equilibrium at 70 to 80 minutes and then it becomes steady and slowly lowered. It was occurred due to the *Kappaphycus alvarezii* has strong adsorption capacity because of the presence of porous surface and vacant space available, it get swollen slowly after accumulation of water inside the cells and after equilibrium the adsorption rate was found decreased due to repulsive forces in molecules and lowered vacant space availability therefore initially the adsorption rate was found initially slow [38]. Similar work was found by various scientists for biosorption of heavy metal such as Cd, Hg, Pb, As, Co, Cu, Mo (VI) [39][40][41][42][43][44][45]

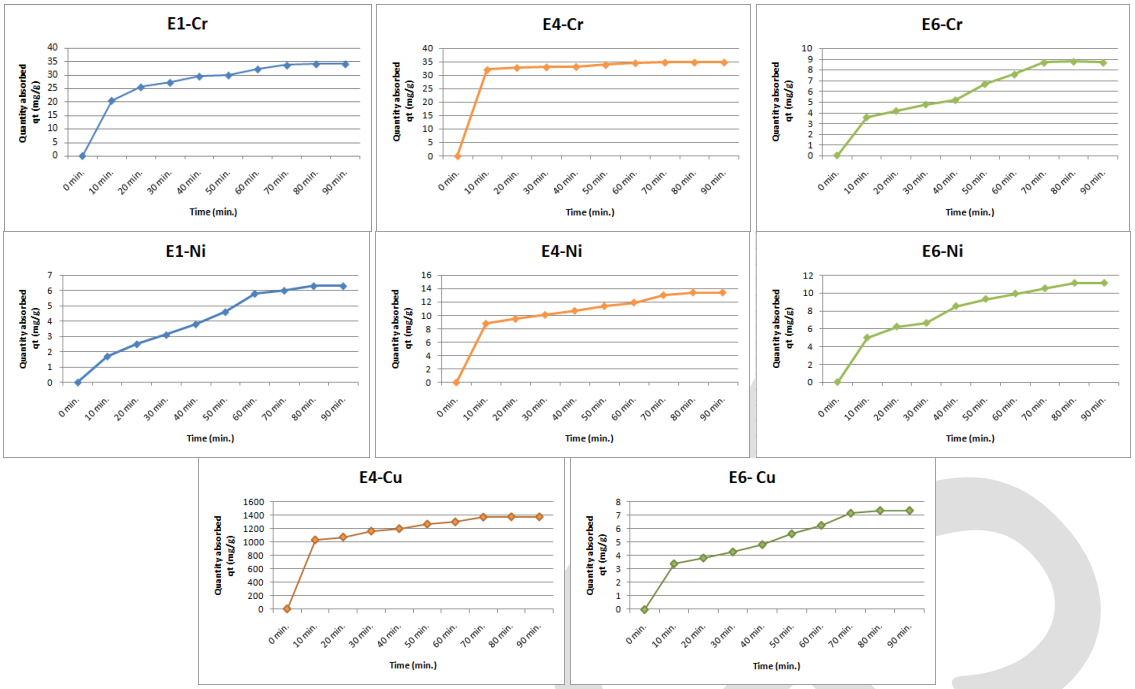

Fig-1 Biosorption capacity of red seaweed *Kappaphycus alvarezii* as function of contact time

The heavy metal such as Cr and Ni removal was observed maximum as 68.78 % and 90.22 % respectively in E1 effluent and Cu removal was observed maximum as 81.53 % in E4 effluent indicated in Figure-2. There are so many literatures available on biosorption treatment of effluent in 250 to 180 minutes by seaweed biomass [46][47][48]. Higher metal affinity is depending on hydrolysis constant, ionic charge and ionic size of individual metals [49][50][51]. In the present study highest metal affinity was found as Ni > Cr > Cu in *Kappaphycus alvarezii*

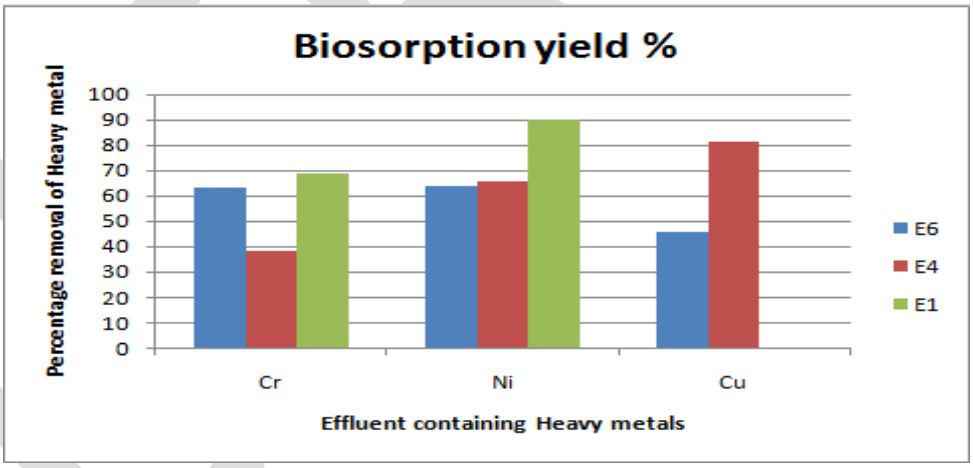

Fig-2 Percentage heavy metal removal

Biosorption isotherms

The equilibrium isotherms such as Langmuir and Freundlich were applied to derive adsorption characteristics such as gain of adsorbate and adsorbate in bulk on surface of adsorbent at equilibrium concentration. The effluent samples E1, E4 and E6 were taken for the removal of heavy metals such as metals Cr, Ni & Cu to evaluate biosorption capability of *Kappaphycus alvarezii*. As mentioned the Langmuir and Freundlich isotherms were successfully applied in the sorption study [52][53]. The Langmuir equation [54] in linerized form is as below.

$$\frac{Ce}{Qe} = \frac{b}{Qo} + \frac{Ce}{Qo} \quad (4)$$

The plot of adsorption (Ce/qe) verses equilibrium concentration (Ce) is shown in Fig-3 to Fig-10 represents the Langmuir model. Table-2 indicates the values of Q_m and b. The vital characteristics of Langmuir model can be stated by constant separation factor RL shown in equation below:

$$R_L = \frac{1}{1+bC0} \quad (5)$$

The RL value shows the adsorption character to be unfavorable (RL > 1), favorable (0 < RL < 1), linear (RL = 1) or irreversible (RL = 0).

The Freundlich isotherm equation [55] is indicated as below:

$$\ln Qe = \ln Kf + \frac{1}{n}\ln Ce \quad (6)$$

Where n and K_f are Freundlich constants; which is determined by slope of the plot and intercept shown in Fig-11 to Fig-18 indicates the intensity and adsorption capability respectively.

Equillibrium studies

The values of Freundlich and Langmuir are represented in Table-2. The plots of Langmuir isotherms shown in Fig-3 to Fig-10 indicate adsorption of metals onto the biomass. The straight lines explains Langmuir model for equilibrium adsorption. The Langmuir and Freundlich model were observed favorable in all metals as shown in Table-2. The Freundlich model was found favorable in all samples except Cr in E4 and E6 & Cu in E4 effluent. The Freundlich isotherm indicates high adsorption capacity of biomass *Kappaphycus alvarezii* with quite rapid progression for metal adsorption.

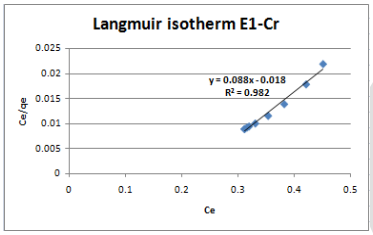

Figure-3

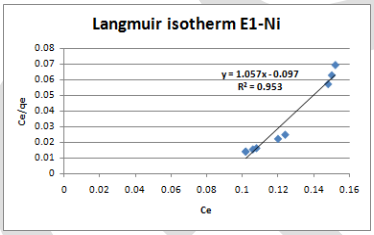

Figure: 4

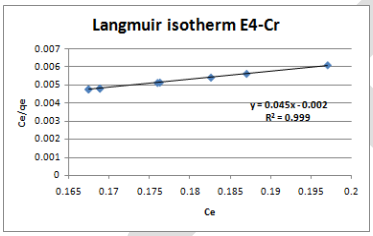

Figure-5

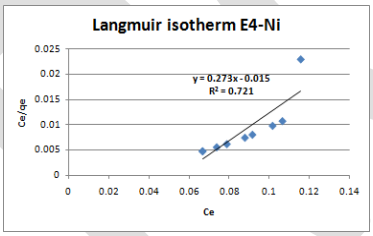

Figure-6

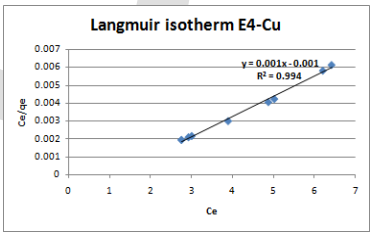

Figure-7

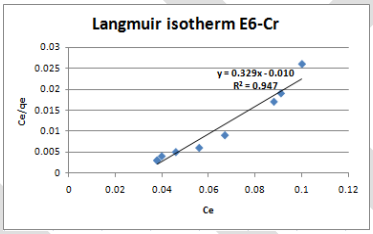

Figure-8

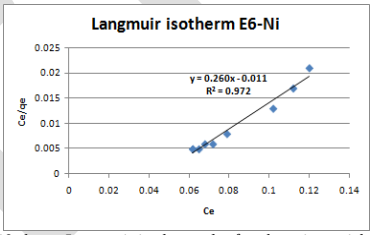

Figure-9

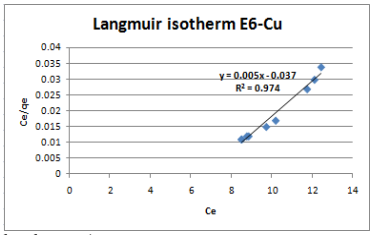

Figure-10

(Fig-3 to Fig-10 shows Langmuir isotherm plot for chromium, nickel and copper)

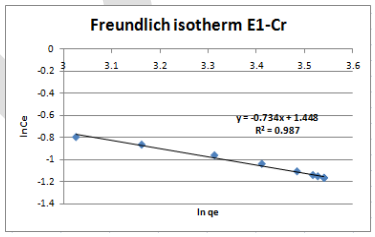

Figure: 11

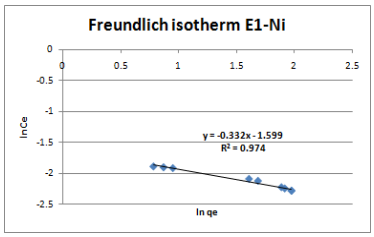

Figure: 12

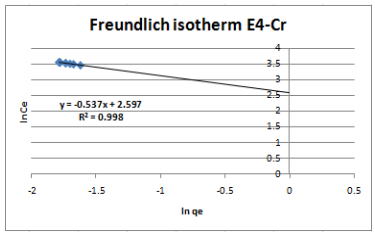

Figure:13

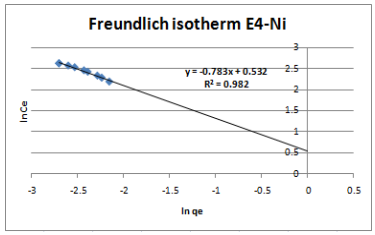

Figure: 14

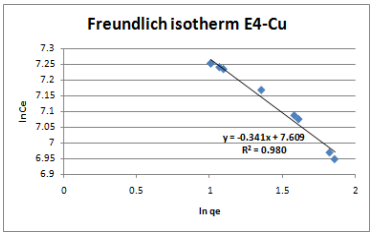

Figure: 15

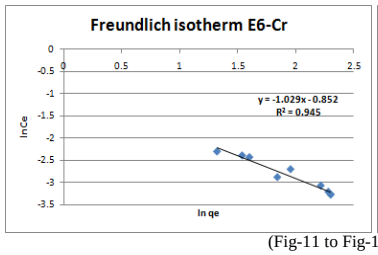

Figure:16

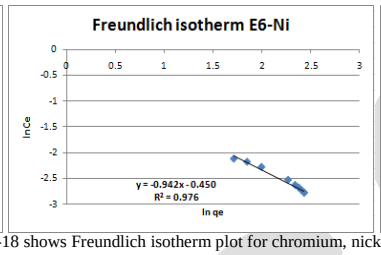

Figure:17

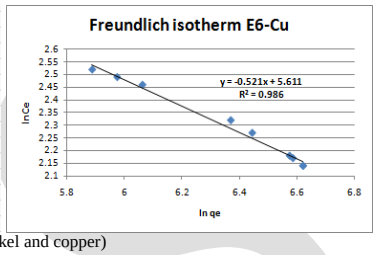

Figure:18

(Fig-11 to Fig-18 shows Freundlich isotherm plot for chromium, nickel and copper)

Table-2: Biosorption isotherm parameter for heavy metal sorption onto *Kappaphycus alvarezii*

Isotherm	Metal	Parameter	Value		
			E1	E4	E6
Langmuir Isotherm	Chromium	R^2	0.982	0.999	0.947
		q_{max}(mg/g)	55.55	500	100
		B	0.204	0.044	0.030
	Nickel	R^2	0.953	0.721	0.972
		q_{max}(mg/g)	10.30	66.66	90.9
		B	0.091	0.054	0.042
	Copper	R^2	-	0.994	0.974
		q_{max}(mg/g)	-	1000	27.02
		B	-	10	7.40
Freundlich isotherm	Chromium	R^2	0.987	0.998	0.945
		K_F	1.362	1.862	0.97
		N	0.69	0.38	1.173
	Nickel	R^2	0.974	0.982	0.976
		K_F	3.012	1.355	1.061
		N	0.62	1.879	2.22
	Copper	R^2	-	0.980	0.986
		K_F	-	2.932	1.919
		N	-	0.131	0.178

Sorption kinetics

The binding of metals was monitored with time. The rapid binding of metals to the biomass was found initially slow and then it become rapid followed by reaching the equilibrium time at 70 to 80 minutes, after 80 minutes no change was observed in equilibrium time. This process occurred because of availability of vacant space inside the biomass cells. The kinetics was studied by the pseudo first and second order rate equation models.

The Lagergren's first order equation describes adsorption rate depended on adsorption capacity of the biomass. It is given as below in linear form (Lagergren, 1898) [56]:

$$\ln (qe - qt) = \ln (qe - K_1 t) \quad (7)$$

The pseudo second order model in linerized form is given by the Ho [57] (Ho, 1995) is:

$$\frac{t}{qt} = \frac{1}{K_2 qe^2} + \frac{1}{qe} t \quad (8)$$

Where, q_e & q_t were the content metals (mg/g) adsorbed at equilibrium & time t and the K is pseudo-second order rate constant of adsorption (g/mg/time). The linear plot of t vs t/qt was obtained which shows the kinetic data best fitted in pseudo-second order model.

The linear plot of ln (qe-qt) vs t for pseudo-first order reaction and t/qt vs t for pseudo-second order reaction of the metal adsorption onto *Kappaphycus alvarezii* was shown in Fig-19 to Fig-34. The correlation coefficients are closer to the correlation coefficient of second-order kinetics indicates that the reaction follows pseudo second order model

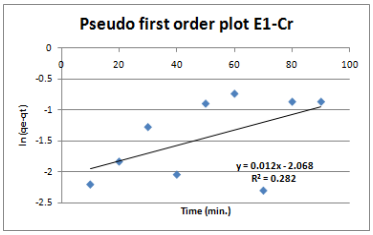

Figure-19

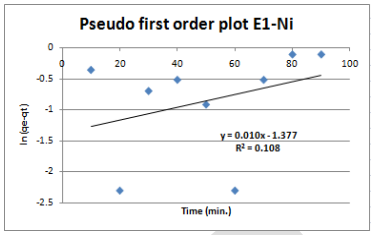

Figure-20

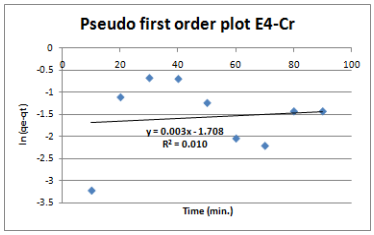

Figure-21

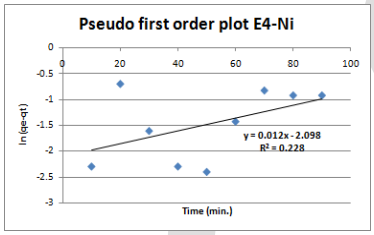

Figure-22

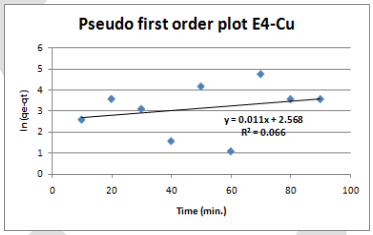

Figure-23

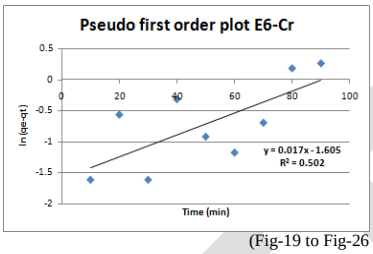

Figure-24

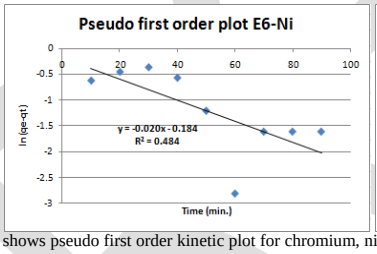

Figure-25

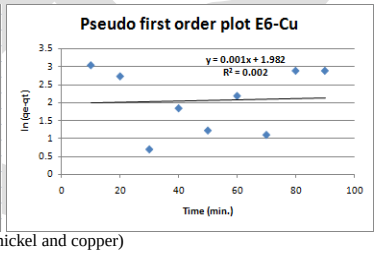

Figure-26

(Fig-19 to Fig-26 shows pseudo first order kinetic plot for chromium, nickel and copper)

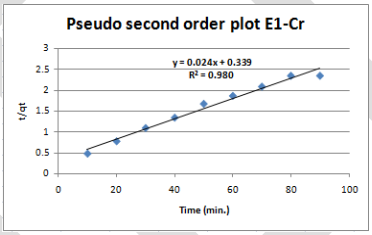

Figure-27

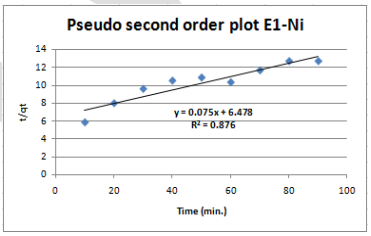

Figure-28

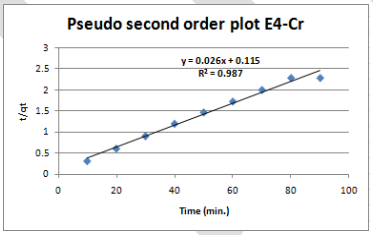

Figure-29

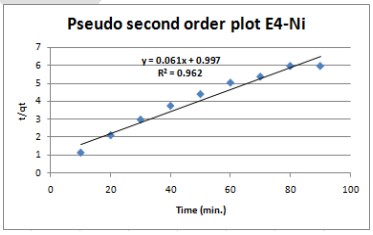

Figure-30

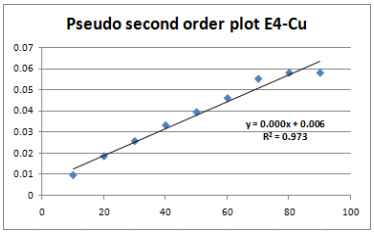

Figure-31

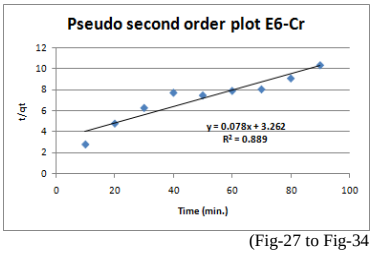

Figure-32

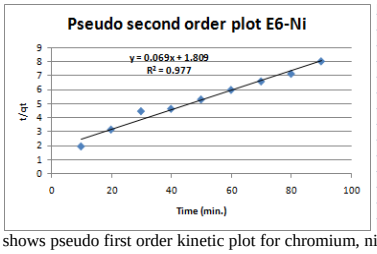

Figure-33

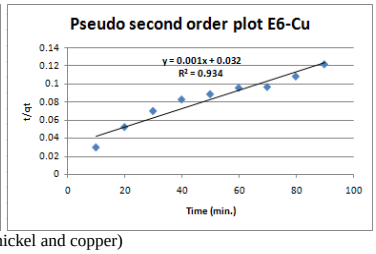

Figure-34

(Fig-27 to Fig-34 shows pseudo first order kinetic plot for chromium, nickel and copper)

Fourier Transform Infrared Interpretation (FTIR)

The spectra analysis shows the functional group variation in the seaweed biomass of *Kappaphycus alvarezii* for before and after treatment of metal containing dye effluents shown in Fig-35 to Fig-38. The recorded spectra gives different adsorption peaks which represents the presence of various functional groups in *Kappaphycus alvarezii* such as O-H alcohol, N-H amino salt, C=N oxime/imine, S=O sulfate, S=O sulfonic acid, C-O aliphatic ether, C-O primary alcohol, C-O vinyl ether, O-H carboxylic acid, P-C organo-phosphorus compound, C-O alkyl aryl ether, C-H alkane, C=C alkane disubstituted (cis), C-F fluro compound, C-O primary alcohol, C-O secondary alcohol, C-O tertiary alcohol, N-O nitro compound, C-O aromatic ester, S=O sulfonamide, S=O sulfoxide. Adsorption of metals inside the biomass of *Kappaphycus alvarezii* indicates alternation of the functional groups of the biomass and by comparison of after treatment spectra show decrease in intensity of peaks and band shifts described in Table-3. The IR spectrum of the biomass shows significant variation in peak frequencies due to binding of metals with active sites of the biomass indicates the presence of ionizabal functional groups inside *Kappaphycus alvarezii* which has potential to interact with other cations [58][59][60]. Thus it play important role in removal of metals from the effluents.

The Image-1 represents Scanning electron microscopy (SEM) of untreated & treated biomass of *Kappaphycus alvarezii* with effluent E1, E4 and E6. The biomass surface was smooth and even but after exposure it resulted to swollen cells and uneven surface. This is due to the damaged cells because of the accumulation of metals. It occupies the free binding sites inside the cells of the biomass represents strong cross linkage of the heavy metals due to ion exchange mechanism [37](M. M. Ghoneim, 2014).

Table-3: Fourier transform infrared analysis (FTIR) Interpretation of *Kappaphycus alvarezii*

Kappaphycus alvarezii	Adsorption bands (cm^{-1})			Assignment
	Initial	Final	Difference	
E_1-effluent	3428.06	3426.27	1.79	O-H stretching alcohol bonded
	2925.56	2925.12	0.44	C-H stretching alkane
	1651.87	1640.08	11.79	C-H aromatic compound bending, C=N stretching imine/oxime, C=C alkane disubstituted (cis)
	1545.93	1543.97	1.96	N-O stretching nitro compound
	1417.43	1412.33	5.1	O-H bending carboxylic acid, O-H alcohol bending, S=O stretching sulfate, C-F fluro compound
	1258.05	1234.64	23.41	C-O stretching aromatic ester, C-O stretching alkyl aryl ether, C-N stretching amine
	1157.83	1127.07	30.76	S=O stretching sulfonamide, S=O stretching sulfone, C-O stretching tertiary alcohol
	1071.23	1069.80	1.43	C-O stretching primary alcohol, S=O stretching sulfoxide, C-O stretching secondary alcohol
E4-effluent	3428.06	3433.50	5.44	O-H stretching alcohol bonded
	2925.56	2925.43	0.13	C-H stretching alkane
	1651.87	1638.31	13.56	C-H aromatic compound bending, C=N stretching imine/oxime, C=C alkane disubstituted (cis)
	1545.93	-	-	N-O stretching nitro compound
	1417.43	1404.24	13.19	O-H bending carboxylic acid, O-H alcohol bending, S=O stretching sulfate, C-F fluro compound
	1258.05	1255.91	2.14	C-O stretching aromatic ester, C-O stretching alkyl aryl ether, C-N stretching amine
	1157.83	1126.90	30.93	S=O stretching sulfonamide, S=O stretching sulfone, C-O stretching tertiary alcohol
	1071.23	1089.98	(-18.75)	C-O stretching primary alcohol, S=O stretching sulfoxide, C-O stretching secondary alcohol
E6-effluent	3428.06	3428.31	(-0.25)	O-H stretching alcohol bonded
	2925.56	2925.32	0.24	C-H stretching alkane
	1651.87	1640.57	11.3	C-H aromatic compound bending, C=N stretching imine/oxime, C=C alkane disubstituted (cis)
	1545.93	-	-	N-O stretching nitro compound
	1417.43	1405.39	12.04	O-H bending carboxylic acid, O-H alcohol bending, S=O stretching sulfate, C-F fluro compound
	1258.05	1253.15	4.9	C-O stretching aromatic ester, C-O stretching alkyl aryl ether, C-N stretching amine
	1157.83	1126.95	30.88	S=O stretching sulfonamide, S=O stretching

				sulfone, C-O stretching tertiary alcohol
	1071.23	1070.86	0.37	C-O stretching primary alcohol, S=O stretching sulfoxide, C-O stretching secondary alcohol

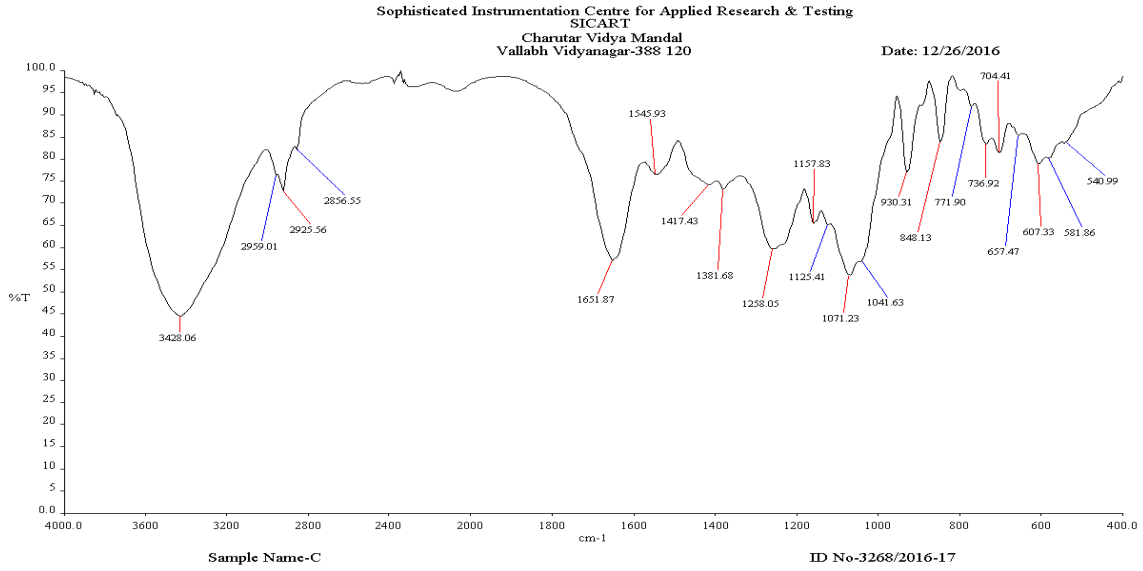

Figure-35

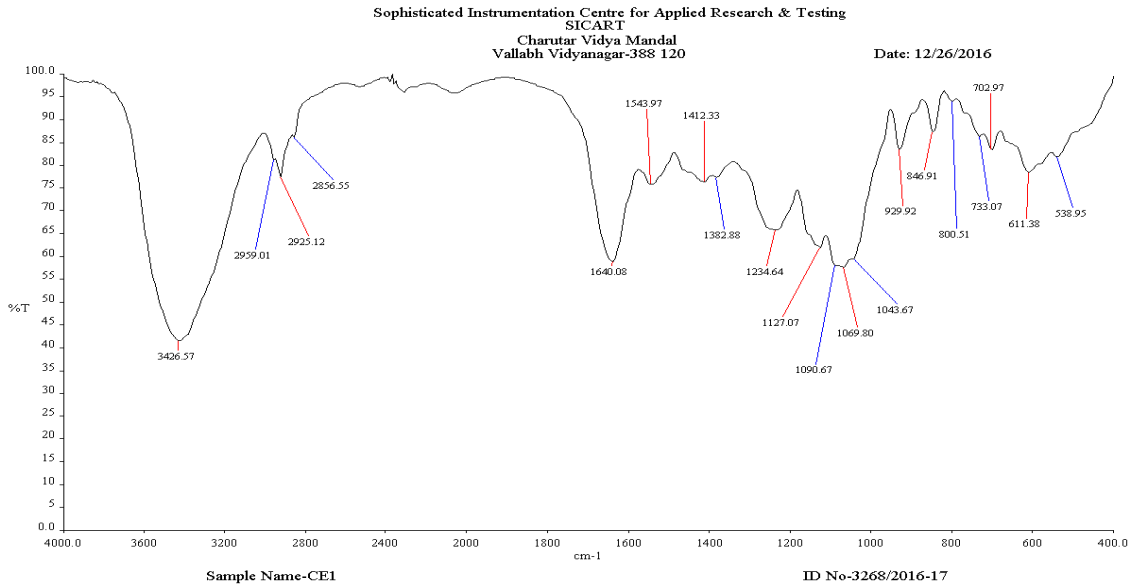

Figure-36

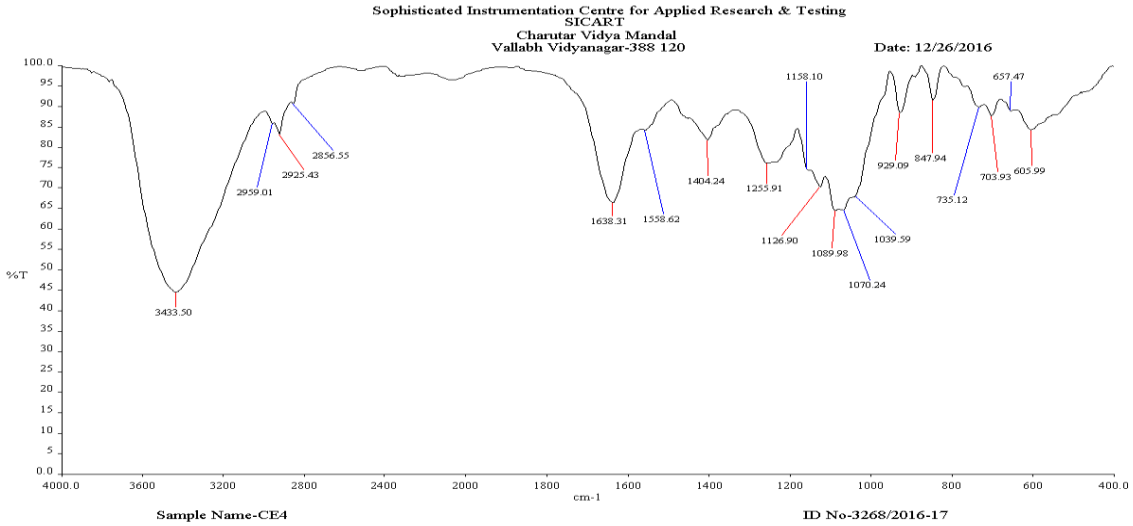

Figure-37

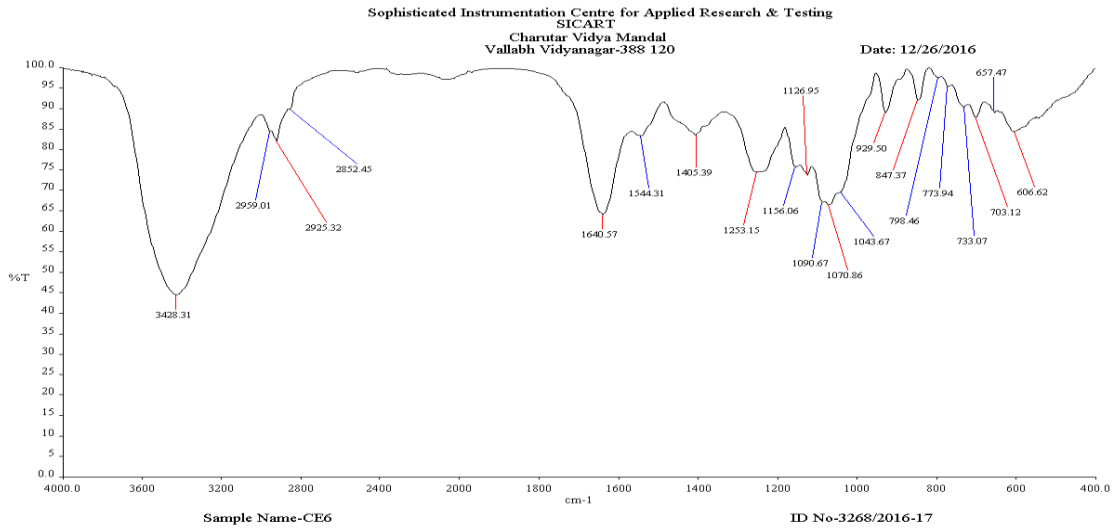

Figure-38

Image-1: Scanning electron microscopy (SEM) of Untreated & Treated *Kappaphycus alvarezii*

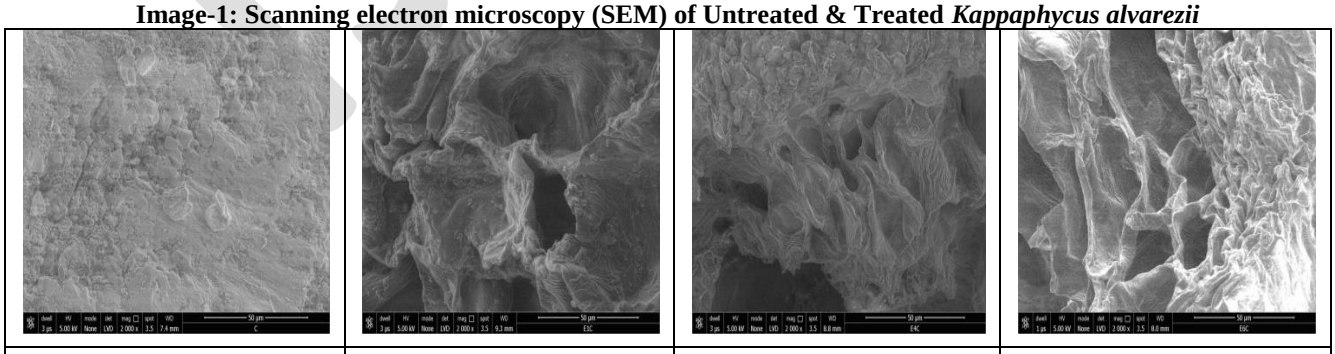

Kappaphycus alvarezii	**E1**	**E4**	**E6**

ACKNOWLEDGMENT

I am thankful to my Co-authors & Mr. Ghanshyam Patel, Dr. Tarosh Patel and Dr. Jaimin Bhatt and Dr. K. K. Tiwari for guidance & Support, also thankful to Sophisticated Instrumentation Centre for Applied Research and Testing (SICART) & Bharuch Enviro Infrastructure Ltd. (BEIL), Ankleshwar for the successful completion of this work.

CONCLUSION

The present study shows that red seaweed biomass of *Kappaphycus alvarezii* has high biosorption capacity for Cr, Ni and Cu. In the present study the highest biosorption was observed as Ni > Cu > Cr as 90.22 % > 81.53 % > 62.93 % respectively in each effluent in 70 to 80 minutes of contact time respectively. The data are well fitted by the Freundlich isotherm and the Langmuir isotherm shows the favorable biosorption of heavy metal and the data on the kinetic studies fitted well which shows the adsorption kinetics of metals by red seaweed biomass of *Kappaphycus alvarezii* followed the pseudo-second order model for biosorption of Cr, Ni and Cu in each effluent shown as E1, E4 & E6. The SEM and FTIR analysis represents strong cross linkage of the metals and functional groups variation which resulted the potential biosorption capability of the biomass. Thus the red biomass *Kappaphycus alvarezii* has considerable potential as biosorbent for the removal of heavy metal from effluent.

REFERENCES:

[1] V. Sivasubramanian "Environmental sustainability using green technologies" Boca Raton, FL: CRC Press, 2016
[2] H. D. Bhimani "Bacterial degradation of Azo Dyes and its derivatives" Thesis PhD, Saurashtra University, Gujarat, India., 2005.
[3] B. H. Hameed, U. G. Akpan, K. P. Wee "Photocatalytic degradation of Acid Red 1 dye using ZnO catalyst in the presence and absence of silver" Desalin. Water Treat 27: 204-209, 2011.
[4] R. H. Souther, T. A. Alspaugh "Textile waste treatment studies" J Water Pollut. Control Fed 29: 918–934, 1957.
[5] N. K. Daud, U. G. Akpan, B. H. Hameed "Decolorization of sunzol black DN conc. in aqueous solution by Fenton oxidation process effect of system parameters and kinetic study" Desalin. Water Treat 37:1–7, 2012.
[6] C. V. Nachiyar, S. Sunkar, G. N. Kumar, A. Karunya, P. B. Ananth "Biodegradation of Acid Blue 113 Containing Textile Effluent by Constructed Aerobic Bacterial Consortia: Optimization and Mechanism" J Bioremed Biodeg 3:162, 2012.
[7] W. Delee, C. O'Neill, F. R. Hawkes, H. M. Pinheiro "Anaerobic treatment of textile effluents: a review" J Chem Technol. Biotechnol 73:323–335, 1998.
[8] S. Mondal "Methods of dye removal from dye house effluent – an overview" Environ Eng Sci 25: 383–396, 2008.
[9] H. S. Rai, M. S. Bhattacharyya, J. Singh, T. K. Bansal, P. Vats, U. C. Banerjee "Removal of dyes from the effluent of textile and dyestuff manufacturing industry: a review of emerging techniques with reference to biological treatment" Crit. Rev. Environmen. Sci. Technol 35: 219–238, 2005.
[10] T. Robinson, G. McMullan, R. Marchant, P. Nigam "Remediation of dyes in textile effluent: a critical review on current treatment technologies with a proposed alternative" Bioresour Technol 77: 247–255, 2001.
[11] F. P. van der Zee, S. Villaverde "Combined anaerobic–aerobic treatment of azo dyes – a short review of bioreactor studies" Water Res 39: 1425–1440, 2005.
[12] M. T. Sulak, H. C. Yatmaz "Removal of textile dyes from aqueous solutions with eco-friendly biosorbent" Desalin. Water Treat 37: 169–177, 2012.
[13] A. Reife, D. Betowski, H. S. Freeman "Dyes and Pigments" Environmental Chemistry, in The Encyclopedia of Environmental Analysis and Remediation, John Wiley & Sons, New York 3: 1442-1465, 1998.
[14] T. Robinson, G. McMullan, R. Marchant, P. Nigam "Remediation of dyes in textile effluent: a critical review on current treatment technologies with a proposed alternative" Bioresource Technol 77: 247–255, 2001.
[15] Y. Fu, T. Viraraghavan "Fungal decolorization of dyewastewaters: a review" Bioresource Technol 79: 251–262, 2001.
[16] K. Y. Pandya, R. V. Patel, R. T. Jasrai, N. Brahmbhatt "Biodecolorization and Biodegradation of reactive azo dyes by *Kappaphycus alvarezii* and optimization of biofertilizing potential" Res J of Recent Sci., 6 (6): 1-5, 2017.
[17] K. Y. Pandya, R. V. Patel, R. T. Jasrai, N. H. Brahmbhatt "Preliminary Study on Potential of Seaweeds in Decolorization Efficacy of Synthetic Dyes Effluent" Int. J. Plant, Animal and Environ Sci., 7: 59-69, 2017.
[18] Z. Aksu "Application of biosorption for the removal of organic pollutants: a review" Process Biochem 40: 997–1026, 2005.
[19] J. Y. Wu, S. C. J. Hwang, C. T. Chen, K. C. Chen "Decolorization of azo dye in a FBR reactor using immobilized bacteria" Enzyme Microb. Technol 37: 102–112, 2005.
[20] A. Ozer, G. Akkaya, M. Turabik "Biosorption of Acid Red 274 (AR274) on *Enteromorpha prolifera* in a batch system" J. Hazard. Mater 126: 119–127, 2005.

[21] G. Akkaya, A. Ozer "Biosorption of Acid Red 274 (AR274) on *Dicranella varia*: determination of equilibrium and kinetic model parameters" Process Biochem 40: 3559–3568, 2005.

[22] **N. Kuyucak "Feasibility of biosorbents application. In: Volesky B (ed) Biosorption of heavy metals" CRC Press, Boca Raton, FL, 371-378, 1990.**

[23] A. G. El-Said, A. M. Gamal "Potential application of orange peel (OP) as an eco-friendly adsorbent for textile dyeing effluents" J of textile and apparel technol and managem 1(3): 1-13, 2012.

[24] M. S. Chiou, H. Y. Li "Adsorption behavior of reactive dye in aqueous solution on chemical cross-linked chitosan beads" Chemosphere 50: 1095–1105, 2003.

[25] Y. C. Wong, Y. S. Szeto, W. H. Cheung, G. McKay "Adsorption of acid dyes on chitosan-equilibrium isotherm analyses" Process Biochem 39: 695–704, 2004.

[26] C. Namasivayam, N. Kanchana, R. T. Yamuna "Waste banana pith as adsorbent for the removal of rhodamine-B from aqueous solutions" Waste Manage.13: 89–95, 1993.

[27] Z. Aksu "Reactive dye bioaccumulation by *Saccharomyces cerevisiae*" Process Biochem 38: 1437–1444, 2003.

[28] Z. Aksu, S. Tezer "Equilibrium and kinetic modelling of biosorption of Remazol Black B by *Rhizopus arrhizus* in a batch system: effect of temperature" Process Biochem 36: 431–439, 2000.

[29] J. Swamy, J. A. Ramsay "The evaluation of white rot fungi in the decoloration of textile dyes" Enzyme Microb Technol 24: 130–137, 1999.

[30] B. Volesky in: B. Volesky (Ed.), Biosorption of Heavy Metals, C CRC Press, Boca Raton, FL, 3, 1990.

[31] N. Kuyucak, B. Volesky "Biosorption by algal biomass. In biosorption of heavy metals; Volesky B", Ed.; CRC Press: Boca Raton, FL, 173-198

[32] F. A. Bertoni, A. C. Medeot, J. C. Gonzalez, L. F. Sala, S. E. Bellu "Application of green seaweed biomass for MoVI sorption from contaminated waters. Kinetic, thermodynamic and continuous sorption studies" J of Colloid and Interface Sci 446: 122–132, 2015.

[33] C. Das, K. Naseera, A. Ram, R. M. Meena, N. Ramaiah "Bioremediation of tannery waste water by a salt-tolerant strain of *Chlorella Vulgaris*" J of Appl Phycol 29: 235-243, 2016.

[34] L. S. Badescu, D. Bulgariu, L. Bulgariu "Alternative utilization of algal biomass (*Ulva* sp.) loaded with Zn (II) ions for improving soil quality" J Appl Phycol 29: 1069-1079, 2016.

[35] S. M. H. Nasab, A. Naji, M. Yousefzadi "Kinetic and equilibrium studies on biosorption of cadmium (II) from aqueous solution by Gracilaria corticata and agar extraction algal waste" J Appl Phycol 29: 1-10, 2017.

[36] A. Siklina, G. D. Nelson, C. E. Bayliss, C. L. Pooley "Bioremediation efficacy – Comparison of nutrient removal from an anaerobic digest waste-based medium by an algal consortium before and after cryopresearvation" J Appl Phycol 29: 1331-1341, 2017.

[37] Y. Xun, Z, Shu-Ping, Z. Wei, C. Hong-You, D. Xiao-Dong, L. Xin-Mei and Y. Zi-Feng "Aqueous dye adsorption on ordered malodorous carbons" Journal of Colloid Interface Science 310, 83–89, 2007.

[38] G. K. Latinwo, L. A. Jimoda, S. E. Agarry, J. A. Adeniran "Biosorption of some heavy metals from Textile Wastewater by Green Seaweed Biomass" Univ J of Env Res and Technol 5 (4): 210-219, 2015.

[39] M. M. Ghoneim, H. S. El-Desoky, K. M. El-Moselhy, Adel Amer, E. H. Abou el-Naga, L. I. Mohamedein, A. E. Al-Prol "Removal of cadmium from aqueous solution using marine green algae, *Ulva lactuca"* Egyptian J of Aqatic Res 40: 235-242, 2014.

[40] N. H. Brahmbhatt and R. V. Patel "Bioremediation potential of *Spirogyra*, toxicity and biosorption on lead (Pb). Indian Hydrobiology" 15 (1): 90-94, 2012.

[41] N. Brahmbhatt, R. V. Patel, R. T. Jasrai "Accumulation of Chromium by Spirogyra Sp. And its Effect on Its Biochemical Constituents" Int J of Green and Herbal Chem 2 (1): 15-19, 2013.

[42] J. I. Nirmal Kumar, C. Oommen and R. N. Kumar "Biosorption of heavy metals from aqueous solution by green marine macroalgae from Okha Port, Gulf of Kutch, India" Am-Euras. J. Agric. Environ. Sci., 6, 317-323, 2009.

[43] G. G. Patel, H. V. Doshi, M. C. Thakur "Biosorption and equilibrium study of Copper by Marine seaweeds from North West Cost of India" J of Env Sci, Toxic and Food Technol 10 (7): 54-64, 2016.

[44] E.A. Bursali, L. Cavas, Y. Seki, S.S. Bozkurt, M. Yurdakoc, Sorption of boron by invasive marine seaweed: *Caulerpa racemosa var. cylindracea*, Chem. Eng. J. 150: 385–390, 2009.

[45] F. A. Bertoni, A. C. Medeot, J. C. Gonzalez, L. F. Sala, S. E. Bellu "Application of green seaweed biomass for MoVI sorption from contaminated waters" Kinetic, thermodynamic and continuous sorption studies. J of Colloid and Interface Sci 446: 122–132, 2015.

[46] M. Rathod, K. Mody, Shaik B "Efficient removal of phosphate from aqueous solutions by red seaweed, *Kappaphycus alverezii"* J of Cleaner Prod 1-10, 2014.

[47] R. Aravindhan, J. R. Rao, B. U. Nair "Removal of basic yellow dye from aqueous solution by sorption on green alga *Caulerpa scalpelliformis"* J of Haz Mat 142: 68–76, 2007.

[48] T. A. Davis, B. Volesky, RHSF Vieira "Sargassum seaweed as biosorbent for heavy metals" Wat Res 34(17): 4270-4278, 2000.

[49] M. Kousha, E. Daneshvar, M. S. Sohrabi, M. Jokar, A. Bhatnagar "Adsorption of acid orange II dye by raw and chemically modified brown macroalga *Stoechospermum marginatum*" Chem Eng J 192: 67–76, 2012.

[50] R. Pandimurugan, S. Thambidurai "Synthesis of seaweed-ZnOPANI hybrid composite for adsorption of methylene blue dye" J of Env Chem Eng 4(1):1332-1347, 2016.

[51] S. E. Agarry, O. O. Ogunleye, O. A. Ajani "Biosorptive removal of cadmium (II) ions from aqueous solution by chemically modified onion skin: batch equilibrium, kinetic and thermodynamic studies" Chem Eng Communications 202: 655-673, 2015.

[52] I. A. W. Tan, B. H. Hameed, A. L. Ahmad "Equilibrium and kinetic studies on basic dye adsorption by oil palm fibre activated carbon" Chem Eng J 127: 111–119, 2007.

[53] B. H. Hameed, A. T. M. Din, A. L. Ahmad "Adsorption of methylene blue onto bamboo-based activated carbon: kinetics and equilibrium studies" J Hazard Mater 141: 819–825, 2007.

[54] B. H. Hameed, D. K. Mahmoud, A. L. Ahmad "Equilibrium modeling and kinetic studies on the adsorption of basic dye by a low-cost adsorbent: Coconut (*Cocos nucifera*) bunch waste" J of Haz Mat 158: 65–72, 2008.

[55] I. D. Mall, V. C. Srivastava, N. K. Agarwal, I. M. Mishra "Removal of congo red from aqueous solution by bagasse fly ash and activated carbon: Kinetic study and equilibrium isotherm analyses" Chemosphere 61: 492–501, 2005.

[56] S. Lagergren "Zur theorie der sogenannten adsorption geloster stoffe" Kungliga Svenska Vetenskapsakademiens Handlingar 24 (4): 1–39, 1898.

[57] Y. S. Ho "Adsorption of Heavy Metals from Waste Streams by Peat" PhD Thesis, University of Birmingham, Birmingham, UK, 1995.

[58] N. Ertugay, Y. K. Bayhan "Biosorption of Cr from aqueous solutions by biomass of *Agricus bisporus*" J of Haz Mater., 154: 432-439, 2008.

[59] O. D. Uluozlu, A. Sari, M. Tuzen "Biosorption of antimony from aqueous solution by lichen (*phusica tribacia*)" Chem Eng J., 163: 382-388, 2010.

[60] X. F. Sun, S. G. Wang, X. W. Liu, W. X. Gong, N. Bao, B. Y. Gao, H. Y. Zhang "Biosorption of malachite green from aqueous solutions onto aerobic granules: kinetic and equilibrium studies" Biores Technol., 99: 3475-3483, 2008.

P&R Publication

International Journal of Engineering Research and general science is an open access peer review publication which is established for publishing the latest trends in engineering and give priority to quality papers which emphasis on basic and important concept through which there would be remarkable contribution to the research arena and also publish the genuine research work in the field of science, engineering and technologies

International Journal Of Engineering Research and General Science
ISSN 2091 - 2730